H2 assisted NH3-SCR over Ag/Al2O3 for automotive applications

Fogel, Sebastian

Publication date:
2013

Document Version
Publisher's PDF, also known as Version of record

Ph.D. Thesis

H_2 assisted NH_3-SCR over Ag/Al_2O_3 for automotive applications

Sebastian Fogel

May 2013

Technical University of Denmark
Department of Physics

Haldor Topsøe A/S

2013-05-14

Preface

The work in this Ph.D. thesis was performed at the R&D Division at Haldor Topsøe A/S, Denmark and at the Technical University of Denmark, Department of Physics. The work was supported by the Danish Council for Strategic Research through grant 09-067233. Project partners were Chalmers University of Technology, Sweden, Amminex A/S, Denmark, Technical University of Denmark and Haldor Topsøe A/S, Denmark.

A lot of people have helped me during my Ph.D. with varying things, from sample analysis to proof reading, from welding to theoretical discussions and everything in between. Without this help I doubt this work would have been possible. First I would like to thank all colleagues in the environmental departments at Topsøe for making my stay there a time to remember. At Topsøe I also want to thank Tais – sometimes I felt you believed in me more than I did, everyone in Miljølab (especially Drago) for help with the test set-up there, everyone in building 10 for help with monolith preparation, Cecile and Jesper for all the work with the set-up, Chi-Mahn for help with SEM, Anders for help with algorithms for engine testing, Magnus, Bjarne, Holger, Kristoffer, Eilif and Karsten for help with the engine testing, Axel and Mark for help with the control both in engine tests and at the test set-up and Susanne for proof reading of articles. At Chalmers I want to thank Stefanie, Louise and Magnus for nice meetings and interesting discussions. My car-buddies, Henrik, Olle and Christian thanks for making the time in the car to and from work enjoyable.

Thanks to my supervisors: Marie for helping me to understand what this was all about in the beginning, Jacob for help with monolith preparation and the theory behind it, Søren for always having time (even when you left DTU) and Dmitry for teaching me the practical aspects of what it means and how to do research. The set-up of supervisors has changed during the years but one thing has been constant Pär. Thank you for being patient and explaining things even when I was slow or reluctant. Your point was (most often) the right, sometimes I just had to find that out for myself.

Finally thanks to my beloved Sara for supporting me throughout these years.

Ravnholm
May 2013

Sebastian Fogel

Abstract

The up-coming strict emission legislation demands new and improved catalysts for diesel vehicle deNO_x. The demand for low-temperature activity is especially challenging. H_2-assisted NH_3-SCR over Ag/Al_2O_3 has shown a very promising low-temperature activity and a combination of Ag/Al_2O_3 and Fe-BEA can give a high NO_x conversion in a broad temperature window without the need to dose H_2 at higher temperatures. The aim of this study has been to investigate the combined Ag/Al_2O_3 and Fe-BEA catalyst system both at laboratory-scale and in full-scale engine-bench testing. The catalysts were combined both in a sequential dual-bed layout and a dual-layer layout where the catalysts were coated on top of each other. The Ag/Al_2O_3 catalyst was also investigated with the aim of improving the sulphur tolerance and low-temperature activity by testing different alumina-supports. A large focus of this study has been the preparation of monolithic catalyst bricks for the catalyst testing.

A high S_{BET} and higher Ag loading gave a high sulphur tolerance and activity. It was believed that the high S_{BET} is needed to give a higher NH_3 adsorption capacity, necessary for the SCR reaction. A higher Ag loading gives more Ag sites and probably a favourable Ag dispersion. Testing with sulphur gave an increased activity of the catalysts. Testing of monolithic catalysts showed a similar activity enhancement after a few standard test cycles. A change in the dispersion or state of Ag can be possible reasons for the activation seen and the activation was believed to be related to Ag and not the alumina.

Small-scale laboratory testing showed that it was preferred to have Ag/Al_2O_3 either upstream or as the outer layer of Fe-BEA. This was attributed to complete NH_3 oxidation over Fe-BEA giving a deficit of NH_3 over the Ag/Al_2O_3 if it was placed downstream or as the inner layer. Full-scale engine testing, on the other hand, showed the opposite for a dual-brick layout. High NO_2 concentrations are believed to give fast-SCR over the Fe-BEA when it was placed upstream of the Ag/Al_2O_3. The activity of the combined catalyst layouts were higher than the activity for individual catalysts when less or no H_2 was co-fed in the small-scale case showing that there were synergistic effects by combining them. The dual-layer layout showed the best performance which is believed to be attributed the short diffusion distance between the layers allowing diffusion of reaction intermediates between them.

Ag/Al_2O_3 only and the combined Ag/Al_2O_3 – Fe-BEA systems were active during the transient NEDC. The NO_x conversions were not very high which is related to the very low temperature of the NEDC and the lower than expected activity of the Ag/Al_2O_3 catalyst seen in stationary testing. The most interesting result was that the catalyst systems showed NO_x conversion already from the start of the cycle, before any NH_3 or H_2 was dosed. NO_x storage over the Ag/Al_2O_3 was believed to be the most likely explanation for this. The NO_x conversion could be enhanced by dosing of NH_3 and H_2 at temperatures lower than 150°C that was used as standard starting temperature of dosing. However, dosing too early inhibited the NO_x conversion.

Dansk resumé

De fremtidige restriktioner i miljølovgivningen for dieselbiler kræver nye og forbedrede katalysatorer, især i lav-temperaturområdet. H_2-assisteret NH_3-SCR over Ag/Al_2O_3 har vist stort potentiale, og en kombination af Ag/Al_2O_3 og Fe-BEA kan give en høj NO_x omsætning i et stort temperaturområde uden der er behov for at dosere H_2 ved højere temperaturer. Målet med denne afhandling har været at undersøge det kombinerede Ag/Al_2O_3 og Fe-BEA system både i laboratorieskala og i fuldskala motortest. Ag/Al_2O_3 blev også undersøgt med det formål at forbedre svovletolerancen og lav-temperatur aktiviteten. Der blev fokuseret på præparation af monolitter til testning.

En høj S_{BET} og en højere Ag-koncentration gav en høj svovltolerance og aktivitet. Den høje S_{BET} gav en høj NH_3-adsorptionskapacitet, og høj Ag-koncentration gav flere sites og muligvis en mere optimal Ag-dispersion. Frisk Ag/Al_2O_3 aktivitet blev højere efter testning både med svovl og NO_2. Aktiveringen formodes at være koblet til Ag og ikke alumina. En ændring i Ag-dispersionen kan være en sandsynlig forklaring.

Monolitforsøgene viste synergieffekter ved at kombinere Ag/Al_2O_3 og Fe-BEA sammenlignet med de individuelle katalysatorer. Det var en fordel at have Ag/Al_2O_3 i en opstrøms eller ydre position i forhold til Fe-BEA i laboratorietest i lille skala. Test i fuldskala gav de modsatte resultater. Forskellen var at Fe-BEA gav en fuldstændig NH_3 omsætning i de første test, og at NO_2 i feeden gav såkaldt "fast-SCR" over Fe-BEA i fuldskala testene. En dual-layer layout gav den bedste aktivitet da H_2 niveauet blev sænket. Det forklares med den korte diffusionsafstand, der giver mulighed for diffusion af reaktionsmellemprodukter. Transiente motortest viste aktivitet helt fra starten af cyklussen, længe inden nogen NH_3 eller H_2 var doseret. Den bedste forklaring på det er NO_x lagring over Ag/Al_2O_3.

Papers

I. S. Fogel, D.E. Doronkin, P. Gabrielsson, S. Dahl, 2012, "Optimisation of Ag loading and alumina characteristics to give sulphur-tolerant Ag/Al_2O_3 catalyst for H_2-assisted NH_3-SCR of NO_x", Appl. Catal. B, 125, 457-464.

II. S. Fogel, D.E. Doronkin, J.W. Høj, P. Gabrielsson, S. Dahl, 2013, "Combination of Ag/Al_2O_3 and Fe-BEA for high-activity catalyst system for H_2-assisted NH_3-SCR of NO_x for light-duty diesel car applications", Top Catal., 56, 14-18.

III. S. Fogel, P. Gabrielsson, 2013, "H_2-assisted NH_3-SCR over Ag/Al_2O_3: An engine-bench study", in manuscript.

IV. D.E. Doronkin, T.S. Khan, T. Bligaard, S. Fogel, P. Gabrielsson, S. Dahl, 2012, "Sulfur poisoning and regeneration of the $Ag/\gamma\text{-}Al_2O_3$ catalyst for H_2-assisted SCR of NO_x by ammonia", Appl. Catal. B, 117-118, 49-58.

V. S. Tamm, S. Fogel, P. Gabrielsson, M. Skoglundh, L. Olsson, 2013, "The effect of the gas composition on hydrogen-assisted NH_3-SCR over Ag/Al_2O_3", Appl. Catal. B, 136-137, 168-176

VI. D.E. Doronkin, S. Fogel, S. Tamm, L. Olsson, T.S. Khan, T. Bligaard, P. Gabrielsson, S. Dahl, 2012, "Study of the "Fast SCR"-like mechanism of H_2-assisted SCR of NO_x with ammonia over Ag/Al_2O_3", Appl. Catal. B, 113-114, 228-236.

Contribution report

I. I performed most of the experimental work and evaluated the results with my co-authors, especially D. Doronkin. I also wrote the manuscript.

II. I prepared the catalyst and evaluated the results with my co-authors. I also wrote the manuscript.

III. I performed all experimental work, interpreted the results and wrote the article.

IV. I participated in the in the planning of experiment strategy and the interpretation of the results, discussion and evaluation of the results. I also performed calculation of required tolerance to sulphur.

V. I prepared the catalysts and prepared that section of the manuscript and participated in the discussion of the results.

VI. I participated in the discussion and evaluation of the results.

Papers not included in the thesis

D.E. Doronkin, S. Fogel, P. Gabrielsson, S. Dahl, 2013, "Ti and Si doping as a way to increase low temperature activity of sulfated Ag/Al_2O_3 in H_2 -assisted NO_x SCR by NH_3", in manuscript.

Table of Contents

1 Introduction

1.1 Background

Diesel engines are completely dominating for heavy-duty vehicles such as trucks and busses. In Western Europe gasoline has had the main market share for light-duty vehicles with an increased share for diesel since the 1990's. The increase in diesel share of new registration was dramatic from the end of the 1990's to the middle of 2000's where it levelled out at around 50% of the market share [1]. One of the reasons for the increased popularity is the lower fuel consumption compared to gasoline vehicles. Diesel is also less costly than gasoline in most European countries. Together, this gives substantially lower operational costs for the owner even though the diesel technology is more costly than the gasoline technology. Many countries e.g. Germany and the UK also have tax incentives to increase sell of low CO_2 emitting cars which include many smaller diesel vehicles [2]. EU legislation that limits the fleet average emitted CO_2 for new vehicles to 130 g/km will be gradually implemented from 2012 to 2015 with a long-term target of 95 g/km in 2020 [3]. This could further increase the incentive for small diesel engines.

Emissions are harmful, both for the environment and for humans. NO_x and especially NO_2 are toxic. Exposure to NO_2 can give respiratory and cardiovascular diseases. NO_x are powerful greenhouse compounds, NO_x is 7-10 times [4] and N_2O is 270 times more powerful than CO_2. NO_x also contributes to acid rain, photochemical smog and ground-level ozone [5]. PM can give asthma and other respiratory effects [6]. CO is highly toxic by blocking the O_2 uptake in the lungs.

Emission legislation was implemented in Europe in the beginning of the 1990's to improve air quality and minimise adverse health effects. The legislation has been revised several times since then, becoming stricter and stricter. The emissions that are limited are CO, HC, PM and NO_x (NO and NO_2). Figure 1 shows the legislative levels for NO_x and PM. Going from the present Euro 5 to

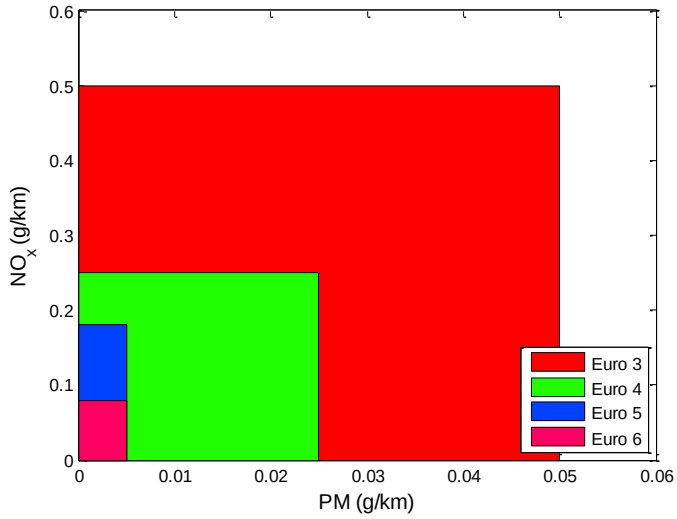

Figure 1 Allowed NO_x and PM levels for European emission legislation for light-duty vehicles, Euro 3 (2000), Euro 4 (2005), Euro 5 (2009) and Euro 6 (2014).

the coming Euro 6 will demand a 56% NO_x reduction. New for PM is that the number of particles will be limited and not only the PM mass. Other countries such as USA have similar legislation [7].

Emission control for gasoline engines is a mature technology and the emissions can be handled relatively easy by a three way catalyst (TWC) that simultaneously removes HC, NO_x and CO. The TWC consists of precious metals Pd and/or Pt combined with Rh. TWC cannot be used in diesel exhaust due to its lean operation with excess oxygen present; reduction of NO_x is especially difficult. Engine improvements and measures are believed not to be sufficient in the future and more advanced aftertreatment technologies are needed to meet upcoming NO_x emission limits. The most promising are selective catalytic reduction (SCR) by NH_3 and NO_x storage and reduction (NSR). The advantage of SCR is that it is a well-known technique that has been used for heavy-duty vehicles for the last 10 years. The disadvantages are the need of storage and refilling of reductant (urea) and limited low-temperature operation. NH_3 are injected to the exhaust prior to the SCR catalyst where they react with NO_x that is reduced to N_2.

$$4NH_3 + 4NO + O_2 \rightarrow 4N_2 + 6H_2O \qquad \text{Equation 1}$$

$$2NH_3 + NO + NO_2 \rightarrow 2N_2 + 3H_2O \qquad \text{Equation 2}$$

$$8NH_3 + 6NO_2 \rightarrow 7N_2 + 12H_2O \qquad \text{Equation 3}$$

HC has been explored as an alternative reductant to NH_3 but the use is so far limited. The advantage with HC would be that it is already available on board the vehicle. However, diesel fuel has a boiling point of ~175-350°C [8] and 20% of the diesel has not evaporated at 300°C [9]. This makes the use of diesel as the reductant at lower temperatures difficult.

The advantage of NSR compared to SCR is that no reductant that needs periodic refilling is needed. The disadvantages are the advanced engine operation related to rich periods and the cost of precious metals. NO is oxidised to NO_2 over e.g. Pt during normal operation and stored as nitrate on the NO_x storage catalyst. The engine is then operated rich (low oxygen level) during short periods of time and the nitrates are decomposed to NO that is reduced over e.g. Rh as in a TWC. Sr- and Ba-oxides are typical NO_x storage materials [10]. Exhaust gas recirculation (EGR) is a complement to SCR and NSR but not sufficient on its own for the upcoming legislation. EGR lowers the oxygen concentration and temperature in the engine cylinder which reduces NO_x formation. The disadvantage of EGR is increased production cost, fuel consumption and higher PM levels [11]. EGR is widely used for heavy- and light-duty vehicles [12].

HC and CO are oxidised over Pt or Pd catalysts. PM or soot which is formed by agglomeration of small carbon particles is removed by filtration. The filter has to be regenerated to avoid build-up of the back-pressure in the exhaust system due to the accumulated soot on the filter. This can either be made in a passive or active way. If the temperature is high enough (250-400°C) NO_2 can react with the soot and oxidise it giving a passive filter regeneration.

$$C + 2NO_2 \rightarrow CO_2 + 2NO \qquad \text{Equation 4}$$

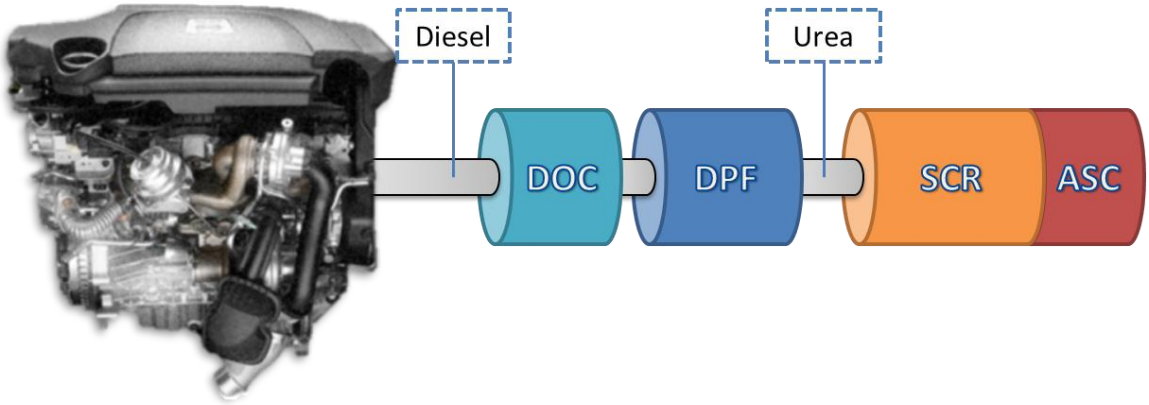

Figure 2 Example of exhaust aftertreatment layout.

The NO_2 can come from up-stream NO to NO_2 oxidation over precious metals, e.g. in a DOC. In active regeneration extra diesel fuel is periodically injected and oxidised over an oxidation catalyst to raise the temperature to 450-600°C which is sufficient to burn off the soot at the filter [10], [13]. Figure 2 shows an example of a layout of a diesel atertreatment system. Included components are an oxidation catalyst (DOC) and a particulate filter (DPF) before and an NH_3 slip catalyst (ASC) after the SCR-catalyst. HC and PM can poison the SCR catalyst and the DOC and DPF are important to prevent this. Urea is often overdosed to maximise the NO_x reduction over the SCR and the ASC is necessary to prevent too high NH_3 concentrations in the tailpipe exhaust.

One of the biggest challenges for NO_x (and other pollutants) removal is, as mentioned above, the low temperature of light-duty exhaust systems. The temperature is typically below 200°C during the standardised new European driving cycle (NEDC) meaning that a lot of NO_x is emitted at very low temperatures [10]. Figure 3 shows an example of accumulated NO_x and engine out temperature during a NEDC for a 1.9 l diesel engine. Today's SCR catalysts, e.g. vanadia-based and Fe-zeolites, are efficient at temperatures above 200-250°C [14]. Cu-zeolite type catalysts have been reported to have very promising low-temperature activity [15–17]; chabazite or chabazite-like structures are especially interesting due to their excellent hydrothermal stability [18–20]. Platinum group metal based catalyst also been proposed but suffer from low selectivity to N_2 and low activity at higher temperatures [21], [22]. Another possible candidate is Ag/Al_2O_3 which has been widely investigated during the last decade.

1.2 Ag/Al_2O_3

The possibility of using Ag/Al_2O_3 as a catalyst for HC-SCR was first reported in the beginning of the 1990's by, among others, Miyadera [23]. HC-SCR is an attractive alternative to conventional urea/NH_3-SCR since the HC reductant already is present and no extra storage is needed. Ag/Al_2O_3 has been widely investigated since the first reports. The effect of e.g. Ag loading [24–28], different HC [29–31] and different support and preparation methods [26], [31–34] have been investigated. However, the limited low-temperature activity is a problem for real life applications. The performance when real diesel fuel is used as reductant can also be questioned [35].

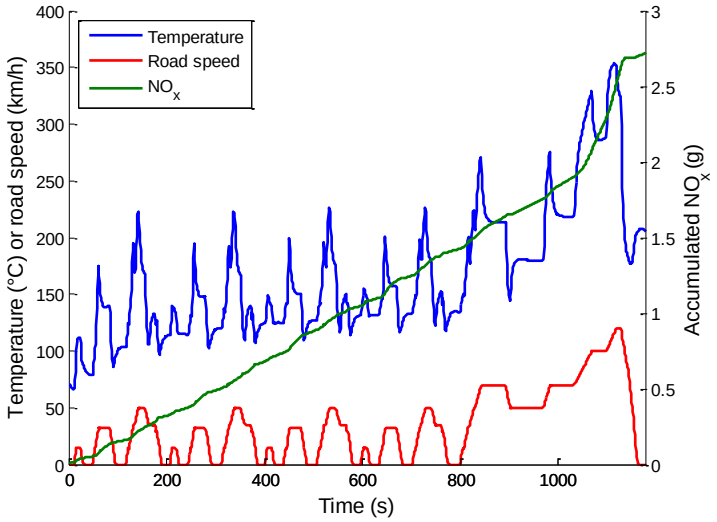

Figure 3 Temperature and accumulated NO_x during NEDC for a 1.9 l diesel engine.

Satokawa [36] was the first to report a dramatic increase in low-temperature activity over Ag/Al_2O_3 by co-feeding H_2. Several reports have confirmed the effect which is now well accepted and widely investigated [37–43]. Richter et al. [44] also showed that Ag/Al_2O_3 is active for H_2-assisted NH_3-SCR and that the catalyst is almost completely inactive without H_2. H_2-assisted NH_3-SCR can even be more active than H_2-assisted HC-SCR. Since the first report there have only been a limited number of reports investigating H_2-assisted NH_3-SCR. The same group that first saw the H_2 effect for NH_3-SCR also investigated the mechanism [45], [46]. They concluded that the role of H_2 was to reduce oxidised Ag species to allow formation of activated oxygen species. These activated oxygen species dehydrogenates NH_3 which reacts with and decompose NO. Shimizu and Satsuma [47] also investigated the mechanism and reached a similar conclusion as the previous authors with H_2 reducing Ag which in turn activates oxygen. They concluded that H_2 facilitated partial reduction and agglomeration of Ag^+ to $Ag_n^{\delta+}$-clusters which activated O_2 to O_2^-. O_2^- activated NH_3 to NH_x and NO to NO_2 which reacted with each other. In another study the same authors showed a high tolerance towards SO_2 poisoning of the Ag/Al_2O_3 catalyst [48]. More recently Chansai et al. [49] investigate the role of H_2 and used NH_3-SCR to avoid interference of HC in their measurements.

The mechanism behind the positive effect of H_2 is still debated and several solutions have been proposed. It is likely that the mechanism is very similar both for HC- and for NH_3-SCR. H_2 has been proposed to reduce Ag which then activates O_2 [39], [45–47]. Ag reduction has also been seen in the presence of CO [41] and conventional SCR [50], [51] and was related to the SCR reaction itself and not the presence of H_2. The proposed effect on Ag reduction could thus come from the enhancement of the SCR reaction by H_2. It is, therefore likely that H_2 participates directly in the reaction. It could either be to enhance formation of some reaction intermediate or removal of some poison [38]. Homogenous gas phase reactions have also been reported to give an important contribution to the overall NO_x conversion and have to be taken into consideration [40], [52–55]. H_2 has been proposed to activate the HC [37], [40], [56] or NO_x [40]. Removal of surface nitrate is another proposed effect [38], [49], [57], [58]. Recently it was shown that the effect of H_2 is very short-lived [49]. Nitrate species was identified to form and disappear at the

same rate as the enhancement of the SCR reaction by short time DRIFT experiments [49]. The nitrate species is probably adsorbed on or close to the active Ag site. It is well known in literature that H_2 enhances the NO to NO_2 oxidation over Ag/Al_2O_3 [38], [50], [56]. Reports both show a positive [24], [59] and a negative effect [39], [50], [56] of replacing NO with NO_2 as the NO_x species. It is then rather NO oxidation to adsorbed NO_x species (ad-NO_x) that is the relevant step and not NO to NO_2 oxidation. NO_2 can directly form these ad-NO_x species [57], [59]. These ad-NO_x species could also poison the active sites on Ag and the removal of these by H_2 [49], [57] seems as a reasonable explanation for the H_2-effect seen.

The sulphur tolerance of a potential automotive catalyst needs to be investigated since sulphur is present in all fuel. SO_2 is the main gas phase sulphur species present in the engine exhaust. Part of the SO_2 is oxidised to SO_3 which can poison the Ag/Al_2O_3 catalyst by forming Ag-sulphates, the oxidation occurs at temperatures above 230°C. Ag-sulphates become unstable and decompose at temperatures above 400°C [60]. Ag/Al_2O_3 has been investigated with respect to sulphur tolerance. The activity is severely decreased at temperatures of 200-450°C [30], [43], [48], [60–62]. At higher temperatures no or low deactivation was seen [60], [61]. Some reports show a severe deactivation even at higher temperatures [59], [63]. Sulphur has also been reported to increase the activity [63], [64]. This has been attributed to formation of Ag_2SO_4 which is believed to be more active than highly dispersed Ag-ions [61], [63]. Higher Ag loaded catalysts are reported to show higher sulphur tolerance [63] [43]. The effect of sulphur is also dependent on the reductant (HC) used [30], [62], [64].

Doping of the alumina with SiO_2 [65] or TiO_2 [65], [66] is reported to increase the sulphur tolerance, which was related to increased acidity of the support which gave less sulphur adsorption. It is widely reported that the activity can be, at least partly, regained by high-temperature treatment (500-650°C) in the presence of H_2 [43], [48], [59], [60]. H_2 in general is reported to have a positive effect on the sulphur tolerance by increasing the sulphur desorption form the catalyst surface [30], [43]. Whether or not Ag- and alumina-sulphates or only Ag-sulphates affects the activity is not clear. Reports have concluded that the poisoning by sulphur is believed to occur on the Ag and that alumina-sulphates does not affect the activity [43], [59], [60]. Alumina-sulphates could even enhance the activity by inhibiting excessive HC combustion [60]. Others have reported that the formation of alumina-sulphates has a negative influence on the activity [63], [66]. Differences in Ag loading and presence of H_2 might explain the differences seen.

A number of studies have tested Ag/Al_2O_3 in real engine exhaust, both in stationary [29], [54], [55], [67], [68] and in transient tests [55], [69]. HC was used as reductant in all reports. Relatively high NO_x conversions were reported. The activity was highly dependent on GHSV [67–69]. Viola [69] reported that a GHSV below 10000 h^{-1} was needed to get a sufficiently high NO_x conversion during transient test cycles (HYWFET, US06 and cold start FTP). Sitshebo et al. [67] reported that the HC present in the exhaust was enough to give a substantial NO_x conversion when H_2 was co-fed. They also showed that the H_2 can be produced on-board via fuel reforming. Lindfors et al. [54] showed a slight deactivation of the Ag/Al_2O_3 catalyst during testing in a real engine exhaust, no deactivation was reported in the other reports.

1.3 Motivation

The ever stricter emission legislation demand new and improved catalysts for deNO_x and innovative ways of utilising them. The low exhaust temperature of modern cars is especially demanding and makes it difficult and costly to meet the demands with today's commercial catalysts. NO_x reduction in a broad temperature window can be obtained by combining low-temperature active Ag/Al_2O_3 and high-temperature active Fe-BEA [70]. A high NO_x conversion could be obtained already at 150-175°C. The benefit of combining the two catalysts was that less H_2 was needed to reach a high NO_x conversion, even at low temperatures. Another advantage was that the tolerance against sulphur poisoning was increased compared to Ag/Al_2O_3 only. The Ag/Al_2O_3 and Fe-BEA system has the potential to meet upcoming legislation with a high low-temperature activity combined with a lower cost related to the use of H_2. This study has been part of a larger research project aimed at further investigated the possibilities of the Ag/Al_2O_3 and Fe-BEA system. The research project included catalyst development on powder-scale, kinetic modelling, theoretical calculations, monolith preparation and testing, full size engine-bench testing and development of a NH_3 and H_2 dosing system for the engine-bench testing.

Most catalyst screening and testing are done in small-scale powder form because of practical reasons. The most important reason for this is that very small amounts of catalysts can be used giving smaller and cheaper testing equipment and easier handling. An important factor when investigating mechanistic aspect is that factors such as mass transfer limitations can be avoided by using small particles. Powder-scale testing was also used in this study to screen different alumina as support for the Ag/Al_2O_3 catalyst. However, to fully evaluate the potential of a promising catalyst it has to be tested as close as possible to real conditions. In the case of automotive catalysts this means as monolithic bricks. A successful transfer of the desired properties found at powder-scale of a catalyst to monolithic-scale is therefore crucial. This can be a key to commercial success of a catalyst and the exact formulations and methods are well guarded secrets of the catalyst companies.

A large focus of this study has, therefore, been the preparation and testing of monolithic catalyst bricks. Small-scale bricks were first prepared followed by scale up of the process to full size 2 l bricks. Different preparation methods and the influence of parameters such as dry-matter and viscosity of washcoating slurries were investigated. The catalytic bricks were both tested in laboratory-scale and on a full size light-duty engine test-bench. The Ag/Al_2O_3 and Fe-BEA was combined both in a sequential dual-bed layout and a dual-layer layout where the catalysts were coated on top of each other. The engine-bench test gave valuable insight into the catalyst performance during real conditions with e.g. poisoning. Laboratory-scale testing with well-defined and controllable conditions was used for an initial test of the different catalyst layouts and to further evaluate the results from engine testing. The Ag/Al_2O_3 catalyst has also been investigated with the aim of improving the sulphur tolerance and low-temperature activity by testing different alumina-supports.

2 Catalyst development

The results presented in this chapter are mainly from Paper I with small parts from papers IV and VI.

2.1 Materials and method

All catalysts were prepared by incipient wetness impregnation to give the desired Ag loading (1-6 wt%). Four different pseudoboehmite alumina precursors that were precalcined at 550, 750 or 1000°C for two hours were compared to commercial γ-Al_2O_3 (Puralox SCFa or TH from Sasol) as a reference sample. The alumina precursors were one from Topsøe, Catapal and Pural from Sasol, and Versal from UOP.

The catalytic activity was tested in a fix-bed quartz flow reactor. Standard test conditions were, 500 ppm NO, 520 ppm NH_3, 1200 ppm H_2, 8.3% O_2, 7% H_2O and balance Ar. 10 ppm SO_2 was added to the feed for sulphur testing. The total flow was 120 Nml/min giving a GHSV of ~50000 h^{-1} based on the whole bed volume (catalyst + SiC). The tests were performed as a ramp down of the temperature from 475 to 130°C at a rate of 2°C/min. For the sulphur testing, the samples were first heated to 475°C and held there for 30 min before being ramped down (2.5°C/min) to 250°C, where SO_2 was introduced and the activity measurement started. The SO_2 was switched off after 1 h at 250°C and the temperature was increased to 670°C and held there for 10 min before being ramped down to 250°C again. The cycle, 1 h at 250°C followed by 10 min at 670°C, was repeated until no difference in activity between the sulphation cycles could be seen. All outlet gases were monitored by FTIR. NO_x conversion was calculated as,

$$X_{NO_x} = \frac{c_{NO_x,in} - c_{NO_x,out}}{c_{NO_x,in}} \qquad \text{Equation 5}$$

where NO_x was the sum of NO, NO_2 and N_2O.

The S_{BET}, pore volume and pore size was measured by N_2-adsorption. NH_3-TPD was conducted in the catalyst test set-up where NH_3 was adsorbed at 90°C in a flow of NH_3 and Ar.

2.2 Results and discussion

XRD showed that the crystallinity of the needle shaped alumina increased when it was calcined at higher temperatures. All samples calcined at 1000°C had, at least partly, transformed from the parent eta/gamma alumina to other, more crystalline, forms such as alpha, delta and/or theta alumina. The test samples showed a wide variety of pore size, volume, size distribution and surface area (S_{BET}). Addition of more Ag did not significantly change the properties.

A series of 1 wt% Ag catalysts with different parent alumina were tested. Figure 4 a) shows an example of temperature dependency of NO_x and NH_3 conversion for fresh 1 wt% Ag/Al_2O_3 from Catapal alumina calcined at 550, 750 and 1000°C. The N_2O level was at most 10 ppm and typically below 5 ppm for all the catalysts tested. The temperature of 50% NO_x conversion (T_{50}) and the NO_x conversion at 250°C were used to compare the samples. Figure 5 shows a clear correlation between T_{50} (a) and NO_x conversion at 250°C (b) and S_{BET}. The optimal S_{BET} for the fresh 1 wt% Ag catalyst tested was found to be 140-220 g/m^2. No clear correlation between activity and other catalyst characteristics were seen. Depending on the S_{BET} of the alumina the catalytic activity was either enhanced or declined when the Ag loading was increased. The NO_x

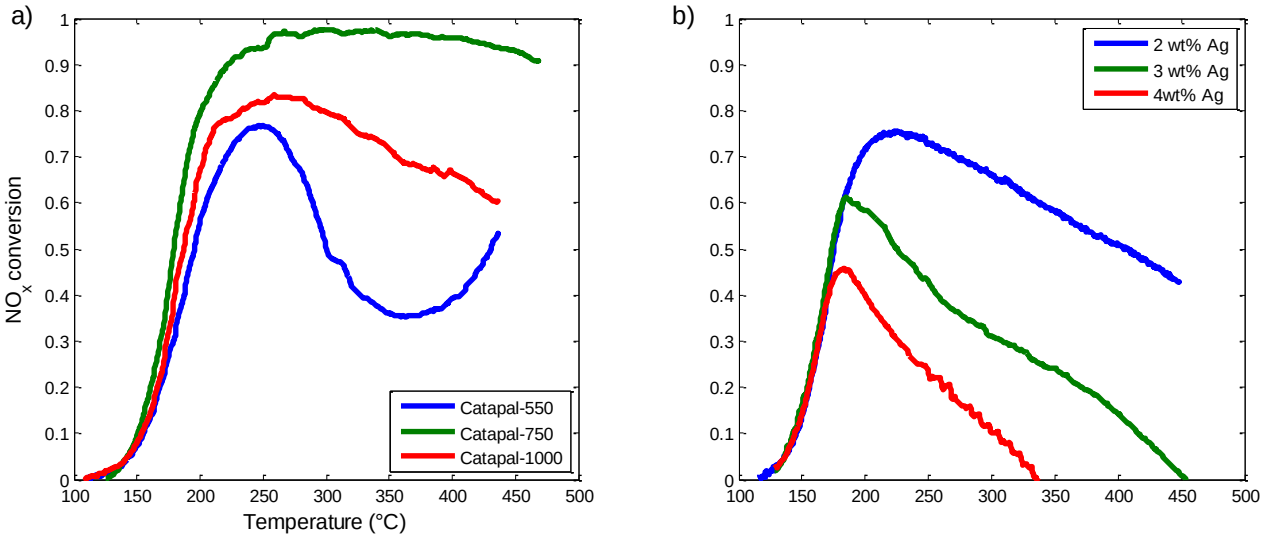

Figure 4 a) Example of NO_x conversion as function of temperature for 1 wt% Ag/Al_2O_3 from Catapal precursor calcined at 550, 750 and 1000°C; b) Comparison of NO_x conversion for Ag/Al_2O_3 with different Ag loading from reference alumina. Reaction conditions: 500 ppm NO, 520 ppm NH_3, 1200 ppm H_2, 8.3% O_2, 7% H_2O and balance Ar, GHSV ~50000 h^{-1} (based on bed volume).

conversion at 250°C increased for samples with S_{BET} >180 m^2/g until it reached its maximum; for lower S_{BET} it was decreased. Figure 4 b) shows an example for the reference catalyst. The activity was the same up to ~170°C for all the Ag loadings. The activity for the 4 wt% Ag sample decreased rapidly at above 170°C and the activity of the 3 wt% Ag sample decreased rapidly at above 200°C. Other catalysts also showed an shift in activity at the lowest temperatures; e.g. 4 wt% Ag/Al_2O_3 from Topsøe-alumina calcined at 550°C had a T_{50} of 170°C compared to 210°C for the same catalyst with 1 wt% Ag. This is discussed more in detail in Chapter 2.3 Conclusions. It was, therefore, concluded that it is the Ag loading/S_{BET} that was the key to activity and not the S_{BET} in itself. Different Ag loadings will therefore correspond to different optimal S_{BET} and vice

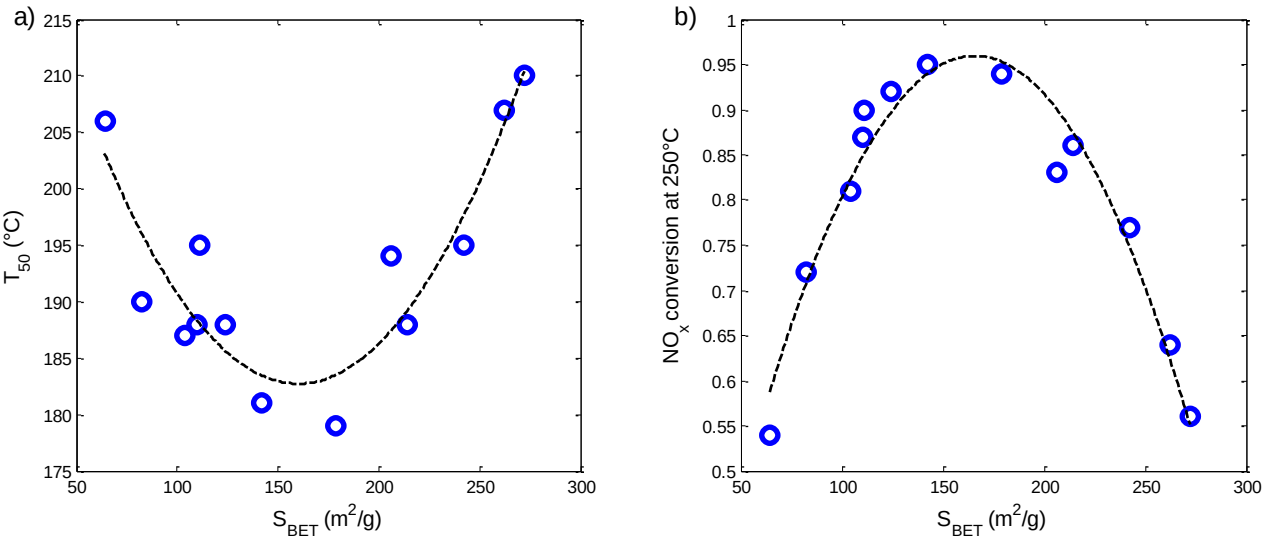

Figure 5 a) T_{50} (temperature of 50% NOx conversion); b) NOx conversion at 250°C; for fresh 1 wt% Ag/Al_2O_3 with respect to S_{BET}. Reaction conditions: 500 ppm NO, 520 ppm NH_3, 1200 ppm H_2, 8.3% O_2, 7% H_2O and balance Ar, GHSV ~50000 h^{-1} (based on bed volume).

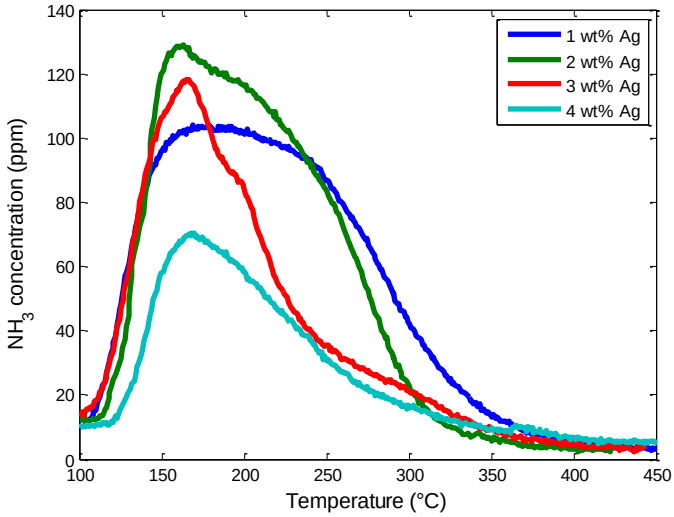

Figure 6 TPD profiles for Ag/Al_2O_3 with 1–4 wt% Ag from reference alumina. Conditions: 100 Nl/min Ar, 5°C/min ramp.

versa. This was also concluded by Zhang et al. [71] for HC-SCR reaction. It should be emphasised that S_{BET} only is a way of quantifying the factors affecting activity such as acidity. Acidity affects, among other things, the NH_3 adsorption capacity of the catalyst which was found to be important. Figure 6 shows that the NH_3 adsorption capacity decreased at temperatures above 200°C as the Ag loading increased for the reference sample series. A lack of NH_3 available for the SCR reaction was believed to be the reason for the loss of activity for the higher Ag loading samples.

The catalysts were tested in the presence of 10 ppm SO_2 to further investigate their applicability. The SO_2 feed was turned off after 1 h at 250°C and the temperature was ramped up to 670°C in

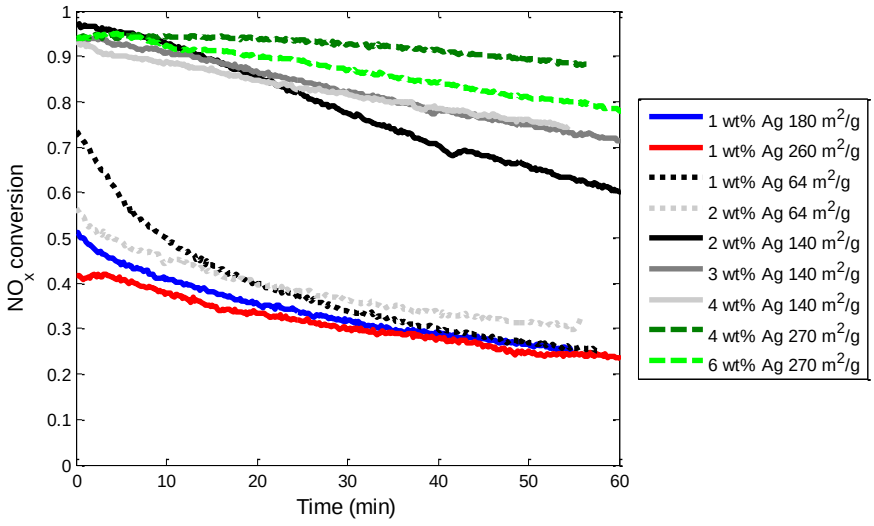

Figure 7 NOx conversion for one sulphur tolerance test cycle at steady-state (no change in activity profile between cycles) for samples with different Ag loading (1-6 wt%) and S_{BET} (64-270 m^2/g). Reaction conditions: T = 250°C, 500 ppm NO, 520 ppm NH_3, 1200 ppm H_2, 10 ppm SO_2, 8.3% O_2, 7% H_2O and balance Ar, GHSV ~50000 h^{-1} (based on bed volume).

order to regenerate the catalytic activity. The cycle was repeated until deactivation stabilised and no difference in activity profile between the cycles was seen, steady-state. Figure 7 shows a comparison of steady-state activity profiles for different samples. The catalysts were deactivated by the presence of SO_2 but could be regenerated and part of the activity regained. The results differed from those of the fresh catalysts with a shift in optimum Ag loading to higher values. It was also clear that a higher S_{BET} was beneficial. The sample that showed the highest NO_x conversion at the end of the deactivation cycle was a high S_{BET} alumina (270 m^2/g) with 4 wt% Ag. The low Ag loading and S_{BET} samples showed poor overall conversion. This was attributed to the higher NH_3 adsorption capacity of the higher S_{BET} alumina since the number of acid sites is proportional to the S_{BET}.

Figure 8 shows a comparison of the temperature dependency of NO_x conversion for fresh catalysts and catalysts after extended testing with sulphur followed by regeneration. A large increase in activity was seen at temperatures above 200°C. However, the activity at lower temperatures decreased and could not be regenerated. Part of the explanation for the increase in activity is believed to be that sulphation of the alumina surface enhances the intensity of Lewis acid sites [66] that increases the NH_3 adsorption capacity of the catalysts; this was also shown by TPD. Another reason was that sulphur poisoned the sites responsible for the unselective NH_3 oxidation seen for fresh high Ag loading catalysts at temperatures above 250-300°C. It is also possible that sulphur poisoning and the high-temperature regeneration affect the Ag dispersion [61].

Dispersion and state of the Ag is believed to be important for the catalytic activity of the Ag catalyst. Both highly dispersed ions [24], [26], [28], [32], [50], [72] and Ag-clusters [34], [73], [74] have been proposed to be the active species for HC-SCR and H_2 promoted HC-SCR. Ag-clusters are reported to form during the SCR reaction by reduction and migration of Ag ions [50], [51], [73]. Ag-clusters [47] and metallic Ag [45], [46] have been reported to be the active

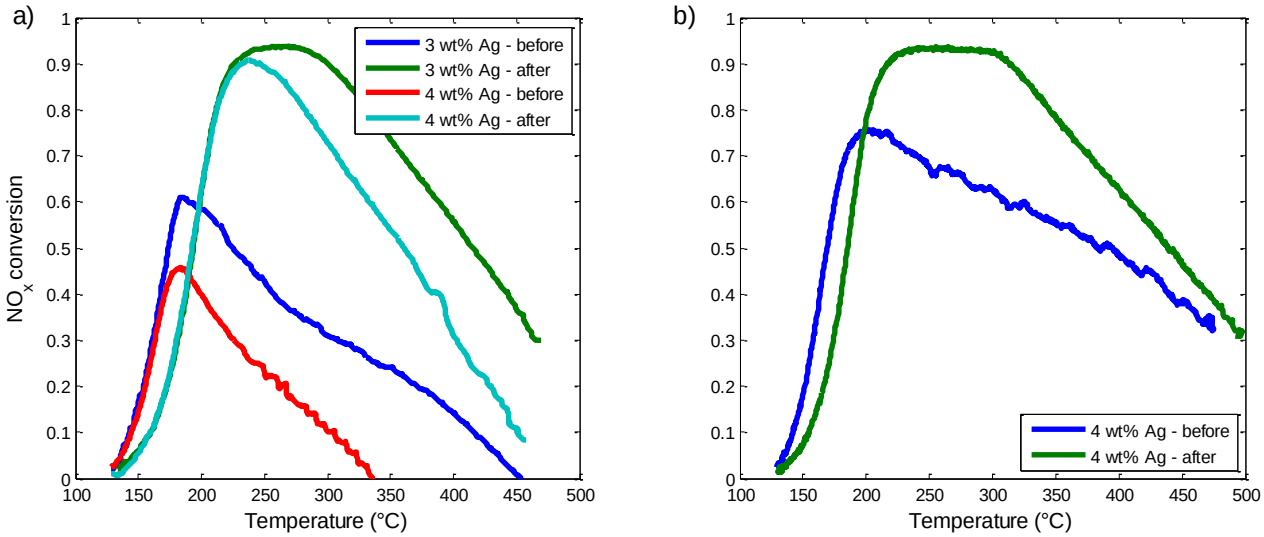

Figure 8 Comparison of NOx conversion as function of temperature for Ag/Al_2O_3 with different Ag loading from a) reference alumina and b) Topsøe alumina, before and after testing with sulphur. Reaction conditions: 500 ppm NO, 520 ppm NH_3, 1200 ppm H_2, 8.3% O_2, 7% H_2O and balance Ar, GHSV ~50000 h^{-1} (based on bed volume)

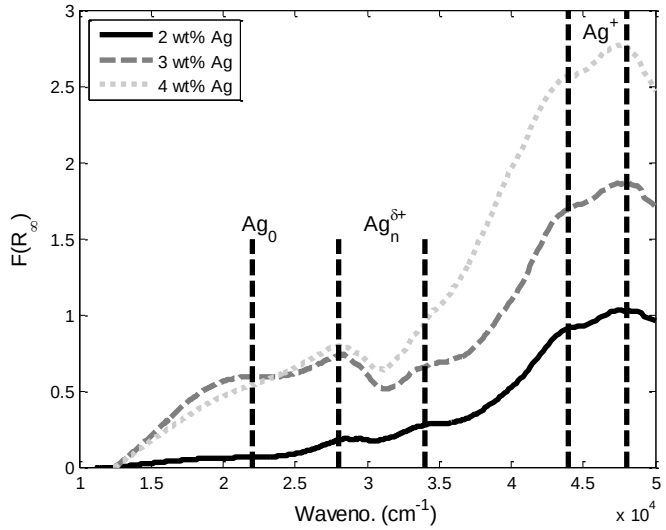

Figure 9 UV–vis spectra for 2–4 wt% Ag/Al_2O_3 from reference alumina. The major peaks attributed to Ag^0, $Ag_n^{\delta+}$ and Ag^+ are indicated.

species for NH_3-SCR.

An increased Ag-loading will affect the state of Ag. An ex-situ study of a number of Ag/Al_2O_3 catalysts from different alumina series with different Ag loadings was performed. When comparing catalyst with the same parent alumina but with different Ag loadings it was seen that the amount of $Ag_n^{\delta+}$-clusters and Ag particles increased as expected from literature. Figure 9 shows an example for 2-4 wt% Ag/Al_2O_3 from reference alumina. It has to be stressed that a higher Ag loading also will give a higher total number of Ag sites. The increased activity seen for high Ag loading samples could, therefore, be related to the increased amount of active sites rather than different types of Ag present. From the tests it was concluded that it is not feasible to get quantitative results from UV-vis studies, nor to compare different series of catalysts. UV-visible spectroscopy is a method that has been widely used to investigate the state of Ag in literature [24], [26], [28], [32], [34]. However, the signal from the alumina itself might interfere with the results from UV-vis [24], Ag is also mobile and can easily form clusters and be re-dispersed as smaller Ag ions on the alumina surface during SCR-conditions [28], [50]. Large Ag particles are, on the other hand, not affected by reduction-oxidation [28]. Ex-situ measurements are, therefore, not necessarily representative for what happens during reaction conditions and it is difficult to identify the active Ag species. Well dispersed Ag ions have been reported to be poisoned by sulphur species on the alumina and Ag-clusters have been reported to give a higher sulphur tolerance [43]. Large Ag particles oxidises NH_3 to a larger extent than Ag ions and clusters [75], [76]. Ag-clusters are, therefore, believed to be preferred over Ag-ions and larger Ag particles as the main Ag-species to get a sulphur tolerant and highly active catalyst. However, it is not possible to fully distinguish between Ag ions and clusters as they might form and disappear during SCR. It could be that sulphur favours the presence of a specific form of Ag and that is what is responsible for the permanent loss in low-temperature activity. Further studies are needed to clarify this.

2.3 Conclusions

The results seen for powdered catalysts with an optimum of high S_{BET} with a high Ag loading can be explained as follows (schematically shown in Figure 10): As Ag loading is increased for a given surface area more active sites will form and the catalytic activity will increase (Figure 10 a). As more metal is loaded the surface will get more and more crowded by Ag-species that form larger and larger clusters/particles. The activity at medium to high temperature (>200-250°C) will start to decrease when the Ag loading becomes higher than the optimal loading since the increased Ag loading will block NH_3 adsorption sites leading to shortage of NH_3 for the SCR reaction (Figure 10 b). From 250-300°C unselective NH_3 oxidation will further decrease the amount of available NH_3, which leads to a reduction of activity. The low-temperature activity is kept constant since NH_3 adsorption still is high and it is, thus, only dependent on the number of available sites. This can also explain the results seen for 1 wt% Ag/Al_2O_3 in Figure 5. The samples with a S_{BET} below 140 m^2/g suffer from low NH_3 adsorption capacity and too crowded Ag giving larger Ag particles. The high S_{BET} samples have too well dispersed Ag and a low amount of sites per S_{BET}. The right balance between amount of Ag and S_{BET} is thus important.

Sulphur, as ad-SO_x species, will poison the catalyst. Part of the poisoning effect is reversible by regeneration at >600-650°C in the presence of H_2. Three main phenomena are seen for the irreversible effects; first, a loss of low-temperature activity; second, an increase in activity above 200-250°C; and third, a decrease in unselective NH_3 oxidation. The loss of low-temperature activity is believed to be related to SO_x bound to the alumina support blocking the sites active at low temperature. By treatment at 950°C this activity can be regenerated but with large loss of higher temperature activity likely related to sintering of Ag particles [28]. SO_x adsorbed on Ag will, unlike SO_x bound to the alumina, be desorbed at 600-650°C [61], [77], thus, allowing these sites to be regenerated. It is thus concluded that there are two different Ag sites present at the catalyst. The increase in activity for the sulphur poisoned catalysts above 200-250°C is related to increased NH_3 storage capacity from more acid sites and also the decreased unselective NH_3 oxidation which is believed to come from blocking of these sites on larger Ag particles. This can

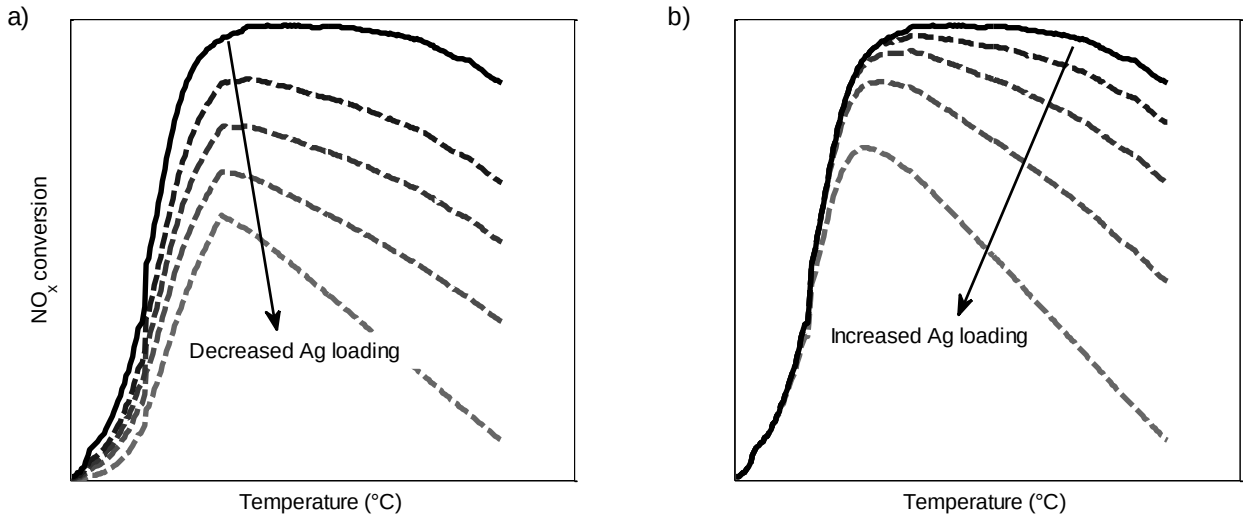

Figure 10 Schematic explanation of influence of Ag loading on activity for a) Ag loadings lower than the optimal Ag loading and b) Ag loadings higher than the optimal Ag loading for any given S_{BET}.

explain why a higher S_{BET} is an advantage; a high S_{BET} can hold more Ag, i.e. more sites, before it becomes too crowded (to large Ag clusters/particles). It could also be that the sulphur influences Ag dispersion towards a dispersion with higher activity at temperatures above 200-250°C and a lower activity at lower temperatures. An addition of Si or Ti will likely affect the Ag dispersion allowing more Ag to be loaded without the negative effects.

2.4 Summary

An optimal S_{BET} of 140-220 m^2/g was found for a series of fresh 1 wt% Ag samples. By testing higher Ag loading samples it was concluded that it was the Ag loading/S_{BET} that was the important measure. By testing the catalysts in the presence of SO_2 followed by regeneration it was found that sulphur irreversibly poisoned the activity below 200°C but also gave a large increase in the activity above 200°C; the activity could be regenerated by high-temperature treatment in the presence of H_2. It was beneficial to have a high S_{BET} since it allowed a higher NH_3 adsorption which is needed for the SCR reaction. A high S_{BET} also allows a higher Ag loading. A high Ag loading will give more available sites and possibly also an optimal dispersion of Ag. A too high Ag loading is believed to give a deficit of NH_3 adsorption capacity on the alumina surface for the SCR reaction at temperatures above 200°C lowering the deNO_x activity. Acidic sites related to sulphur increases the NH_3 adsorption capacity of the catalyst giving an increased activity above 200°C.

3 Monolith preparation: effect of slurry properties

3.1 Theoretical background

The principle of the preparation process of coated catalytic monoliths, so called washcoating, is as follows [78]:

1. The powder catalyst is mixed with water or some other solvent and binder into slurry.
2. The catalyst particle size is reduced in e.g. a ball mill.
3. The catalyst slurry is coated onto the monolith. Different techniques can be used, e.g.
    a. The monolith can be partly or fully immersed into the slurry.
    b. The slurry can be drawn through the monolith either by gravitational forces or by suction.
4. Excess slurry is removed with e.g. pressurised air.
5. The monolith is dried.
6. Steps 3-5 are repeated until the desired catalyst loading is reached.
7. The monolith is calcined to fixate the coat to the monolith and remove any residue solvent or pH adjuster. The monoliths can also be calcined after each single coat layer if steps 3-5 are repeated.

During the coating process the pores in the support wall take up the liquid in the slurry while the solid particles are too big to enter the support and are deposited on the wall forming a filter cake [78], [79]. A viscous film will form outside the filter cake when the excess slurry is removed from the channels. The thickness of the film is dependent on the properties of the slurry, such as viscosity, and the speed at which the excess liquid is removed, i.e. dependent the external force used [79]. The liquid uptake will be larger in subsequent coats since the previous coat layer also will absorb liquid, in addition to the substrate material. To avoid channel blocking the solid content or dry matter (DM) has to be lowered to get less viscous slurry. Binders are used to increase the interparticle adhesion of the catalyst and the anchoring to the substrate wall [78], [80]. The properties of the slurry can be adjusted with different additives such as dispersion or wetting agents to give the desired properties [80].

The DM of the slurry will directly affect the catalyst loading on the substrate. A high DM of the slurry is preferred since it will give a higher coat loading per impregnation [81]. The substrate can only take up a certain amount of liquid and a higher DM of the slurry will give a higher amount of catalyst deposited related to the liquid uptake. The amount deposited is also related to the viscosity and yield stress of the slurry. Useful slurries are normally Bingham plastic:

$$\sigma = \sigma_0 + \mu\dot{\gamma} \qquad \text{Equation 6}$$

where σ is the shear stress, σ_0 is the yield stress, μ is the viscosity and $\dot{\gamma}$ is the shear rate. Figure 11 schematically shows the shear stress as a function of shear rate for a Bingham plastic fluid.

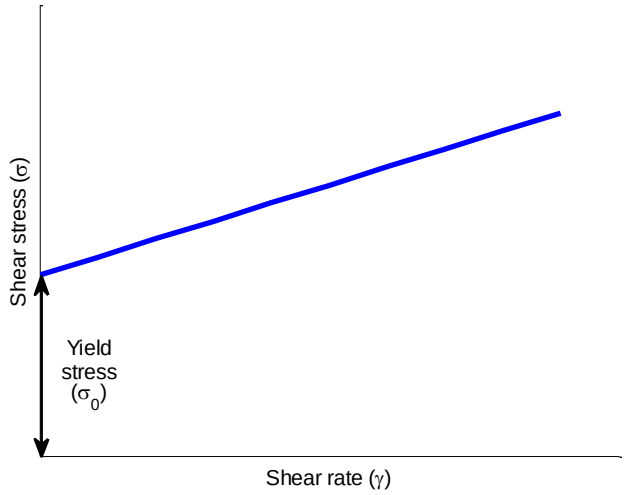

Figure 11 Schematic figure of shear stress as function of shear rate for a Bingham plastic fluid.

The yield stress is marked in the figure and the viscosity is represented by the slope of the curve. If the DM is low the yield stress will be close to zero and the slurry will be Newtonian [82]. If the shear stress is lower than the yield stress the medium (in this case the slurry) is immobile [79]. This happens in the monolith channels; as the substrate walls take up the liquid the DM will increase together with viscosity and yield stress, eventually making the catalyst to deposit on the substrate wall. Thus, by increasing the yield stress it is possible to manipulate the amount of catalyst deposited on the wall. This can be done by adding thickener agents which has a very high yield stress in comparison to viscosity, enough to affect the yield stress of the whole slurry [83].

Too viscous slurry will lead to channel blocking of the monolith substrate. pH and DM are the most important factors for controlling the viscosity of the slurry [79]. The effect of pH is connected to the surface charge of the alumina. An increased pH will give a more negatively charged surface from the equilibrium

$$sOH + OH^- \rightleftarrows sO^- + H_2O \qquad \text{Equation 7}$$

where s denotes the surface. A decreased pH gives a more positively charged surface according to

$$sOH + H^+ \rightleftarrows sOH_2^+ \qquad \text{Equation 8}$$

If the particles have low or zero charge they will agglomerate and the slurry will become more viscous. A larger charge, either positive or negative, will lead to repulsion between the particles [82]. The isoelectric point of alumina is at a pH of 7-8 [81]. A lower or higher pH is, therefore, appropriate for alumina [78], [81]. Changing pH can be enough to ensure stable slurry with an appropriate viscosity. The viscosity can also be lowered by using a dispersion agent that hinders particle agglomeration [81]. The effect of the dispersion agent can e.g. be electrostatic by charging the surface (as with pH) or steric by adding a polymer that hinders the particles to come into contact with each other [82]. The length of the monolith is also of importance. A

longer monolith will give a higher DM and viscosity at the end of the channel due to more and more liquid being absorbed by the monolith, which may lead to channel blocking.

Desired properties of the coated monoliths are high mechanical strength (so that the catalyst is not lost due to vehicle vibrations) and low diffusion resistance (so that the whole catalyst layer is utilised). Particle size is a crucial parameter in order to get a catalyst coat with good adherence to the monolith (high mechanical strength). The particle size should be in the same size range as the macropores of the cordierite support (5 μm) to allow anchoring to the support [78], [84]. Interfacial forces between the particles also play an important role [84]. Too small particles can give a very dense coat with diffusion limitations and too large particles can give irregular coats with poorer adherence [78], [84]. Smaller particles also leads to a higher viscosity of the slurry which will affect the coating process [81]. Cracks can form in the coat layer during drying. The cracks will form where the coat is thickest, typically in the corners of the monolith channels [85].

The target of the washcoating and slurry studies was an as high as possible coat loading of the monolith bricks to minimise the number of repeated coatings. The parameters that could be tuned were DM and viscosity. Viscosity is linked to DM and a change in DM will affect the viscosity. The viscosity could also be adjusted by pH and additives such as thickening and dispersion agents. Particle size was not believed to affect the coating properties to any larger extent. It does, however, influence the mechanical stability of the coat. The effect of slurry properties and different additives on coating capability was investigated in an empirical way and the success was evaluated based on if the monolith channels were blocked or not. If the coating tests were successful the DM or viscosity was increased up to the point when coating became unsuccessful. The effect of modifying agents is very complex and very much based on empirical work.

3.2 Materials and method

Based on the results in Chapter 2 Catalyst development a Topsøe high surface area alumina (300 m^2/g) was chosen as the catalyst carrier material. The catalysts were, except for the first washcoating tests, prepared by incipient wetness impregnation. Wetness impregnation followed by spray dying was investigated as an alternative method to incipient wetness impregnation for catalyst preparation. The difference of scale between catalyst powder tests and monolith test are significant, from a couple of grams to several kilograms of catalyst and wetness impregnation was believed to be a more effective way of preparing larger amounts of catalyst. For the first washcoating test a wetness impregnation method was used instead. The alumina was mixed with excess H_2O and ball-milled to a typical d_{50} of 2.5-3.0 μm. $AgNO_3$ was added to the slurry under intense stirring in sufficient amount to give the desired load of 6 wt% Ag and the slurry was spray-dried to produce fine catalyst powder. The small alumina particles agglomerated during spray drying giving a d_{50} of 17 μm. No further particle size reduction was made. The S_{BET} of the prepared catalyst was 270 m^2/g. The catalyst also had a high pore volume (0.9 cm^3/g), i.e. high ability of the catalyst powder to take up liquid, and it was not possible to get a DM higher than approximately 35%.

XRD showed no traces of Ag and that the alumina was eta/gamma phase with approximately 20% alpha phase. ICP analysis showed a content of 6.1 wt% for the first batch and 6.6 wt% for the second batch prepared.

All slurries and monoliths were prepared following the scheme described in Chapter 3.1 Theoretical background, unless stated otherwise. The Fe-BEA monoliths were prepared using a Topsøe standard recipe. The particle size was reduced by shaking the slurry with glass beads (2-3 mm) in a paint shaker. Depending on the size of the monolith they were either dipped in the slurry (d=2 cm monoliths) or the slurry was poured from the top and allowed to flow through the monolith. The support material was 400 cpsi cordierite that was cut to the desired size when necessary. Three different sizes of cylindrical monoliths were prepared; small size, 21x20 mm (dxh) (V=7 mL), medium size, 49x76 mm (dxh) (V=140 mL) and full size, 140x130 mm (dxh) (V=2 L).

pH was adjusted either by using HNO_3 or NH_4OH. The binder used was colloidal silica (Levasil 200N) in 14-18 wt% of total DM. Particle size was measured by laser diffraction with a Malvern Mastersizer 2000 (Malvern Instruments, UK). The viscosity was measured with a cup and bob Bohlin Visco 88 Viscometer (Malvern Instruments, UK). The yield stress and viscosity was calculated by varying the shear rate and measuring the shear stress. The dry matter (DM) or solid content of the slurries was measured using a Mettler Toledo HB 43 (the sample was heated by a halogen lamp to evaporate all liquid and the weight loss was measured). Scanning electron microscope (SEM) image was acquired on a Philips XL30 ESEM-FEG. The sample was mounted in epoxy and ground to reveal the cross section.

3.3 Results and discussion

3.3.1 Topsøe alumina

The activity of the catalyst prepared by wetness impregnation and spray-drying was lower compared to a 4 wt% reference catalyst (Figure 12). Spray-drying is known to give a very good metal distribution which is often desired. However, the catalyst development showed that the optimal Ag/Al_2O_3 also needs some larger clusters of Ag to retain a high activity when the catalyst was sulphur poisoned (Chapter 2 Catalyst development). It is believed that the spray-drying gave too dispersed Ag on the catalyst surface giving a lower activity. More Ag was also likely trapped in the bulk of the catalyst and not directly available for SCR compared to the incipient wetness impregnated catalyst where more Ag is present on the catalyst surface. By increasing the amount of Ag added and by investigating the process further it should be possible to get the same activity on a spray-dried catalyst. This was, however, beyond the scope of this study and it was decided to use the conventional incipient wetness impregnation method instead. It was also shown that the gain in time and simplicity was not as large as expected for the wetness impregnation and spray-dry method. Incipient wetness impregnation was, therefore chosen for the further catalyst preparation.

Figure 13 shows the influence of pH on viscosity, pH of the as prepared slurry was 7. The highest viscosity was found at pH close to 7 as expected from literature. A decreased pH gave a substantially lower yield stress while an increase in pH had no significant effect. The viscosity was not affected to the same extent by pH. Based on the higher yield stress it was decided to use

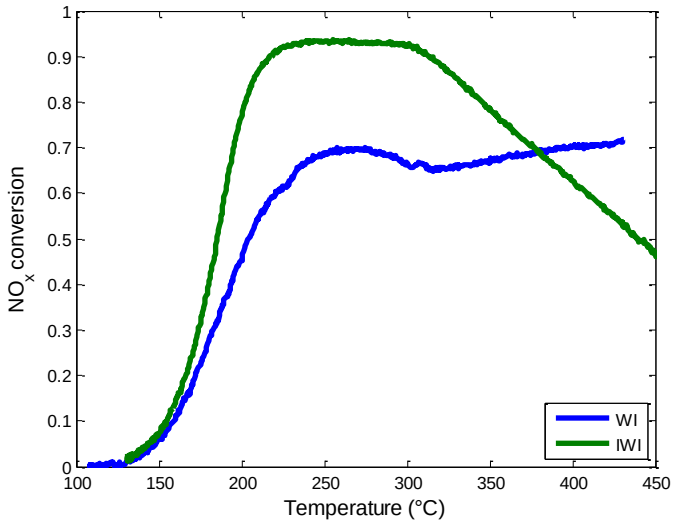

Figure 12 Comparison of NO_x conversion as function of temperature for wetness impregnated (WI) 6 wt% Ag/Al_2O_3 and incipient wetness impregnated (IWI) 4 wt% Ag/Al_2O_3 from Topsøe alumina (S_{BET} 270m^2/g). Reaction conditions: 500 ppm NO, 520 ppm NH_3, 1200 ppm H_2, 8.3% O_2, 7% H_2O and balance Ar, GHSV ~50000 h^{-1} (based on bed volume).

a pH of around 10. The DM had to be somewhat lower than the maximum since the slurry sedimented within a few minutes at the highest DM. A thickener agent (Kelzan) was added to compensate for the lower viscosity and yield stress and to stabilise the slurry. The polymer based agent increased the yield stress without affecting the viscosity to any larger extent; allowing more catalyst to be deposited in each coating.

Washcoating of a small test series of monoliths (Table 1) showed that it was rather complex to interpret the results. Other factors such as the time that pressurised air is used to remove the excess slurry from the monolith channels will also affect the amount of catalyst that is deposited; as will small differences in pH. Slurries prepared in identical manners could also display

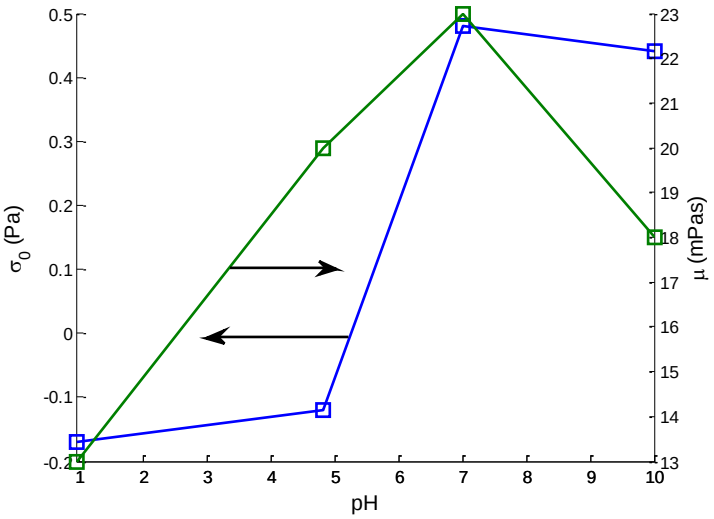

Figure 13 Influence of pH on viscosity and yield stress for 6 wt% Ag/Al_2O_3, DM 35%.

different properties showing that they were not completely stable. As seen for sample 1 and 2 in Table 1 similar slurry properties can give different results. However, a clear correlation between DM, viscosity and loading was seen. DM and viscosity is not independent of each other. E.g. sample 4 had a DM that was almost half of that of sample 5 with yield stress in the same range and showed a loading that was only ¼ of that of sample 5. Sample 6 showed that it was possible to compensate for a lower DM by increasing the yield stress (compared to sample 5).

Table 1 Catalyst loading as function of slurry properties for 5 cm length monoliths, pH 10.

Sample	1	2	3	4	5	6
σ_0 (Pa)	-0.13	-0.12	0.091	1.6	1.8	4.7
μ (mPas)	6.5	7.7	12	7.4	13	16
DM	29	29	32	16	31	27
Loading (g/l)	21	27	33	7.9	31	31

Visual inspection of the slurry was an important method to evaluate its potential for washcoating in complement with viscosity measurements. It was also evident that the length of the monolith played an important role. The slurry had to be made thinner in order to avoid channel blocking when 8 cm monoliths were used instead of the 5 cm monoliths used before. On the other hand, the amount of catalyst deposited was in general higher. It was concluded that a high yield stress (up to 5 Pa) was possible if the viscosity was kept below approximately 25 mPas. The monoliths had to be coated three times to reach the desired catalyst load of 120-140 g/l. To avoid channel blocking the DM was lowered to approximately 19 wt% in the second and to 17 wt% in the third washcoat to get less viscous slurry. The catalyst loading in the subsequent steps was higher than in step 1, also reported in literature [83], in contrast to [81] who showed a lower loading in subsequent steps. The difference seen might be explained by differences in viscosity; a low viscosity will give a smaller contribution from viscous film formation which might explain why the loading per coating decreased for Ref [81].

During particle size reduction in the paint shaker the viscosity tended to increase dramatically making the slurry more gel-like then liquid due to a lowering of pH and the smaller particles themselves [81]. The change in pH is likely due to new alumina surfaces being formed which will change pH towards that of neutral powder [83]. A high viscosity during shaking makes the particle size reduction ineffective since the catalyst particles are not able to move freely in the slurry and come in contact with the glass beads and are, therefore, not crushed. By carefully monitoring and adjusting pH during the shaking it was still possible to obtain a reasonable particle size distribution (d_{50}=3.2 μm). The slurry was diluted to a DM of 20-23% to decrease viscosity to make it possible to separate the glass beads used for crushing and to be able to later coat the monoliths.

A series of small size monoliths (21x20 mm) were prepared from the wetness impregnated and spray-dried catalyst. The desired loading could be reached in two coatings instead of three as in the initial tests since the monoliths were shorter and thicker slurry could be used. When the same slurry was used for several monoliths it became visibly thicker since the monolith substrate took up proportionally more water than catalyst; giving the remaining slurry a higher DM. This gave an increase in loading for the monoliths dipped after each other in the same slurry. The same trend could be seen both for the first and the second coating. The Ag/Al_2O_3

catalyst can be made more active by sulphur treatment (Chapter 2 Catalyst development). The monoliths were, therefore, impregnated with sulphur by a pore volume impregnation method. The monoliths were submerged in an ammonium sulphite solution; the pores of both the catalyst and the monolith substrate were, thus, filled with liquid. The amount of sulphur impregnated was determined by the amount of liquid that was taken up by the monolith and the sulphur concentration of the liquid. Excess water was removed with pressurized air. The monoliths were frozen (-30°C) and the water was removed by sublimation in a vacuum chamber. Freeze drying is believed to prevent formation of sulphur concentration gradients in the monoliths during drying and has also been used for catalyst preparation, giving a high dispersion of the metal on the catalyst support [31]. The amount of sulphur added could be controlled close to the targeted amount. The monoliths were used for the development of a kinetic model (Paper V). Dual-layer monoliths were prepared from incipient wetness impregnated Ag/Al_2O_3 to investigate different possibilities of combining Ag/Al_2O_3 with Fe-BEA. They were denoted as dual-layer-X/Y where X was the outer layer and Y the inner layer catalyst, Ag means Ag/Al_2O_3 and Fe means Fe-BEA. The ratio between the two catalysts was 1:1 on weight basis with the same total loading as the single catalyst bricks. Catalysts with Ag loading of both 6 and 4 wt% were prepared. 4 wt% Ag loading was prepared since that was believed to be a more optimal loading than 6 wt%. The 4 wt% Ag monoliths were used for activity testing in Paper II (Chapter 4.1.1 Small-scale laboratory testing: Ag/Al_2O_3 and Fe-BEA combinations). Unlike the previous test three coatings were needed to meet the targeted loading for Ag/Al_2O_3 monoliths (Ag-only) and two coatings of Ag/Al_2O_3 for the dual-layer bricks. The targeted slurry properties were met without addition of thickener for the 4 wt% Ag samples. This again shows that it was challenging to work with the present alumina and that the reproducibility is questionable. More details about the slurries and monoliths can be found in Appendix B.

The adhesion of the coat layer of the first catalyst series was somewhat poor and parts of the coat had fallen off in the catalyst container. If the coat falls off even when no extensive force is placed on the monolith even more might fall off from the vibrations and high gas flow behind an engine. A likely explanation for the poor coat adherence was believed to be the large particle size (d_{50} = 17 μm). However, the catalyst prepared by incipient wetness impregnation followed by particle size reduction in the paint shaker (to d_{50}=3.2 μm) did not show any significant improvement compared to the ones prepared by wetness impregnation and spray-drying.

A SEM study of the incipient wetness impregnated 6 wt% Ag samples was conducted to investigate the condition of the coat and adherence of it. Figure 14 shows SEM images of dual-layer-Fe/Ag and –Ag/Fe. The damages and mayor cracks seen in the pictures are believed to come from the preparation process of the samples for the SEM study. The faint vertical line for Ag/Al_2O_3 in Figure 14 e) might be the boundary between layers. No clear boundaries or separation from the multiple coatings layers could, however, be seen for any other sample. The coat thickness was larger for dual-layer-Ag/Fe compared to dual-layer-Fe/Ag as expected from the somewhat higher catalyst loading (165 and 150 g/l). The boundary between Ag/Al_2O_3 and Fe-BEA showed no tendency to separate which means that there was a good adherence between the two. There was a clear difference in density between the Ag/Al_2O_3 and Fe-BEA layers; the smaller particles of Fe-BEA allowed a much denser structure. Fe-BEA also showed a better interaction with the cordierite support compared to Ag/Al_2O_3. This is likely related to the smaller Fe-BEA particles being able to more freely enter the macro-pores of the cordierite

allowing better anchoring of the coat layer (Figure 14 c, e and f). The smaller cracks seen likely comes from shrinkage of the thick coat layers during drying, this was especially frequent in the corners where the layer was thickest. The difference in density between the Ag/Al_2O_3 and Fe-BEA layers mean that they might shrink to different extents; further adding stress to the coats, leading to crack formation (Figure 14 f).

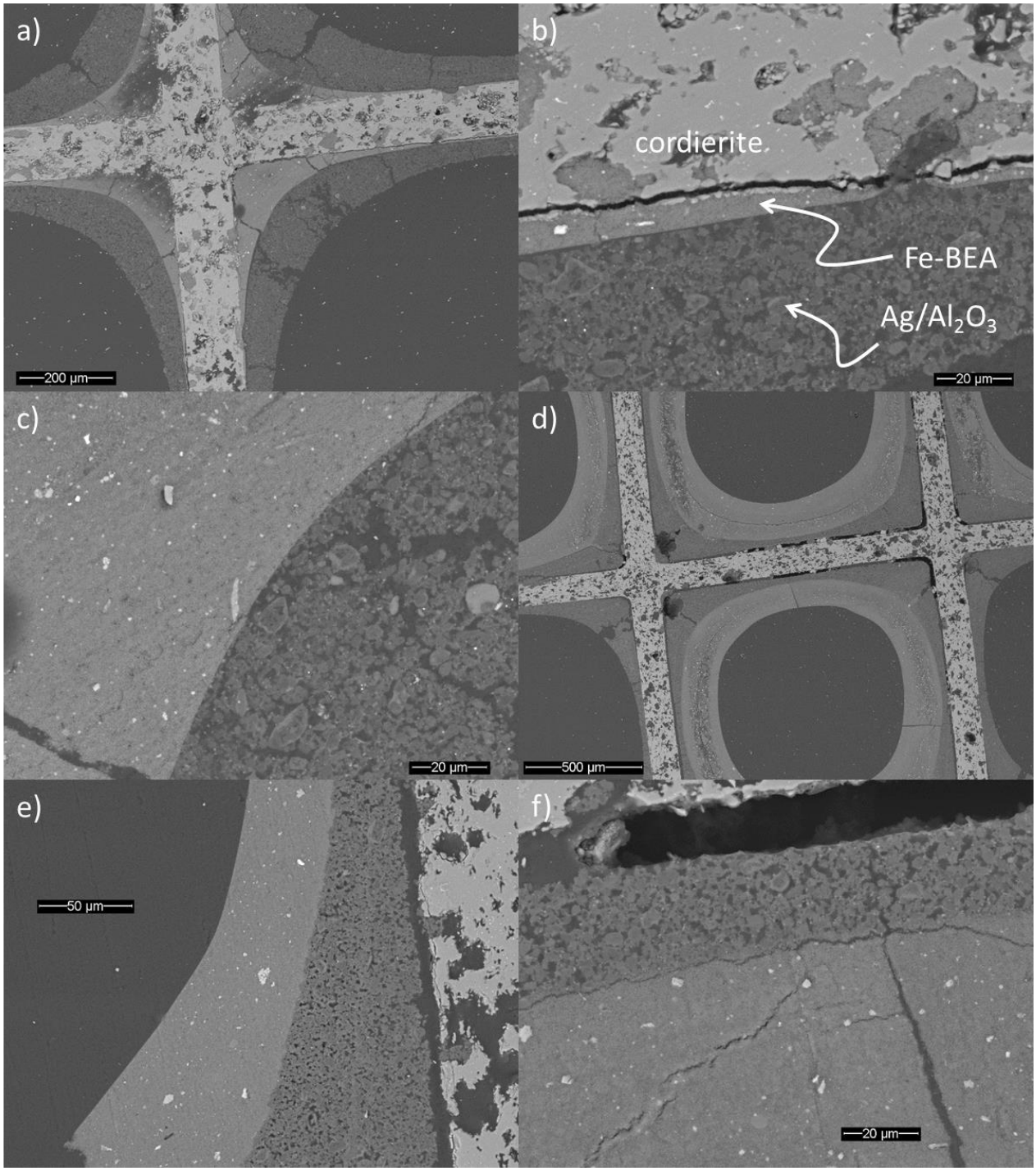

Figure 14 SEM images of 6 wt% Ag catalyst combined with Fe-BEA, a-c) dual-layer-Fe/Ag and d-f) dual-layer-Ag/Fe.

The conclusion from this test was that the alumina used was not optimal for washcoating. First the catalyst was somewhat difficult to work with since the large pore volume restricts the DM of the slurries and the reproducibility of results was low. This will make it challenging to scale up the procedure to full size samples. Second, the mechanical stability of the coat on the monoliths was believed to be a bit too low for engine tests with vibrations and periodical high flows. Different alumina was, therefore, used for later monolith preparation.

3.3.2 Siralox alumina

Catalyst development showed that the low-temperature performance of the catalyst could be improved by impregnation of small amounts of Si or Ti (1-2 wt%) [86]. T_{50} was improved by 10°C and sulphur tolerance was more or less similar compared to the previous best Ag/Al_2O_3. The same result was shown for commercial Si-alumina (Siralox 5/230, Sasol Germany, 3 wt% Si). Cordierite monoliths were washcoated with $Ag/Si\text{-}Al_2O_3$ to further investigate the performance of the doped catalyst. The monolithic catalysts were both prepared and tested at lab-scale (140 ml) and in full-scale engine tests (2 l) (Paper III and Chapter 4 Monolith testing).

The catalyst could not form completely homogenous slurry when mixed with water due to hard catalyst agglomerates. These agglomerates sedimented in a matter of a few minutes and stirring in a dissolver were not enough to break them apart. A few minutes (~3) in the paint shaker were enough to break the agglomerates and create more homogenous slurry. Table 2 shows the particle size reduction as an effect of shaking time. There was a large decrease in particle size after 9 min of shaking. The most dramatic decrease in particle size is believed to occur in the very first minutes (not measured). There was also a reasonable decrease between 9 and 12 min. More than 12 min only gave a small particle size decrease. There is a limit to how small the particles in the slurry can become which is dependent on the size and the hardness of the glass beads. An even longer time in the shaker will, therefore, not reduce the particle size any further. 12 min seems to be a reasonable time for further studies based on these results since it gives small enough particles and a reasonable particle distribution. The slurry should give good adhesive capabilities of the coat.

Table 2 Effect of time in paint shaker (2-3 mm glass beads) on particle size of the prepared washcoat slurry for $Ag/Si\text{-}Al_2O_3$.

Time (min)	$d_{0.1}$ (µm)	$d_{0.5}$ (µm)	$d_{0.9}$ (µm)
0	10.9	45.5	119
9	1.51	4.29	11.18
12	1.42	3.62	8.96
15	1.42	3.49	8.14
18	1.35	3.17	7.04

Different dispersion agents were tested to allow a higher DM in the slurry, thus simplifying the washcoating process. Compared to the previously used alumina the Si-alumina had a smaller pore volume and was easier to work with. A basic dispersion agent was preferred over an acidic since the thickener used (Kelzan) could not be used at a too low pH.

Four basic dispersion agents were tested; BYK-E-420, Darvan 821A, Dispex A40 and AMP-90. Darvan and Dispex gave fast sedimentation and BYK gave no visible effect on the slurry viscosity; neither was, therefore, considered any further. AMP-90 gave visibly thinner slurry. However, the results could not be repeated and the large effect seen in the beginning is believed

to be due to a pH rise by adding the AMP-90 which has a high pH of 13. Moreover, AMP-90 caused formation of foam in the slurry; addition of an anti-foam agent (Silfoam SE47) could not fully prevent this. AMP-90 was, therefore, discarded as a viable dispersion agent.

Instead, an acidic dispersion agent ($Al(NO_3)_3$) was tested. The agent lowered the viscosity significantly when pH was kept below ~4.5. The slurry actually became too thin to give a high catalyst loading. The viscosity could be altered by increasing the pH. However, the viscosity was too sensitive too small changes in pH for this to be a feasible method. This is also why a thickening agent was used previously since it stabilizes the slurry. As mentioned above, the thickening agent could not be used at the low pH as it was not completely dissolved. This was compensated by the higher possible DM. The higher possible DM comes both from the use of the dispersion agent and from the smaller volume of the catalyst.

The catalyst was added in three steps to try to maximise the DM without getting too thick slurry from very small particles. The main part was added in the first step and shaken for 6 min. A smaller portion (around 11% of the total catalyst amount) was then added and the slurry was shaken another 3 min before a third portion (around 7% of the total catalyst amount) of catalyst was added. This was followed by an additional 3 min in the shaker giving a total time of 12 min. By adding the catalyst in different steps and allowing different shaking times a wide size distribution, while at the same time maintaining a small particle size for the main part, can be obtained which should ensure good adhesive properties of the coat. The particle size was d_{10}=1.69, d_{50}=4.92 and d_{90}=13.3 μm which was similar to after 9 min of shaking in Table 2 but with a higher DM. The resulting slurry was thin enough to allow a good separation from the beads while still maintaining a DM of 37-39 wt% which was substantially higher than that of the previous catalyst tested (20-25 wt%). Table 3 shows the properties for three prepared slurries. A higher DM gives a higher viscosity but does not seem to affect the yield stress which only varied slightly between the samples. A viscosity above ~30-34 mPas was too thick and led to blocking of the monolith channels.

Table 3 Slurry properties for three slurries where the catalyst was added in three steps (after 0, 6 and 9 min of shaking). The total shaking time with glass beads in a paint shaker was 12 min.

	Slurry 1	Slurry 2	Slurry 3
pH	4.3	4.0	4.6
σ_0 (Pa)	0.785	0.878	1.14
μ (mPas)	34.6	27.3	27.1
DM (wt%)	39.0	37.4	37.3

Medium and large size monoliths were prepared and tested (Paper III and Chapter 4 Monolith testing). Even with the higher DM than in previous studies (37 compared to 20-25 wt%) it was not possible to get the desired loading (120-140 g/l) in one coating and the monoliths had to be coated twice. For the second coating the slurry had to be thinner. Some channel blocking could not be avoided for the full size monoliths due to the length (127 mm) of them. More details about the monoliths can be found in Appendix B.

The adhesion of the coat layers was much better than for previous samples. By simply visually examining the samples it could be seen the coat had a more “glossy” finish which is an indication

of a denser and thus more adhesive coat. This is attributed to the smaller volume and the particle size distribution of the catalyst.

3.4 Conclusions

Two different alumina were used as carriers for the Ag/Al_2O_3 based on the results from catalyst development; a Topsøe high surface area alumina and a commercial Si-alumina. A wetness impregnation method combined with spray drying was first used as an alternative to standard incipient wetness impregnation for the Topsøe alumina. The goal was to simplify the catalyst preparation when the process was scaled up from small-scale powder tests (a couple of grams) to full size monolith washcoating (several kilograms). However, catalyst activity tests indicated that some of the activity was lost compared to reference catalyst. This likely comes from a different Ag dispersion on the catalyst. The gain in time and simplicity was also lower than anticipated. Incipient wetness impregnation was, therefore, used for the further catalyst preparation.

The highest possible DM of slurries prepared from the Topsøe alumina was low since the alumina had a high pore volume. A low DM leads to low coat loadings and the washcoating process had to be repeated two to three times to meet the desired loading (120-140 g/l). One way to increase the loading for a given DM is to increase the yield stress of the slurry. This should be made without increasing the viscosity which may lead to channel blocking of the monoliths. A thickener agent was successfully used. The thickener also stabilised the slurry which was very sensitive to small changes in pH. However, it was difficult to work with the alumina due to the high pore volume ("fluffiness") and it was difficult to fully reproduce the results making it challenging to scale up the results to larger monolith bricks. The adherence of the coat layer, both seen as parts of the coat falling off and by a SEM study, was also considered a bit low.

The Si-alumina had a smaller pore volume and was easier to handle and a higher DM was possible. To improve the properties of the washcoat slurries a series of dispersion agents was tested of which $Al(NO_3)_3$ gave positive results. The thickener agent used previously could not be completely dissolved at the low pH of the acidic dispersion agent. Without addition of a thickener the slurry was too thin to get a high coat loading. Instead the DM was increased by adding catalyst in three steps during particle size reduction. Even though a higher DM was possible, two subsequent coatings were needed to meet the desired loading. It was difficult to prepare full size monoliths since there was a tendency for channel blocking at the end of the channels. The monoliths had a visible better adherence compared to the previous ones.

4 Monolith testing

The results presented in this chapter are from Papers II and III.

4.1 Materials and method

Catalytic monoliths in three different sizes were prepared and tested. The smallest size was 21x20 mm and they were tested in the "small-scale" laboratory test set-up with flows around 1.7 Nl/min. The monoliths became more challenging to prepare as they got bigger and the next size was 49x76 mm monoliths that were tested in the "medium-scale" laboratory test set-up at flows around 70 Nl/min. The last size was full-scale 2 l monoliths tested after a passenger car engine with flows around 132 Nm^3/h during stationary tests.

4.1.1 Small-scale laboratory testing: Ag/Al_2O_3 and Fe-BEA combinations

The tested small size (21x20 or 10 mm) cylindrical monoliths were prepared by washcoating cordierite, according to the process described in Chapter 3.3.1 Topsøe alumina. The catalyst activity was tested in a stainless-steel tubular flow reactor with a feed of 250 ppm NO, 275 ppm NH_3, 0, 250 or 600 ppm H_2, 12% O_2, 6% H_2O and balance N_2. The total gas flow was adjusted to give the desired GHSV (15000, 30000 or 60000 h^{-1}). The tests were performed as a ramp down of the temperature from 400 to 150°C; NO_x and ammonia concentrations were allowed to stabilize at each step. All outlet gases were monitored by FTIR. NO_x conversion was calculated according to Equation 5. More details can be found in Paper II.

4.1.2 Medium-scale laboratory testing

The tested medium size (49x76 mm) cylindrical monoliths were prepared by washcoating cordierite according to the process described in Chapter 3.3.2 Siralox alumina.

In a conventional test set-up an oven/furnace is used to heat the feed gases before entering the reactor. The whole reactor with feed lines can alternatively be placed inside the oven/furnace. This is a robust technique that is well proven. However, it suffers from slow heating and cooling rates when the dimensions of the system increase, mostly due to the large mass of the piping, the reactor and of the surrounding air that has to be heated. In a real vehicle exhaust system the only heat comes from the hot exhaust gas itself. A "new" test set-up was, therefore, designed with the intention of building a more compact unit with fast heating and cooling rates. The ultimate goal was to be able to perform transient runs to more closely mimic the operation of an engine during real-life driving.

Figure 15 shows a schematic picture of the set-up, all gases and liquid H_2O were controlled with mass flow controllers. All lines after the heater were made of steel. N_2 and air were first heated in a small gas heater before the desired feed gases was added to the hot stream. Steam was produced by passing liquid H_2O to a heated metal block were it rapidly evaporated. The distance between the heater and the reactor was not large enough to allow a sufficient mixing to get a homogenous gas feed and a metal mixer was added which proved satisfactory. However, the heating and cooling rates became significantly slower due to the relatively large mass of the mixer. During heating a large part of the energy was used to heat the mixer and once heated the mixer heated the cool gas when the system was meant to cool down. It was, thus, not possible to run the system transient. The mixer may be omitted if the distance between the heater and the reactor is increased and/or the dimensions of the tubes are smaller to give an increased

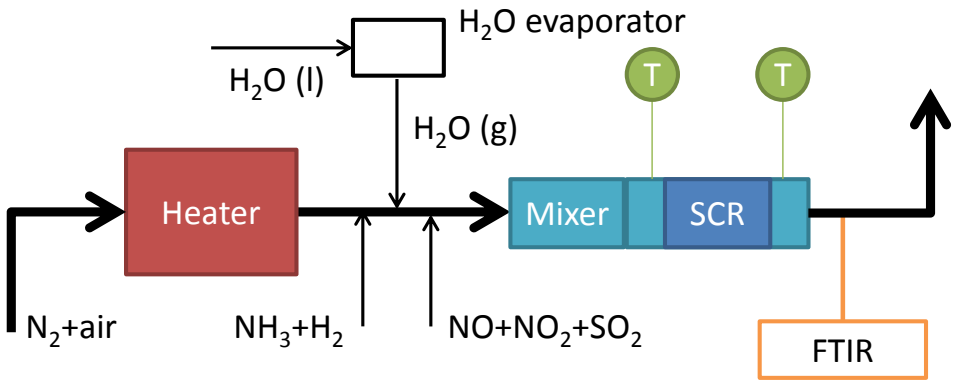

Figure 15 Schematic layout of laboratory set-up.

turbulence ($Re = vd/\mu$). Another issue with the test set-up was the too narrow temperature operating window of the heater. The heater could not provide sufficient power to reach the desired temperature of ~650°C without breaching the low flow limit. There are more robust gas heaters available on the market which is believed to be able to provide the desired power and operate with a larger temperature window. Nonetheless, the principal design of the test set-up proved satisfactory and by replacing the heater and re-building the lines slightly it is believed that close to transient testing is possible.

A standard feed of 500 ppm NO, 500 ppm NH_3, 1000 ppm H_2, 8% O_2, 12% H_2O and balance N_2 was used for activity testing. NO was mixed with air to allow oxidation to NO_2 in order to investigate the influence of NO_2 on the reaction. NO_2/NO_x ratios of 0.25, 0.5, 0.75 and 0.95 was tested and compared to the standard feed (NO_2/NO_x=0). Tests were also performed without adding H_2. The outlet gas was analysed by a FTIR after the catalyst. Inlet concentrations were taken from the given set-points (verified by empty reactor tests). The GHSV was 30000 or 33000 h^{-1} depending on the size of the tested catalyst brick. More details can be found in Paper III.

4.1.3 Engine-bench testing

The tested full size (140x130 mm) cylindrical monoliths were prepared by washcoating cordierite according to the process is described in Chapter 3.3.2 Siralox alumina. Four different layouts were tested; Ag/Al_2O_3 (Ag-only), Fe-BEA (Fe-only), Fe-BEA upstream of Ag/Al_2O_3 (dual-brick-Fe/Ag) and Ag/Al_2O_3 upstream of Fe-BEA (dual-brick-Ag/Fe). Figure 16 shows a schematic layout of the test set-up. The engine was a Euro 5 rated 2.0 l, 120 kW, five-cylinder direct-injected Volvo diesel engine equipped with EGR. Two catalyst bricks, either two of the same type (Ag- and Fe-only) or one of each type (dual-brick-Fe/Ag and dual-brick-Ag/Fe), with a total volume of 4 l were placed after the engine. Both stationary and transient tests were performed. The NO_x and NH_3 levels were allowed to reach steady-state during the stationary testing. For transient tests the New European driving cycle (NEDC) were used. NO_x (NO and NO_2), N_2O, NH_3 and H_2O was measured by FTIR and HC by Horiba MEXA. Conversions were calculated by switching the sample point between inlet and outlet of the catalyst bricks.

NH_3 was supplied from a gas bottle by a mass flow controller. H_2 was supplied by feeding NH_3 to a cracker were it was converted to H_2 and N_2; some unreacted NH_3 also remained in the stream (Figure 16). NH_3 flow to the cracker was controlled by a mass flow controller. The NH_3 and H_2 dosing system with NH_3 cracker was supplied by Amminex A/S Denmark. During stationary

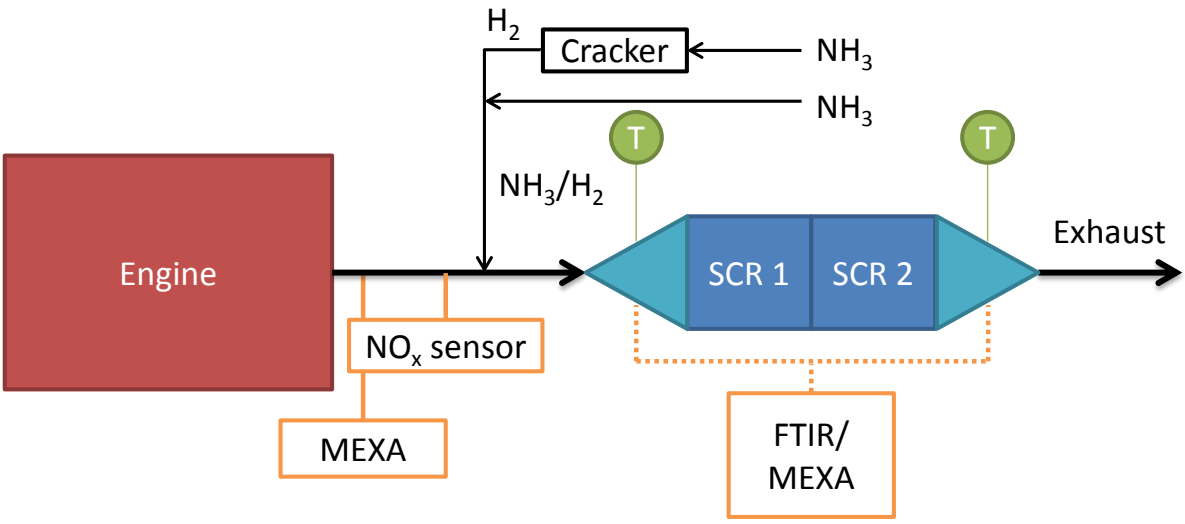

Figure 16 Schematic layout of engine bench test set-up.

tests the amount of reductant (NH_3 and H_2) dosed was controlled by online calculations from the actual NO_x concentrations (NO_x sensors) with fixed NH_3 (ANR) and H_2 (HNR) to NO_x ratios. During transient testing reductant dosing was either controlled by online calculations as in the case of stationary testing with dosing starting when the exhaust gas temperature was above 150°C or as pre-calculated values based on NO_x and flow inlet values from previous reference tests. Tests with dosing from 120°C were conducted to investigate if the total cycle NO_x conversion could be enhanced by earlier reductant dosing. ANR of 0.8 and HNR of 2 or 0 (no H_2 co-feeding) were used for all test. More details can be found in Paper III.

4.2 Results and discussion

4.2.1 Small-scale laboratory testing: Ag/Al_2O_3 and Fe-BEA combinations

Paper II investigated different combinations of Ag/Al_2O_3 and Fe-BEA. Fe-BEA is known to be highly active for NH_3-SCR above 250°C [87–90]. By combining Ag/Al_2O_3 and Fe-BEA a catalytic system with a high activity in a broad temperature window (200-500°C) could be obtained; without the need to dose H_2 necessary for the Ag/Al_2O_3 at higher temperatures [70]. The two catalysts were both combined in a sequential dual-brick layout and in a dual-layer layout. The dual-brick layouts are denoted dual-brick-Ag/Fe (Ag/Al_2O_3 brick upstream of a Fe-BEA brick) and dual-brick-Fe/Ag (Fe-BEA upstream of Ag/Al_2O_3). The dual-layer layouts were denoted dual-layer-Ag/Fe (Ag/Al_2O_3 on top of Fe-BEA) and dual-layer-Fe/Ag (Fe-BEA on top of Ag/Al_2O_3). They were compared to Ag/Al_2O_3 (Ag-only) and Fe-BEA (Fe-only) only bricks. Figure

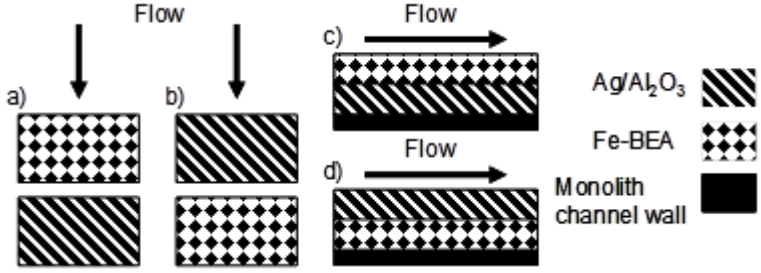

Figure 17 The different monolith layouts tested a) dual-brick-Fe/Ag, b) dual-brick-Ag/Fe, c) dual-layer-Fe/Ag and d) dual-layer-Ag/Fe.

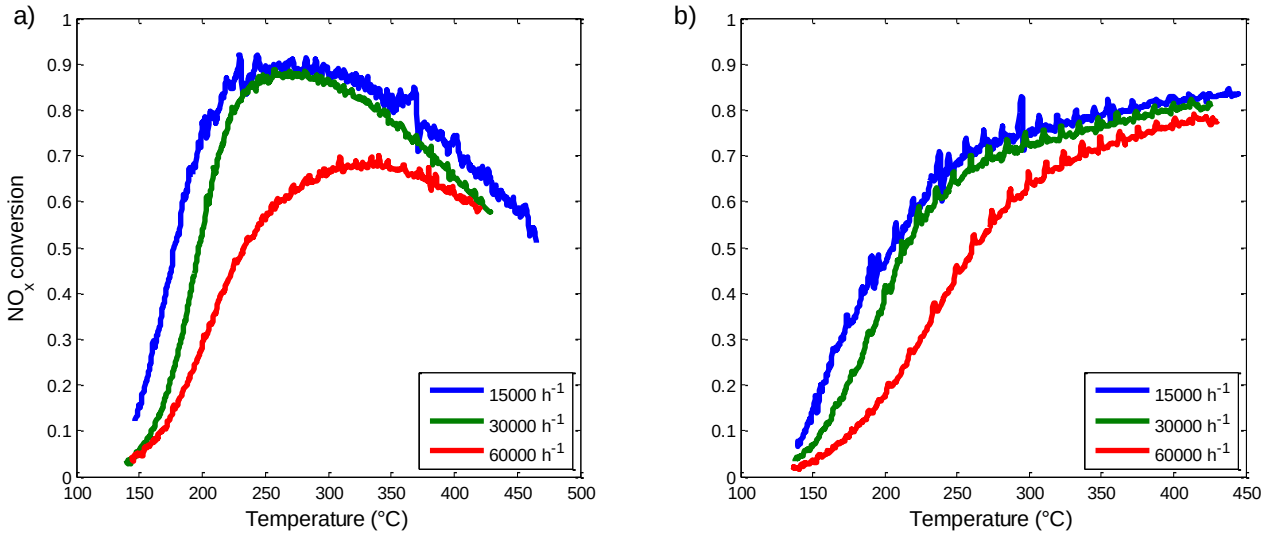

Figure 18 Dependency of GHSV on activity for a) Ag-only and b) Fe-only. Reaction conditions: 250 ppm NO, 275 ppm NH_3, 600 ppm H_2, 12% O_2, 6% H_2O and balance N_2, GHSV ~15000, 30000 or 60000 h^{-1}.

17 shows a schematic picture of the tested layouts. The GHSV was in all cases identical for the whole catalytic system.

Ag/Al_2O_3 has been reported to be sensitive when it comes to GHSV [8], [68], [69]. Viola [69] showed that a GHSV above 10000 h^{-1} negatively affected the activity over Ag/Al_2O_3 for HC-SCR in an engine bench test. Figure 18 shows the influence of GHSV on activity for a) Ag-only and b) Fe-only. The catalysts were tested at GHSV of 15000, 30000 and 60000 h^{-1}. Ag/Al_2O_3 was, as seen, more sensitive to GHSV than Fe-BEA. Fe-BEA showed a slightly lower NO_x conversion when the GHSV was increased from 15000 to 30000 h^{-1} while Ag/Al_2O_3 showed a larger decrease at temperatures below approximately 220°C. Both catalysts showed a lower NO_x conversion at a GHSV of 60000 h^{-1}, here the difference was even more pronounced between the two. It was, therefore, decided to use the lowest GHSV of 15000 h^{-1} in this study.

Figure 19 a) shows a comparison of the activity for the tested layouts. It was clear that it was preferred to have Ag/Al_2O_3 in the upstream or outer layer position compared to Fe-BEA and the NO_x conversion was close to that of Ag-only. Dual-brick-Fe/Ag and dual-layer-Fe/Ag, on the other hand, showed a performance close to that of Fe-BEA. The poorer performance of dual-brick-Fe/Ag and dual-layer-Fe/Ag was attributed to unselective NH_3 conversion over the Fe-BEA leading to a deficit of NH_3 for the downstream/bottom-layer Ag/Al_2O_3, Figure 19 b). H_2 oxidation might also be contributing, it was, however, not possible to measure this with the equipment available.

Figure 20 shows the influence of H_2 concentration on the performance of the Ag/Al_2O_3 upstream/outer layer layouts, Ag-only and Fe-only was included for comparison. Ag-only lost a lot of its activity when the H_2 concentration was lowered and it was completely inactive without H_2 present. However, the combined layouts retained their activity above 200°C when H_2 was lowered from 600 to 250 ppm. Dual-layer-Ag/Fe even retained most of its activity from 300°C and up without any H_2 present and it out-performed Fe-only. This is remarkable since the Ag/Al_2O_3 was shown to be inactive without H_2 and that only half the amount of Fe-BEA was

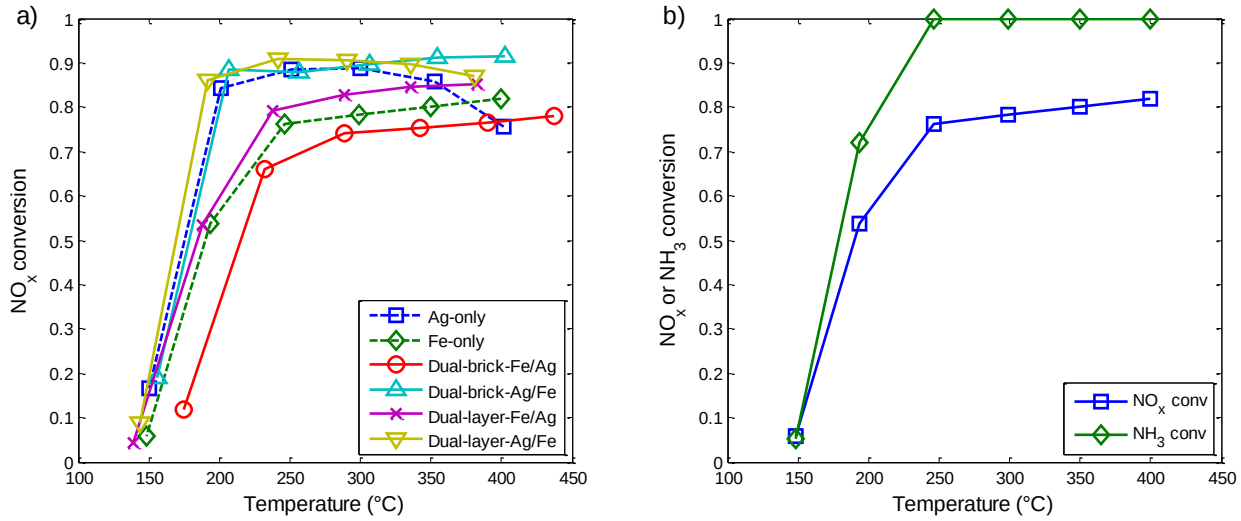

Figure 19 a) comparison steady-state NO_x conversion as function of temperature for dual-brick-Ag/Fe, dual-brick-Fe/Ag, dual-layer-Ag/Fe, dual-layer-Fe/Ag, Ag-only and Fe-only (600 ppm H_2); b) steady-state NO_x and NH_3 conversion as function of temperature for Fe-only. Reaction conditions: 250 ppm NO, 275 ppm NH_3, 600 ppm H_2, 12% O_2, 6% H_2O and balance N_2, GHSV ~15000 h^{-1}.

present compared to Fe-only. The latter might be explained by the fact that the Fe-BEA layer was very dense, as seen in Figure 14, which might give diffusion limitations through the layer which could mean that it was only the top part of the layer that was utilized for SCR-reaction.

Metkar et al. [18] proposed that it was beneficial to have a thinner layer Fe-BEA in a dual-layer layout compared to a thicker layer in a shorter brick. Diffusion limitations due to the Fe-BEA layer being too dense might also inhibit the reaction over Ag/Al_2O_3 in dual-layer-Fe/Ag reducing the positive effects of combining the two. A simple way of investigating this is to prepare monolithic catalyst with different Fe-BEA loading (coat thickness) and investigate the effect of GHSV. If an increase in GHSV can be compensated by a thicker coat this indicates that there are no diffusion limitations. On the other hand, if the activity only is dependent on GHSV regardless of coat thickness there might be diffusions limitations. The temperature has to be chosen so that the overall reaction is in the kinetically controlled regime (lower temperature) to be able to

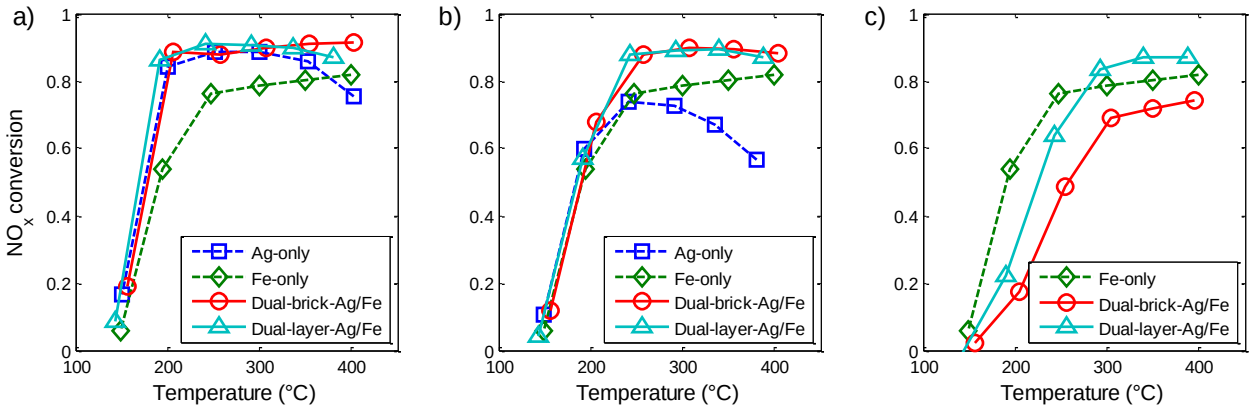

Figure 20 Steady-state NO_x conversion as function of temperature for dual-brick-Ag/Fe, dual-layer-Ag/Fe, Ag-only and Fe-only with a) 600 ppm H_2, b) 250 ppm H_2 and c) 0 ppm H_2. Reaction conditions: 250 ppm NO, 275 ppm NH_3, 0, 250 or 600 ppm H_2, 12% O_2, 6% H_2O and balance N_2, GHSV ~15000 h^{-1}.

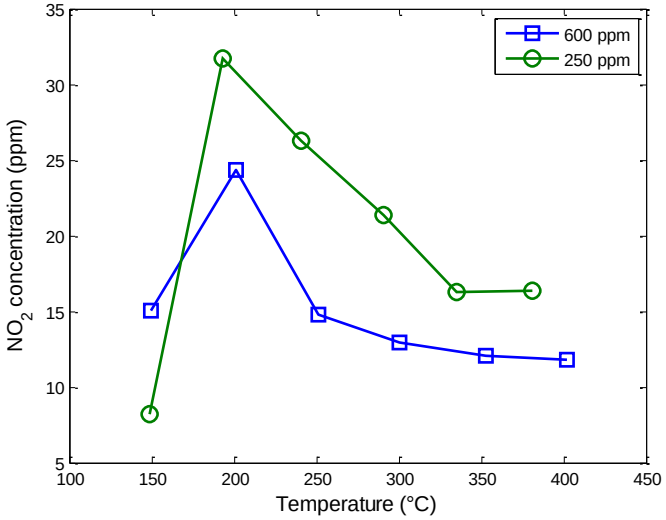

Figure 21 Steady-state NO_2 formation over Ag-only with different H_2 concentrations. Reaction conditions: 250 ppm NO, 275 ppm NH_3, 600 or 250 ppm H_2, 12% O_2, 6% H_2O and balance N_2, GHSV ~15000 h^{-1}.

evaluate any effect of the coat layer being too dense. This was, however, beyond the scope of this study.

It is well known in literature that H_2 enhances the NO to NO_2 oxidation over Ag/Al_2O_3 [38], [50], [56]. NO_2 formation was also seen for the fresh catalysts in the previous powder tests (Paper I). Prolonged exposure to sulphur reduced the NO to NO_2 oxidation. Figure 21 shows NO_2 out from Ag-only when 600 or 250 ppm H_2 was used; without H_2, NO_2 was only seen at 400°C (8 ppm). The NO_2 formed over Ag/Al_2O_3 was believed to react over Fe-BEA according to the so called "fast-SCR" reaction [18], [91] when the latter was placed downstream. The fast-SCR reaction over Fe-BEA makes it more active than Ag/Al_2O_3. The formation of NO_2 and fast-SCR was believed to be one of the reasons why it was beneficial to have Ag/Al_2O_3 upstream/as outer layer of Fe-BEA. However, since H_2 was a prerequisite for excessive NO to NO_2 oxidation over Ag/Al_2O_3 this could not fully explain the results seen for dual-layer-Ag/Fe in Figure 20 c). Here it was speculated that the short diffusion distance between the two catalyst layers was the key and that some reaction intermediate, which could still be NO_2, migrates between the layers. The tests conducted in this study did not give any conclusive answers to the observed synergistic effect of the dual-layer layout. To investigate this more advanced ways of measuring is needed compared to just measuring before and after the monolith bricks as in this study. It might be possible to identify potential reaction intermediates by e.g. measuring inside the monolith channel.

4.2.2 Stationary engine-bench testing

Paper III investigated the performance of Ag/Al_2O_3, Fe-BEA and a dual-brick combination of the two in an engine-bench. A core sample of the tested Ag/Al_2O_3 and a fresh Ag/Al_2O_3 sample were tested in a laboratory test set-up to further evaluate the results from the engine tests.

Figure 22 shows the steady state NO_x conversion for the tested layouts (Ag-only, Fe-only, dual-brick-Fe/Ag and dual-brick-Ag/Fe) as function of temperature in the engine-bench. Ag-only showed an unexpectedly low NO_x conversion in the whole temperature range and Fe-only a

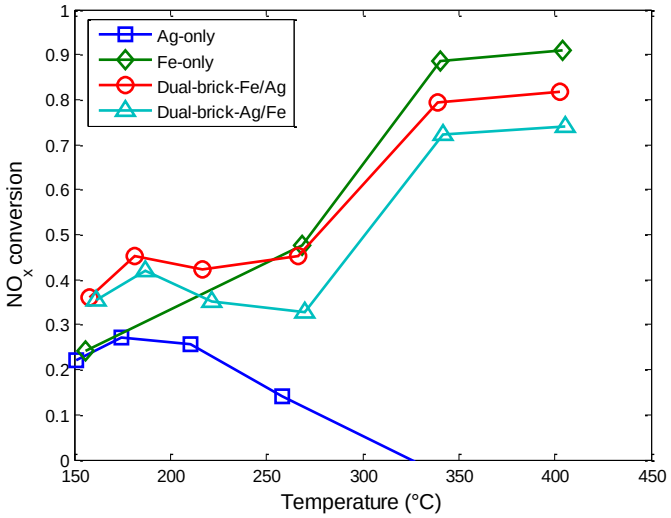

Figure 22 Engine bench stationary steady-state NO_x conversions as function of temperature for the different catalyst layouts. The layouts including Ag/Al_2O_3 are tested with NH_3 and H_2 dosing and Fe-only with only NH_3 dosing.

higher than expected NO_x conversion at 150°C and a 90% NO_x conversion at 340 and 400°C. The combined catalyst systems (dual-brick-Fe/Ag and dual-brick-Ag/Fe) showed an activity profile that was a combination of that of Ag/Al_2O_3 and Fe-BEA with a local maximum at 180°C corresponding to that over Ag/Al_2O_3 and a sharp increase in activity above 270°C related to Fe-BEA. The performance of the combined systems was better than that of the individual catalysts at the lowest temperatures. Above 270°C Fe-only was preferred over the combined systems. It was also preferred to have Fe-BEA as the upstream catalyst (dual-brick-Fe/Ag) compared to having Ag/Al_2O_3 upstream. This contradicts the previous results (Figure 19), where there was a clear advantage of having Ag/Al_2O_3 upstream.

No unselective NH_3 oxidation was seen in the engine tests in contrast to the small-scale

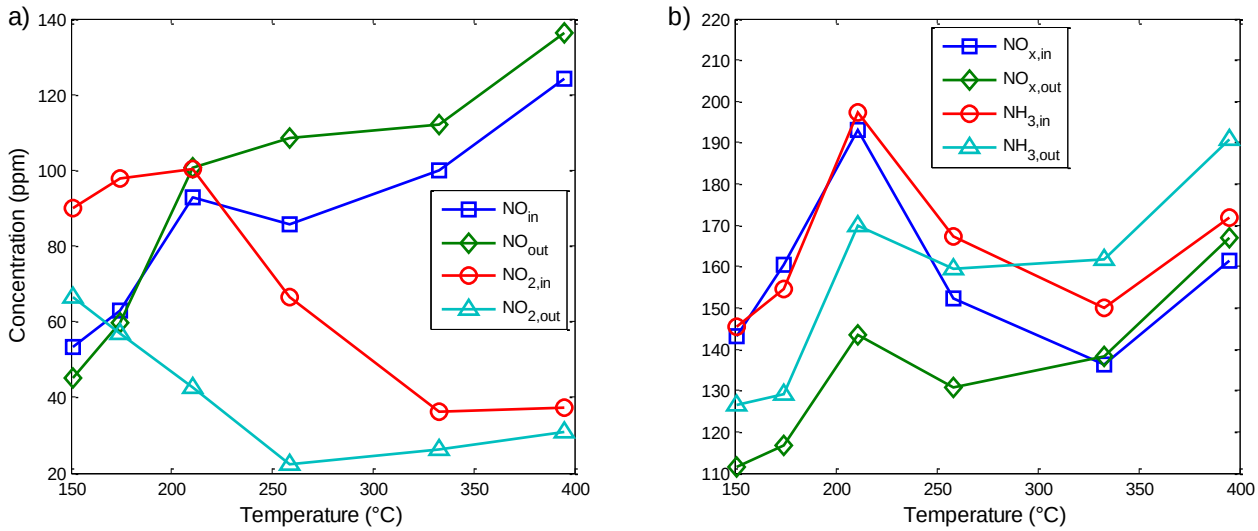

Figure 23 Engine bench stationary steady-state concentrations as function of temperature for Ag-only with NH_3 and H_2 dosing.

laboratory tests. Figure 23 shows the NO, NO_2, NO_x and NH_3 concentrations for Ag-only. The high NO_2/NO_x levels was believed to give fast-SCR over the Fe-BEA [18], [91], which would further explain why Fe-BEA was preferred in an upstream position; having Ag/Al_2O_3 as the upstream catalyst will lower the NO_2 levels, thus reducing the system deNO_x activity. Typically it is expected that some 10% of the total NO_x is NO_2. Here, the levels were up to 60% at the lowest temperatures and 18-20% at 400°C. The high NO_2 concentrations seen were attributed to the high EGR rates (20-60%) [11], [92–94]. NO was produced over Ag-only from 220°C and up from NO_2 to NO reduction and there seems to be a connection between NO_2 concentration and NO_x conversion.

The NH_3 to H_2 cracker was used as a way of providing on-board H_2 to eliminate the need of an extra storage tank for the H_2. The NH_3 could either come from urea decomposition prior to the cracker or from NH_3 stored in a metal ammine salt [95]. The maximum cracking capacity of the system limited the amount of NH_3 and H_2 that could be dosed which affected the maximum possible NO_x conversion negatively. It was mainly H_2 that was limited and the amount dosed was estimated to be 1-1.6 times the NO_x, compared to the set-point of 2. The lower than expected H_2 dosing would have affected the performance of the catalyst negatively; especially in the 200-300°C range (Paper V). The overdosing of NH_3 seen (Figure 23 b) came from the NO_x sensors, used for controlling the amount NH_3 and H_2 dosed, measuring a NO_x level that was slightly higher than the one measured by FTIR and MEXA systems. This could be accounted for by the dosing algorithm in future tests. In-situ NH_3 formation over the Ag/Al_2O_3 could also contribute to the higher than expected NH_3 concentration seen in Figure 23 b.

In-situ NH_3 formation was observed in a preliminary test and it was concluded that it was formed over the Ag/Al_2O_3. NH_3 formation over Ag/Al_2O_3 has been reported in literature [9], [40], [58], [96], [97]. The NH_3 formation in these studies was attributed to the reaction of NO with H_2 [58], [96], hydrolysis of N-containing hydrocarbons (without H_2) [40] or reaction of HC and NO_x [97]. Figure 24 shows the NH_3 out of the catalyst together with the HC concentration. When the

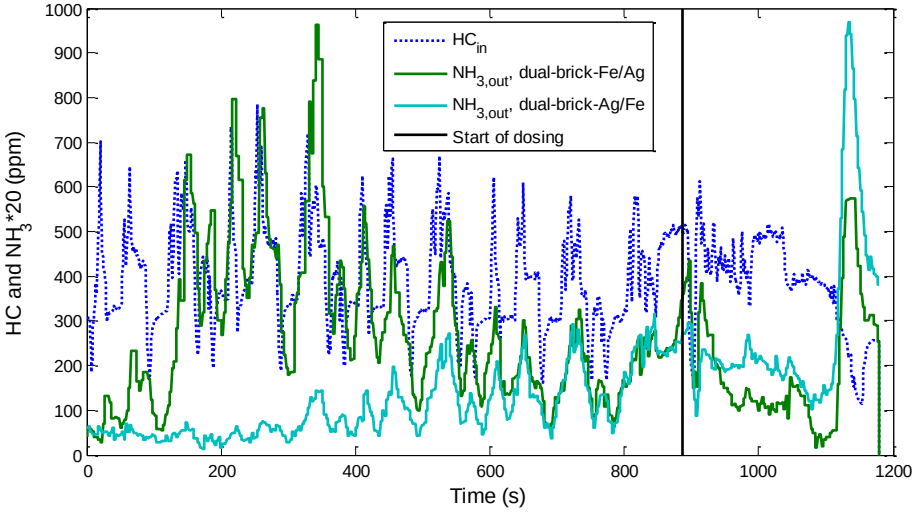

Figure 24 NH_3 concentration out of the catalysts compared to HC out from the engine (in to the catalysts) during NEDC for dual-brick-Ag/Fe and dual-brick-Fe/Ag. Black vertical line represents start of NH_3 and H_2 dosing.

Fe-BEA was placed downstream of the Ag/Al_2O_3 less NH_3 was initially seen which is related to NH_3 storage over the Fe-BEA. When the temperature was increased in the end of the test cycle a larger NH_3 desorption could be seen. No conclusive NH_3 formation was seen in the test presented here. The difference between the preliminary tests and the test presented here, is likely related to different HC levels in the exhaust (the HC level was up to 2-2.5 times higher in the preliminary test) [97].

An interesting question when testing Ag/Al_2O_3 in a real engine exhaust is if the unburned HC present in the exhaust can enhance the activity via HC-SCR. Sitshebo et al. [67] reported a noticeable NO_x conversion from the HC present in the exhaust; especially if H_2 was present. The HC conversion was low in the tests reported here for Ag-only and given the low NO_x conversion it is difficult to evaluate whether HC-SCR contributed to the overall NO_x conversion or not. The HC conversion was higher in a preliminary test which also showed a higher NO_x conversion, this might indicate that HC-SCR plays a role in the total NO_x conversion. The preliminary test had HC concentrations that were 2-2.5 times higher than in the present tests. The amount reacted NH_3 to amount reacted NO_x was low in the test presented here which indicates that something besides NH_3-SCR was responsible for the NO_x conversion. Contribution from HC-SCR can thus neither be concluded nor excluded.

Three possible explanations for the low activity over Ag/Al_2O_3 were proposed.

- A H_2 deficit of over the Ag/Al_2O_3, only allowing NO_x reduction via NO_2.
- The catalyst was deactivated, not allowing the expected H_2-assisted NH_3 SCR to commence.
- NO_2 inhibits the activity when NO_2 is present in larger concentrations even when H_2 is present. This could be indirect due to NO_2 poisoning of NO active sites [39].

Figure 25 shows the results from laboratory testing of a core sample from the Ag/Al_2O_3 brick used in the engine tests. The catalyst was completely deactivated. In the figures it is seen the activity was regained in a second test directly after the first. The activity was not further enhanced by in-situ treatment at 500°C and treatment at 500°C in a furnace in an atmosphere of air. Possible reasons for the deactivation are oxidation of the Ag and poisoning from soot. Oxidised Ag can be reduced at temperatures below 450°C by H_2, i.e. during the first standard deNO_x test [39], [50]. Soot can be oxidised by NO_2 in the temperature range of 250-400°C [10] and NO_2 from H_2 induced NO oxidation could explain the reactivation seen in Figure 25. Soot oxidation by NO_2 might also explain the increase in NO out during engine testing. Soot poisoning or Ag oxidation were believed to be the reasons for the deactivation seen.

Several reports have replaced NO with NO_2, either partly or completely, for HC-SCR with varying results. Replacing the NO by NO_2 has been reported to enhance or to not affect the activity and make bare Al_2O_3 active [24], [59] or to reduce the activity [39], [50], [56]. A difference between the cited reports are the HC species used, the reports showing a positive effect [24], [59] both used propene while those showing no or negative effect ([39], [50], [56]) used saturated alkanes (propane or decane), which might affect the results. The HC present in the exhaust is a close match to the composition of the diesel fuel with mainly longer straight HC species. Richter et al.

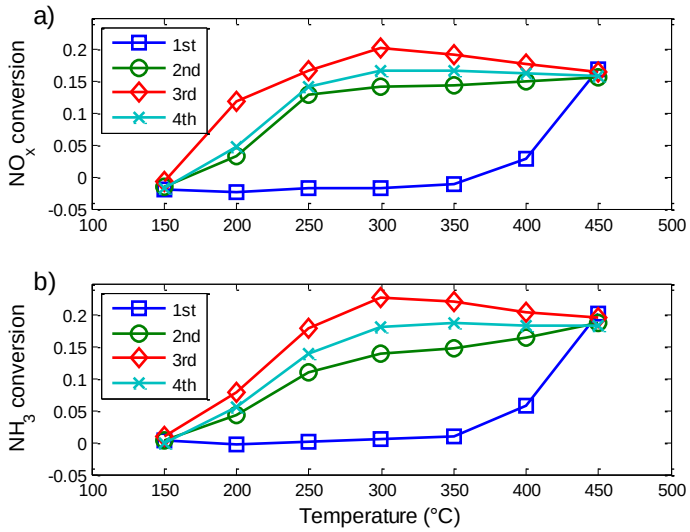

Figure 25 a) NO_x and b) NH_3 conversion as function of temperature for core sample from engine tested Ag/Al_2O_3. 1st test and 2nd test were before and 3rd test and 4th test were after regeneration (in-situ at 500°C and in oven at 550°C). Reaction conditions: 500 ppm NO, 500 ppm NH_3, 1000 ppm H_2, 8% O_2, 12% H_2O and balance N_2, GHSV ~33000 h^{-1}.

[39] attributed the negative NO_2 effect to NO_2 poisoning the catalyst. Literature suggests that H_2 enhanced the NO_x reduction also when NO_2 was used instead of NO [39], [50], [56].

Figure 26 shows the influence of NO_2/NO_x ratio for a 4 wt% Ag/Al_2O_3 sample tested in the laboratory set-up (without any HC present). The activity was enhanced after the NO_2/NO_x testing campaign compared to before during a standard test (without NO_2) and it is in good agreement with the results from the small-scale test with the same GHSV (Figure 18). Paper I and IV (Chapter 2 Catalyst development) showed that the catalyst was activated by testing with sulphur present in the gas, which was attributed to increased NH_3 adsorption capacity and a decreased unselective NH_3 oxidation. Since no sulphur was present in Figure 26 another mechanism had to be responsible for the catalyst activation. Possible reasons might be a change in the dispersion or state of Ag. Such changes during the SCR have been reported in literature [47], [50], [51].

Addition of NO_2 had no significant impact on NO_x conversion for the catalyst at medium temperatures (250-300°C) when H_2 was co-fed as seen in Figure 26. However, the activity was increased at both lower and higher temperatures. The activity increase was most enhanced at the lowest and highest temperatures. Since 0.5 NO_2/NO_x was the first test (after the standard test) the lower activity seen are believed to be related to the sample not being fully activated. The catalyst did not show any activity for a pure NO feed when no H_2 was present. Addition of NO_2 gave a low activity which was largely independent on the NO_2 level. A difference was only seen for the highest concentrations at the lowest temperatures. It is not unreasonable to have 25% NO_2 a in the exhaust; either from the engine as in this study or after a DOC [12]. The negative effect of NO_2 reported in literature for HC-SCR ([39], [50], [56]) seems to be related to the HC-SCR reaction itself and is not believed to be relevant for NH_3-SCR even in the presence of HC in the engine exhaust.

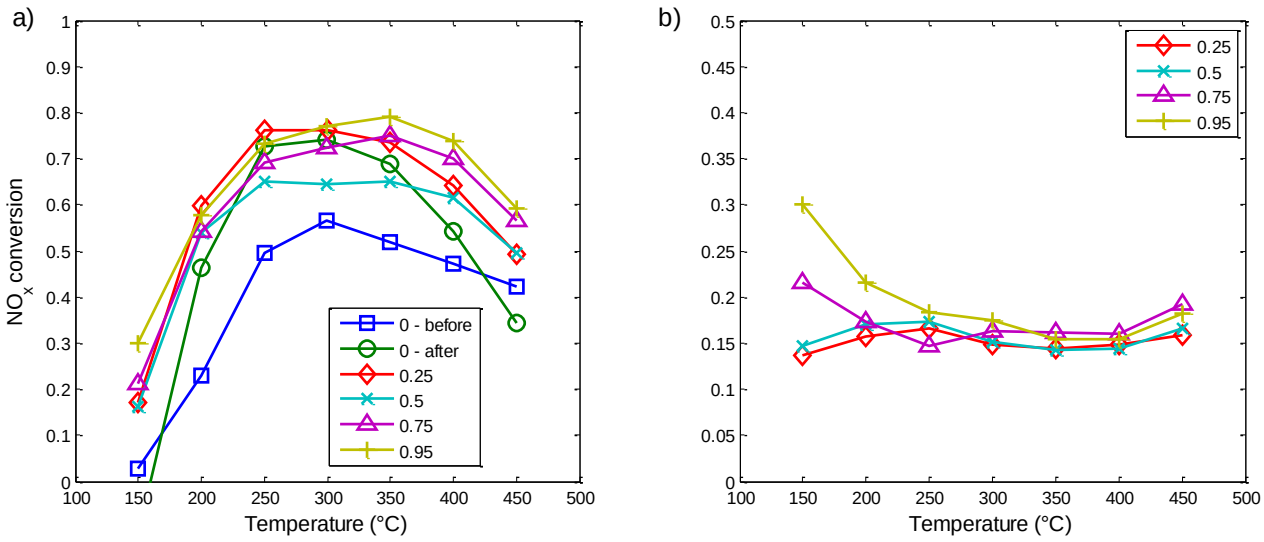

Figure 26 NO_x conversion as function of temperature for different NO_2/NO_x ratios (indicated in legend); a) with H_2 and b) without H_2. Reaction conditions: 500 ppm NO, 500 ppm NH_3, 0 or 1000 ppm H_2, 8% O_2, 12% H_2O and balance N_2, GHSV ~30000 h^{-1}.

To discuss and understand the effect of NO_2, the view of the SCR mechanism has to be roughly outlined. The perception for this work is that NO is activated over Ag sites to ad-NO_x species that is reduced to N_2 with NH_3 at sites on the alumina. NO_2 can directly form these ad-NO_x species which could explain why deNO_x activity was seen over bare alumina in Paper VI, which is also reported in literature [24], [59]. Without H_2 the NO is too strongly bound as ad-NO_x to the Ag sites poisoning them [49], [57] and no deNO_x activity can be seen. Too much NO_2 will poison the sites on the alumina responsible for ad-NO_x to N_2 reduction [39] and H_2 are able to reduce this effect which explains the limit for deNO_x when no H_2 was present (Paper VI and Figure 26 b). In Paper V a global SCR reaction stoichiometry was found to be 1:1:2 for NO:NH_3:H_2, one of the H_2 molecules is believed to be related to removal of the strongly bound ad-NO_x to Ag sites while the other on is related to inhibition of the NO_2 poisoning effect. One difference seen between the two tests without NO_2 in Figure 26 was that the more active sample showed up to ten times more NO_2 at the outlet, which again points to NO oxidation being a key parameter for the mechanism. This enhanced oxidation might also be the effect of the activation seen. The enhancing effect of NO_2 seen in this study can thus be explained as follows.

- At temperatures below 250°C the activation of NO is the rate determining step and the presence of NO_2 is able to react directly over the alumina increasing the total conversion.
- At medium temperatures activation of NO is no longer the rate determining step and NO_2 does not affect the global conversion.
- Above 300°C a high unselective H_2 oxidation [39](Paper V) gives a deficit of H_2 available for removal of the NO ad-NO_x species from Ag sites [49], [57] which is compensated by the presence of NO_2.

Based on the results in Figure 26, a complete lack of H_2 over the catalyst does not seem to be the cause for the low NO_x conversion seen for Ag-only in the engine testing (Figure 22). If no H_2 was present the NO_x conversion below 250°C should have been lower and it should have been higher

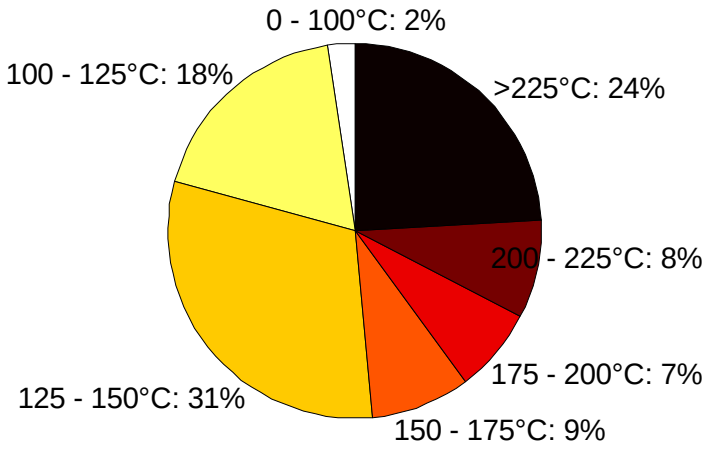

Figure 27 NO_x temperature distribution on mole basis measured directly before the catalysts for transient NEDC.

at higher temperatures given the NO_2/NO_x ratios in the engine tests. The tested core sample also had a lower catalyst loading than expected (60% of the expected), indicating a non-uniform loading which will affect the activity negatively by giving a higher relative GHSV for the catalyst (Figure 18). It is concluded that the lower than expected deNO_x activity seen for Ag/Al_2O_3, both in Ag-only and the combined systems, comes from catalyst deactivation related to soot or Ag oxidation, the lower than intended H_2 and low specific catalyst coat loading.

4.2.3 Transient engine-bench testing

Paper III also investigated the performance of the Ag/Al_2O_3 and Fe-BEA during transient testing. Figure 27 shows the NO_x distribution over different temperature intervals for the NEDC. The conditions were, as seen, very demanding for SCR with more than 50% of the total emitted NO_x being emitted below 150°C and only 32% above 200°C. A further implication of the low temperature was NH_3 and H_2 dosing. In the standard case NH_3 and H_2 was dosed when the temperature was above 150°C. The temperature was stable above 150°C after around 830 s. In another case, dosing started when the temperature was above 120°C (after 250 s) to investigate the potential benefit of earlier NH_3 and H_2 dosing. Urea dosing is normally started at 180-200°C which would severely limit the possibility for SCR during the NEDC. To be able to dose NH_3 at lower temperatures can, therefore, be a key to meeting the strict legislation targets.

Figure 28 shows the accumulated NO_x over the NEDC used for transient tests. The total NO_x conversion over the cycle were 22, 15, 18 and 22% for Ag-only, Fe-only, dual-brick-Fe and dual-brick-Ag, respectively, the conversion was adjusted for differences in inlet amount. Figure 29 show the total NO_x conversion as function of time during the NEDC. The large increase in NO_x out (Figure 28) and drop in NO_x conversion (Figure 29) seen after approximately 1100 s coincides with the highest temperature. Unfortunately, that also meant that the GHSV increased from maximum 30000 h^{-1} during urban driving to 70000 h^{-1}, which will affect Ag/Al_2O_3 negatively (Figure 18). The high flow also gave a NH_3 and H_2 deficit due to the maximum NH_3 cracking limit of the dosing system, further limiting possible NO_x conversion. The low maximum NO_x conversion over Ag/Al_2O_3 seen in the stationary tests obviously also limited the deNO_x

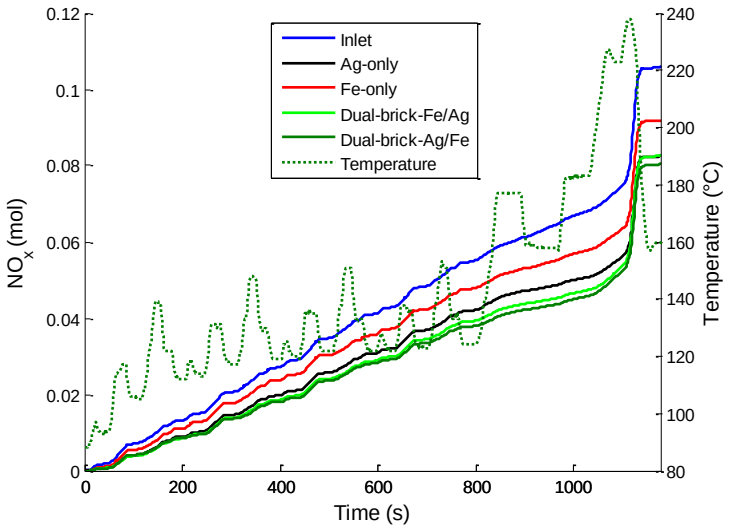

Figure 28 Accumulated NO_x during NEDC for Ag-only, Fe-only, dual-brick-Fe/Ag and dual-brick-Ag/Fe compared to inlet NO_x, NH_3 and H_2 dosing (only NH_3 for Fe-only).

performance of the catalyst system. The advantage of having Ag/Al_2O_3 upstream of Fe-BEA could be related to HC-SCR over the former and that HC oxidation over Fe-BEA inhibits the deNO_x reaction if Ag/Al_2O_3 is placed downstream. Another possible reason could be NH_3 adsorption over Fe-BEA since the Fe-only layout showed very little NH_3 out during the NEDC. This would give a NH_3 deficit over the downstream Ag/Al_2O_3.

The NEDC was roughly divided into three parts based on the performance of the catalysts. During the first part which was the first 250 s of the cycle the performance was dual-brick-Ag/Fe ≈ dual-brick-Fe/Ag > Ag-only >> Fe-only. The second part was 250-1000 s and the performance was dual-brick-Ag/Fe > dual-brick-Fe/Ag > Ag-only > Fe-only. During the last part

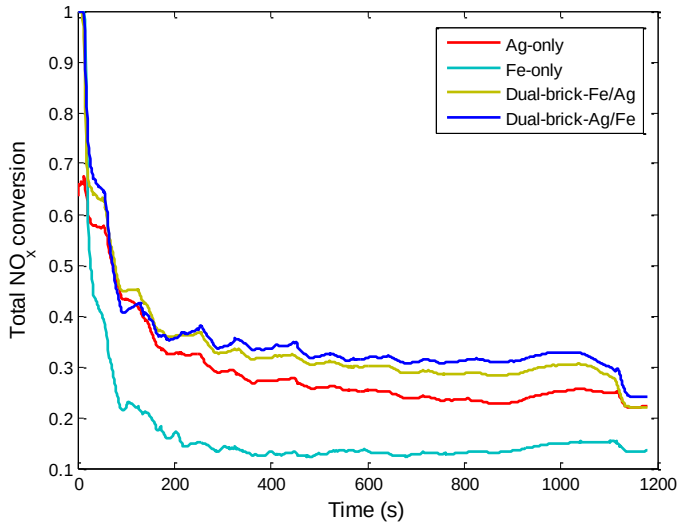

Figure 29 Total NO_x conversions as function of time during NEDC for Ag-only, Fe-only, dual-brick-Fe/Ag and dual-brick-Ag/Fe, NH_3 and H_2 dosing, (only NH_3 for Fe-only).

(>1000 s) Ag-only did instead show the best deNO_x performance and the performance order was Ag-only > Fe-only ≈ dual-brick-Ag/Fe ≈ dual-brick-Fe/Ag. The main advantage of Ag-only was seen at the highest temperatures (220-240°C), see Figure 29.

NH_3 and H_2 dosing started after 830 s which led to the conclusion that SCR could not account for the activity seen during the first parts of the cycle. Instead it is believed that NO_x storage is responsible for the NO_x conversion seen at low temperatures. Tsukamoto et al. [98] showed that NO_x storage could be enhanced by addition of TiO_2 to the catalysts and they attributed this to the formation of more storage sites due to a better Ag dispersion. It is believed that the SiO_2 content in the catalyst used in this study will improve NO_x storage in the same way as TiO_2 since SiO_2 doping done in conjunction to this work showed similar improvements as TiO_2 with respect to activity [86]. NO-TPD during dry conditions showed a relatively large NO_x storage capacity of the Ag/Al_2O_3, however, the presence of H_2O will lower the capacity. Brosius et al. [57] has shown that the NO_x adsorption capacity was dramatically enhanced by replacing NO with NO_2 in the presence of H_2O. NO_x storage, therefore, seems to be the best explanation for the NO_x conversion seen at the low temperature when no NH_3 or H_2 was dosed. Figure 30 shows no excessive NO_x desorption during the cycle. The expected NO_x desorption when the temperature increased in the later part of the cycle was believed to be compensated by increased SCR activity. The difference between the Ag/Al_2O_3 containing catalysts and Fe-only was clear. The former showed NO_x conversion directly from the start of the cycle while the latter showed a NO_x out that was closer to the NO_x in.

No overall effect on NO_x conversion was seen by dosing NH_3 and H_2 from 120°C compared to the standard temperature of 150°C. A closer inspection of total NO_x conversion as function of time (Figure 31) showed that the decline in NO_x conversion was more rapid up to approximately 400 s of the cycle when dosing started at 120°C (after 250 s) compared to at 150°C (after 830 s). The NO_x conversion then increased for the 120°C dosing case while it remained almost constant for the 150°C dosing case and in the end they showed the same conversion. This is explained as follows: Up to 400 s NH_3 inhibits NO_x storage and possibly fast-SCR [99]. When the catalyst has

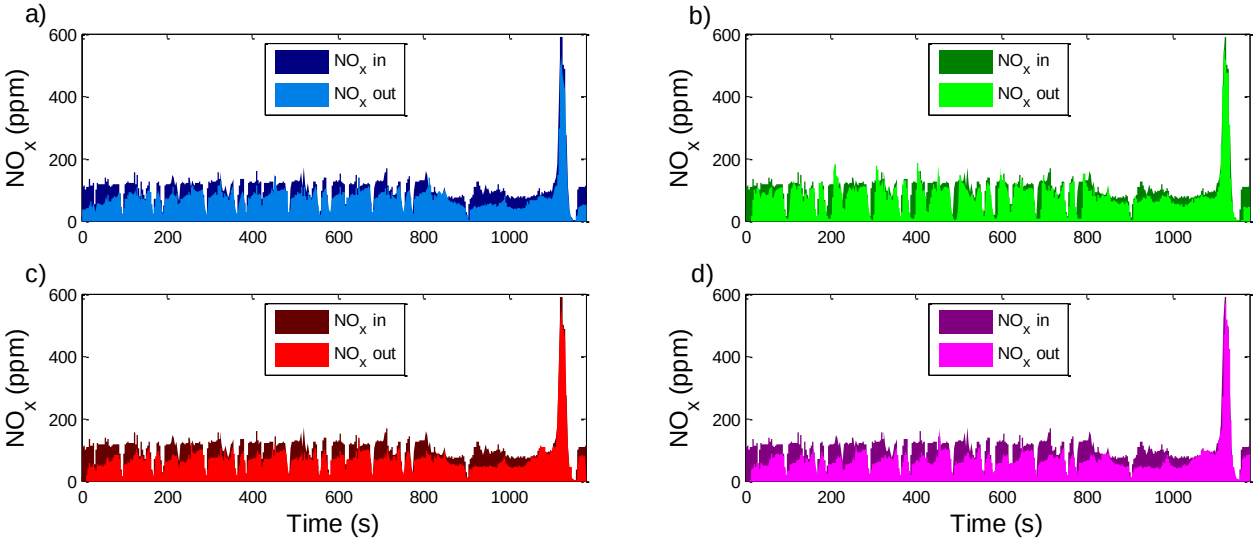

Figure 30 NO_x before (NO_x in) and after (NO_x out) catalysts during NEDC; a) Ag-only, b) Fe-Only, c) dual-Fe/Ag and d) dual-Ag/Fe, NH_3 and H_2 dosing (only NH_3 for Fe-only).

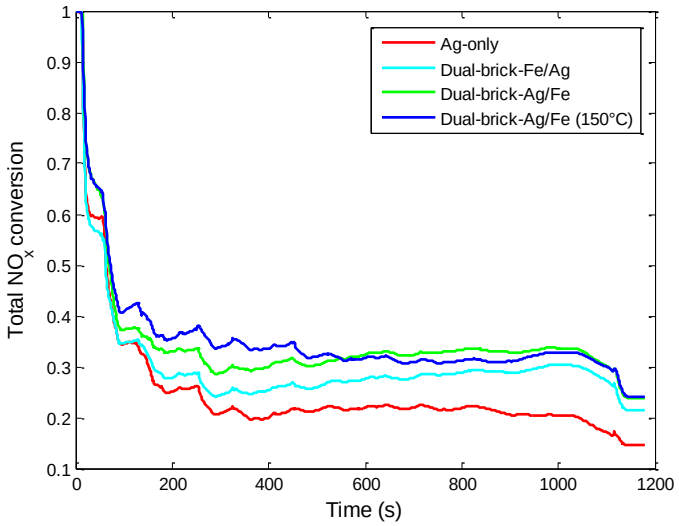

Figure 31 Total NO_x conversions as function of time during NEDC for Ag-only, dual-brick-Fe/Ag, dual-brick-Ag/Fe with NH_3 and H_2 dosing from 120°C. Dual-brick-Ag/Fe with NH_3 and H_2 dosing from 150°C is included for comparison.

been warmed up there is some SCR activity in addition to NO_x storage, seen as the increase in NO_x conversion. When dosing also starts in the original dosing case both strategies show the same NO_x conversion. By starting to dose NH_3 and H_2 a bit later the negative effect could be avoided while the positive is retained. The increased activity seen when dosing started earlier shows that there are some SCR activity even at temperatures as low as 120°C.

4.3 Conclusions

Laboratory testing of small monolith bricks showed synergistic effects of combining Ag/Al_2O_3 and Fe-BEA. It was preferred to have Ag/Al_2O_3 as the upstream brick in a dual-brick layout and as the outer layer in a dual-layer layout. The dual-layer layout was preferred when the H_2 concentration in the feed was lowered. The positive effect of having Ag/Al_2O_3 as the upstream/outer layer catalyst was attributed to formation of NO_2 over the Ag/Al_2O_3 giving fast-SCR over Fe-BEA and unselective NH_3 oxidation over Fe-BEA giving a NH_3 deficit over the Ag/Al_2O_3 when it is placed downstream.

During stationary engine-bench testing on the other hand, no unselective NH_3 oxidation was seen over Fe-BEA. The level of NO_2 out from the engine was also very high and it was preferred to have Fe-BEA in an upstream position in a dual-brick layout. Ag/Al_2O_3 showed a very low activity which was attributed to deactivation related to soot or Ag oxidation of the catalyst, the lower than intended H_2 level and low catalyst coat loading.

Transient tests (NEDC) showed high NO_x conversion from the start of the cycle, before any NH_3 or H_2 was dosed. The most likely explanation is believed to be NO_x storage over the Ag/Al_2O_3. The overall cycle conversion was, however, low which is mainly attributed to very demanding conditions with a lot of the NO_x being emitted at very low temperatures (<150°C).

5 Overall conclusions and future outlook

5.1 Conclusions

From the catalyst development it was concluded that a high S_{BET} and higher Ag loading gives a high sulphur tolerance and a high deNO_x activity. A high Ag loading gives more active sites and probably a more favourable Ag dispersion. A too high Ag loading reduces the NH_3 adsorption capacity while sulphur increases it due to formation of acid sites. The high S_{BET} is believed to allow more Ag and give a higher NH_3 adsorption capacity, necessary for the SCR reaction. The high Ag loading and high S_{BET} catalyst showed a high tolerance towards sulphur poisoning.

A similar activity enhancement (de-greening) was seen from laboratory-scale testing of monolithic catalysts as was seen for powder catalysts during testing with sulphur. NO_2 was present in the feed for the monolithic tests which might affect the results. It might also be that the observed activity enhancement for the powder catalyst is more related to the testing itself than the presence of sulphur. It is believed that the activation is related to Ag and not the alumina as an increased NO to NO_2 oxidation was seen for the monolithic catalyst after it was activated. Possible reasons for this activation might be a change in the dispersion or state of Ag.

Ag/Al_2O_3 was combined with Fe-BEA to give a catalyst with a high activity in a broad temperature range without the need to continuously having to dose H_2 to get activity over the Ag/Al_2O_3. Small-scale monolith tests showed that it was preferred to have Ag/Al_2O_3 either as the upstream brick in a dual-brick layout or as the outer layer in a dual-layer layout. The opposite could give complete NH_3 oxidation over Fe-BEA leading to a NH_3 deficit over Ag/Al_2O_3. Full-scale engine testing contradicted these results and showed that Fe-BEA was preferred as the upstream brick in a dual-brick layout. The presence of NO_2 in the feed giving fast-SCR over Fe-BEA and no unselective NH_3 oxidation in the engine tests are believed to explain the observed difference between the two tests. The activity of the combined catalyst layouts were higher than the activity for individual catalysts when less or no H_2 was co-fed showing that there were synergistic effects by combining them. The dual-layer layout showed the best performance which is believed to be attributed the short diffusion distance between the layers allowing dispersion of reaction intermediates between them.

Transient engine bench testing showed that Ag/Al_2O_3 and a combined Ag/Al_2O_3 – Fe-BEA system was active during the NEDC. The NO_x conversion was not very high which is related to both the very low temperature of the NEDC and the low activity of the Ag/Al_2O_3 catalyst seen from stationary testing. The most interesting result was that the catalyst systems showed NO_x conversion already from the start of the cycle before any NH_3 or H_2 was dosed. NO_x storage over the Ag/Al_2O_3 was believed to be the most likely explanation for this. The NO_x conversion could be enhanced by dosing of NH_3 and H_2 at temperatures lower than 150°C that was used as the standard dosing temperature. Dosing at too low temperature, however, inhibited the NO_x conversion.

5.2 Future

The mechanism behind the synergistic effects of combining Ag/Al_2O_3 and Fe-BEA is not fully investigated. Especially the effect of the dual-layer layout is not completely understood and further studies are needed. The de-greening seen for the high Ag loading and high S_{BET} catalysts

was first attributed to the effect of sulphur poisoning. A similar effect was seen for the later tests when no SO_2 was present and the possible mechanism should be further investigated. The sulphur tolerance was only tested for powder catalyst and the possible impact of sulphur on monolithic catalysts needs to be evaluated. It would also be interesting to further investigate which state of Ag and which Ag dispersion that is the most optimal over Ag/Al_2O_3 and if it is affected by sulphur.

The preliminary engine tests showed NH_3 formation over the Ag/Al_2O_3. This could potentially enhance the low-temperature activity for combined catalyst system with a downstream catalyst that can store the formed NH_3. The main explanation for the NO_x conversion seen at the start of the NEDC (before any NH_3 or H_2 was dosed) was believed to be NO_x storage over Ag/Al_2O_3. NO-TPD during dry conditions also showed a substantially storage capacity. More NO_x storage/adsorption tests with H_2O present are needed to fully evaluate the potential of Ag/Al_2O_3 for NO_x storage. It was believed that the Ag/Al_2O_3 catalyst was poisoned by soot during the engine testing. Future test should, therefore include DPF prior to the SCR catalysts. More catalyst, either by increasing the catalyst loading or adding more/larger bricks, is also needed to reduce the GHSV. It is also believed that the results can be improved by tailor-made dosing algorithms that take the possible NO_x storage and other mechanism into consideration.

6 References

[1] "New Passenger Car Registrations - Breakdown by Specification Share of Diesel," *European automobile manufacturers' association*, 2010. [Online]. Available: http://www.acea.be/collection/statistics. [Accessed: 01-May-2013].

[2] "Overview of CO2-based motor vehicle taxes in the EU," *European automobile manufacturers' association*, 2013. [Online]. Available: http://www.acea.be/collection/taxation_background/. [Accessed: 01-May-2013].

[3] "Reducing CO2 emissions from passenger cars," *European Commission: Climate Action*, 2013. [Online]. Available: http://ec.europa.eu/clima/policies/transport/vehicles/cars/index_en.htm. [Accessed: 01-May-2013].

[4] G. Lammel and H. Graßl, "Greenhouse effect of NOx," *Environmental Science and Pollution Research*, vol. 2, no. 1, pp. 40–45, Jul. 1995.

[5] K. Skalska, J. S. Miller, and S. Ledakowicz, "Trends in NOx abatement: a review," *The Science of the total environment*, vol. 408, no. 19, pp. 3976–89, Sep. 2010.

[6] A. Sydbom, A. Blomberg, S. Parnia, N. Stenfors, T. Sandström, and S. E. Dahlén, "Health effects of diesel exhaust emissions.," *The European respiratory journal*, vol. 17, no. 4, pp. 733–46, Apr. 2001.

[7] "Emission standards," *DieselNet*. [Online]. Available: http://www.dieselnet.com/standards/. [Accessed: 02-May-2013].

[8] S. J. Schmieg, R. J. Blint, and L. Deng, "Control strategy of the removal of NOx from diesel engine exhaust using hydrocarbon selective catalytic reduction," *SAE International Journal of Fuels and Lubricants*, vol. 1, no. 1, pp. 1540–1552, 2008.

[9] S. J. Schmieg, T. M. Sloane, and R. J. Blint, "Catalysts for lean-burn engine exhaust aftertreatment using hydrocarbon selective catalytic reduction," *SAE International Journal of Fuels and Lubricants*, vol. 2, no. 2, pp. 323–336, 2009.

[10] M. V Twigg, "Catalytic control of emissions from cars," *Catalysis Today*, vol. 163, no. 1, pp. 33–41, Apr. 2011.

[11] M. K. Khair and H. Jääskeläinen, "Exhaust Gas Recirculation," *DieselNet Technology Guide*, 2012. [Online]. Available: http://www.dieselnet.com/tech/engine_egr.php. [Accessed: 06-Mar-2013].

[12] T. V Johnson, "Vehicular Emissions in Review," *SAE International Journal of Engines*, vol. 5, no. 2, pp. 216–234, 2012.

[13] C.-J. Karlsson and K. Telborn, "Method and sytem for diesel particle filter regeneration," Patent WO 2012/030273 A12012.

[14] T. V Johnson, "Review of diesel emissions and control," *International Journal of Engine Research*, vol. 10, no. June, pp. 275–285, Oct. 2009.

[15] S. Brandenberger, O. Kröcher, A. Tissler, and R. Althoff, "The State of the Art in Selective Catalytic Reduction of NOx by Ammonia Using Metal-Exchanged Zeolite Catalysts," *Catalysis Reviews*, vol. 50, no. 4, pp. 492–531, Oct. 2008.

[16] K. Kamasamudram, N. W. Currier, X. Chen, and A. Yezerets, "Overview of the practically important behaviors of zeolite-based urea-SCR catalysts, using compact experimental protocol," *Catalysis Today*, vol. 151, no. 3–4, pp. 212–222, Jun. 2010.

[17] M. Colombo, I. Nova, and E. Tronconi, "A comparative study of the NH3-SCR reactions over a Cu-zeolite and a Fe-zeolite catalyst," *Catalysis Today*, vol. 151, no. 3–4, pp. 223–230, Jun. 2010.

[18] P. S. Metkar, M. P. Harold, and V. Balakotaiah, “Selective catalytic reduction of NOx on combined Fe- and Cu-zeolite monolithic catalysts: Sequential and dual layer configurations,” *Applied Catalysis B: Environmental*, vol. 111–112, pp. 67–80, Sep. 2011.

[19] D. W. Fickel, E. D. Addio, J. A. Lauterbach, and R. F. Lobo, “The ammonia selective catalytic reduction activity of copper-exchanged small-pore zeolites,” *Applied Catalysis B: Environmental*, vol. 102, no. 3–4, pp. 441–448, 2011.

[20] S. J. Schmieg, S. H. Oh, C. H. Kim, D. B. Brown, J. H. Lee, C. H. F. Peden, and D. Heui, “Thermal durability of Cu-CHA NH3-SCR catalysts for diesel NOx reduction,” *Catalysis Today*, vol. 184, no. 1, pp. 252–261, 2012.

[21] C. N. Costa and A. M. Efstathiou, “Low-temperature H2-SCR of NO on a novel Pt/MgO-CeO2 catalyst,” *Applied Catalysis B: Environmental*, vol. 72, no. 3–4, pp. 240–252, Mar. 2007.

[22] M. Leicht, F. J. P. Schott, M. Bruns, and S. Kureti, “NOx reduction by H2 on WOx/ZrO2-supported Pd catalysts under lean conditions,” *Applied Catalysis B: Environmental*, vol. 117–118, no. 2, pp. 275–282, May 2012.

[23] T. Miyadera, “Alumina-supported silver catalysts for the selective reduction of nitric oxide with propene and oxygen-containing organic compounds,” *Applied Catalysis B: Environmental*, vol. 2, no. 2–3, pp. 199–205, Jun. 1993.

[24] K. A. Bethke and H. H. Kung, “Supported Ag Catalysts for the Lean Reduction of NO with C3H6,” *Journal of Catalysis*, vol. 172, pp. 93–102, 1997.

[25] Z. Wang, M. Yamaguchi, I. Goto, and M. Kumagai, “Characterization of Ag/Al2O3 de-NOx catalysts by probing surface acidity and basicity of the supporting substrate,” *Physical Chemistry Chemical Physics*, vol. 2, pp. 3007–3015, 2000.

[26] K. Shimizu, J. Shibata, H. Yoshida, A. Satsuma, and T. Hattori, “Silver-alumina catalysts for selective reduction of NO by higher hydrocarbons : structure of active sites and reaction mechanism,” *Applied Catalysis B: Environmental*, vol. 30, pp. 151–162, 2001.

[27] F. C. Meunier, R. Ukropec, C. Stapleton, and J. R. H. Ross, “Effect of the silver loading and some other experimental parameters on the selective reduction of NO with C3H6 over Al2O3 and ZrO2 -based catalysts,” *Applied Catalysis B: Environmental*, vol. 30, pp. 163–172, 2001.

[28] K. Arve, F. Klingstedt, K. Eränen, D. Y. Murzin, L. Čapek, J. Dedecek, Z. Sobalik, B. Wichterlová, K. Svennerberg, L. R. Wallenberg, and J.-O. Bovin, “Analysis of the State and Size of Silver on Alumina in Effective Removal of NOx from Oxygen Rich Exhaust Gas,” *Journal of Nanoscience and Nanotechnology*, vol. 6, no. 4, pp. 1076–1083, Apr. 2006.

[29] K. Masuda, K. Tsujimura, K. Shinoda, and T. Kato, “Silver-promoted catalyst for removal of nitrogen oxides from emission of diesel engines,” *Applied Catalysis B: Environmental*, vol. 8, no. 1, pp. 33–40, Feb. 1996.

[30] K. Shimizu, M. Tsuzuki, and a Satsuma, “Effects of hydrogen and oxygenated hydrocarbons on the activity and SO2-tolerance of Ag/Al2O3 for selective reduction of NO,” *Applied Catalysis B: Environmental*, vol. 71, no. 1–2, pp. 80–84, Feb. 2007.

[31] H. Kannisto, H. H. Ingelsten, and M. Skoglundh, “Ag–Al2O3 catalysts for lean NOx reduction—Influence of preparation method and reductant,” *Journal of Molecular Catalysis A: Chemical*, vol. 302, no. 1–2, pp. 86–96, Apr. 2009.

[32] K. Arve, L. Capek, F. Klingstedt, K. Eränen, L.-E. Lindfors, D. Y. Murzin, J. Dedecek, Z. Sobalik, and B. Wichterlova, “Preparation and characterisation of Ag/alumina

catalysts for the removal of NOx emissions under oxygen rich conditions," *Topics in Catalysis*, vol. 30/31, no. 1–4, pp. 91–95, 2004.
[33] A. Sultana, M. Haneda, T. Fujitani, and H. Hamada, "Influence of Al2O3 support on the activity of Ag/Al2O3 catalysts for SCR of NO with decane," *Catalysis Letters*, vol. 114, no. 1–2, pp. 96–102, Feb. 2007.
[34] D. Y. Yoon, J.-H. Park, H.-C. Kang, P. S. Kim, I.-S. Nam, G. K. Yeo, J. K. Kil, and M.-S. Cha, "DeNOx performance of Ag/Al2O3 catalyst by n-dodecane: Effect of calcination temperature," *Applied Catalysis B: Environmental*, vol. 101, no. 3–4, pp. 275–282, Jan. 2011.
[35] G. B. Fisher, C. L. DiMaggio, D. Trytko, K. M. Rahmoeller, and M. Sellnau, "Effects of Fuel Type on Dual SCR Aftertreatment for Lean NOx Reduction," *SAE International Journal of Fuels and Lubricants*, vol. 2, no. 2, pp. 313–322, 2009.
[36] S. Satokawa, "Enhancing the NO/C3H8/O2 Reaction by Using H2 over Ag/Al2O3 Catalysts under Lean-Exhaust Conditions.," *Chemistry Letters*, vol. 3, no. 3, pp. 294–295, 2000.
[37] J. Shibata, K. Shimizu, S. Satokawa, A. Satsuma, and T. Hattori, "Promotion effect of hydrogen on surface steps in SCR of NO by propane over alumina-based silver catalyst as examined by transient FT-IR," *Physical Chemistry Chemical Physics*, vol. 5, no. 10, p. 2154, 2003.
[38] R. Burch, J. P. Breen, C. J. Hill, B. Krutzsch, B. Konrad, E. Jobson, L. Cider, K. Eränen, F. Klingstedt, and L.-E. Lindfors, "Exceptional Activity for NO x Reduction at Low Temperatures Using Combinations of Hydrogen and Higher Hydrocarbons on Ag/Al 2 O 3 Catalysts," *Topics in Catalysis*, vol. 30/31, pp. 19–25, Jul. 2004.
[39] M. Richter, U. Bentrup, R. Eckelt, M. Schneider, M.-M. Pohl, and R. Fricke, "The effect of hydrogen on the selective catalytic reduction of NO in excess oxygen over Ag/Al2O3," *Applied Catalysis B: Environmental*, vol. 51, no. 4, pp. 261–274, Aug. 2004.
[40] K. Eränen, F. Klingstedt, K. Arve, L.-E. Lindfors, and D. Y. Murzin, "On the mechanism of the selective catalytic reduction of NO with higher hydrocarbons over a silver/alumina catalyst," *Journal of Catalysis*, vol. 227, no. 2, pp. 328–343, Oct. 2004.
[41] B. Wichterlova, P. Sazama, J. P. Breen, R. Burch, C. J. Hill, L. Capek, and Z. Sobalik, "An in situ UV–vis and FTIR spectroscopy study of the effect of H and CO during the selective catalytic reduction of nitrogen oxides over a silver alumina catalyst," *Journal of Catalysis*, vol. 235, no. 1, pp. 195–200, Oct. 2005.
[42] J. P. Breen and R. Burch, "A review of the effect of the addition of hydrogen in the selective catalytic reduction of NOx with hydrocarbons on silver catalysts," *Topics in Catalysis*, vol. 39, no. 1–2, pp. 53–58, Sep. 2006.
[43] K. Shimizu, T. Higashimata, M. Tsuzuki, and A. Satsuma, "Effect of hydrogen addition on SO2 tolerance of silver–alumina for SCR of NO with propane," *Journal of Catalysis*, vol. 239, no. 1, pp. 117–124, Apr. 2006.
[44] M. Richter, R. Fricke, and R. Eckelt, "Unusual Activity Enhancement of NO Conversion over Ag/Al2O3 by Using a Mixed NH3/H2 Reductant Under Lean Conditions," *Catalysis Letters*, vol. 94, no. 1/2, pp. 115–118, Apr. 2004.
[45] E. Kondratenko, V. Kondratenko, M. Richter, and R. Fricke, "Influence of O2 and H2 on NO reduction by NH3 over Ag/Al2O3: A transient isotopic approach," *Journal of Catalysis*, vol. 239, no. 1, pp. 23–33, Apr. 2006.
[46] V. Kondratenko, U. Bentrup, M. Richter, T. Hansen, and E. Kondratenko, "Mechanistic aspects of N2O and N2 formation in NO reduction by NH3 over

Ag/Al2O3: The effect of O2 and H2," *Applied Catalysis B: Environmental*, vol. 84, no. 3–4, pp. 497–504, Dec. 2008.
[47] K. Shimizu and A. Satsuma, "Reaction Mechanism of H 2 -Promoted Selective Catalytic Reduction of NO with NH 3 over Ag/Al2O3," *Journal of Physical Chemistry C*, vol. 111, pp. 2259–2264, 2007.
[48] K. Shimizu and A. Satsuma, "Hydrogen assisted urea-SCR and NH3-SCR with silver–alumina as highly active and SO2-tolerant de-NOx catalysis," *Applied Catalysis B: Environmental*, vol. 77, no. 1–2, pp. 202–205, Nov. 2007.
[49] S. Chansai, R. Burch, and C. Hardacre, "The use of Short Time on Stream (STOS) transient kinetics to investigate the role of hydrogen in enhancing NOx reduction over silver catalysts," *Journal of Catalysis*, vol. 295, pp. 223–231, Nov. 2012.
[50] P. Sazama, L. Capek, H. Drobna, Z. Sobalik, J. Dedecek, K. Arve, and B. Wichterlova, "Enhancement of decane-SCR-NO over Ag/alumina by hydrogen. Reaction kinetics and in situ FTIR and UV–vis study," *Journal of Catalysis*, vol. 232, no. 2, pp. 302–317, Jun. 2005.
[51] J. P. Breen, R. Burch, C. Hardacre, and C. J. Hill, "Structural investigation of the promotional effect of hydrogen during the selective catalytic reduction of NOx with hydrocarbons over Ag/Al2O3 catalysts.," *The journal of physical chemistry. B*, vol. 109, no. 11, pp. 4805–7, Mar. 2005.
[52] K. Eränen, L.-E. Lindfors, F. Klingstedt, and D. Y. Murzin, "Continuous reduction of NO with octane over a silver/alumina catalyst in oxygen-rich exhaust gases: combined heterogeneous and surface-mediated homogeneous reactions," *Journal of Catalysis*, vol. 219, no. 1, pp. 25–40, Oct. 2003.
[53] K. Arve, E. Popov, M. Rönnholm, F. Klingstedt, J. Eloranta, K. Eränen, and D. Murzin, "From a fixed bed Ag-alumina catalyst to a modified reactor design: how to enhance the crucial heterogeneous-homogeneous reactions in HC-SCR," *Chemical Engineering Science*, vol. 59, no. 22–23, pp. 5277–5282, Dec. 2004.
[54] L.-E. Lindfors, K. Eränen, F. Klingstedt, and D. Y. Murzin, "Silver/alumina catalyst for selective catalytic reduction of NOx to N2 by hydrocarbons in diesel powered vehicles," *Topics in Catalysis*, vol. 28, no. 1–4, pp. 185–189, 2004.
[55] F. Klingstedt, K. Eränen, L.-E. Lindfors, S. Andersson, L. Cider, C. Landberg, E. Jobson, L. Eriksson, T. Ilkenhans, and D. Webster, "A Highly Active Ag/Alumina Catalytic Converter for Continuous HC-SCR During Lean-Burn Conditions: From Laboratory to Full-Scale Vehicle Tests," *Topics in Catalysis*, vol. 30/31, no. 1–4, pp. 27–30, Jul. 2004.
[56] S. Satokawa, J. Shibata, K. Shimizu, A. Satsuma, and T. Hattori, "Promotion effect of H2 on the low temperature activity of the selective reduction of NO by light hydrocarbons over Ag/Al2O3," *Applied Catalysis B: Environmental*, vol. 42, no. 2, pp. 179–186, May 2003.
[57] R. Brosius, K. Arve, M. Groothaert, and J. Martens, "Adsorption chemistry of NOx on Ag/Al2O3 catalyst for selective catalytic reduction of NOx using hydrocarbons," *Journal of Catalysis*, vol. 231, no. 2, pp. 344–353, Apr. 2005.
[58] K. Shimizu, J. Shibata, and A. Satsuma, "Kinetic and in situ infrared studies on SCR of NO with propane by silver–alumina catalyst: Role of H2 on O2 activation and retardation of nitrate poisoning," *Journal of Catalysis*, vol. 239, no. 2, pp. 402–409, Apr. 2006.

[59] F. C. Meunier and J. R. H. Ross, “Effect of ex situ treatments with SO2 on the activity of a low loading silver–alumina catalyst for the selective reduction of NO and NO2 by propene,” *Applied Catalysis B: Environmental*, vol. 24, no. 1, pp. 23–32, Jan. 2000.
[60] J. P. Breen, R. Burch, C. Hardacre, C. J. Hill, B. Krutzsch, B. Bandl-Konrad, E. Jobson, L. Cider, P. G. Blakeman, L. J. Peace, M. V Twigg, M. Preis, and M. Gottschling, “An investigation of the thermal stability and sulphur tolerance of Ag/γ-Al2O3 catalysts for the SCR of NOx with hydrocarbons and hydrogen,” *Applied Catalysis B: Environmental*, vol. 70, no. 1–4, pp. 36–44, Jan. 2007.
[61] A. Abe, N. Aoyama, S. Sumiya, N. Kakuta, and K. Yoshida, “Effect of SO2 on NOx reduction by ethanol over Ag/Al2O3 catalyst,” *Catalysis Letters*, vol. 51, pp. 5–9, 1998.
[62] Q. Wu, Q. Feng, and H. He, “Disparate effects of SO2 on the selective catalytic reduction of NO by C2H5OH and IPA over Ag/Al2O3,” *Catalysis Communications*, vol. 7, no. 9, pp. 657–661, Sep. 2006.
[63] P. W. Park and C. L. Boyer, “Effect of SO 2 on the activity of Ag / g-Al 2 O 3 catalysts for NO x reduction in lean conditions,” *Applied Catalysis B: Environmental*, vol. 59, pp. 27–34, 2005.
[64] T. N. Angelidis, S. Christoforou, A. Bongiovanni, and N. Kruse, “On the promotion by SO2 of the SCR process over Ag/Al2O3 : influence of SO2 concentration with C3H6 versus C3H8 as reductant,” *Applied Catalysis B: Environmental*, vol. 39, pp. 197–204, 2002.
[65] N. Jagtap, S. B. Umbarkar, P. Miquel, P. Granger, and M. K. Dongare, “Support modification to improve the sulphur tolerance of Ag/Al2O3 for SCR of NOx with propene under lean-burn conditions,” *Applied Catalysis B: Environmental*, vol. 90, no. 3–4, pp. 416–425, Aug. 2009.
[66] J. Li, Y. Zhu, R. Ke, and J. Hao, “Improvement of catalytic activity and sulfur-resistance of Ag/TiO2–Al2O3 for NO reduction with propene under lean burn conditions,” *Applied Catalysis B: Environmental*, vol. 80, pp. 202–213, 2008.
[67] S. Sitshebo, A. Tsolakis, and K. Theinnoi, “Promoting hydrocarbon-SCR of NOx in diesel engine exhaust by hydrogen and fuel reforming,” *International Journal of Hydrogen Energy*, vol. 34, no. 18, pp. 7842–7850, Sep. 2009.
[68] K. Kim, K. M. Chun, S. Song, H. S. Han, and H. Gu, “Hydrogen Effect on the DeNOx Efficiency Enhancement of Fresh and Aged Ag/Al2O3 HC-SCR in a Diesel Engine Exhaust,” *SAE International*, no. 2011–01–1278, 2011.
[69] M. B. Viola, “HC-SCR Catalyst Performance in Reducing NOx Emissions from a Diesel Engine Running Transient Test Cycles,” *SAE Technical paper series*, no. 2008–01–2487, 2008.
[70] A. Stakhev, S. Dahl, I. Gekas, and P. L. T. Gabrielsson, “Process and catalyst system for SCR of NOx,” Patent EP 2 301 650 A12011.
[71] R. Zhang and S. Kaliaguine, “Lean reduction of NO by C3H6 over Ag/alumina derived from Al2O3, AlOOH and Al(OH)3,” *Applied Catalysis B: Environmental*, vol. 78, no. 3–4, pp. 275–287, Feb. 2008.
[72] X. She and M. Flytzani-Stephanopoulos, “The role of AgOAl species in silver–alumina catalysts for the selective catalytic reduction of NOx with methane,” *Journal of Catalysis*, vol. 237, no. 1, pp. 79–93, Jan. 2006.
[73] A. Satsuma, J. Shibata, A. Wada, Y. Shinozaki, and T. Hattori, “In-situ UV-Visible Spectroscopic Study for Dynamic Analysis of Silver Catalyst,” *Science And Technology in Catalysis*, vol. 145, pp. 235–238, 2003.

[74] S. T. Korhonen, A. M. Beale, M. A. Newton, and B. M. Weckhuysen, “New Insights into the Active Surface Species of Silver Alumina Catalysts in the Selective Catalytic Reduction of NO,” *Journal of Physical Chemistry C*, vol. 115, pp. 885–896, 2011.
[75] V. Demidyuk, C. Hardacre, R. Burch, A. Mhadeshwar, D. Norton, and D. Hancu, “Aromatic hydrocarbons and sulfur based catalyst deactivation for selective catalytic reduction of NOx,” *Catalysis Today*, vol. 164, no. 1, pp. 515–519, Apr. 2011.
[76] L. Zhang, C. Zhang, and H. He, “The role of silver species on Ag / Al 2 O 3 catalysts for the selective catalytic oxidation of ammonia to nitrogen,” *Journal of Catalysis*, vol. 261, no. 1, pp. 101–109, 2009.
[77] Q. Wu, H. Gao, and H. He, “Conformational Analysis of Sulfate Species on Ag/Al2O3 by Means of Theoretical and Experimental Vibration Spectra,” *Journal of Physical Chemistry B*, vol. 110, pp. 8320–8324, 2006.
[78] T. Nijhuis, A. Beers, T. Vergunst, I. Hoek, F. Kapteijn, and J. Moulijn, “Preparation of monolithic catalysts,” *Catalysis Reviews*, vol. 43, no. 4, pp. 345–380, Mar. 2001.
[79] W. B. Kolb, A. A. Papadimitriou, R. L. Cerro, D. D. Leavitt, and J. C. Summers, “The ins and outs of coating monolithic structures,” *Chemical engineering progress*, vol. 89, no. 2, pp. 61–67, 1993.
[80] W. P. Addiego, I. M. Lachman, J. L. Williams, M. R. Williams, and K. E. Zaun, “High surface area washcoated substrate and method for producig same,” Patent US005212130A1993.
[81] C. Agrafiotis and A. Tsetsekou, “The effect of processing parameters on the properties of γ-alumina washcoats deposited on ceramic honeycombs,” *Journal of Materials Science*, vol. 35, pp. 951 – 960, 2000.
[82] R. J. Pugh and L. Bergström, Eds., *Surface and colloid chemistry in advanced ceramics processing*. New York: Marcel Dekker Inc, 1994.
[83] A. K. Mogalicherla and D. Kunzru, “Effect of method of preparation on activity of Pd/Al2O3 monolith catalysts,” *The Canadian Journal of Chemical Engineering*, vol. 9999, pp. 367–375, 2010.
[84] C. Agrafiotis and A. Tsetsekou, “The effect of powder characteristics on washcoat quality . Part I : Alumina washcoats,” *Journal of the European Ceramic Society*, vol. 20, no. 7, pp. 815–824, Jun. 2000.
[85] L. Villegas, F. Masset, and N. Guilhaume, “Wet impregnation of alumina-washcoated monoliths: Effect of the drying procedure on Ni distribution and on autothermal reforming activity,” *Applied Catalysis A: General*, vol. 320, pp. 43–55, Mar. 2007.
[86] D. E. Doronkin, S. Fogel, P. Gabrielsson, and S. Dahl, “Ti and Si doping as a way to increase low temperature activity of sulfated Ag/Al2O3 in H2 -assisted NOx SCR by NH3,” *In manuscript*, 2013.
[87] P. Balle, B. Geiger, D. Klukowski, M. Pignatelli, S. Wohnrau, M. Menzel, I. Zirkwa, G. Brunklaus, and S. Kureti, “Study of the selective catalytic reduction of NOx on an efficient Fe/HBEA zeolite catalyst for heavy duty diesel engines,” *Applied Catalysis B: Environmental*, vol. 91, no. 3–4, pp. 587–595, Sep. 2009.
[88] P. Balle, B. Geiger, and S. Kureti, “Selective catalytic reduction of NOx by NH3 on Fe/HBEA zeolite catalysts in oxygen-rich exhaust,” *Applied Catalysis B: Environmental*, vol. 85, no. 3–4, pp. 109–119, Jan. 2009.
[89] C. He, Y. Wang, Y. Cheng, C. K. Lambert, and R. T. Yang, “Activity, stability and hydrocarbon deactivation of Fe/Beta catalyst for SCR of NO with ammonia,” *Applied Catalysis A: General*, vol. 368, no. 1–2, pp. 121–126, Oct. 2009.

[90] R. G. Silver, M. O. Stefanick, and B. I. Todd, “A study of chemical aging effects on HDD Fe–zeolite SCR catalyst,” *Catalysis Today*, vol. 136, no. 1–2, pp. 28–33, Jul. 2008.
[91] A. Grossale, I. Nova, and E. Tronconi, “Study of a Fe–zeolite-based system as NH3-SCR catalyst for diesel exhaust aftertreatment,” *Catalysis Today*, vol. 136, no. 1–2, pp. 18–27, Jul. 2008.
[92] M. J. Pipho, D. B. Kittelson, and D. D. Zarling, “NO2 Formation in a Diesel Engine,” *SAE Technical paper series*, no. 910231, 1991.
[93] H. Yamada, K. Misawa, D. Suzuki, K. Tanaka, J. Matsumoto, M. Fujii, and K. Tanaka, “Detailed analysis of diesel vehicle exhaust emissions: Nitrogen oxides, hydrocarbons and particulate size distributions,” *Proceedings of the Combustion Institute*, vol. 33, no. 2, pp. 2895–2902, Jan. 2011.
[94] J. J. Chong, A. Tsolakis, S. S. Gill, K. Theinnoi, and S. E. Golunski, “Enhancing the NO2/NOx ratio in compression ignition engines by hydrogen and reformate combustion, for improved aftertreatment performance,” *International Journal of Hydrogen Energy*, vol. 35, no. 16, pp. 8723–8732, Aug. 2010.
[95] T. Johannessen, H. Schmidt, A. M. Frey, and C. H. Christensen, “Improved Automotive NOx Aftertreatment System: Metal Ammine Complexes as NH3 Source for SCR Using Fe-Containing Zeolite Catalysts,” *Catalysis Letters*, vol. 128, no. 1–2, pp. 94–100, Jan. 2009.
[96] J. P. Breen, R. Burch, C. Hardacre, C. J. Hill, and C. Rioche, “A fast transient kinetic study of the effect of H2 on the selective catalytic reduction of NOx with octane using isotopically labelled 15NO,” *Journal of Catalysis*, vol. 246, no. 1, pp. 1–9, Feb. 2007.
[97] C. L. DiMaggio, G. B. Fisher, K. M. Rahmoeller, and M. Sellnau, “Dual SCR Aftertreatment for Lean NOx Reduction,” *SAE International Journal of Fuels and Lubricants*, vol. 2, no. 1, pp. 66–77, 2009.
[98] Y. Tsukamoto, H. Nishioka, D. Imai, Y. Sobue, N. Takagi, T. Tanaka, and T. Hamaguchi, “Development of New Concept Catalyst for Low CO 2 Emission Diesel Engine Using NOx Adsorption at Low Temperatures,” *SAE International*, vol. 2012–01–03, 2012.
[99] A. Grossale, I. Nova, and E. Tronconi, “Ammonia blocking of the ‘Fast SCR’ reactivity over a commercial Fe-zeolite catalyst for Diesel exhaust aftertreatment,” *Journal of Catalysis*, vol. 265, no. 2, pp. 141–147, Jul. 2009.

Appendix

A. List of abbreviations

γ	Shear rate
μ	Viscosity
σ_0	Yield stress
σ	Shear stress
ad-NO_x	Adsorbed Nox species
ASC	Ammonia slip catalyst
d	Diameter
DM	Dry matter - solid content
DOC	Diesel oxidation catalyst
DPF	Diesel particulate filter
d_x	Particle size distribution, x denotes the percentage of particles that is of a size less than the stated value
FTIR	Fourier transform infrared spectroscopy
GHSV	Gas hourly space velocity
HC	Hydrocarbons
NSR	Nox storage and reduction
PM	Particulate matter
Re	Reynolds number
S_{BET}	Surface area calculated using the Brunauer, Emmet and Teller method
SCR	Selective catalytic reduction
SEM	Scanning electron microscope
T_{50}	Temperature for 50% Nox conversion
TPD	Temperature programmed desorption
TWC	Three way catalyst
v	Velocity
XRD	X-ray diffraction

Ag-only	Catalyst brick with only Ag/Al_2O_3
Dual-brick-Ag/Fe	Dual brick layout with Ag/Al_2O_3 upstream of Fe-BEA
Dual-brick-Fe/Ag	Dual brick layout with Fe-BEA upstream of Ag/Al_2O_3
Dual-layer-Ag/Fe	Dual layer layout with Ag/Al_2O_3 as the outer layer of Fe-BEA
Dual-layer-Fe/Ag	Dual layer layout with Fe-BEA as the outer layer of Ag/Al_2O_3
Fe-only	Catalyst brick with only Fe-BEA

B. Monolith preparation

Topsøe alumina (6 wt% Ag/Al_2O_3) – catalyst for Paper V

Table B-1 Properties of slurry used for coating monoliths

Washcoat no.	1	2
pH	9.5	-
σ_0 (Pa)	5.12	3.66
μ (mPas)	26.0	19.3
DM (wt%)	21.9	20.3

Table B-2 Properties of small-scale monoliths (21x20 mm). Monoliths A-C was dipped after each other in the same slurry during coat 1 and D-E in another slurry. During coat 2 A-B and C-E was dipped in different slurries.

Monolith	A	B	C	D	E
Coat 1					
(g/L)	53.0	60.8	71.8	53.5	52.2
(wt.%)	13.8	15.4	18.0	14.3	13.8
Coat 2					
(g/L)	70.2	74.9	65.5	62.4	65.7
(wt.%)	15.4	15.9	14.1	14.3	14.8
Final					
(g/L)	112	125	126	105	107
(wt.%)	25.3	27.1	27.9	24.7	24.7

Table B-3 Amount sulphur in the monoliths after sulphur impregnation.

Monolith	B	C	D	E
S [wt.%]	0.65	0.53	0.64	0.59

Topsøe alumina – 6 wt% Ag/Al_2O_3 catalysts for SEM images

Table B-4 Slurry properties for 6 wt% Ag/Al_2O_3. The slurry for coat 2 was made by diluting slurry 1. The slurry for coat 3 was the same as for coat 2.

Washcoat no.	1	2	3
pH	10.7	-	-
σ_0 (Pa)	5.58	5.09	-
μ (mPas)	27.0	15.6	-
DM (wt%)	18.3	16.8	18.3

Table B-5 Properties for 6 wt% Ag/Al_2O_3 small-scale monoliths (21x20 mm). A-B are Ag/Al_2O_3 and C-E are dual-layer monoliths with C with Ag/Al_2O_3 as the inner layer and D-E with Fe-BEA as the inner layer.

Monolith	A	B	C	D	E
Coat 1					
(g/L)	38.5	41.2	39.2	62.5*	75.8*
(wt.%)	13.7	14.6	14.0	22.2*	26.9*
Coat 2					
(g/L)	48.3	51.4	48.4	89.6	99.7
(wt.%)	15.1	15.9	15.2	26.1	27.9
Coat 3					
(g/L)	57.8	61.2	99.0*	-	-
(wt.%)	15.7	16.3	26.9*	-	-
Final					
(g/L)	128	135	165	129	149
(wt.%)	45.5	47.8	59.0	45.7	52.8

* Fe-BEA

Topsøe alumina – 4 wt% Ag/Al_2O_3 catalysts for Paper II

Table B-6 Slurry properties for 4 wt% Ag/Al_2O_3. The slurry for coat 2 was made by diluting slurry 1 and slurry 3 by diluting slurry 2.

Washcoat no.	1	2	3
pH	10.	-	-
σ_0 (Pa)	5.84	3.75	3.01
μ (mPas)	12.1	8.62	8.69
TS (wt%)	23.6	17.8	14.9

Table B-7 Properties for 4 wt% Ag/Al_2O_3 small-scale monoliths (21x20 mm). A is Ag/Al_2O_3 and B-E are dual-layer monoliths with B-C with Ag/Al_2O_3 as the inner layer and D-E with Fe-BEA as the inner layer.

Monolith	A	B	C	D	E
Coat 1					
(g/L)	42.2	46.5	40.8	35.7*	36.8*
(wt.%)	14.6	16.2	14.6	12.5*	12.4*
Coat 2					
(g/L)	41.2	50.3	45.0	43.6*	46.4*
(wt.%)	12.5	15.1	14.0	13.6*	13.9*
Coat 3					
(g/L)	36.8	86.8*	76.5*	54.4	60.8
(wt.%)	9.89	23.8*	20.7*	14.9	16.0
Coat 4					
(g/L)	-	-	-	36.5	36.5
(wt.%)	-	-	-	8.72	7.41
Final					
(g/L)	120	173	163	170	177
(wt.%)	29.4	35.6	34.1	37.4	37.3

* Fe-BEA

Siralox alumina – catalysts for Paper III

Table B-8 Properties for 4 wt% Ag/Si-Al_2O_3 medium size monoliths (140 ml), A-B are Ag/Al_2O_3 and C-D are dual-layer monoliths with Fe-BEA as the inner layer.

Monolith	A	B	C	D
Coat 1				
(g/L)	80.6	70.5	60.1*	63.8*
(wt.%)	27.4	22.8	19.9*	20.7*
Coat 2				
(g/L)	95.4	107	78.2	60.8
(wt.%)	25.5	28.2	21.7	16.7
Final				
(g/L)	161	162	126	111
(wt.%)	35.4	34.3	29.5	26.6
* **Fe-BEA**				

Table B-9 Properties for 4 wt% Ag/Si-Al_2O_3 full size monoliths (2 l).

Monolith	A	B
Coat 1		
(g/L)	71.1	57.6
(wt.%)	23.8	19.2
Coat 2		
(g/L)	86.2	74.1
(wt.%)	20.1	24.0
Final		
(g/L)	132	119
(wt.%)	30.6	28.5

Paper I

Applied Catalysis B: Environmental 125 (2012) 457–464

Contents lists available at SciVerse ScienceDirect

Applied Catalysis B: Environmental

journal homepage: www.elsevier.com/locate/apcatb

Optimisation of Ag loading and alumina characteristics to give sulphur-tolerant Ag/Al_2O_3 catalyst for H_2-assisted NH_3-SCR of NO_x

Sebastian Fogel[a,b,*], Dmitry E. Doronkin[b], Pär Gabrielsson[a], Søren Dahl[b]

[a] Haldor Topsøe A/S, Nymøllevej 55, 2800 Kgs. Lyngby, Denmark
[b] Center for Individual Nanoparticle Functionality (CINF), Department of Physics, Technical University of Denmark, Fysikvej 307, 2800 Kgs. Lyngby, Denmark

ARTICLE INFO

Article history:
Received 20 February 2012
Received in revised form 14 June 2012
Accepted 18 June 2012
Available online 30 June 2012

Keywords:
Ag/Al_2O_3
NH_3
SCR
H_2
Sulphur tolerance

ABSTRACT

A series of Ag/Al_2O_3 catalysts with different alumina precursors and different Ag loadings were tested for H_2 assisted NH_3-SCR of NO. The catalysts were characterised (BET, XRD, NH_3-TPD, ICP-OES, TEM and UV–vis spectroscopy) and tested as fresh catalyst, during long-term cycling tests with SO_2 present and after the sulphur testing. The aim was to find an optimal configuration of the Ag/Al_2O_3 catalyst for automotive applications. Catalysts with a high sulphur tolerance during long-term SO_2 cycling (1 h with 10 ppm SO_2 at 250 °C followed by 10 min regeneration at 670 °C, repeated until no difference between cycles was seen) were demonstrated. The high sulphur tolerance and activity was attributed to high surface areas of the catalyst supports, together with a high Ag loading. The high surface area allows a larger NH_3 storage on the surface which is previously reported necessary for the SCR reaction. A higher Ag loading will affect the state of Ag by increasing the ratio of Ag-clusters and particles to highly dispersed Ag ions. SO_2-poisoned Ag-clusters and particles can be regenerated by the high temperature treatment in the deNO_x feed, highly dispersed Ag ions cannot.

1. Introduction

Up to now it has been possible to meet the ever stricter emission limits for light-duty diesel vehicles by direct engine management and tuning and use of diesel particulate filters (DPF) and/or oxidation catalysts (DOC). This will not be possible in the future, to meet the upcoming legislation an aftertreatment system will be needed for NO_x reduction [1]. Options for such reduction are selective catalytic reduction (SCR) by urea, lean NO_x trap (LNT) and further tuning of the engine like exhaust gas recirculation (EGR). SCR is very effective and is today being widely used for heavy-duty trucks and seems like an attractive way to go, since its high efficiency makes it possible to tune the engines for better fuel efficiency [2]. The first applications with SCR for passenger cars are already on the road in Europe and the USA.

The critical point for all applications is, however, the low-temperature (100–250 °C) activity of the catalyst. In order to reduce NO_x in the cold part of the test cycles, the engine manufacturers have to take measures to increase the exhaust temperature by engine management, which reduces the overall efficiency of the system. Hydrocarbon (HC)-SCR over Ag/Al_2O_3 has been known for quite some time [3] and is widely investigated. Addition of hydrogen is known to enhance the low-temperature activity [4,5]. Richter et al. [6] have showed that Ag/Al_2O_3 also is active for NH_3-SCR when H_2 is co-fed; with NO_x conversion starting at 150 °C. However, since then there have been only few reports about NH_3-SCR on Ag/Al_2O_3.

Although not entirely unambiguous, most studies show that the activity of Ag/Al_2O_3 is decreased by sulphur which is normally present in automotive exhaust. Those showing the opposite may be attributed to the reaction conditions, reductant, temperature, etc. According to the results of Breen et al. [7], catalyst deactivation by SO_2 only occurs at temperatures of about 230–400 °C for HC-SCR. At lower temperatures, the oxidation of SO_2 to SO_3 supposed to be crucial for the catalyst deactivation does not occur. At higher temperatures, the formed Ag-sulphate becomes unstable. The same results have been showed by Shimizu and Satsuma [8] with deactivation at 250 °C but not at 200 °C for H_2-assisted NH_3-SCR. H_2 is reported to facilitate activity regeneration after sulphur poisoning [9]. Different sulphur tolerance for different HC reductants has been shown [10,11]. Testing the sulphur tolerance is therefore very important when evaluating Ag/Al_2O_3 catalysts for automotive SCR.

This study aims to find the optimal formulation of the Ag/Al_2O_3 catalyst for H_2-assisted NH_3-SCR for automotive applications under realistic conditions. A series of different alumina precursors were thermally pretreated to give alumina supports with varying characteristics to see how the different characteristics influence catalyst performance. Different Ag loadings were also tested. Emphasis of

* Corresponding author at: Haldor Topsøe A/S, Nymøllevej 55, 2800 Kgs. Lyngby, Denmark. Tel.: +45 2275 4125.
E-mail address: sefo@topsoe.dk (S. Fogel).

0926-3373/$ – see front matter © 2012 Elsevier B.V. All rights reserved.
http://dx.doi.org/10.1016/j.apcatb.2012.06.014

this study is on the sulphur tolerance and the regeneration possibilities of the sulphated catalyst.

2. Experimental

2.1. Catalyst preparation

Four different pseudoboehmite alumina precursors were tested: one from Topsøe, Catapal and Pural from Sasol, and Versal from UOP. The alumina precursors were precalcined at 550, 750 and 1000 °C for 2 h. The resulting alumina samples were then impregnated with $AgNO_3$ (99.8% purity) by the incipient wetness method to give the desired amount of Ag (1, 2, 3, 4 or 6 wt%). Following the impregnation, the samples were first dried in air at room temperature and then at 100 °C over night. They were thereafter calcined at 550 °C for 2 h. Reference catalysts based on γ-Al_2O_3 (Puralox SCFa or TH from Sasol) were prepared by the same method. Before testing, the samples were pressed, crushed and sieved to give fractions of 150–300 μm.

The catalysts were designated, A, C, P, R and V for Topsøe, Catapal, Pural, reference and Versal alumina, respectively. The letters are followed by the intended Ag loading and by the alumina precalcination temperature, e.g. A1-550 (1 wt% Ag on Topsøe alumina precalcined at 550 °C).

2.2. Catalyst characterisation

The specific surface areas (S_{BET}) of the catalysts were measured by N_2-adsorption by single point or by multipoint BET using either a Quantachrome Monosorb or Autosorb. The difference between results obtained by single and multipoint BET was less than 10% for seven samples tested by both methods; S_{BET} is therefore given regardless of method used. Multipoint BET was also used to get information on pore volume and pore size distribution.

The crystal phase of the catalysts was investigated by X-ray diffraction (XRD) on a Philips PW3040/60 diffractometer using Cu Kα radiation. The alumina crystal size was estimated applying the Scherrer equation to the reflex from the 440 crystal plane ($2\theta = 67°$).

Inductively coupled plasma-optical emission spectroscopy (ICP-OES) with a Perkin Elmer Optima 3000 was used to verify the Ag-content of the catalysts.

TEM measurements were carried out in a TECNAI T20 transmission electron microscope equipped with an Oxford Instruments EDX detector. For the measurements the catalyst powder was dispersed on a copper TEM grid covered with a lacey carbon film. Images were acquired using DigitalMicrograph from Gatan Inc.

UV–visible reflectance spectroscopy on a Varian Cary 300 was used to investigate the state of Ag in the catalysts. The spectra were converted into the Kubelka–Munk function ($F(R_\infty)$).

Temperature programmed desorption (TPD) of NH_3 was conducted in the catalyst test setup (see below) and with the same amount of catalyst (45 mg). Prior to the experiment, the catalyst was pretreated in a flow of Ar (100 N ml/min) for 30 min at 500 °C. After that the sample was cooled down and NH_3 was then adsorbed at 90 °C (monitored by FTIR), followed by a switch back to Ar-flow to remove gaseous NH_3. When the NH_3 signal was below 10 ppm, the temperature ramp was started (5 °C/min).

2.3. Catalyst activity testing

The catalyst activity was tested in a fixed-bed quartz flow reactor (inner diameter 4 mm). 45 mg of the catalyst was diluted with 100 mg of SiC giving a bed height of ~12 mm. The catalyst was held in place by quartz wool plugs.

A standard deNO_x feed of 500 ppm NO, 520 ppm NH_3, 1200 ppm H_2, 8.3% O_2, 7% H_2O and balance Ar was used for activity testing. For sulphur testing, 10 ppm SO_2 was added to the feed. The total flow was 120 N ml/min giving a GHSV of ~50,000 h^{-1} based on the whole bed volume (catalyst + SiC) and a GHSV of ~100,000 h^{-1} based on the catalyst volume. The gases were controlled by mass flow controllers, and water was fed by a syringe pump (ISCO 100 DM). The gases were either supplied by AGA (Ar and O_2) or Air Liquide.

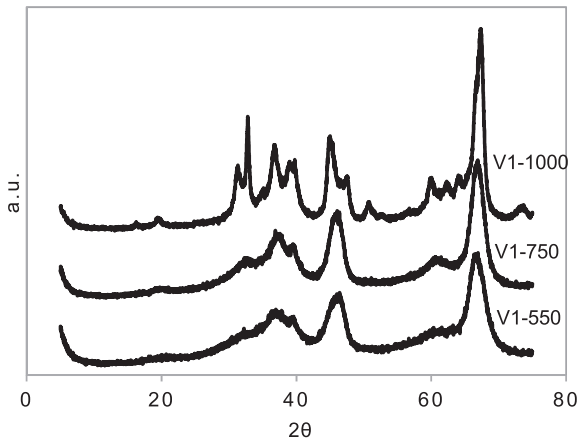

Fig. 1. XRD of Versal, calcined at 550, 750 and 1000 °C, respectively.

During activity testing, the samples were heated to 475 °C and held there for 30 min before being ramped down to 130 °C at a rate of 2 °C/min during which the activity was measured. For sulphur testing, the samples were first heated to 475 °C and held there for 30 min before being ramped down (2.5 °C/min) to 250 °C, where SO_2 was introduced and the activity measurement started. After 1 h at 250 °C, SO_2 was switched off and the temperature was increased to 670 °C and held there for 10 min before being ramped down to 250 °C again. Then the cycle, 1 h at 250 °C followed by 10 min at 670 °C, was repeated until no difference in activity between the sulphation cycles could be seen.

Outlet gases were analysed using a Thermo Fisher Nicolet 6700 FTIR analyzer, equipped with a 2-m gas cell. All gas capillaries and the FTIR gas cell were heated to >130 °C to avoid condensation of water and formation of ammonium nitrate.

NO_x conversion was calculated as $(c_{NOx,in} - c_{NOx,out})/c_{NOx,in}$, where NO_x was the sum of NO, NO_2 and N_2O.

3. Results

3.1. Catalyst characteristics

Characteristics for the different 1 wt% Ag loading catalysts are listed in Table 1. The A- and the V-series had surface areas in the same range for each pretreatment temperature (4–11% variation), the C-series had somewhat lower (11–16%) and the P-series had significantly lower surface areas (48–62%) compared to A. The P-series had a higher pore diameter as compared to the others (3–5 times). The C-series showed a much narrower pore-size distribution than the rest of the samples. The measured Ag loading was close to the target value for the samples tested. The target Ag loading will therefore be used throughout this report.

Increasing the Ag loading did not significantly alter the characteristics as can be seen for P1-1000 and P2-1000. This is in accordance with previously reported results [12,13]. The S_{BET} for 1 wt% Ag samples will therefore be used for higher Ag loading samples.

The crystallinity of the samples increased with increased precalcination temperature of the samples seen by XRD spectra. Fig. 1 shows the XRD spectra for the V-series. V1-550 and V1-750 was a mixture of eta and gamma phase and V1-1000 was a mixture of eta

Table 1
Characteristics (surface area (S_{BET}), pore volume (V_{pore}), pore diameter (D_{pore}), Ag loading, crystal phase of the alumina, crystal size and NO_x conversion at 250 °C before and after testing with sulphur) for the four boehmite alumina-series tested, Topsøe alumina (A), Catapal (C), Pural (P) and Versal (V), together with the reference γ-alumina (R). The alumina designator is followed by the Ag load and by the temperature at which the boehmite was calcined.

Catalyst	S_{BET} (m^2/g)	V_{pore} (cm^3/g)	D_{pore} (Å)	Ag loading (wt%)		Alumina phase	Crystal size (Å)	NO_x conversion at 250 °C	
				Target	Measured			Fresh	After sulphur testing
A1-550	272	–	–	0.99	–	eta/gamma	37	0.56	–
A1-750	214	0.94	171	0.99	–	eta/gamma	43	0.86	–
A1-1000	124	–	–	1.1	0.92	eta/gamma (traces of alpha and theta)	–	0.92	–
C1-550	242	0.49	75	1.0	–	eta/gamma	42	0.77	–
C1-750	179	0.48	101	1.0	1	eta/gamma	51	0.94	0.51
C1-1000	104	–	–	1.0	–	eta/theta	–	0.81	–
P1-550	111	–	–	1.0	–	eta/gamma	85	0.90	–
P1-750	82.2	1.2	514	1.0	0.99	eta/gamma	96	0.72	–
P1-1000	64.4	–	–	1.0	–	theta and delta	–	0.54	0.73
P2-1000	62.2	–	–	2.0	1.8	–	–	0.081	0.56
V1-550	262	–	–	1.0	–	eta/gamma	36	0.64	0.42
V1-750	206	0.92	178	1.0	–	eta/gamma	45	0.83	–
V1-1000	110	–	–	1.0	–	eta/theta	–	0.87	–
R1	142	–	–	1.0	0.87	eta/gamma	57	0.95	–

–, not analysed.

and theta phase. The same trend as for the V-series can be seen for the A-, C- and P-series as well. All the samples calcined at 1000 °C were, at least partly, converted from eta or gamma-alumina to more crystalline phases, alpha, delta and/or theta, Table 1.

The surface areas of the gamma-alumina were proportional to the reciprocal crystal size (Fig. 2). This indicates either a cylindrical or "needle" shape or a spherical shape of the alumina crystals. TEM images of R1 were used to confirm a "needle" shape of the alumina crystals (supporting information, S1).

In conclusion, the aluminas chosen had "needle" shape and displayed a wide range of S_{BET}, pore volumes and sizes. We therefore had a representative series of alumina precursors for our tests.

3.2. Catalyst activity of 1 wt% Ag samples (without SO_2)

The catalysts were tested in the standard deNO_x feed (without SO_2), the temperature was ramped down from 475 to 130 °C at a rate of 2 °C/min. Fig. 3 shows the temperature dependency of NO_x conversion for the C-series. C1-750 was almost identical to the reference sample (not shown) and they both showed a very promising activity; comparable to those reported in the literature for Cu- and Fe-zeolites [2]. The NH_3 conversion followed the NO_x conversion close to stoichiometry at temperatures up to 250 °C. The N_2O level was at most 10 ppm and typically below 5 ppm for all the catalysts tested.

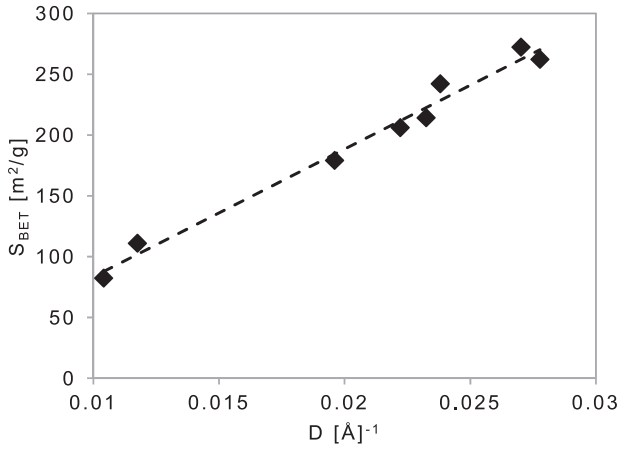

Fig. 2. Correlation between S_{BET} and crystal size.

The light-off temperature (T_{50}), temperature of 50% NO_x conversion, was used to display the low-temperature activity. Fig. 4a shows a clear correlation between T_{50} and the S_{BET} for 1 wt% Ag catalysts. A decrease in T_{50}, i.e. an increase in low-temperature activity, was seen when the S_{BET} was increased from its lowest values. It levelled out at S_{BET} ~140 g/m^2. When S_{BET} got higher than ~200 g/m^2, T_{50} started to increase. Thus, for fresh catalysts there was an optimum S_{BET} range of about 140–220 g/m^2. The same trend with an optimal S_{BET}, in the same range, can be seen for NO_x conversion at 200 (not shown) and 250 °C (Fig. 4b).

No direct correlation between activity and pore volume or pore size distribution could be seen.

3.3. Sulphur tolerance of 1 wt% Ag-samples

Since all diesel fuels normally contain small amounts of sulphur we conducted tests with SO_2 in the feed. A realistic level of SO_2 in low-sulphur diesel exhaust is below 1 ppm [7]. Our data for 0.5–10 ppm SO_2 (not shown) indicate that the degree of sulphur poisoning of Ag/Al_2O_3 is cumulative and depends on the total SO_2 exposure rather than on SO_2 concentration. Therefore, we used 10 ppm of SO_2 in the tests to decrease the testing time. Most modern diesel vehicles are equipped with a DPF [2]. The DPF is regenerated

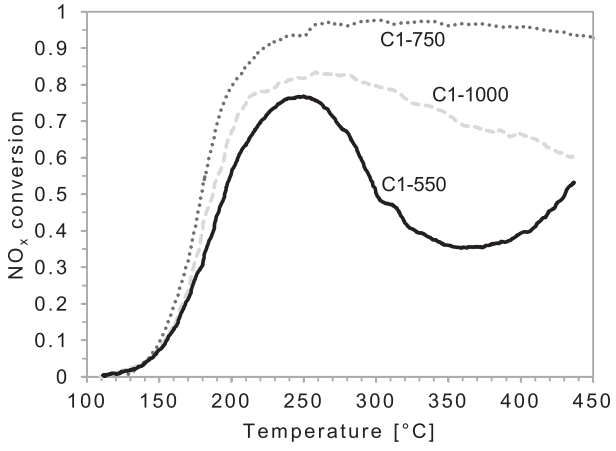

Fig. 3. Dependence of NO_x conversion on the reaction temperature for fresh Catapal-series. Reaction conditions: 500 ppm NO, 520 ppm NH_3, 1200 ppm H_2, 8.3% O_2, 7% H_2O and balance Ar, GHSV ~50,000 h^{-1} (based on bed volume).

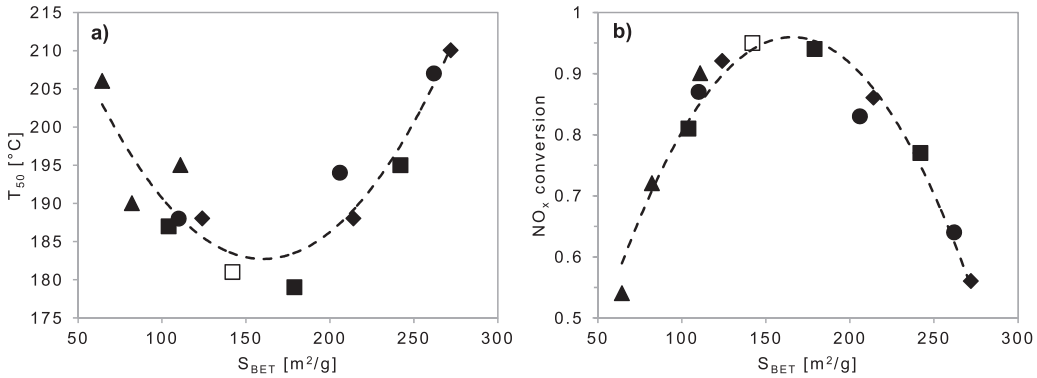

Fig. 4. (a) T_{50} (temperature of 50% NO_x conversion) and (b) NO_x conversion at 250 °C; for fresh sample-series of A ("diamond"), C ("filled square"), P ("triangle"), V ("circle") and R ("open square") 1 wt% Ag catalysts with respect to S_{BET}. Reaction conditions: 500 ppm NO, 520 ppm NH_3, 1200 ppm H_2, 8.3% O_2, 7% H_2O and balance Ar, GHSV ~50,000 h^{-1} (based on bed volume).

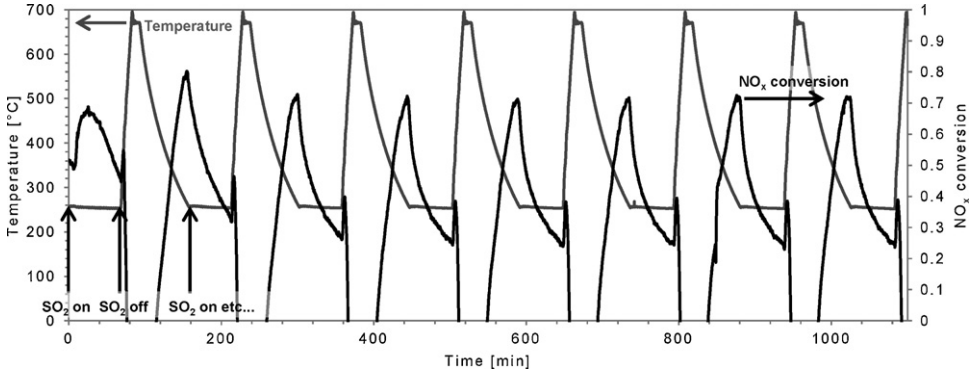

Fig. 5. Sulphur tolerance – regeneration cycling for P1-1000. Only the first eight cycles are shown. Reaction conditions: 500 ppm NO, 520 ppm NH_3, 1200 ppm H_2, 0 or 10 ppm SO_2, 8.3% O_2, 7% H_2O and balance N_2, GHSV ~50,000 h^{-1} (based on bed volume).

by burning off the soot at elevated temperatures at regular intervals. To mimic real life conditions and to investigate whether the catalyst could be regenerated by an increased temperature or not, like during DPF regeneration, the catalysts were first subjected to sulphur for 1 h at 250 °C. This roughly corresponds to the amount of sulphur a typical catalyst is subjected to between DPF regenerations, about 900 km of driving [14]. Sulphur was then turned off, and the temperature was increased to 670 °C and held there for 10 min to simulate regeneration of the catalyst. When the temperature once again had reached 250 °C, sulphur was again turned on and the cycle started all over again (Fig. 5). This was repeated 20 times giving a total time on stream with sulphur of 20 h.

The sulphur tolerance was tested for three of the samples representing low, medium and high surface areas to see if the same trend as for fresh catalysts with an optimal S_{BET} around 140–220 g/m^2 could be seen. The samples tested were P1-1000, C1-750 and V1-550. Fig. 5 shows the first eight cycles for P1-1000; the trends for C1-750 and V1-500 (not shown) were similar. All catalysts were severely deactivated by SO_2 and it was possible to regenerate part of the activity. Both P1-1000 and V1-550 showed a higher SCR activity at the start of cycle two (regenerated activity) compared to at the start of cycle one (fresh activity). The regenerated activity declined after cycle two before it reached a steady value. C1-750, on the other hand, did not show this increase in activity between the start of cycle one and cycle two.

After 3–6 cycles, the regenerated (after 10 min at 670 °C without SO_2) and sulphated activity (after 1 h with SO_2) became stabilised and the deactivation profile was identical for subsequent cycles, this will be referred to as "steady-state". Fig. 6 shows one sulphation cycle at this steady-state for the three catalysts tested. The low surface-area sample (P1-1000) showed the highest regenerated activity followed by the medium and high surface area samples (C1-750 and V1-550). P1-1000 showed a much more rapid decrease in NO_x conversion. At the end of the sulphation cycle all samples had the same activity.

An interesting and surprising observation was that P1-1000 had a higher NO_x conversion after exposure to SO_2 and regeneration (at steady-state) than it had as a fresh sample under the same

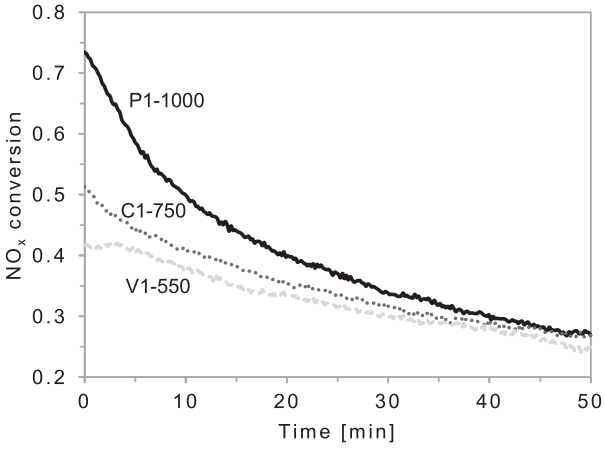

Fig. 6. NO_x conversion for one sulphur tolerance test cycle at steady-state (no change in deactivation profile between cycles) for P1-1000, C1-750 and V1-550, representing low (64 m^2/g), medium (180 m^2/g) and high (260 m^2/g) surface areas, respectively. Reaction conditions: T = 250 °C, 500 ppm NO, 520 ppm NH_3, 1200 ppm H_2, 10 ppm SO_2, 8.3% O_2, 7% H_2O and balance Ar, GHSV ~50,000 h^{-1} (based on bed volume).

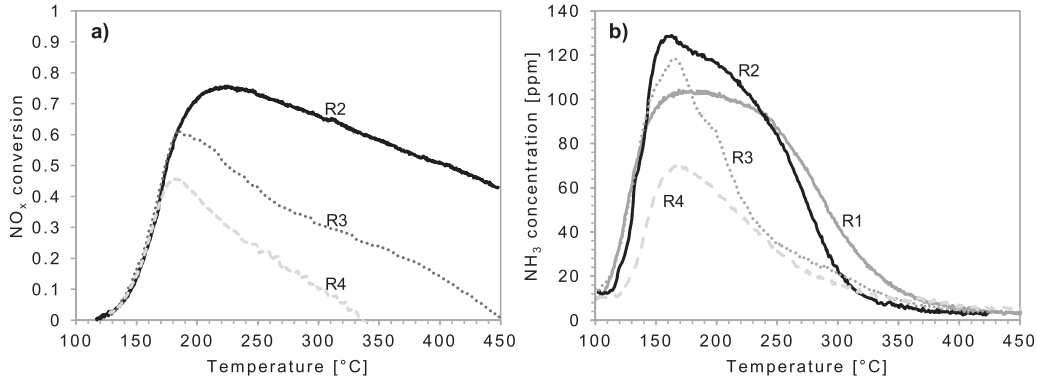

Fig. 7. (a) Dependence of NO_x conversion on the reaction temperature for fresh reference-series, 2–4 wt% Ag (R2, R3 and R4). Reaction conditions: 500 ppm NO, 520 ppm NH_3, 1200 ppm H_2, 8.3% O_2, 7% H_2O and balance Ar, GHSV ~50,000 h^{-1}(based on bed volume) and (b) NH_3-TPD profiles for reference-series with 1–4 wt% Ag (R1, R2, R3 and R4). Conditions: 100 N ml/min Ar, 5 °C/min ramp.

conditions; 72 and 54%, respectively (Figs. 4b and 6). The catalyst was activated by sulphur. The activity was also increased for about 30 min during cycle one, before decreasing (Fig. 5). An initial increase of activity upon sulphur poisoning was also reported for propane and propene-SCR by Shimizu et al. [9] and Park and Boyer [12], the latter attributed it to the formation of silver-sulphate.

The higher regenerated NO_x conversion of P1-1000 indicates that a high Ag loading/S_{BET} is advantageous for higher sulphur tolerance for the catalyst. Higher Ag loading samples were therefore prepared.

3.4. Catalytic activity of higher Ag loading catalysts

Fig. 7a compares the NO_x conversion for fresh R-catalyst with 2, 3 and 4 wt% Ag in the standard deNO_x feed during temperature ramping (475–130 °C). The activity curves follow each other closely up to ~170 °C for the three samples. The NO_x conversion for the higher Ag loading catalysts was significantly lower at higher temperatures. This cannot entirely be explained by unselective NH_3 oxidation since NH_3 conversion followed the NO_x conversion up to 250 °C for the 3 and 4 wt% Ag-samples (through the whole temperature range for the 2 wt% Ag sample). At temperatures above 250 °C, NH_3 oxidation could contribute to the decrease in NO_x conversion. A lack of NH_3 adsorbed on the catalyst surface, which is thought to be necessary for the NH_3-SCR of NO_x [15,16], can be a possible explanation for low NO_x conversion for high Ag loading catalysts. NH_3 adsorption capacity was estimated by NH_3-TPD for R1, R2, R3 and R4 (Fig. 7b). The ammonia adsorption capacity at temperatures above 200 °C decreased when the Ag loading increased above 2 wt%. It can be seen as a general trend that a higher amount of Ag led to lower activity at higher temperatures due to lower NH_3 adsorption capacity, possibly due to Ag blocking the strongest NH_3 adsorption acid sites on the alumina.

3.5. Sulphur tolerance of higher Ag loading catalysts

P2-1000, R2, R3, R4, A4-550 and A6-550 catalysts were prepared and tested for sulphur tolerance in the same way as previously done with 1 wt% Ag catalysts (10 ppm SO_2 for 1 h at 250 °C followed by 10 min regeneration at 670 °C). This was repeated until no difference could be seen between the cycles (steady-state), at least ten cycles (10 h on stream with SO_2) were run.

All tested catalysts showed a similar behaviour as that of P1-1000 (Fig. 5) with an initial increase of the activity during cycle one and an increased activity after regeneration at the beginning of cycle two. The regenerated and sulphated activities became stable after a few cycles and no differences could be seen between subsequent cycles, steady-state. Fig. 8 shows the deactivation during one of these steady-state sulphation-cycles; P1-1000 was included for comparison. Increasing the Ag loading did not increase the regenerated activity for the low S_{BET}-sample (P1- and P2-1000). P2-1000 did, on the other hand, show a slower deactivation than P1-1000 when SO_2 was present in the feed. The higher S_{BET}-samples all showed a similar regenerated activity around 93–94% NO_x conversion. R2 showed a slightly higher regenerated activity but at the same time a more rapid deactivation; i.e. lower sulphur tolerance. A4-550 was the most sulphur-tolerant catalyst and showed a very low deactivation during the test. NO_x conversion dropped from 94 to 88%, corresponding to a decrease in NO_x reduction rate of 25% (assuming first order kinetics and the reactor being an ideal plug-flow-reactor). R3, and R4 showed an almost identical deactivation profile; this together with the fact that A6-550 showed lower sulphur tolerance than A4-550 points to that there is an optimum Ag load for each alumina type (likely linked to different S_{BET} giving different amounts of acid sites).

Fig. 9a shows a comparison of the activity during temperature ramp-down in standard deNO_x feed (no SO_2) for R3 and R4 before and after sulphur testing. R3 and R4 showed very similar behaviour up to ~170 °C for fresh and up to ~240 °C for sulphated catalysts. At higher temperatures the NO_x conversion profiles deviated a lot. This stresses the necessity to combine different testing, in this case

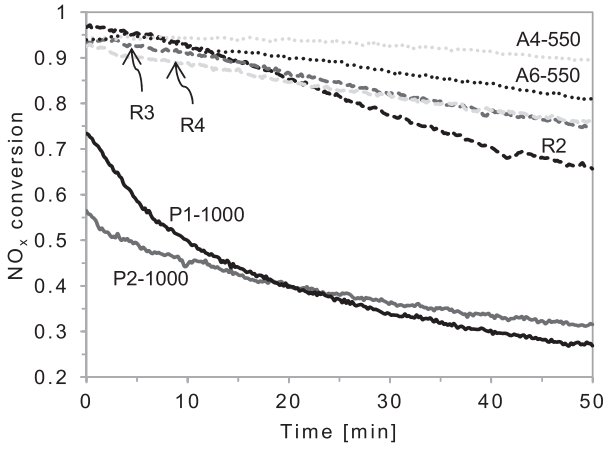

Fig. 8. NO_x conversion for one sulphur tolerance test cycle at steady-state (no change in deactivation profile between cycles) for higher Ag load samples, P1-1000, P2-1000, R2, R3, R4, A4-550 and A6-550, representing low (64 m^2/g), medium (140 m^2/g) and high (270 m^2/g) surface areas, respectively. Reaction conditions: T = 250 °C, 500 ppm NO, 520 ppm NH_3, 1200 ppm H_2, 10 ppm SO_2, 8.3% O_2, 7% H_2O and balance Ar, GHSV ~50,000 h^{-1} (based on bed volume).

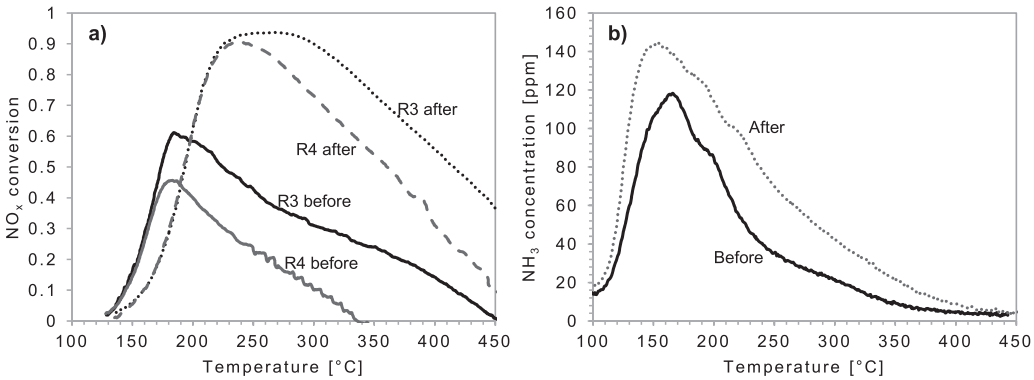

Fig. 9. (a) Comparison of the dependence of NO_x conversion on the reaction temperature for reference catalyst, 3 and 4 wt% Ag (R3 and R4), before and after testing with sulphur. Reaction conditions: 500 ppm NO, 520 ppm NH_3, 1200 ppm H_2, 8.3% O_2, 7% H_2O and balance Ar, GHSV ~50,000 h^{-1} (based on bed volume) and (b) NH_3-TPD profiles for reference catalyst with 3 wt% Ag (R3) before and after testing with sulphur. Conditions: 100 N ml/min Ar, 5 °C/min ramp.

sulphur testing at 250 °C and temperature ramping (475–130 °C), to be able to distinguish the performance of different catalysts. By subjecting the catalyst to SO_2 followed by regeneration there is a huge gain in maximum and higher-temperature activity. At the same time, the low-temperature activity cannot be fully regained. Fig. 9b shows the difference in NH_3 adsorption capacity before and after testing with sulphur for 3 wt% Ag reference catalyst. Sulphur increased the NH_3 adsorption capacity which could be part of the explanation for the increase in activity after testing with sulphur.

3.6. UV–vis spectra

Many reports show that increasing the Ag loading will affect the state of Ag [17–21]. An increase in Ag loading will give more Ag clusters/nanoparticles relative to highly dispersed Ag-ions. UV–vis spectroscopy is a widely used method to investigate the state of Ag [17–21]. Spectra were taken for P1- and P2-1000, A4- and A6-550 and R2, R3 and R4. Fig. 10 shows the spectra for the latter series. Broad peaks were seen at bands of around 21,000–23,000, 28,000, 34,000–35,000 and above 40,000 cm^{-1}. The band at 22,000 cm^{-1} has been attributed to larger metallic Ag nanoparticles (~10 nm), the peaks at 28,000 and 34,000–35,000 cm^{-1} to $Ag_n^{\delta+}$-clusters and above 40,000 cm^{-1} to dispersed Ag^+-ions [22,23]. From Fig. 10 it is clear that the intensities for the bands attributed to Ag-clusters and nanoparticles increased as the Ag loading increased from 2 to 3 and 4 wt%. The same trend with an increase in the amounts of Ag present as clusters or nanoparticles in the catalysts with higher Ag loading was also seen for the A- and P-series (not shown). Thus, the UV–vis

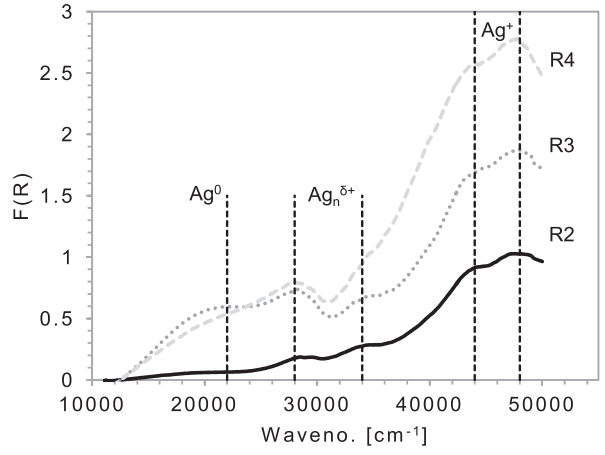

Fig. 10. UV–vis spectra for reference-series with 2–4 wt% Ag. The major peaks attributed to Ag^0, $Ag_n^{\delta+}$ and Ag^+ are indicated.

results qualitatively indicate that the samples with higher Ag loading had a higher ratio of cluster and particles to dispersed ions. These indications are in agreement with those previously reported in the literature.

4. Discussion

The correlation between T_{50} and NO_x conversion at 250 °C (near maximum) and S_{BET} (Fig. 4) is clear. It should be emphasised that the different S_{BET} stems from different calcinations temperatures of the alumina precursor and that other characteristics like crystal phase also is affected (Fig. 1). Different crystal phases of the alumina may affect the Ag and alumina interaction. Zhang and Kaliaguine [13] concluded that impregnation of AlOOH with Ag gave a Ag–O–Al bond whereas impregnation of Ag on a γ-Al_2O_3 gave more dispersed Ag due to less –OH groups available. In our study all precursors were precalcined and the alumina were dehydrated meaning the effect of surface –OH groups would be small. It was only the samples calcined at 1000 °C that showed any significant change in crystal phase of the alumina. The results for those samples did not stand out from the others. We, therefore, attribute the difference in deNO_x activity for the different catalysts to differences in surface area between the precursors rather than an effect of difference in crystal phase and crystallinity. However, S_{BET} and crystallinity (Fig. 2) are closely related to each other so influence on the performance from different crystallinity of the samples cannot be ruled out. We also found no correlation between other textural characteristics, such as pore volume or pore size distribution and activity. This supports the hypothesis that it is the correlation between Ag loading and surface area of the alumina catalysts carrier that is the influencing parameter. A higher Ag loading/S_{BET} will affect the dispersion and state of Ag as well as the acid–basic properties of the alumina support. Different Ag loadings will therefore correspond to different optimal S_{BET} and vice versa, this was also concluded by Zhang and Kaliaguine [13] for HC-SCR reaction.

Fig. 6 shows the importance of Ag loading/S_{BET} for sulphur tolerance, the low S_{BET} sample (P1-1000) shows the highest regenerated activity. However, there was a limit to the maximum possible activity for low S_{BET} catalysts, shown by a lower regenerated activity for P2-1000 (Fig. 8). We attribute this to a lack of available NH_3 on the surface due to fewer acid sites available for NH_3 adsorption. The latter was demonstrated by TPD (Fig. 7b) for reference catalyst catalysts with different Ag loading (1–4 wt%). Alumina carriers with higher S_{BET} are therefore of more interest for production of catalysts with higher activity. The higher number of acid sites stems from the higher geometrical area and the amounts of acid sites are proportional to the S_{BET}. To obtain similar or higher Ag loading/S_{BET}

as for the most sulphur-tolerant 1 wt% sample (P1-1000), more Ag was loaded on to the high S_{BET} alumina. The samples (R2, R3, R4, A4- and A6-550) all demonstrated much higher regenerated NO_x conversion (93–97%) compared to any of the 1 wt% Ag/Al_2O_3. R4 showed a sulphur tolerance very similar to the one for R3, and A6-500 showed a lower tolerance than A4-550 indicating that there is an optimal Ag loading for sulphur tolerance; the same trend that could be seen for fresh catalysts. Ag loading/S_{BET} is a trade-off between having as many stabilised active Ag-sites as possible and having acid sites available for NH_3 adsorption.

We attribute the large difference in sulphur tolerance between low and high Ag loading catalysts to the different types of Ag present, highly dispersed Ag-ions and partly charged Ag-clusters and metallic Ag-nanoparticles. Similar conclusions were made by Shimizu et al. [9], who investigated sulphur tolerance for propane-SCR over Ag/Al_2O_3 with different Ag loadings. They concluded that H_2 promotes removal of Ag-sulphates and that higher Ag loading samples gave higher sulphur tolerance. The samples with the highest Ag loading had a larger part of the Ag present as partly charged Ag-clusters compared to lower loading samples. For HC-SCR dispersed Ag is believed to be most active for NO SCR with a high selectivity towards N_2. Ag-clusters and particles are, on the other hand, more active for HC combustion and NO reduction to unwanted N_2O [18]. We observed that the NH_3 conversion deviated from that of NO at temperatures above 250–300 °C and a somewhat higher N_2O production over fresh catalysts with higher Ag loading in agreement with findings for HC-SCR. After sulphation and regeneration, however, no unwanted NH_3 oxidation and N_2O levels below 3–5 ppm were seen. Any NH_3 oxidation is unwanted, since it means that less NH_3 is available as reductant. Moreover, oxidation of NH_3 to NO or N_2O lead to negative NO_x conversion.

When the catalyst is subjected to SO_2 both the Ag and the alumina support will be affected [24]. The difference is that Ag-sulphates can be decomposed at the regeneration temperature used in this report (670 °C) whereas alumina sulphates cannot [25,26]. We suggest in a previous study [14] that it is only the Ag-clusters and particles, and not the dispersed Ag-ions that can be regenerated. After a few sulphation cycles all alumina is permanently sulphated, leading to blockage of the dispersed Ag-ions. This would then explain why the activity in the lowest temperature range, where Ag-ions are believed active, are permanently lost (Fig. 9a). The Ag-clusters and particles are, on the other hand regenerated. When SO_2 once again is switched on, the activity starts to decrease as Ag-sulphates are formed. Meunier and Ross [24] reported that sulphation of alumina only to a small extent affects the catalyst activity at high temperatures (486 °C) for HC-SCR and that it is the sulphation of Ag that is responsible for the decrease in activity reported. They also suggested that the reaction takes place in a different way over dispersed Ag-ions and over metallic (clusters and particles) Ag which could also be part of the explanation of the higher activity of the catalysts with more Ag-clusters and particles seen after exposure to SO_2. The fact that the sulphation of alumina only plays a minor roll in the total decrease in activity at higher temperatures (above 200 °C) is supported by the results in this report with high NO_x conversion over sulphated catalysts (Fig. 9a). However, the sulphation of alumina will severely affect the catalytic activity at lower temperatures, possibly by blocking active dispersed Ag-ions.

One reason for the increase in high-temperature activity seen for sulphated catalysts (Fig. 9a) is that sulphation of the alumina leads to formation of strong Lewis acid sites on the catalyst surface [27] and, thus, a higher NH_3-adsorption capacity at higher temperatures which was also shown by NH_3-TPD (Fig. 9b). The increase in NH_3 adsorption capacity is believed to explain the initial increase in activity during the first 30 min of the first sulphation cycle. It is also believed to partly explain the increase in regenerated activity between the first and the second sulphation cycle for the high Ag loading/S_{BET} samples, e.g. P1-1000 (Fig. 5). The fresh catalyst was limited by the availability of adsorbed ammonia. When the catalyst was subjected to sulphur, the ammonia adsorption capacity and thus the activity increased, seen as the initial (30 min) activity increase. Reduction of Ag-ions to Ag-clusters could also contribute [9]. Yoon et al. [21] showed that the amount of Ag-clusters/nanoparticles increases as the calcination temperature was increased for their 2 wt% Ag-catalyst (550–800 °C). The high regeneration temperature of 670 °C we used will therefore likely lead to the formation of more Ag-clusters on the catalyst surface as well as other structural changes. These changes are stabilised after a few sulphation and regeneration cycles and are believed, beside the increased NH_3 adsorption capacity, to be another reason for to the enhanced activity of the sulphated samples. Sulphation also seems to block NH_3 oxidation sites, since NO_x and NH_3 conversion profiles were close to stoichiometric during the whole temperature range tested for sulphated catalysts. The suppression of NH_3 oxidation is, however, only of importance at temperatures above 250–300 °C where fresh high Ag loading catalysts started to show unselective NH_3 oxidation. Similar conclusions were made by Demidyuk et al. for HC-SCR [28].

Our results indicate that having a larger part of Ag present as Ag-clusters is favourable over having larger Ag-nanoparticles. The oxidation of NH_3 increased for all the fresh catalyst series as the S_{BET} was decreased; the samples with the highest Ag to S_{BET} ratio probably had the highest amounts of Ag nanoparticles. The NH_3 oxidation was also most prominent over P2-1000 and R4; the samples with the highest Ag loading/S_{BET}. Large Ag-particles have been reported to be more active for NH_3 oxidation [29,30]. A4-550, showing the best performance, had a medium Ag to S_{BET} ratio indicating less Ag-nanoparticles. It still had, as indicated by the UV–vis spectra, a favourably higher ratio of clusters and particles to highly dispersed Ag-ions when compared to the lowest Ag loading samples. This indicates that Ag-clusters are more active for NO_x SCR than metallic Ag-particles. Formation of larger Ag-particles will also reduce the relative amount of available Ag-sites which also is likely to give a lower activity.

5. Conclusions

A series of Ag/Al_2O_3 catalysts with different alumina precursors and different Ag loadings giving a wide range of characteristics was prepared. Most of the samples tested were gamma alumina; those precalcined at 1000 °C were of higher alumina phases. Alumina phase changes are not believed to affect the performance to any larger extent. The catalysts were tested as fresh catalysts, during and after sulphation. Catalysts with high sulphur tolerance were demonstrated (NO_x conversion ~90% at 250 °C with 10 ppm SO_2). At $T > 200$ °C catalysts with high Ag loading were activated after short sulphur exposure. Low-temperature activity (<200 °C) was, however, lost after exposure to sulphur with a shift of T_{50} by 15–20 °C towards higher temperatures for the best catalysts. The completely different results obtained for fresh and sulphated catalysts stresses the importance to include sulphur in the activity testing; or at least as a type of "de-greening" process.

To obtain high activity and sulphur tolerance we found that the important characteristic of the support is a high S_{BET} which is proportional to the amount of acid sites. This together with a high Ag loading gives a sulphur tolerant and active catalyst. Having as many stabilised active Ag-sites as possible (a high Ag loading) and having acid sites available for NH_3 adsorption (S_{BET}) is a trade-off. A high S_{BET} is needed because it gives a higher overall NH_3 adsorption capacity (more acid sites) compared to low S_{BET} catalysts. A high Ag loading/S_{BET} is wanted since it affects the state of Ag by

increasing the ratio of Ag-clusters and particles to highly dispersed Ag ions. SO_2-poisoned Ag-clusters and particles can be regenerated by treatment in the deNO_x feed at 670 °C, highly dispersed Ag ions cannot. In practise this regeneration should coincide with the DPF regeneration in an engine exhaust.

Acknowledgments

This work was supported by The Danish Council for Strategic Research through grant 09-067233. TEM images were acquired with the support of Center for Electron Nanoscopy (DTU CEN) and of Dr. Thomas W. Hansen. Analysis and characterisation were performed at Topsøe by several colleagues whose help is greatly acknowledged.

The authors also wish to thank Dr. Jakob Weiland Høj for the fruitful discussions and Susanne Friis Madsen for proof reading the article.

Appendix A. Supplementary data

Supplementary data associated with this article can be found, in the online version, at http://dx.doi.org/10.1016/j.apcatb.2012.06.014.

References

[1] M.V. Twigg, Catalysis Today 163 (2011) 33–41.
[2] T.V. Johnson, International Journal of Engine Research 10 (2009) 275–285.
[3] T. Miyadera, Applied Catalysis B 2 (1993) 199–205.
[4] S. Satokawa, Chemistry Letters 3 (2000) 294–295.
[5] R. Burch, J.P. Breen, C.J. Hill, B. Krutzsch, B. Konrad, E. Jobson, L. Cider, K. Eränen, F. Klingstedt, L.-E. Lindfors, Topics in Catalysis 30–31 (2004) 19–25.
[6] M. Richter, R. Fricke, R. Eckelt, Catalysis Letters 94 (2004) 115–118.
[7] J.P. Breen, R. Burch, C. Hardacre, C.J. Hill, B. Krutzsch, B. Bandl-Konrad, E. Jobson, L. Cider, P.G. Blakeman, L.J. Peace, M.V. Twigg, M. Preis, M. Gottschling, Applied Catalysis B 70 (2007) 36–44.
[8] K. Shimizu, A. Satsuma, Applied Catalysis B 77 (2007) 202–205.
[9] K. Shimizu, T. Higashimata, M. Tsuzuki, A. Satsuma, Journal of Catalysis 239 (2006) 117–124.
[10] K. Shimizu, M. Tsuzuki, A. Satsuma, Applied Catalysis B 71 (2007) 80–84.
[11] Q. Wu, Q. Feng, H. He, Catalysis Communications 7 (2006) 657–661.
[12] P.W. Park, C.L. Boyer, Applied Catalysis B 59 (2005) 27–34.
[13] R. Zhang, S. Kaliaguine, Applied Catalysis B 78 (2008) 275–287.
[14] D. Doronkin, T.S. Khan, T. Bligaard, S. Fogel, P. Gabrielsson, S. Dahl, Applied Catalysis B 117-118 (2012) 49–58.
[15] V. Kondratenko, U. Bentrup, M. Richter, T. Hansen, E. Kondratenko, Applied Catalysis B 84 (2008) 497–504.
[16] D. Doronkin, S. Fogel, S. Tamm, L. Olsson, S. Dahl, Applied Catalysis B 113-114 (2012) 228–236.
[17] K.A. Bethke, H.H. Kung, Journal of Catalysis 172 (1997) 93–102.
[18] K. Shimizu, J. Shibata, H. Yoshida, A. Satsuma, T. Hattori, Applied Catalysis B 30 (2001) 151–162.
[19] K. Arve, L. Čapek, F. Klingstedt, K. Eränen, L.-E. Lindfors, D.Y. Murzin, J. Dědeček, Z. Sobalik, B. Wichterlová, Topics in Catalysis 30/31 (2004) 91–95.
[20] K. Arve, F. Klingstedt, K. Eränen, D.Y. Murzin, L. Čapek, J. Dědeček, Z. Sobalik, B. Wichterlová, K. Svennerberg, L.R. Wallenberg, J.-O. Bovin, Journal of Nanoscience and Nanotechnology 6 (2006) 1076–1083.
[21] D.Y. Yoon, J.-H. Park, H.-C. Kang, P.S. Kim, I.-S. Nam, G.K. Yeo, J.K. Kil, M.-S. Cha, Applied Catalysis B 101 (2011) 275–282.
[22] A.N. Pestryakov, A.A. Davydov, Journal of Electron Spectroscopy and Related Phenomena 74 (1995) 195–199.
[23] P. Sazama, L. Čapek, H. Drobná, Z. Sobalík, J. Dědeček, K. Arve, B. Wichterlová, Journal of Catalysis 232 (2005) 302–317.
[24] F.C. Meunier, J.R.H. Ross, Applied Catalysis B 24 (2000) 23–32.
[25] A. Abe, N. Aoyama, S. Sumiya, N. Kakuta, K. Yoshida, Catalysis Letters 51 (1998) 5–9.
[26] Q. Wu, H. Gao, H. He, Journal of Physical Chemistry B 110 (2006) 8320–8324.
[27] J. Li, Y. Zhu, R. Ke, J. Hao, Applied Catalysis B 80 (2008) 202–213.
[28] V. Demidyuk, C. Hardacre, R. Burch, A. Mhadeshwar, D. Norton, D. Hancu, Catalysis Today 164 (2011) 515–519.
[29] L. Zhang, C. Zhang, H. He, Journal of Catalysis 261 (2009) 101–109.
[30] L. Zhang, H. He, Journal of Catalysis 268 (2009) 18–25.

Paper II

Top Catal
DOI 10.1007/s11244-013-9921-8

ORIGINAL PAPER

Combination of Ag/Al_2O_3 and Fe-BEA for High-Activity Catalyst System for H_2-Assisted NH_3-SCR of NO_x for Light-Duty Diesel Car Applications

S. Fogel · D. E. Doronkin · J. W. Høj · P. Gabrielsson · S. Dahl

Abstract Low-temperature active Ag/Al_2O_3 and high-temperature active Fe-BEA zeolite were combined and tested for H_2-assisted NH_3-selective catalytic reduction (SCR) of NO_x. The catalysts were either washcoated onto separate monoliths that were placed up- or downstream of each other (dual-brick layout) or washcoated on top of each other in a sandwiched layout (dual-layer). Our results showed that it is highly preferred to have Ag/Al_2O_3 as the upstream or outer layer catalyst. Fe-BEA showed a high NH_3 oxidation giving an NH_3 deficit over the Ag/Al_2O_3. Ag/Al_2O_3 formed NO_2 which enhanced the activity over Fe-BEA through the "fast"-SCR reaction when Fe-BEA was placed downstream or as inner layer. When no H_2, which is needed for the SCR reaction over Ag/Al_2O_3, was added, the dual-layer layout was preferred. The shorter diffusion distance between the layers is a probable explanation.

Keywords Ag/Al_2O_3 · Fe-BEA · Monoliths · H_2 · NH_3 · SCR

1 Introduction

Two of the most promising alternatives to meet the upcoming strict NO_x emission regulations for diesel cars in Europe and the USA are lean NO_x traps (LNT) and selective catalytic reduction (SCR) [1, 2]. One disadvantage of the LNT over SCR is the need to run the engine rich for shorter periods of time to regenerate the LNT. NH_3-SCR is widely used for heavy-duty trucks and also for light-duty passenger cars. It is a proven and well-known technique.

State-of-the-art light-duty engines generate exhaust with very low temperatures (below 200–250 °C) during a large part of the standardized test cycles [2]. Applying the SCR catalyst technology for light-duty passenger cars therefore requires that the catalyst is able to reduce NO_x at these low temperatures. The currently used Fe-zeolites or V-based catalysts work well at higher temperatures [1]. One way to increase the NO_x reduction performance in the low-temperature part of its operation is to increase the exhaust temperature by engine measures or to heat the catalyst electrically. This will, however, give an undesirable fuel penalty.

A promising candidate for low-temperature NH_3-SCR is Ag/Al_2O_3, which has shown high activity when H_2 is co-fed [3]. Without H_2, Ag/Al_2O_3 is inactive for NH_3-SCR. Ag/Al_2O_3 is reported to be deactivated by sulfur, both for hydrocarbon (HC) and NH_3-SCR [4, 5]. By tuning the Ag loading and surface area of the Ag/Al_2O_3 we have shown that it is possible to get a high sulfur tolerant catalyst [6]. H_2-SCR over metal-oxide supported Pt or Pd catalysts is another option that shows a high activity at temperatures as low as 100–150 °C [7, 8]. However, the low activity at temperatures above 200 °C and rather poor selectivity (Pt-based catalysts) limits its practical use.

An obvious drawback of NH_3-SCR over Ag/Al_2O_3 is the necessity to co-supply H_2, which will give an increased fuel penalty as compared to using only NH_3 for other SCR catalysts. By combining the low-temperature active Ag/Al_2O_3 with Fe-BEA active at higher temperatures, it is

S. Fogel · J. W. Høj · P. Gabrielsson
Haldor Topsøe A/S, Nymøllevej 55, 2800 Kgs. Lyngby, Denmark

S. Fogel (✉) · D. E. Doronkin · S. Dahl
CINF, Technical University of Denmark, Fysikvej 307, 2800 Kgs. Lyngby, Denmark
e-mail: sefo@topsoe.dk

Published online: 26 February 2013

possible to get a system that shows high low- and high high-temperature activity; without having to dose H_2 at the higher temperatures. This decreases the fuel penalty of the combined system compared to a Ag/Al_2O_3 system. Fe-BEA is a well-known and tested catalyst that shows high hydrothermal stability [9–11] and sulfur tolerance [9, 12].

There are several ways of combining the low-temperature (Ag/Al_2O_3) and the high-temperature (Fe-BEA) catalysts, e.g. as two (or more) separate bricks (monoliths), as washcoated on each end of a single monolith brick, as multiple layers washcoated on top of each other or as combinations of the mentioned layouts. In a recent publication, Cu-zeolite as the low-temperature and Fe-zeolite as the high-temperature active catalyst were combined and tested as separate bricks and in a two-layer layout [13].

This study aims to investigate a combined NH_3-SCR system for automotive applications comprising a combination of Ag/Al_2O_3 active at low temperatures and Fe-BEA active at higher temperatures. We tested a dual-brick layout (two separate monoliths) and a dual-layer layout (a single monolith with two sandwiched catalyst layers).

2 Materials and Methods

Ag/Al_2O_3 catalyst (4 wt% Ag) was prepared by incipient wetness impregnation of $AgNO_3$ (99.8 % purity) of pre-calcined (500 °C) Topsøe boehmite-alumina. A commercial Fe-BEA (1 wt% Fe) was used as the high-temperature catalyst. The catalysts were washcoated onto cordierite monoliths (400 cpsi) to give the desired total loads of catalysts of 120–140 g/l. After washcoating, the monoliths were dried and calcined at 500 °C for 2 h. In the case of the two-layer washcoat layout, the Ag/Al_2O_3:Fe-BEA ratio was 1:0.9–1 based on mass.

The catalyst activity was tested in a stainless-steel tubular flow reactor (id = 22 mm). The tested monoliths had a diameter of 2.1 cm and a height of 2 or 1 cm (dual-brick layout) to get the same shape and total volume for all tested layouts. The monoliths were wrapped in a thick layer of quartz wool to avoid gas slip between the reactor wall and the catalyst. The feed gas was pre-heated in the oven in a 160-cm-long capillary. A deNO_x feed of 250 ppm NO, 275 ppm NH_3, 600, 250 or 0 ppm H_2, 12 % O_2, 6 % H_2O and balance N_2 was used for activity testing. Technical air was used after purification with a Parker K-MT 3 LAB adsorption dryer. The gases were controlled by UNIT Celerity mass flow controllers, and water was fed by a syringe pump (ISCO 100 DM) through a heated capillary. The total flow was 1,730 Nml/min giving a GHSV of $\sim$15,000 h^{-1} based on the monolith volume. During activity testing, the samples were heated to 400 °C and held there for 60 min before stepwise decrease to 150 °C. NO_x and ammonia concentrations were allowed to stabilize at each step. Outlet gases were analyzed using a Thermo Fisher Nicolet 6700 FTIR analyzer, equipped with a 2-m gas cell. All gas capillaries and the FTIR gas cell were heated to >130 °C to avoid condensation of water and formation of ammonium nitrate. NO_x conversion was calculated as $(c_{NO_x,IN} - c_{NO_x,OUT})/c_{NO_x,IN}$, where NO_x is the sum of NO, NO_2 and N_2O.

Scanning electron microscope (SEM) image was acquired on a Philips XL30 ESEM-FEG. The sample was mounted in epoxy and ground to reveal the cross section.

3 Results and Discussion

3.1 Comparison of Layouts

Figure 1 shows the four different layouts tested; dual-brick with either Fe-BEA or Ag/Al_2O_3 as upstream monolith (dual-brick-Fe and -Ag) and dual layer with either Fe-BEA or Ag/Al_2O_3 as the outer layer (dual-layer-Fe and -Ag). In addition, single monoliths with Ag/Al_2O_3 (Ag-only) or Fe-BEA (Fe-only) were tested. Figure 2 shows the temperature dependency of NO_x conversion for the tested monoliths. The best performance was achieved by dual-layer-Ag, dual-brick-Ag and Ag-only; the performance was comparable for these three up to $\sim$350 °C. Dual-layer-Fe and dual-brick-Fe showed much lower NO_x conversions, comparable with Fe-only, dual-layer-Fe showed a small advantage over Fe-only at temperatures above $\sim$250 °C.

One thing worth noting from Fig. 2 is the relatively low maximum NO_x conversion of Fe-only (0.8); it would be expected to reach closer to 1 at the highest temperatures tested in this study. Since sufficient time was allowed to saturate the Fe-BEA at each temperature tested, NH_3 storage [14] could be ruled out. Excess amount of NH_3 in the feed gas may inhibit the activity of Fe-BEA. With an NO:NH_3 ratio of 1:1.1 in the tests, this might explain the somewhat lower than expected maximum NO_x conversion of Fe-BEA.

NH_3 conversion for Ag-only followed the NO_x conversion closely, meaning that the unreacted NH_3 and NO_x

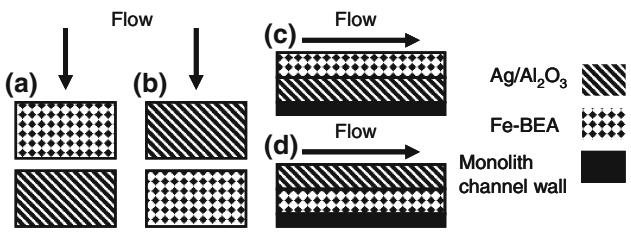

Fig. 1 The different monolith layouts tested **a** dual-brick-Fe, **b** dual-brick-Ag, **c** dual-layer-Fe and **d** dual-layer-Ag

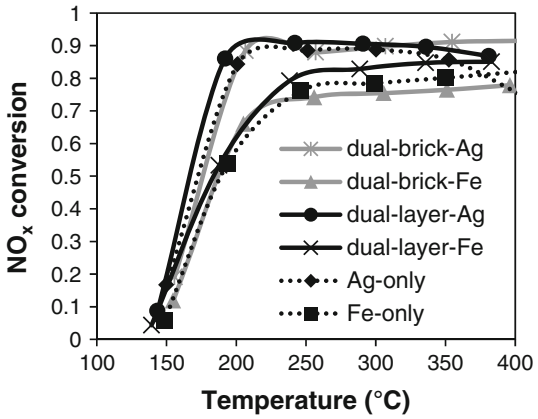

Fig. 2 Comparison of temperature dependency of NO_x conversion for dual-brick-Ag, dual-brick-Fe, dual-layer-Ag, dual-layer-Fe, Ag-only and Fe-only (600 ppm H_2)

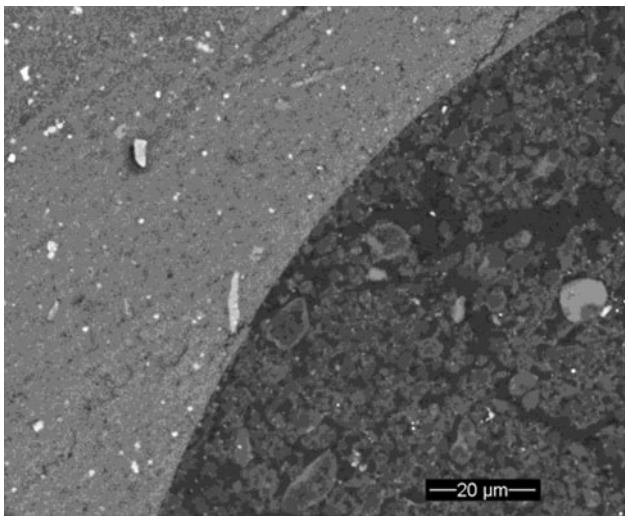

Fig. 3 SEM image of a dual-layer 6 wt% Ag/Al_2O_3 (*darker material* on the *right*) and Fe-BEA (*lighter material* on the *left*)

would pass to any downstream catalyst brick or layer. Fe-only, on the other hand, showed close to 100 % NH_3 conversion (not shown) at temperatures above 200 °C, indicating excessive NH_3 oxidation. In the dual-brick configuration the GHSV for each brick is twice as high as the GHSV for the single monoliths tested. To investigate whether the GHSV would influence NH_3 conversion over the Fe-only, a test with a GHSV of 30,000 h^{-1} was performed; the result was the same with complete NH_3 oxidation at temperatures above 200 °C. A lack of NH_3 over the downstream (inner layer) Ag/Al_2O_3 is, therefore, a likely explanation for the lower NO_x conversion over the dual-brick-Fe and dual-layer-Fe systems. Another possible explanation could be H_2 oxidation over the Fe-BEA. Ag/Al_2O_3 is, as will be discussed later (Fig. 4), sensitive when it comes to H_2 level.

Metkar et al. [13] reported that diffusion limitations could be an issue for Fe-BEA at temperatures above 250–300 °C, meaning that the entire catalyst layer is not utilized for SCR activity. They proposed that a thinner Fe-BEA catalyst layer in a dual-layer layout could be more efficient than a shorter separate monolith in a dual-brick layout with the same catalyst mass. This could help explain the difference seen in Fig. 1 for dual-layer-Fe and dual-brick-Fe. SEM images of monoliths comparable to the ones tested (6 wt% instead of 4 wt% Ag/Al_2O_3) (Fig. 3) showed that the Fe-BEA layer is much denser than the Ag/Al_2O_3 layer, this could further indicate that gas diffusion occurs more readily in the Ag/Al_2O_3 layer compared to in the Fe-BEA layer.

It is also well-known that the SCR reaction over Fe-zeolites is much faster when equimolar amounts of NO and NO_2 are fed to the catalysts, so called "fast"-SCR [13, 15]. The Ag/Al_2O_3 only test showed a maximum of 25 ppm NO_2 in the effluent at 200 °C; at the other temperatures tested the level was between 10 and 15 ppm. The "fast"-SCR reaction over Fe-BEA is therefore likely contributing to the positive effect of having Ag/Al_2O_3 as the upstream/outer layer catalyst.

The use of H_2 as a co-reductant in addition to NH_3 will increase the fuel penalty. It is therefore of interest to minimize the H_2 usage. Figure 4 compares the NO_x conversion for dual-layer-Ag, dual-brick-Ag and Ag-only at different H_2 levels (600, 250 and 0 ppm); Fe-only is included for comparison. For Ag-only, the NO_x conversion dropped drastically when the H_2 level was lowered to 250 ppm, when H_2 was removed the catalyst was completely inactive. The dual-layer-Ag and dual-brick-Ag layouts compensated the lack of activity of Ag/Al_2O_3 due to H_2-shortage with activity of the Fe-BEA and kept the same activity with 250 ppm H_2 as with 600 ppm at 250 °C and above. No clear difference could be seen between the dual-layer-Ag and dual-brick-Ag. However, when H_2 was removed, the dual-layer-Ag showed a higher NO_x conversion compared to dual-brick-Ag. At 350 and 400 °C the NO_x conversion of the dual-layer-Ag was very close to that with 600 and 250 ppm H_2. It can therefore be concluded that the total H_2 usage can be lowered by optimizing the amount of H_2 dosed at different temperatures.

For the Ag-only the NH_3 conversion closely follows the NO_x conversion when the H_2 level was lowered from 600 to 250 and to 0 ppm (no activity seen). For the combined system this will mean that NO_x and NH_3 will pass to the Fe-BEA layer/brick with the same NH_3:NO_x ratio as over the Ag/Al_2O_3 layer/brick. As mentioned previously the "fast"-SCR reaction over Fe-BEA is likely to contribute to the high NO_x conversion over the combined system. When H_2 was lowered to 250 ppm, NO_2 levels of between 10 and 30 ppm were seen over Ag-only, as with 600 ppm H_2 the highest level was seen at 200 °C. Without H_2, NO_2 was

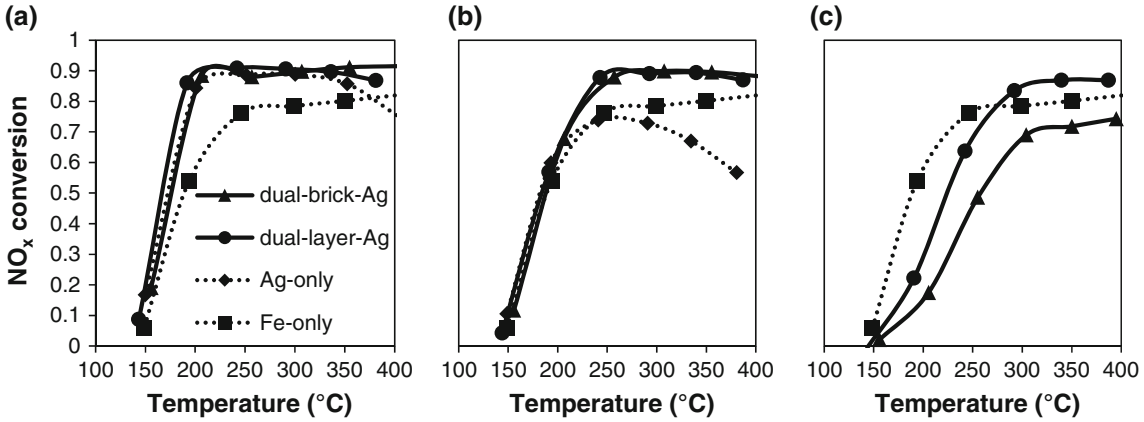

Fig. 4 Temperature dependency of NO_x conversion for dual-brick-Ag, dual-layer-Ag, Ag-only and Fe-only with **a** 600 ppm H_2, **b** 250 ppm H_2 and **c** 0 ppm H_2

only seen at 400 °C with a level of 10 ppm. The NO_2 effect is, therefore, also a viable explanation for the positive effect of the combined catalyst layout with lower H_2 levels present. However, NO to NO_2 oxidation cannot fully explain the positive effect of the dual-layer layout compared to Fe-BEA-only (Fig. 4c) when no H_2 is dosed.

In our previous study of the mechanism of H_2-assisted NH_3-SCR [16] we found that NO to NO_2 oxidation is a vital step in the reaction. NO_2 is continuously formed on the surface and is reacting with NO and NH_3. The shorter diffusion distance between Ag/Al_2O_3 and Fe-BEA in the dual-layer layout could therefore mean that more NO_2 is available for the "fast"-SCR reaction over the Fe-BEA than in a dual-brick layout where only the NO_2 not reacted over the Ag/Al_2O_3 is available. NO to NO_2 oxidation is believed to be dependent on the presence of H_2 [16] and might, therefore, not be able to fully explain what is seen in Fig. 4c. Formation of some other unknown intermediate over Ag/Al_2O_3 or over Fe-BEA which, due to the short diffusion distance, is then available for the other catalyst, might, therefore, also be a contributing factor to the synergistic effect seen for the dual-layer layout with Ag/Al_2O_3 as the outer layer. This will need more research; as will the effect of the HC present in a real exhaust gas, which will also work as NO_x reductant over Ag/Al_2O_3.

4 Conclusions

Different layouts of combined Ag/Al_2O_3 and Fe-BEA catalyst systems were tested and compared to Ag/Al_2O_3 and Fe-BEA-only systems. The systems tested were dual-brick, one monolith brick in front of the other, and dual-layer, the catalysts washcoated on top of each other. Having Ag/Al_2O_3 as the outer layer or upstream brick yields the best performance. The performance was as good as, or better than Ag/Al_2O_3 or Fe-BEA-only systems. We attribute this to two different things. First, having Fe-BEA in front of Ag/Al_2O_3 suppresses the activity of the latter due to complete NH_3 oxidation without having full NO_x conversion leading to a NH_3 deficit on the Ag/Al_2O_3. Second, formation of NO_2 over Ag/Al_2O_3 is believed to enhance the activity over Fe-BEA through the "fast"-SCR reaction when Fe-BEA is placed downstream (or as inner layer) of the Ag/Al_2O_3.

To minimize the fuel penalty due to H_2 dosing, different levels of H_2, necessary for Ag/Al_2O_3 to be active, were tested. When less H_2 than in the standard case (600 ppm) was used, the combined Ag/Al_2O_3 and Fe-BEA systems outperformed Ag/Al_2O_3-only, since the loss in activity over Ag/Al_2O_3 was compensated for by the activity of Fe-BEA. When no H_2 was used, the dual-layer-Ag layout outperformed dual-brick-Ag. It also outperformed Fe-only at temperatures above 250 °C clearly indicating synergistic effects of the combined system compared to one catalyst only systems. We believe that the shorter diffusion distance in the case of dual-layer layout explains why it outperforms the other layouts. NO_2 or other intermediates formed over either of the layers are able to diffuse to the other layer and thus enhancing the activity of the layout as a whole.

Acknowledgments This work was supported by The Danish Council for Strategic Research through Grant 09-067233.

References

1. Johnson TV (2009) Int J Eng Res 10:275–285
2. Twigg MV (2011) Catal Today 163:33–41
3. Richter M, Fricke R, Eckelt R (2004) Catal Lett 94:115–118
4. Breen JP, Burch R, Hardacre C, Hill CJ, Krutzsch B, Bandl-Konrad B, Jobson E, Cider L, Blakeman PG, Peace LJ, Twigg MV, Preis M, Gottschling M (2007) Appl Catal B 70:36–44
5. Shimizu K, Satsuma A (2007) Appl Catal B 77:202–205

6. Fogel S, Doronkin DE, Gabrielsson P, Dahl S (2012) Appl Catal B 125:457–464
7. Costa CN, Efstathiou AM (2007) Appl Catal B 72:240–252
8. Leicht M, Schott FJP, Bruns M, Kureti S (2012) Appl Catal B 117–118:275–282
9. Balle P, Geiger B, Klukowski D, Pignatelli M, Wohnrau S, Menzel M, Zirkwa I, Brunklaus G, Kureti S (2009) Appl Catal B 91:587–595
10. Balle P, Geiger B, Kureti S (2009) Appl Catal B 85:109–119
11. He C, Wang Y, Cheng Y, Lambert CK, Yang RT (2009) Appl Catal A 368:121–126
12. Silver RG, Stefanick MO, Todd BI (2008) Catal Today 136:28–33
13. Metkar PS, Harold MP, Balakotaiah V (2011) Appl Catal B 111–112:67–80
14. Lindholm A, Sjövall H, Olsson L (2010) Appl Catal B 98:112–121
15. Grossale A, Nova I, Tronconi E (2008) Catal Today 136:18–27
16. Doronkin DE, Fogel S, Tamm S, Olsson L, Khan TS, Bligaard T, Gabrielsson P, Dahl S (2011) Appl Catal B 113–114:228–236

Paper III

H_2-assisted NH_3-SCR over Ag/Al_2O_3: An engine-bench study

*Sebastian Fogel and Pär Gabrielsson**
Haldor Topsøe A/S, Nymøllevej 55, 2800 Kgs. Lyngby, Denmark
* corresponding author: tel. +45 2275 4184, pg@topsoe.dk

Abstract

A combined catalyst system of Ag/Al_2O_3 and Fe-BEA was tested in a light-duty engine bench for H_2-assisted NH_3-SCR. Ag/Al_2O_3 was used to provide a high low-temperature activity, while Fe-BEA can provide a high activity at higher temperatures without the need to co-feed H_2. The catalysts were combined in a sequential dual-brick layout and compared to Ag/Al_2O_3 and Fe-BEA only. The aim of the study was to investigate the performance of the catalysts in real life exhaust in contrast to synthetic gas. The catalysts were both tested during stationary and transient conditions. Transient testing was carried out with the New European Driving Cycle (NEDC). Laboratory tests were performed to complement the results from engine tests. Ag/Al_2O_3 showed a lower NO_x conversion in stationary engine tests than expected. This was investigated further in a laboratory test set-up and was attributed to deactivation by soot and/or Ag oxidation, low H_2 levels and low specific catalyst loading. NO_2 increased the catalytic activity at below 250 and above 300°C. For the combined systems, it was preferred to have Fe-BEA in an upstream position of Ag/Al_2O_3 compared to the opposite. The high engine out NO_2/NO_x ratio, giving fast-SCR over the Fe-BEA, was believed to be the reason. At low temperature, the activity over the combined systems was higher than that for the individual catalysts showing that there were synergy effects of combining Ag/Al_2O_3 and Fe-BEA. The transient tests also showed that there were synergistic effects of combining Ag/Al_2O_3 and Fe-BEA. However, the overall cycle NO_x conversion was low due to very demanding conditions with a lot of the NO_x being emitted at below 150°C. The order of performance based on an overall conversion during the NEDC was dual-brick with Ag/Al_2O_3 upstream = Ag/Al_2O_3 only > dual-brick Fe-BEA upstream > Fe-BEA only. The Ag/Al_2O_3 containing layouts showed a noticeable NO_x conversion from the start of the cycle, i.e. before any NH_2 or H_2 was dosed. We believe that the NO_x conversion seen came from NO_x storage on the Ag/Al_2O_3.

Keywords: Ag/Al_2O_3; SCR; NH_3; H_2; Fe-BEA, engine bench testing

1 Introduction

The upcoming Euro 6 and Euro VI emissions legislation for light- and heavy-duty diesel vehicles in Europe is very strict. It calls for large reductions of, among others, NO_x. It is well accepted that some type of exhaust aftertreatment will be needed for light-duty vehicles, as has been the case for heavy-duty vehicles for many years. For heavy-duty vehicles selective catalytic reduction (SCR) has almost completely penetrated the market. For light-duty vehicles there are other options in addition to SCR, with lean NO_x traps (LNT) being the main one; SCR catalyst and LNT can also be combined [1]. Today there are light-duty passenger cars equipped with SCR being sold in Europe that meet Euro 6 standards. Another wide-spread technique is exhaust gas recirculation (EGR) which often is used together with SCR on heavy-duty vehicles or as a single

measure to reach present NO_x legislation (Euro 5) on light-duty vehicles. EGR lowers the oxygen concentration and temperature in the engine cylinder which reduces NO_x formation [2].

The main challenge for the NO_x removal both for light- and heavy-duty vehicles is the low-temperature activity (<200-250^{o}C). Today's SCR catalysts, e.g. vanadia-based and Fe-zeolites, are efficient at higher temperatures [3]. Cu-zeolite type catalysts have been reported to have very promising low-temperature activity [4–6] ; chabazite or chabazite-like structures are especially interesting due to their excellent hydrothermal stability [7–9]. Platinum group metal-based catalyst has also been proposed but suffers from low selectivity to N_2 and has a limited temperature window of operation since they oxidize the NH_3 at temperatures above 200°C [10], [11]. Ag/Al_2O_3 is a promising candidate that has been reported to have high low-temperature activity, when H_2 is co-fed with either hydrocarbons (HC) [12–14] or NH_3 as the reductant [15], [16]. We have previously investigated the mechanism [17], [18] and sulfur tolerance [19], [20] of NH_3-SCR with H_2 over Ag/Al_2O_3 and showed a promising low-temperature activity and stability of the catalyst. A large draw-back of NH_3-SCR over Ag/Al_2O_3 is that the catalyst is inactive without H_2 in contrast to HC-SCR which is active from 250-300°C even without H_2 [12–14]. Thus, we combined Ag/Al_2O_3 with Fe-BEA in a previous study and showed that the amount of H_2 needed can be reduced without sacrificing the activity over the combined catalyst system [21]. Fe-BEA shows high activity from 250-300°C [5], [6], [22]. Since diesel exhaust contains a lot more compounds than are possible to include in simulated exhaust, the catalyst system has to be tested under real conditions to fully evaluate the potential of it. Compounds, such as unburned hydrocarbons, particulates, residues from engine lubricant oil and even traces of metal from engine wear [23] could potentially affect the catalyst performance. There is a number of reports that test Ag/Al_2O_3 in real diesel exhaust for HC-SCR [24–29]; to our knowledge, there are none using urea/NH_3 as the reductant. The reported NO_x conversions were dependent on the type of HC species used, HC/NO_x ratio, GHSV and amount of H_2 used.

In this study, we aim to investigate the performance of Ag/Al_2O_3, Fe-BEA and a combination of the two in the exhaust of a light-duty engine mounted on an engine dynamometer for H_2-assisted NH_3-SCR. We tested the catalysts both under stationary and transient conditions. Transient testing was made with the New European Driving Cycle (NEDC). Laboratory tests were performed to complement results from the engine tests.

2 Materials and method

2.1 Catalyst preparation

Ag/Al_2O_3 catalyst (4 wt% Ag) was prepared by incipient wetness impregnation of $Si\text{-}Al_2O_3$ (Siralox 5/320, courtesy of Sasol Germany) with $AgNO_3$ (99.8% purity). The prepared catalyst was dried at room temperature and at 100°C and later calcined at 500°C. The Fe-BEA was a commercial 1 wt% Fe catalyst. The catalysts were washcoated onto cordierite monolith bricks (400 cpsi) to give the desired catalyst loading (120-160 g/l). We used 5.6x5.0" (dxh) (2 l) bricks for engine testing and 4.9x7.6 cm (dxh) (0.14 ml) bricks for laboratory tests. The catalyst bricks were dried at room temperature in flowing air and calcined at 500°C for 2 h after the washcoating. Core samples, 4.9x7.4 cm (dxh), were taken from the Ag/Al_2O_3 catalyst used in the engine tests and were tested in the laboratory test set-up.

2.2 Engine dynamometer testing

A 2.0 l, 120 kW, five-cylinder direct-injected Volvo diesel engine equipped with EGR was used for engine dynamometer testing. The engine was rated to Euro 5 emission standard. A standard low-sulfur (<10 ppm) diesel was used. The engine was mounted on a Horiba DYNAS$_3$ HT250 engine dynamometer test rig. The two catalyst bricks (4 l in total volume) were placed directly after each other, approximately 75 cm after the engine. NH_3 and H_2 were dosed approximately 30 cm before the catalysts. The temperature was measured before and after the catalysts. The exhaust gas was analyzed by two Horiba MEXA 7170D and one FTIR (Gasmet 4000). Together, they can measure NO, NO_2, N_2O, NH_3, CO, CO_2, H_2O, O_2 and hydrocarbons (HC). HC was measured as total HC based on C_1-equivalents.

One MEXA was placed directly after the engine and used as a reference of engine out concentrations. The second MEXA and the FTIR were coupled to the same sample line; sampling could either be carried out before or after the catalysts by switching the sample point in the engine dynamometer control program. Figure 1 shows a schematic picture of the set-up. NO_x (NO and NO_2), N_2O, NH_3 and H_2O were measured by FTIR and HC, O_2, CO and CO_2 by MEXA (unless stated otherwise). Conversions (NO_x, NH_3 and HC) were calculated by comparing catalyst inlet and outlet levels by switching the sample point.

NH_3 was supplied from a gas bottle by a mass flow controller. H_2 was supplied by feeding NH_3 to a cracker, where it was converted to H_2 and N_2; some unreacted NH_3 also remained in the stream. NH_3 flow to the cracker was controlled by a mass flow controller. During stationary tests, the amount of NH_3 and H_2 dosed was controlled by online calculations from the actual NO_x concentrations (measured by NO_x sensors) and flow with fixed NH_3 (ANR) and H_2 (HNR) to NO_x ratios. During transient testing, NH_3 and H_2 dosing were either controlled by online calculations, as in the case of stationary testing with dosing starting when the exhaust gas temperature was above 150°C, or as pre-calculated values based on NO_x and flow inlet values from previous reference tests. The pre-calculated values were used to allow dosing from 120°C by circumventing the low-temperature limit of reductant dosing below 150°C due to an electronic shut down of the NO_x sensors used for calculating the amount NH_3 and H_2 to be dosed. The same ANR and HNR, 0.8 and 2, respectively, were used in all tests.

Table 1 shows the engine settings and relevant data for the six stationary points tested. The points were chosen to give comparable NO_x concentrations and total flows. The inlet NO_x levels varied significantly, they were in general lowest in the first test (Ag-only). At each point, temperature, NO_x level and NH_3 level were allowed to reach steady-state before changing the conditions. Tests were performed with (NH_3 and H_2 dosing) and without co-feeding of H_2 (only NH_3 dosing) and without any reductant dosing at all. Measurements were made before and after the catalysts. For transient tests, the New European Driving Cycle (NEDC) was used. It comprises four urban cycles and one extra urban cycle (highway cycle) and has a total road distance of 11 km and takes 1180 s to complete. Figure 2 shows the road speed during the NEDC and the engine out temperature. The engine was operated under high speed and low throttle conditions (3500 rpm/0%) for approximately 20 min prior to the start of the NEDC to cool down the exhaust system. The inlet gas temperature at the start of the cycle was 60°C.

Four layouts were tested: Ag/Al_2O_3 (Ag-only), Fe-BEA (Fe-only), Fe-BEA upstream of Ag/Al_2O_3 (dual-brick-Fe/Ag) and Ag/Al_2O_3 upstream of Fe-BEA (dual-brick-Ag/Fe). A total of two bricks (4 l of catalysts) was used

in all cases; either two of the same type (Ag- and Fe-only) or one of each type (dual-brick-Fe/Ag and dual-brick-Ag/Fe).

2.3 Laboratory testing

Testing was also carried out in a laboratory set-up. Figure 3 shows a schematic picture of the set-up. N_2 and air were first heated in a gas heater before the desired feed gases were added. The resulting feed was passed through a mixer to ensure a homogenous composition before entering the reactor and the monolithic catalyst. All gases and liquid H_2O were controlled with mass flow controllers. All lines after the heater were made of steel. H_2O was evaporated by passing liquid H_2O to a heated metal block, where it was rapidly evaporated; the lines after the evaporator was heated to 180°C to avoid condensation. The temperature was measured by thermocouples before and after the catalyst.

A standard feed of 500 ppm NO, 500 ppm NH_3, 1000 ppm H_2, 8% O_2, 12% H_2O and balance N_2 was used for activity testing. NO was mixed with air to allow oxidation to NO_2 in order to investigate the influence of NO_2 on the reaction. NO_2/NO_x ratios of 0.25, 0.5, 0.75 and 0.95 were tested and compared to the standard feed (NO_2/NO_x = 0). Tests were also performed without adding H_2. The outlet gas was analyzed by a FTIR (Gasmet 4000) after the catalyst. Inlet concentrations were taken from the given set-points (verified by empty reactor tests). The FTIR-lines were heated to 180°C to avoid H_2O condensation and NH_4NO_3 formation. The GHSV was 30000or 33000h^{-1} depending on the size of the tested catalyst brick.

2.4 TPD

NH_3 and NO-TPD were carried out in a fixed-bed flow reactor, where 0.5 g of the powder catalyst (of a particle size of 150-300 μm) was used. The catalyst was treated in N_2 at 500°C for 30 min. prior to adsorption of NO or NH_3. NO was adsorbed at 40°C (2000 ppm, 10% O_2, balance N_2) and NH_3 at 150°C (2100 ppm, balance N_2). Excess NO or NH_3 was removed by switching back to pure N_2, before the temperature was ramped up (2°C/min) to 500°C (NO-TPD) or 650°C (NH_3-TPD) in a pure N_2 atmosphere.

3 Results and discussion

3.1 Stationary tests

Figure 4 shows NO_x conversions for the four layouts tested (Ag-only, Fe-only, dual-brick-Fe/Ag and dual-brick-Ag/Fe) as a function of temperature for the NH_3 and H_2 dosing case during stationary tests. Ag-only showed an unexpectedly low NO_x conversion in the whole temperature range, and Fe-only showed a higher than expected NO_x conversion at 150°C and a 90% NO_x conversion at 340 and 400°C. The combined catalyst systems (dual-brick-Fe/Ag and dual-brick-Ag/Fe) showed an activity profile that was a combination of that of Ag/Al_2O_3 and Fe-BEA with a local maximum at 180°C corresponding to that of Ag/Al_2O_3 and a sharp increase in activity at above 270°C related to Fe-BEA. The performance of the combined systems was better than that of the individual catalysts at the lowest temperatures. At above 270°C, Fe-only was preferred over the combined systems. It was also preferred to have Fe-BEA as the upstream catalyst (dual-brick-Fe/Ag) compared to having Ag/Al_2O_3 upstream. This contradicts our previous results, where there was a clear advantage of having Ag/Al_2O_3 upstream [21]. We attributed this, among other things, to a complete NH_3 conversion over Fe-BEA giving a deficit of NH_3 over the downstream catalyst. In this study, no such unselective NH_3 oxidation was seen (Figure 5). Figure 5 shows that there were very small differences in NO_x

conversion between NH_3 and H_2 dosing and only NH_3 dosing for Ag-only and the combined systems. Since the effect of H_2 is very pronounced [15], this was highly unexpected and will be discussed later. There was even some NO_x conversion, when no NH_3 or H_2 was dosed below 200°C for Ag-only (not shown).

The ratio between the amounts of converted NH_3 and converted NO_x over the catalysts varied between 0.8 and 1.2 and in most cases it was close to 1 for the Fe-BEA containing layouts, in good agreement with the expected results [5], [6], [22]. Most of the deNO_x activity is believed to occur on the Fe-BEA (Figure 4) for the combined systems. Thus, the somewhat low NH_3 conversion seen for the combined system (Figure 5) can be explained by an overstoichiometric dosing of NH_3 due to unreacted NH_3 present in the H_2 stream from the NH_3 to H_2 cracker (Figure 1). Ag-only, on the other hand, showed lower values at up to 270°C (0.4-0.6); at higher temperatures, the NH_3 conversion was negative and the NO_x conversion was slightly negative giving large positive values. The low NH_3/NO_x ratio for Ag-only indicates that it is not only the main SCR reactions that were responsible for the NO_x conversion.

Figure 6 shows the NO, NO_2, NO_x and NH_3 concentrations for Ag-only. NO_2 concentrations in and out were a bit higher, and NH_3 in was a bit lower relative to total NO_x compared to the other layouts. The inlet NO_2 level was very high, it is typically expected that some 10% of the total NO_x is NO_2. Here, the levels were up to 60% at the lowest temperatures and 18-20% at 400°C. The high NO_2 levels are attributed to the high EGR rate, 60, 50, 40, 30, 20 and 20% seen for the six temperature points, respectively (low to high temperature). The air fuel ratios (AFR) roughly had the same values as the EGR rate. EGR lowers the peak temperature in the engine cylinders and thus the NO_x level [2]. However, NO_2 has been reported not to be affected to a larger extent which will increase the NO_2/NO_x ratio [30–32]. NO_x was primarily removed as NO_2 at the lowest temperatures (<250°C) (Figure 6). NO was produced over Ag-only from 220°C and up by NO_2 to NO reduction. A close resemblance between NO_x conversion and NO_2 level for Ag-only (Figure 4 and Figure 6) can be seen. Figure 7 shows the NO_2/NO_x ratio and NO_x conversion for Ag-only; there was a clear likeness of the two at temperatures above 200°C, indicating a relation between the two. This was not seen for any of the other layouts (not shown).

Fe-BEA has, as other Fe-zeolites, been reported to be very active when equimolar amounts of NO_2 and NO are co-fed, so called “fast-SCR” [6], [22]. The high NO_2/NO_x ratio allowing fast-SCR, which makes Fe-BEA more active than Ag/Al_2O_3, is believed to be the reason for the high deNO_x activity seen for Fe-only and why Fe-BEA was preferred as the upstream catalyst (dual-brick-Fe/Ag) in the combined systems. Having Ag/Al_2O_3 upstream will mean that less NO_2 is present for fast-SCR over the Fe-BEA with a lower system deNO_x activity as the consequence. Fast-SCR has also been reported to suppress NH_3 oxidation [22]. Our previous study [21] did, in contrast to this study, only have NO present as the NO_x compound. NO to NO_2 oxidation over Ag/Al_2O_3 which could later react over the Fe-BEA was, together with unselective NH_3 oxidation over Fe-BEA, believed to be the reasons why Ag/Al_2O_3 was preferred as the upstream catalyst in the previous study. The difference in feed gas composition is believed to explain the difference seen between the two studies.

The NH_3 outlet concentration was higher than the inlet concentration at above 300°C, indicating NH_3 formation. Since all points are taken at steady-state and that the same analysis equipment was used for both inlet and outlet measurements, experimental errors can be excluded. Still, a simple N-balance between inlet and outlet NO_x and NH_3 shows an excess of N-containing species at the outlet, this can be considered close to the experimental uncertainty. NH_3 formation over Ag/Al_2O_3 has been reported in the

literature [33–37]. The NH_3 formation was in these studies attributed to the reaction of NO with H_2 [33], [34], hydrolysis of N-containing hydrocarbons (without H_2) [35] or reaction of HC and NO_x [36]. In a preliminary test prior to the one reported here, NH_3 formation was observed during transient testing. No conclusive NH_3 formation could be seen in the present test. The difference between the preliminary test and the present test was the HC level. DiMaggio et al. [36] showed that NH_3 formation is dependent on H_2 level, temperature and C:N ratio. The higher HC level in the preliminary test (up to 2-2.5 times higher) could therefore be the reason why NH_3 formation was seen in that test and not in the present one. NH_3 formed over an upstream catalyst and then stored on the downstream catalyst, e.g. Fe-BEA, is similar to what has been proposed for combined LNT and SCR systems [38]. It can be a very interesting way to boost low-temperature activity and the potential problem of urea decomposition and formation of deposits at temperatures <190°C [3]. Thus, further investigation of the potential NH_3 formation over Ag/Al_2O_3 is interesting but beyond the scope of this study.

This study also wanted to investigate if the hydrocarbons present in the exhaust could contribute to the total NO_x conversion by HC-SCR. Sitshebo et al. [28] reported that unburned HC present in the exhaust could give a noticeable NO_x conversion; especially when H_2 was present. It should be noted that the 4 wt% Ag catalyst used here might not be suited for HC-SCR. An optimal Ag loading for HC-SCR is often reported to be around 2 wt% [14], [25], [26]. No larger HC conversion over Ag/Al_2O_3 (Ag-only) was seen. Fe-BEA (Fe-only), on the other hand, showed a higher HC conversion, and it is reasonable to believe that the HC conversion seen for the combined systems comes from the Fe-BEA. Given the low NO_x conversion over Ag-only and the low ratio of reacted NH_3 to NO_x, HC-SCR might still contribute. The low NO_x and HC conversion, however, makes it hard to clearly see this.

The set-points for ammonia (ANR) and hydrogen dosing (HNR) were 0.8 and 2, respectively. The actual amount of NH_3 dosed was higher (Figure 6), especially when both NH_3 and H_2 were dosed due to the unreacted NH_3 in the stream from the cracker. It was even a bit higher for the combined systems (not shown). An overdosing of NH_3 is believed not to affect Ag/Al_2O_3 [18]. However, it might affect Fe-BEA and thus the combined systems [4–6], [39]. Since no measurement of H_2 was possible, the actual amount dosed can only be estimated indirectly. The H_2 level was estimated both based on the given set-point to the H_2 dosing system and the amount of unreacted NH_3 in the stream from the cracker. Both estimations gave similar results. The difference in NH_3 concentration seen when both NH_3 and H_2 was dosed compared to only NH_3 is also an evidence that H_2 was in fact dosed. The estimated H_2 level dosed was a bit low due to the maximum NH_3 cracking capacity limit of the cracker system. In the worst cases (at 220°C), the H_2/NO_x ratio was 1 (set-point HNR 2), in most other cases 1.4-1.6. The lack of H_2 will affect the activity, since Ag/Al_2O_3 is sensitive to H_2 concentration; especially in the region 200-300°C [18] and can partly explain the low activity over Ag/Al_2O_3.

As stated above, the performance of Ag/Al_2O_3 was lower than expected, both in Ag-only and in the combined layouts. It was also unexpected that the NO_x conversion was very similar whether or not H_2 was co-fed. There was also an apparent relation between NO_2/NO_x ratio and NO_x conversion. Three possible explanations can be proposed: 1) a H_2 deficit of over the Ag/Al_2O_3, only allowing NO_x reduction via NO_2 [17]; 2) the catalyst was deactivated, not allowing the expected H_2-assisted NH_3 SCR to commence; and 3) the presence of NO_2 inhibits the performance of the catalyst. The latter could indirectly be due to NO_2 poisoning of NO active sites [14].

The H_2 concentration was low, as stated above, which will affect the activity of Ag/Al_2O_3 in a highly negative way. However, it should be high enough to show a higher difference in activity between NH_3 and H_2 dosing and only NH_3 dosing. Whether H_2 was available over the whole catalysts or not cannot, however, be concluded from these tests. Excessive H_2 oxidation in the first part of the catalyst brick would give a H_2 deficit downstream. Several reports have shown that replacing NO with NO_2, either completely or partially, as the NO_x compound reduces the NO_x conversion for HC-SCR, with or without H_2 present [13], [14], [40]. Other reports, on the other hand, have shown the opposite, they also showed that bare Al_2O_3 was active when NO_2 was fed [41], [42]. A difference between the cited reports is the HC species used. The reports showing a positive effect [41], [42] both used propene, while those showing no or negative effect ([13], [14], [40]) used saturated alkanes (propane or decane), which might affect the results. The HC present in the exhaust is a close match to the composition of the diesel fuel with mainly longer straight HC species. We have recently shown that Ag/Al_2O_3 (and Al_2O_3) was active for NH_3-SCR (without H_2), when mixtures of NO and NO_2 are used [17]. The activity was, however, much lower than for H_2-assisted NH_3-SCR of NO and limited to a maximum of 30% NO_x conversion regardless of NO_2/NO_x ratio. The stability of the catalyst during operation is of course crucial for it to be of any real interest, and the possibility of deactivation of the Ag/Al_2O_3 has to be considered. The catalyst in the study had been used in a previous preliminary test sequence and it had then been stored in air.

To investigate the possible reasons for the low NO_x conversion seen, a core sample of the brick used for engine testing was taken. The first noticeable thing was the low weight of the sample which corresponded to a coat loading of only 60% of the expected weight. This points to the monolith brick having a non-uniform coat (the sample was taken from the inlet of the brick); there was some channel blocking that will contribute to this meaning that the coat loading of the part of the monolith available for SCR, excluding blocked channels, was low giving a low specific coat loading of the monolith. The low specific coat loading will in itself affect the $deNO_x$ performance, since Ag/Al_2O_3 is sensitive to GHSV. Figure 8 shows a comparison of standard tests, before and after attempted regeneration. The standard test in the lab-scale reactor showed that the catalyst was almost completely inactive; it only started to show activity at 400°C. However, a second test following the first one showed that the catalyst had been reactivated. The activity was still low; NO_x conversion below 15%. The catalyst was heated to 500°C in the reactor in the presence of 1000 ppm H_2, 9% O_2 and balance N_2 to further try to regenerate it. No difference was seen in activity, and the catalyst was heated to 550°C for 4 h in an oven in an atmosphere of air to burn off soot. After the treatment, the catalyst was completely “clean” and showed no visible traces of soot. The first standard test after the oven treatment showed a small gain in NO_x conversion. A second test showed a somewhat lower NO_x conversion comparable to that before the regeneration attempts of the sample. Prior to the lab-scale and the engine bench testing, the catalyst had been stored in air for some weeks. Oxidation of Ag could be one of the deactivation mechanisms seen. Oxidized Ag can be reduced at temperatures below 450°C, i.e. during the first standard $deNO_x$ test [14], [40]. Soot is oxidized by NO_2 in the temperature range of 250-400°C [43], which could explain the increase seen in NO out during engine testing. NO_2 from H_2 induced NO oxidation being able to oxidize soot might be the reason for the reactivation seen in Figure 8.

Figure 9 shows the influence of NO_2/NO_x ratio for a 4 wt% Ag/Al_2O_3 sample. The activity of the sample during a standard test (no NO_2) was enhanced after the NO_2/NO_x testing campaign compared to before. The higher activity was also seen in later tests and the activation is considered permanent. It is, therefore, concluded that the catalyst needs to be activated before it reaches its maximum activity, similar to what

was found in our previous study [20]. In that study we investigated the sulfur tolerance of Ag/Al_2O_3 catalysts and related an increased activity for high Ag loading samples to activation by sulfur. The results of this study show that testing under standard $deNO_x$ conditions is, in itself, enough to activate the catalyst. It is speculated that this need for de-greening is related to dispersion and possibly the state of Ag on the catalyst. Further investigations with a similar protocol as in [20] is needed to fully understand the de-greening effect. The presence of NO_2 increased the activity below 250°C and above 300°C when H_2 was co-fed, the effect was largest at the lowest and highest temperatures tested. The first test conducted was the one with an NO_2/NO_x ratio of 0.5 which showed a lower activity than the other tests. This lower activity is believed to be related to the sample not being fully activated, it might be that the activation is related to or enhanced by the presence of NO_2. We have previously speculated that NO to NO_2 oxidation is an important step in the reaction mechanism of NO reduction [17]. The results in this study seem to support that conclusion. The $deNO_x$ activity was very low, when no H_2 was co-fed, and it was not dependent of the NO_2 level, except at 150°C, where the NO_2/NO_x ratio of 0.95 showed a much higher conversion, and 0.75 showed a somewhat higher NO_x conversion (Figure 9 b). Since the difference in activity was larger between no NO_2 at all and 0.25 or 0.95 NO_2/NO_x it is concluded that smaller quantities of NO_2 is enough to enhance the activity. It is not unreasonable to have 25% NO_2 in the exhaust; either from the engine as in this study or after a DOC [1].

Based on the results in Figure 9 a complete lack of H_2 over the catalyst does not seem to be the cause for the low NO_x conversion seen for Ag-only in the engine testing (Figure 4 and Figure 7). If no H_2 was present the NO_x conversion below 250°C should have been lower and it should have been higher at higher temperatures given the NO_2/NO_x ratios in the engine tests. It is concluded that the lower than expected $deNO_x$ activity seen for Ag/Al_2O_3, both in Ag-only and the combined systems, comes from catalyst deactivation related to soot and possibly Ag oxidation, the lower H_2 than was intended and low specific catalyst coat loading giving a high GHSV. The presence of NO_2 in the engine exhaust is believed to explain the relatively high NO_x conversion seen when no H_2 was fed.

3.2 Transient tests

Figure 10 shows the NO_x distribution over different temperature intervals for the NEDC. The conditions were, as seen, very demanding for SCR with more than 50% of the total NO_x emitted being emitted below 150°C and only 32% above 200°C. Table 2 shows the gas composition during the NEDC. A further implication of the low temperature was NH_3 and H_2 dosing. In the standard case, NH_3 and H_2 were dosed when the temperature was above 150°C. The temperature was stable above 150°C after around 830 s. In another case, dosing started when the temperature was above 120°C (after 250 s) to investigate the potential benefit of earlier NH_3 and H_2 dosing.

Figure 11 shows the accumulated NO_x at the outlet of the tested catalyst layouts. The inlet NO_x amount (measured with the reference MEXA) varied somewhat compared to the reference test. With the difference in the inlet NO_x taken into account, the total NO_x conversion over the cycles was 22, 15, 18 and 22% for Ag-only, Fe-only, dual-brick-Fe and dual-brick-Ag, respectively. This was a small change compared to what is reported in Figure 11. However, the difference can be assumed to be within the margin of experimental error. There was a large increase in emitted NO_x after around 1100 s of the cycle corresponding to highway driving and the highest engine load (Figure 2). Since this large increase in emitted NO_x corresponds to the highest temperatures, a large NO_x conversion can be expected. However, the high load resulted in a large

increase in GHSV, from maximum 30000 h^{-1} during urban driving to 70000 h^{-1} during the highway part. Ag/Al_2O_3 is sensitive to GHSV [27], [29], [44], and a GHSV of 70000 h^{-1} is high. Another issue was NH_3 and H_2 dosing. Due to inconsistent measurements from the NO_x sensors, the level dosed varied. The amount of NH_3 dosed varied between 0.3 and 2 times the NO_x concentration between the start of dosing (after around 830 s) and 1100 s and down to 0.2 of NO_x at the highest flows and temperatures (the set-point was 0.8). H_2 dosing was estimated (no H_2 analysis was available) to be between 0.8 and 2 times the NO_x concentration between the start of dosing and 1100 s and down to 0.2 of NO_x at the highest flows and temperatures (the set-point was 2). Thus, there was a clear shortage of NH_3 and H_2 available for the SCR reaction, when the temperature and emitted NO_x was at their highest, severely affecting the SCR activity. Figure 12 shows this as the drop in the total NO_x conversion after 1100 s.

By looking more closely at the accumulated NO_x profiles (Figure 11) and instantaneous total NO_x conversion (Figure 12) they can roughly be divided into three different parts: The first part was 0-250 s of the NEDC, which is almost one and a half urban cycles. In this part the performance was dual-brick-Ag/Fe ≈ dual-brick-Fe/Ag > Ag-only >> Fe-only. The second part was 250-1000 s, urban driving and first part of high-way driving, the temperature was <180°C; performance was dual-brick-Ag/Fe > dual-brick-Fe/Ag > Ag-only > Fe-only. The last part was >1000 s; in this part dual-brick-Ag/Fe did no longer perform better than the other layouts; the order was instead Ag-only > Fe-only ≈ dual-brick-Ag/Fe ≈ dual-brick-Fe/Ag. The difference mainly occurred when the temperature was at its highest (220-240°C). Given the fact that no NH_3 or H_2 was dosed until the temperature reached 150°C (after 830 s) and the low temperatures during the NEDC, it seems unlikely that SCR was responsible for the relatively high NO_x conversion seen in the early stages of the cycle. A 37% total NO_x conversion was e.g. seen for dual-brick-Ag/Fe after 250 s with a temperature that only reached maximum 140°C. Even though NH_3 was present on the catalyst surface at the start of the NEDC from previous testing, it seems unlikely that any H_2 would be present. The fact that NH_3 was present at the start of the cycle could be seen as a slow but steady release of NH_3, as the temperature was gradually increased (not shown). NH_3-TPD confirmed that NH_3 would still be present at both Fe-BEA (not shown) and Ag/Al_2O_3 (Figure 13 b) given the temperatures seen by the catalysts prior to the NEDC (160-270°C). With the high NO_2/NO_x ratios shown (Table 2) and the presence of NH_3 over the catalysts, SCR over Fe-BEA is a possibility. The low activity of Fe-only contradicts this theory. Another possible explanation to the NO_x conversion seen at low temperatures is NO_x storage over the catalysts.

Even though Fe-BEA has been reported to store small amounts of NO_x [5], [45], the H_2O present in the exhaust is believed to inhibit the storage making this insignificant [5]. Ag/Al_2O_3 has also been reported to be able to store NO_x [46–50], it has even been considered as NO_x storage catalyst due to its supposedly good storage capabilities [51]. It is vital that O_2 is present during adsorption to allow oxidation of NO to ad-NO_x species. NO-TPD was performed for Ag/Al_2O_3 to investigate the potential of NO_x storage (adsorption at 40°C), Figure 13 a). Since all catalysts had been used in NO_x containing streams at relatively low temperature (160-270°C), peak 2 can be assumed to be filled at the start of the cycle and it is only NO_x adsorption peak 1 that is considered to play a larger role during NEDC. The NO_x adsorption capacity from the TPD-results was enough to explain the results seen during NEDC. However, the TPD was performed under dry conditions and H_2O will lower the NO_x storage capacity. Brosius et al. [46] showed a noticeable adsorption capacity when NO was replaced by NO_2 even when H_2O was present. With the results presented in literature [46], [51], NO_x storage over Ag/Al_2O_3 is believed to be a valid explanation of the NO_x conversion seen at temperatures below 140-160°C during the NEDC in this study.

Figure 14 shows the inlet and outlet NO_x levels for the tested systems. The NO_x level was in all cases higher or equal at the catalyst inlet compared to the outlet, i.e. no excessive desorption of NO_x during the cycle. The difference between Ag/Al_2O_3 and Fe-BEA was emphasized. It is clearly seen that Ag-only and the combined layouts showed NO_x conversion right from the start of the NEDC, whereas Fe-only showed NO_x outlet levels closer to the inlet levels. Again this indicates NO_x storage over Ag/Al_2O_3 as the main mechanism behind the NO_x conversion seen. The temperature never reached higher than 250°C during the cycle, meaning that part of the NO_x stored on the catalysts likely remained even after the cycle. However, the main part of the NO_x stored will be desorbed during the ramp up in temperature starting after around 950 s. When the temperature increases, so does the activity of the catalysts; this should be seen as a lower NO_x level after the catalysts. However, the NO_x level after the catalyst was similar to the level before the catalysts from 1000 s of the cycle. We believe that two facts are responsible: 1) the GHSV increases with the temperature which will lower the activity of the Ag/Al_2O_3; and 2) the NO_x desorbed from the catalysts gives a higher NO_x level over the catalyst than that of the feed; this excessive NO_x reacts over the catalysts meaning that the NO_x level over the catalyst was higher than expected but still not higher than the inlet level. In other words, the increase in NO_x from desorption was compensated for by the SCR reaction. A NO_x-level that is higher than the feed will also lead to shortage of NH_3 and H_2, since these are dosed based on inlet NO_x-level, further limiting possible NO_x conversion. Catalyst models and advanced dosing algorithms can compensate for this but is beyond the scope of this study.

While NO_x storage is believed to be the main cause of NO_x conversion during the first two identified parts of the NEDC (0-250 s and 250-1000 s), SCR of NO_x seems to be the best explanation for the NO_x conversion seen in the last phase, since the rapid temperature rise would desorb NO_x rather than adsorb and store it as believed at the earlier phases. This implies that Ag/Al_2O_3 not only stores NO_x better than Fe-BEA, it also shows a higher SCR activity under NEDC conditions. However, the results indicate synergistic effect of combining Ag/Al_2O_3 and Fe-BEA during parts of the cycle. HC was stored on Ag/Al_2O_3 during the low temperature parts of the cycle and then released, as the temperature increased during the latter part of the NEDC. The total HC conversion over the cycle was 27, 73, 14 and 29% for Ag-only, Fe-only, dual-brick-Fe/Ag and dual-brick-Ag/Fe, respectively. HC-SCR might therefore contribute to the NO_x conversion seen. HC-SCR could be one reason for the advantage of having Ag/Al_2O_3 upstream of Fe-BEA. Another could be that excessive NH_3 adsorption on Fe-BEA hinders the activity over the downstream Ag/Al_2O_3 due to a NH_3 deficit. A step response test in the laboratory set-up (0 to 300 ppm NH_3) showed that the NH_3 adsorption capacity of Fe-BEA was large enough to give a large delay in NH_3 exiting the catalyst which could potentially affect the performance of the Ag/Al_2O_3, when the latter was placed downstream of the former.

Dosing of NH_3 and H_2 already from 120°C (after 250 s) compared to dosing from 150°C (after 830 s) did not give any difference in the total NO_x conversion for the combined layouts. Again, indicating that it was not the SCR reaction that was responsible for the NO_x conversion during the main part of the NEDC. However, a detailed investigation of total NO_x conversion as a function of time (Figure 15) showed interesting results. The decline in NO_x conversion was more rapid up to approximately 400 s of the cycle, when dosing started at 120°C as compared to at 150°C; also seen as a steeper increase in the accumulated NO_x curves (not shown). After approximately 400 s, the NO_x conversion increased, and in the end it reached the same value as in the 150°C dosing case. This is explained as follows: Up to 400 s, NH_3 inhibits NO_x storage and possibly fast-SCR [39]. When the catalyst has been warmed up, there is some SCR activity in addition to NO_x storage, seen as the increase in NO_x conversion. When dosing also starts in the original dosing case, both strategies

show the same NO_x conversion. We believe that by optimizing the dosing further, the negative effect of NH_3 can be removed, and a higher total NO_x conversion could be reached. It can thus be concluded that there is some SCR activity even at temperatures down to 120°C.

4 Conclusions

Stationary engine tests showed that a combination of Ag/Al_2O_3 and Fe-BEA gave the highest deNO_x activity below 270°C, while Fe-BEA only was preferred at higher temperatures. For the combined systems, it was preferred to have Fe-BEA in an upstream position of Ag/Al_2O_3 compared to the opposite. The high engine out NO_2/NO_x ratio giving fast-SCR over the Fe-BEA was believed to be the reason. At low temperatures, the activity over the combined systems was higher than that of the individual catalysts showing that combining Ag/Al_2O_3 and Fe-BEA gave synergy effects. Ag/Al_2O_3 showed an unexpectedly low activity which we attribute to deactivation by soot and/or Ag oxidation, low H_2 levels and low specific catalyst loading. Fresh Ag/Al_2O_3 catalysts showed a high activity in laboratory scale tests. The catalyst was activated by subsequent test runs pointing to the need to de-green the catalyst prior to using it. The mechanism and a more precise de-greening protocol need to be investigated further. The catalytic activity below 250 and above 300°C was enhanced by addition of NO_2 as part of the NO_x. An NO_2 level of 25% was enough to give the enhancement; increasing NO_2 only showed a small effect.

Transient NEDC tests also showed synergistic effects when combining Ag/Al_2O_3 and Fe-BEA. However, the overall cycle NO_x conversion was low. It should be noted that the conditions for SCR were very tough during the NEDC with 50% of the total emitted NO_x being emitted below 150°C and only 32% above 200°C, which severely affects the possibility for SCR. The order of performance based on overall conversion was dual-brick-Ag/Fe = Ag-only > dual-brick-Fe/Ag > Fe-only. The performance varied during different parts of the NEDC. The dual-brick layouts performed best at the lowest temperatures and before any NH_3 or H_2 was dosed, and Ag-only performed best when the temperature was highest. The latter was related to a higher SCR activity. The low overall NO_x conversion seen is partly related to the same reasons as those for the stationary tests: deactivation by soot and/or Ag oxidation, low H_2 levels and low specific catalyst loading of the Ag/Al_2O_3. The high GHSV during the highway part of the cycle also contributed to the low SCR activity. The Ag/Al_2O_3 containing layouts showed a noticeable NO_x conversion from the start of the cycle, i.e. before any NH_2 or H_2 was dosed. We believe that the NO_x conversion seen comes from NO_x storage on the Ag/Al_2O_3.

The Ag/Al_2O_3 – Fe-BEA system shows potential, but further studies are needed. Tests with a higher catalyst volume and DPF filter should be conducted to obtain a lower GHSV and avoid poisoning by soot. An advanced dosing algorithm should also be developed that includes NO_x adsorption and desorption for a more accurate NH_3 and H_2 dosing.

Acknowledgements

This work was supported by The Danish Council for Strategic Research through grant 09-067233. Magnus Skoglundh, Louise Olsson and Stefanie Tamm from Competence Centre of Catalysis at Chalmers University of Technology are gratefully acknowledged for valuable discussions. Amminex A/S is gratefully acknowledged for supplying the NH_3 and H_2 dosing system. Thanks also to Magnus Lewander and his team

at Topsøe Engine test center for their help with the engine-bench testing and to Susanne Friis Madsen for proof reading of the manuscript.

References

[1] T. V Johnson, “Vehicular Emissions in Review,” *SAE International Journal of Engines*, vol. 5, no. 2, pp. 216–234, 2012.

[2] M. K. Khair and H. Jääskeläinen, “Exhaust Gas Recirculation,” *DieselNet Technology Guide*, 2012. [Online]. Available: http://www.dieselnet.com/tech/engine_egr.php. [Accessed: 06-Mar-2013].

[3] T. V Johnson, “Review of diesel emissions and control,” *International Journal of Engine Research*, vol. 10, no. June, pp. 275–285, Oct. 2009.

[4] S. Brandenberger, O. Kröcher, A. Tissler, and R. Althoff, “The State of the Art in Selective Catalytic Reduction of NOx by Ammonia Using Metal-Exchanged Zeolite Catalysts,” *Catalysis Reviews*, vol. 50, no. 4, pp. 492–531, Oct. 2008.

[5] K. Kamasamudram, N. W. Currier, X. Chen, and A. Yezerets, “Overview of the practically important behaviors of zeolite-based urea-SCR catalysts, using compact experimental protocol,” *Catalysis Today*, vol. 151, no. 3–4, pp. 212–222, Jun. 2010.

[6] M. Colombo, I. Nova, and E. Tronconi, “A comparative study of the NH3-SCR reactions over a Cu-zeolite and a Fe-zeolite catalyst,” *Catalysis Today*, vol. 151, no. 3–4, pp. 223–230, Jun. 2010.

[7] P. S. Metkar, M. P. Harold, and V. Balakotaiah, “Selective catalytic reduction of NOx on combined Fe- and Cu-zeolite monolithic catalysts: Sequential and dual layer configurations,” *Applied Catalysis B: Environmental*, vol. 111–112, pp. 67–80, Sep. 2011.

[8] D. W. Fickel, E. D. Addio, J. A. Lauterbach, and R. F. Lobo, “The ammonia selective catalytic reduction activity of copper-exchanged small-pore zeolites,” *Applied Catalysis B: Environmental*, vol. 102, no. 3–4, pp. 441–448, 2011.

[9] S. J. Schmieg, S. H. Oh, C. H. Kim, D. B. Brown, J. H. Lee, C. H. F. Peden, and D. Heui, “Thermal durability of Cu-CHA NH3-SCR catalysts for diesel NOx reduction,” *Catalysis Today*, vol. 184, no. 1, pp. 252–261, 2012.

[10] C. N. Costa and A. M. Efstathiou, “Low-temperature H2-SCR of NO on a novel Pt/MgO-CeO2 catalyst,” *Applied Catalysis B: Environmental*, vol. 72, no. 3–4, pp. 240–252, Mar. 2007.

[11] M. Leicht, F. J. P. Schott, M. Bruns, and S. Kureti, “NOx reduction by H2 on WOx/ZrO2-supported Pd catalysts under lean conditions,” *Applied Catalysis B: Environmental*, vol. 117–118, no. 2, pp. 275–282, May 2012.

[12] S. Satokawa, “Enhancing the NO/C3H8/O2 Reaction by Using H2 over Ag/Al2O3 Catalysts under Lean-Exhaust Conditions.,” *Chemistry Letters*, vol. 3, no. 3, pp. 294–295, 2000.

[13] S. Satokawa, J. Shibata, K. Shimizu, A. Satsuma, and T. Hattori, “Promotion effect of H2 on the low temperature activity of the selective reduction of NO by light hydrocarbons over Ag/Al2O3,” *Applied Catalysis B: Environmental*, vol. 42, no. 2, pp. 179–186, May 2003.

[14] M. Richter, U. Bentrup, R. Eckelt, M. Schneider, M.-M. Pohl, and R. Fricke, “The effect of hydrogen on the selective catalytic reduction of NO in excess oxygen over Ag/Al2O3,” *Applied Catalysis B: Environmental*, vol. 51, no. 4, pp. 261–274, Aug. 2004.

[15] M. Richter, R. Fricke, and R. Eckelt, “Unusual Activity Enhancement of NO Conversion over Ag/Al2O3 by Using a Mixed NH3/H2 Reductant Under Lean Conditions,” *Catalysis Letters*, vol. 94, no. 1/2, pp. 115–118, Apr. 2004.

[16] K. Shimizu and A. Satsuma, “Hydrogen assisted urea-SCR and NH3-SCR with silver–alumina as highly active and SO2-tolerant de-NOx catalysis,” *Applied Catalysis B: Environmental*, vol. 77, no. 1–2, pp. 202–205, Nov. 2007.

[17] D. E. Doronkin, S. Fogel, S. Tamm, L. Olsson, T. S. Khan, T. Bligaard, P. Gabrielsson, and S. Dahl, "Study of the 'Fast SCR'-like mechanism of H2-assisted SCR of NOx with ammonia over Ag/Al2O3," *Applied Catalysis B: Environmental*, vol. 113–114, pp. 228–236, Feb. 2012.

[18] S. Tamm, S. Fogel, P. Gabrielsson, M. Skoglundh, and L. Olsson, "The effect of the gas composition on hydrogen-assisted NH3-SCR over Ag/Al2O3," *Applied Catalysis B: Environmental*, vol. 136–137, pp. 168–176, Jun. 2013.

[19] D. E. Doronkin, T. Suvra, T. Bligaard, S. Fogel, P. Gabrielsson, and S. Dahl, "Sulfur poisoning and regeneration of the Ag/g-Al2O3 catalyst for H2-assisted SCR of NOx by ammonia," *Applied Catalysis B: Environmental*, vol. 117–118, pp. 49–58, 2012.

[20] S. Fogel, D. E. Doronkin, P. Gabrielsson, and S. Dahl, "Optimisation of Ag loading and alumina characteristics to give sulphur-tolerant Ag/Al2O3 catalyst for H2-assisted NH3-SCR of NOx," *Applied Catalysis B: Environmental*, vol. 125, pp. 457–464, 2012.

[21] S. Fogel, D. E. Doronkin, J. W. Høj, P. Gabrielsson, and S. Dahl, "Combination of Ag/Al2O3 and Fe-BEA for High-Activity Catalyst System for H2-Assisted NH3-SCR of NOx for Light-Duty Diesel Car Applications," *Topics in Catalysis*, vol. 56, no. 1, pp. 14–18, Feb. 2013.

[22] P. Balle, B. Geiger, and S. Kureti, "Selective catalytic reduction of NOx by NH3 on Fe/HBEA zeolite catalysts in oxygen-rich exhaust," *Applied Catalysis B: Environmental*, vol. 85, no. 3–4, pp. 109–119, Jan. 2009.

[23] W. A. Majewski, "What Are Diesel Emissions," *DieselNet Technology Guide*, 2012. [Online]. Available: http://www.dieselnet.com/tech/emi_intro.php. [Accessed: 06-Mar-2013].

[24] K. Masuda, K. Tsujimura, K. Shinoda, and T. Kato, "Silver-promoted catalyst for removal of nitrogen oxides from emission of diesel engines," *Applied Catalysis B: Environmental*, vol. 8, no. 1, pp. 33–40, Feb. 1996.

[25] L.-E. Lindfors, K. Eränen, F. Klingstedt, and D. Y. Murzin, "Silver/alumina catalyst for selective catalytic reduction of NOx to N2 by hydrocarbons in diesel powered vehicles," *Topics in Catalysis*, vol. 28, no. 1–4, pp. 185–189, 2004.

[26] F. Klingstedt, K. Eränen, L.-E. Lindfors, S. Andersson, L. Cider, C. Landberg, E. Jobson, L. Eriksson, T. Ilkenhans, and D. Webster, "A Highly Active Ag/Alumina Catalytic Converter for Continuous HC-SCR During Lean-Burn Conditions: From Laboratory to Full-Scale Vehicle Tests," *Topics in Catalysis*, vol. 30/31, no. 1–4, pp. 27–30, Jul. 2004.

[27] M. B. Viola, "HC-SCR Catalyst Performance in Reducing NOx Emissions from a Diesel Engine Running Transient Test Cycles," *SAE Technical paper series*, no. 2008–01–2487, 2008.

[28] S. Sitshebo, A. Tsolakis, and K. Theinnoi, "Promoting hydrocarbon-SCR of NOx in diesel engine exhaust by hydrogen and fuel reforming," *International Journal of Hydrogen Energy*, vol. 34, no. 18, pp. 7842–7850, Sep. 2009.

[29] K. Kim, K. M. Chun, S. Song, H. S. Han, and H. Gu, "Hydrogen Effect on the DeNOx Efficiency Enhancement of Fresh and Aged Ag/Al2O3 HC-SCR in a Diesel Engine Exhaust," *SAE International*, no. 2011–01–1278, 2011.

[30] M. J. Pipho, D. B. Kittelson, and D. D. Zarling, "NO2 Formation in a Diesel Engine," *SAE Technical paper series*, no. 910231, 1991.

[31] H. Yamada, K. Misawa, D. Suzuki, K. Tanaka, J. Matsumoto, M. Fujii, and K. Tanaka, "Detailed analysis of diesel vehicle exhaust emissions: Nitrogen oxides, hydrocarbons and particulate size distributions," *Proceedings of the Combustion Institute*, vol. 33, no. 2, pp. 2895–2902, Jan. 2011.

[32] J. J. Chong, A. Tsolakis, S. S. Gill, K. Theinnoi, and S. E. Golunski, "Enhancing the NO2/NOx ratio in compression ignition engines by hydrogen and reformate combustion, for improved aftertreatment performance," *International Journal of Hydrogen Energy*, vol. 35, no. 16, pp. 8723–8732, Aug. 2010.

[33] K. Shimizu, J. Shibata, and A. Satsuma, "Kinetic and in situ infrared studies on SCR of NO with propane by silver–alumina catalyst: Role of H2 on O2 activation and retardation of nitrate poisoning," *Journal of Catalysis*, vol. 239, no. 2, pp. 402–409, Apr. 2006.

[34] J. P. Breen, R. Burch, C. Hardacre, C. J. Hill, and C. Rioche, “A fast transient kinetic study of the effect of H2 on the selective catalytic reduction of NOx with octane using isotopically labelled 15NO,” *Journal of Catalysis*, vol. 246, no. 1, pp. 1–9, Feb. 2007.

[35] K. Eränen, F. Klingstedt, K. Arve, L.-E. Lindfors, and D. Y. Murzin, “On the mechanism of the selective catalytic reduction of NO with higher hydrocarbons over a silver/alumina catalyst,” *Journal of Catalysis*, vol. 227, no. 2, pp. 328–343, Oct. 2004.

[36] C. L. DiMaggio, G. B. Fisher, K. M. Rahmoeller, and M. Sellnau, “Dual SCR Aftertreatment for Lean NOx Reduction,” *SAE International Journal of Fuels and Lubricants*, vol. 2, no. 1, pp. 66–77, 2009.

[37] S. J. Schmieg, T. M. Sloane, and R. J. Blint, “Catalysts for lean-burn engine exhaust aftertreatment using hydrocarbon selective catalytic reduction,” *SAE International Journal of Fuels and Lubricants*, vol. 2, no. 2, pp. 323–336, 2009.

[38] B. Pereda-Ayo, D. Duraiswami, and J. R. González-Velasco, “Control of NOx storage and reduction in NSR bed for designing combined NSR–SCR systems,” *Catalysis Today*, vol. 172, no. 1, pp. 66–72, Aug. 2011.

[39] A. Grossale, I. Nova, and E. Tronconi, “Ammonia blocking of the ‘Fast SCR’ reactivity over a commercial Fe-zeolite catalyst for Diesel exhaust aftertreatment,” *Journal of Catalysis*, vol. 265, no. 2, pp. 141–147, Jul. 2009.

[40] P. Sazama, L. Capek, H. Drobna, Z. Sobalik, J. Dedecek, K. Arve, and B. Wichterlova, “Enhancement of decane-SCR-NO over Ag/alumina by hydrogen. Reaction kinetics and in situ FTIR and UV–vis study,” *Journal of Catalysis*, vol. 232, no. 2, pp. 302–317, Jun. 2005.

[41] K. A. Bethke and H. H. Kung, “Supported Ag Catalysts for the Lean Reduction of NO with C3H6,” *Journal of Catalysis*, vol. 172, pp. 93–102, 1997.

[42] F. C. Meunier and J. R. H. Ross, “Effect of ex situ treatments with SO2 on the activity of a low loading silver–alumina catalyst for the selective reduction of NO and NO2 by propene,” *Applied Catalysis B: Environmental*, vol. 24, no. 1, pp. 23–32, Jan. 2000.

[43] M. V Twigg, “Catalytic control of emissions from cars,” *Catalysis Today*, vol. 163, no. 1, pp. 33–41, Apr. 2011.

[44] S. J. Schmieg, R. J. Blint, and L. Deng, “Control strategy of the removal of NOx from diesel engine exhaust using hydrocarbon selective catalytic reduction,” *SAE International Journal of Fuels and Lubricants*, vol. 1, no. 1, pp. 1540–1552, 2008.

[45] D. Klukowski, P. Balle, B. Geiger, S. Wagloehner, S. Kureti, B. Kimmerle, a. Baiker, and J.-D. Grunwaldt, “On the mechanism of the SCR reaction on Fe/HBEA zeolite,” *Applied Catalysis B: Environmental*, vol. 93, no. 1–2, pp. 185–193, Nov. 2009.

[46] R. Brosius, K. Arve, M. Groothaert, and J. Martens, “Adsorption chemistry of NOx on Ag/Al2O3 catalyst for selective catalytic reduction of NOx using hydrocarbons,” *Journal of Catalysis*, vol. 231, no. 2, pp. 344–353, Apr. 2005.

[47] J. Li, Y. Zhu, R. Ke, and J. Hao, “Improvement of catalytic activity and sulfur-resistance of Ag/TiO2–Al2O3 for NO reduction with propene under lean burn conditions,” *Applied Catalysis B: Environmental*, vol. 80, pp. 202–213, 2008.

[48] R. Zhang and S. Kaliaguine, “Lean reduction of NO by C3H6 over Ag/alumina derived from Al2O3, AlOOH and Al(OH)3,” *Applied Catalysis B: Environmental*, vol. 78, no. 3–4, pp. 275–287, Feb. 2008.

[49] X. She and M. Flytzani-Stephanopoulos, “The role of AgOAl species in silver–alumina catalysts for the selective catalytic reduction of NOx with methane,” *Journal of Catalysis*, vol. 237, no. 1, pp. 79–93, Jan. 2006.

[50] I. Nadjar, J.-M. Trichard, P. Costa, and G. Djéga-Mariadassou, “Selective reduction of NOx in diesel exhaust with hydrocarbons over alumina in NEDC conditions,” *Topics in Catalysis*, vol. 42–43, no. 1–4, pp. 27–31, May 2007.

[51] Y. Tsukamoto, H. Nishioka, D. Imai, Y. Sobue, N. Takagi, T. Tanaka, and T. Hamaguchi, “Development of New Concept Catalyst for Low CO 2 Emission Diesel Engine Using NOx Adsorption at Low Temperatures,” *SAE International*, vol. 2012–01–03, 2012.

Table 1 Data for stationary points, GHSV based on a total of 4 l catalyst.

	Engine settings								
T (°C)	Speed (rpm)	Torque (Nm)	GHSV (h^{-1})	NO_x (ppm)	O_2 (%)	H_2O (%)	CO_2 (%)	CO (ppm)	HC[a] (ppm)
160	2800	15	33000	140-150	16	4.0	3.4	1000	240-280
180	2800	30	34000	160-180	15	4.6	4.5	840	170-220
220	2800	50	36000	190-230	14	5.5	5.3	560	100-150
270	2740	75	34000	150-210	11	7.0	6.9	280	60-100
340	2330	125	33000	130-160	7.8	9.2	9.6	200	30-60
400	1835	200	33000	160-210	5.2	11	11	480	16-25
[a] The level was in the higher range for Ag-only.									

Table 2 Typical gas composition during NEDC.

Component	Concentration (%)	Component	Concentration (ppm)
O_2	10-20	CO	300-1200
H_2O	2-8	HC	150-400[a]
CO_2	0-9	NO_2/NO_x	0.3-0.6[b]
[a] Level was down to 50 ppm in shorter periods of time, [b] Lower at end of cycle (<0.3).			

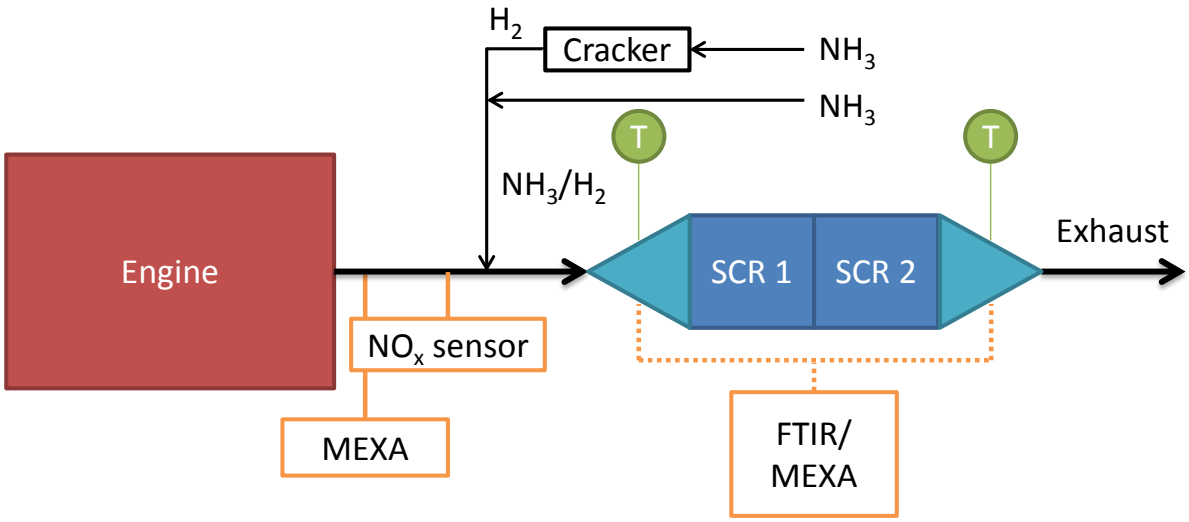

Figure 1 Schematic layout of engine bench test set-up

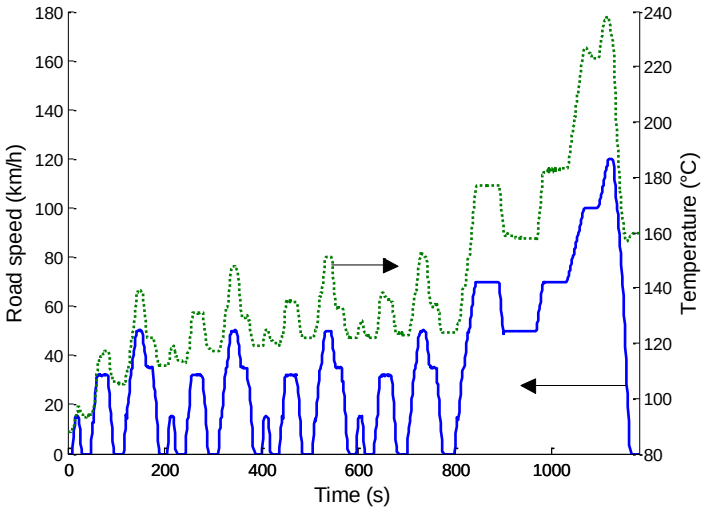

Figure 2 NEDC, road speed and actual temperature.

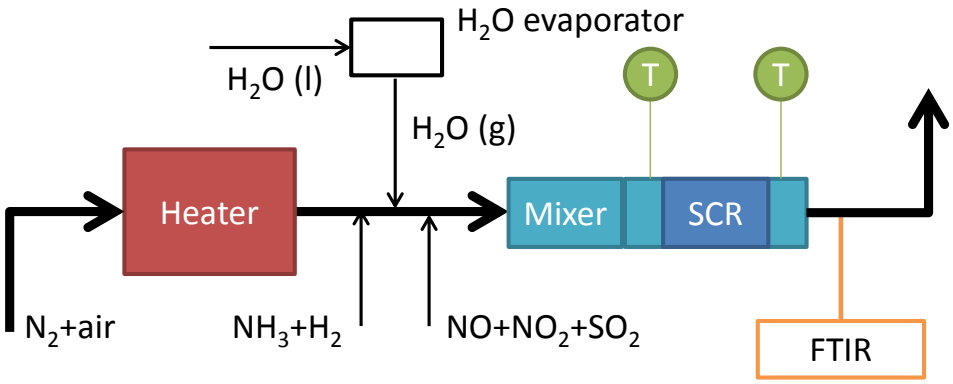

Figure 3 Schematic layout of laboratory set-up.

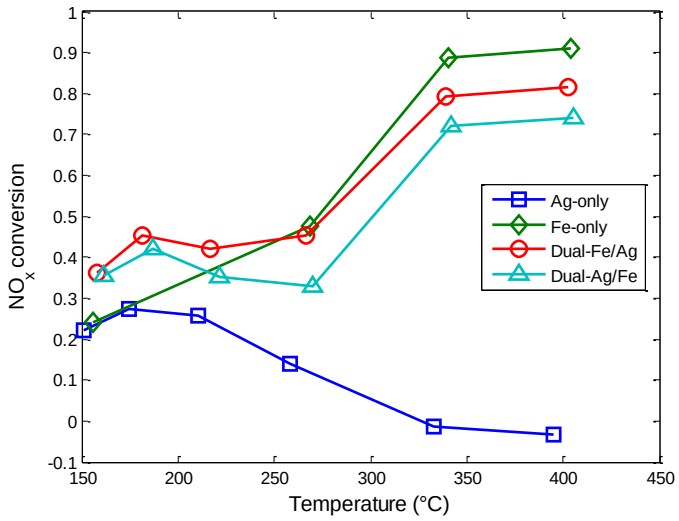

Figure 4 Engine bench stationary steady-state NO_x conversions as function of temperature for the different catalyst layouts at steady-state. The layouts including Ag/Al_2O_3 are tested with NH_3 and H_2 dosing and Fe-only with only NH_3 dosing.

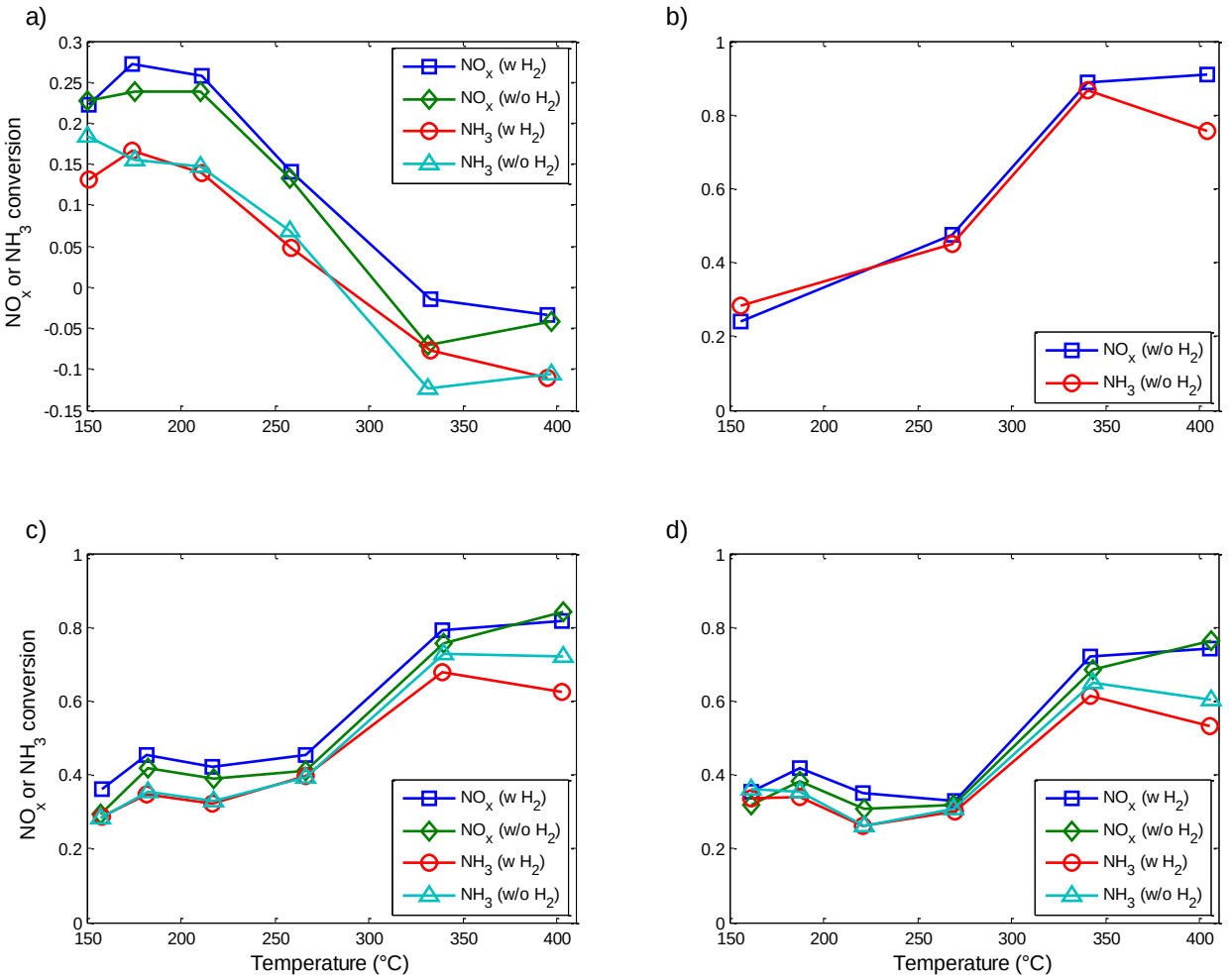

Figure 5 Engine bench stationary steady-state NO_x and NH_3 conversions as a function of temperature for a) Ag-only, b) Fe-only, c) dual-Fe/Ag and d) dual-Ag/Fe. The systems were tested both with NH_3 and H_2 dosing (w H_2) and with only NH_3 dosing (w/o H_2).

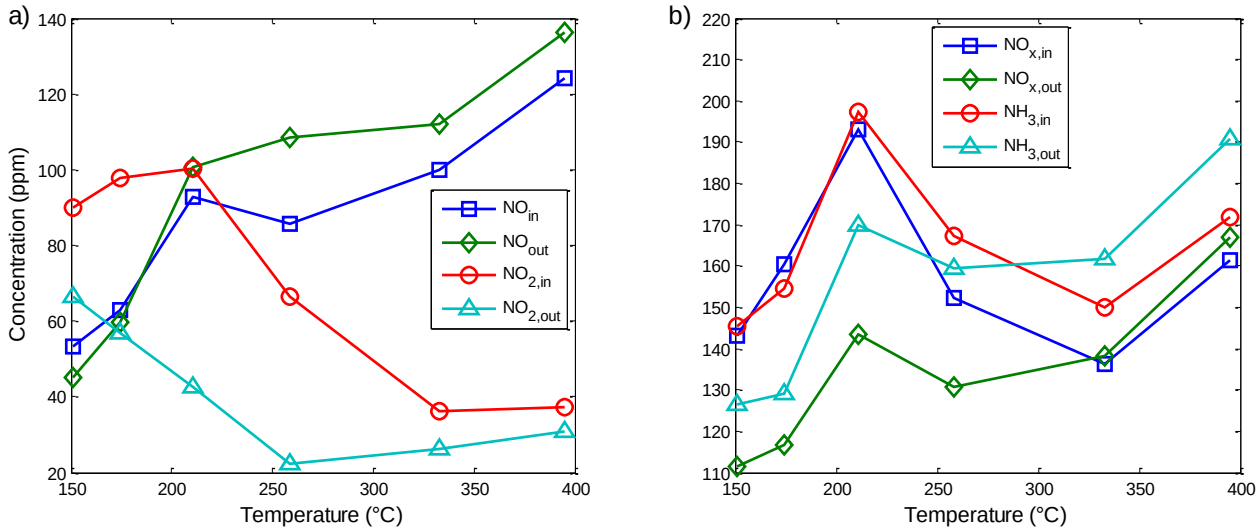

Figure 6 Engine bench stationary steady-state concentrations as function of temperature for Ag-only with NH_3 and H_2 dosing.

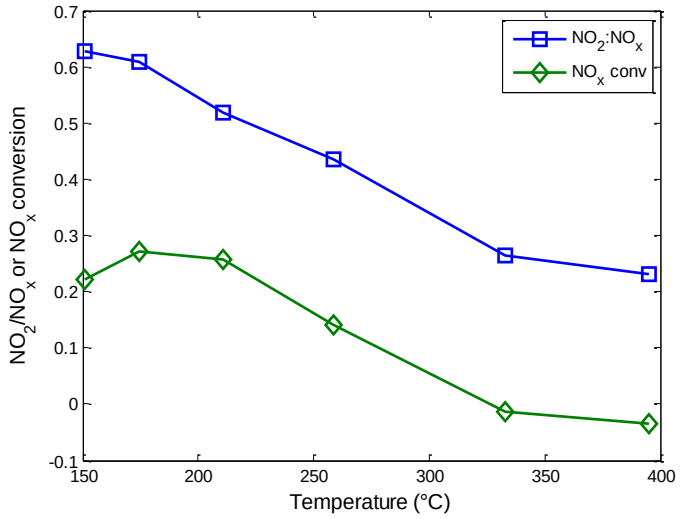

Figure 7 Engine bench stationary steady-state NO_2/NO_x ratios vs. NO_x conversions as function of temperature for Ag-only, NH_3 and H_2 dosing.

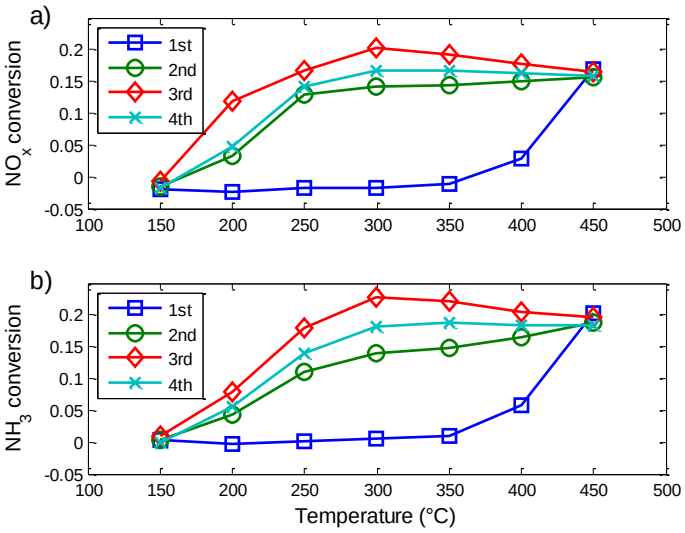

Figure 8 Temperature dependency of NO_x (a) and NH_3 (b) conversion for core sample after engine tests. 1st test and 2nd test before and 3rd test and 4th test after regeneration (in-situ at 500°C and in oven at 550°C). Reaction conditions: 500 ppm NO, 500 ppm NH_3, 1000 ppm H_2, 8% O_2, 12% H_2O and balance N_2, GHSV ~33000 h^{-1}.

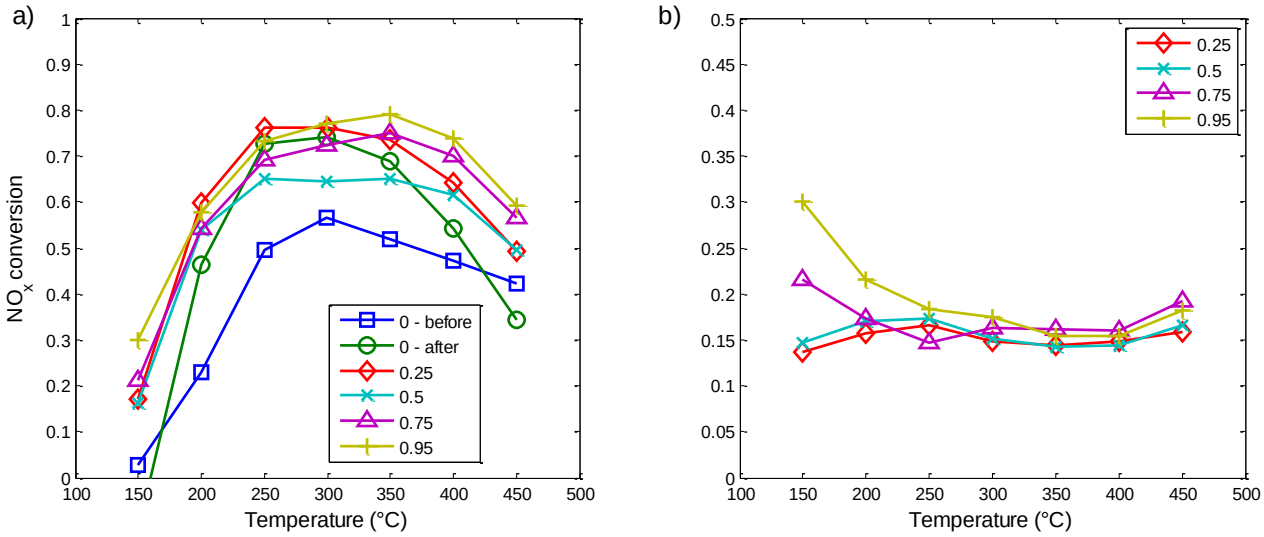

Figure 9 NO_x conversion as function of temperature for different NO_2/NO_x ratios (indicated in legend); a) with H_2 and b) without H_2. Reaction conditions: 500 ppm NO, 500 ppm NH_3, 0 or 1000 ppm H_2, 8% O_2, 12% H_2O and balance N_2, GHSV ~30000 h^{-1}.

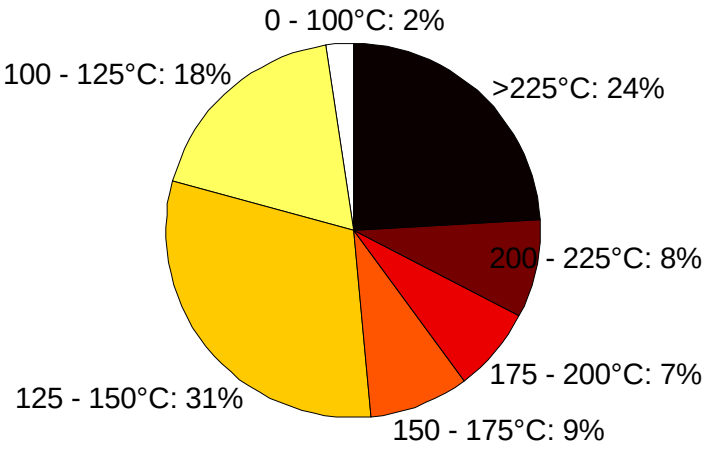

Figure 10 NO_x temperature distribution on mole basis measured directly before the catalysts for transient NEDC.

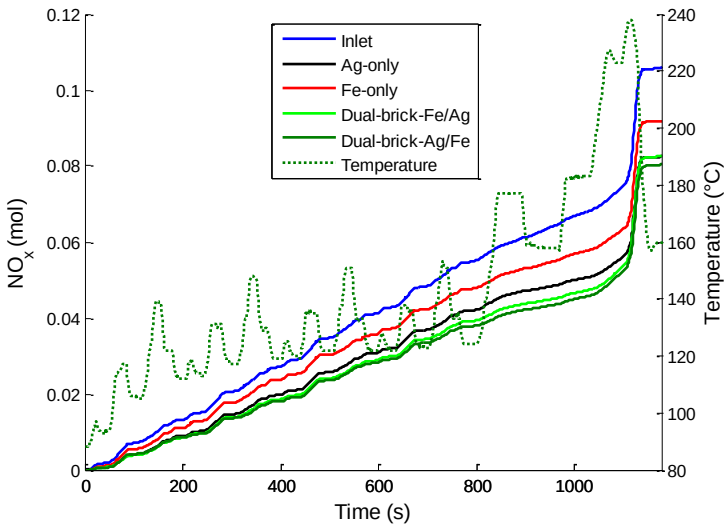

Figure 11 Accumulated NO_x during NEDC for Ag-only, Fe-only, dual-brick-Fe/Ag and dual-brick-Ag/Fe compared to inlet NO_x, NH_3 and H_2 dosing (only NH_3 for Fe-only).

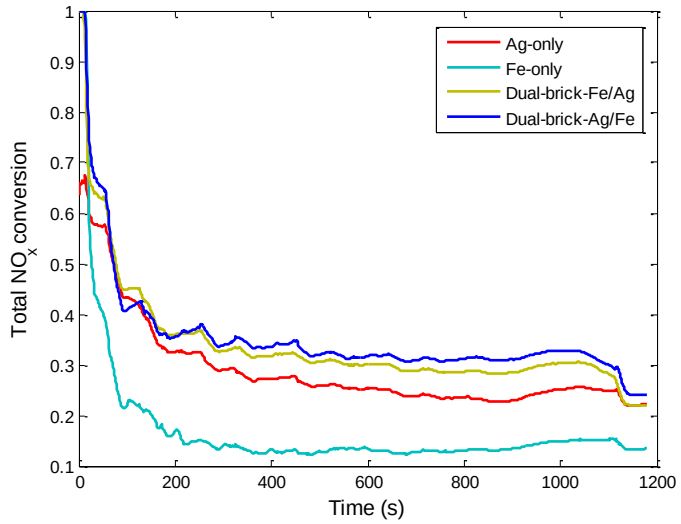

Figure 12 Total NO_x conversions as function of time during NEDC for Ag-only, Fe-only, dual-brick-Fe/Ag and dual-brick-Ag/Fe, NH_3 and H_2 dosing, (only NH_3 for Fe-only).

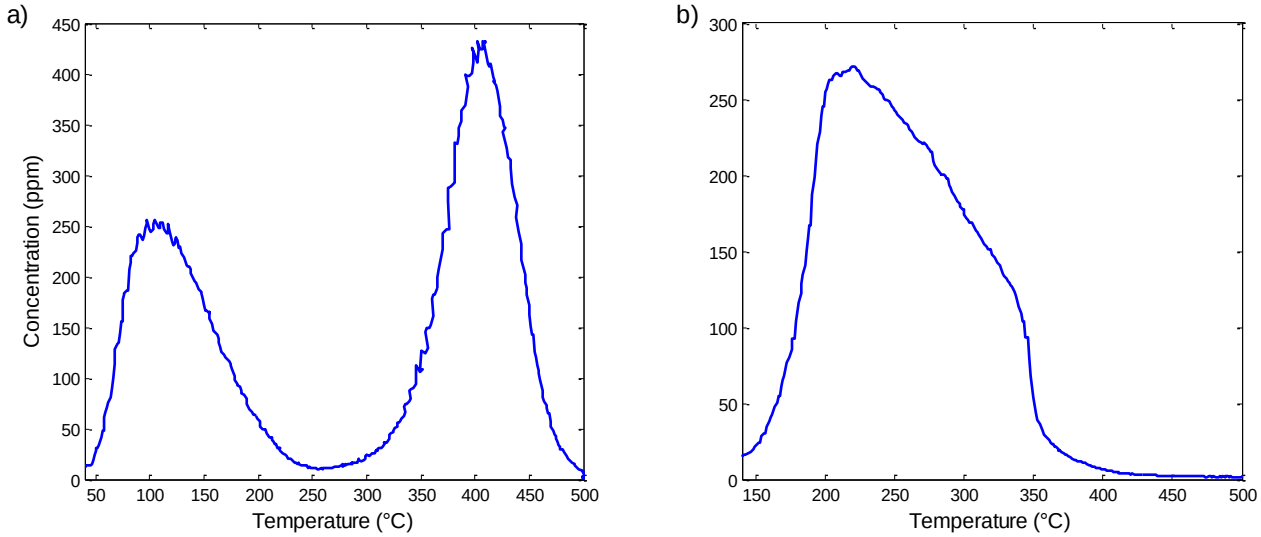

Figure 13 a) NO-TPD, saturation temperature 40°C, and b) NH_3-TPD saturation temperature 150°C, of Ag/Al_2O_3.

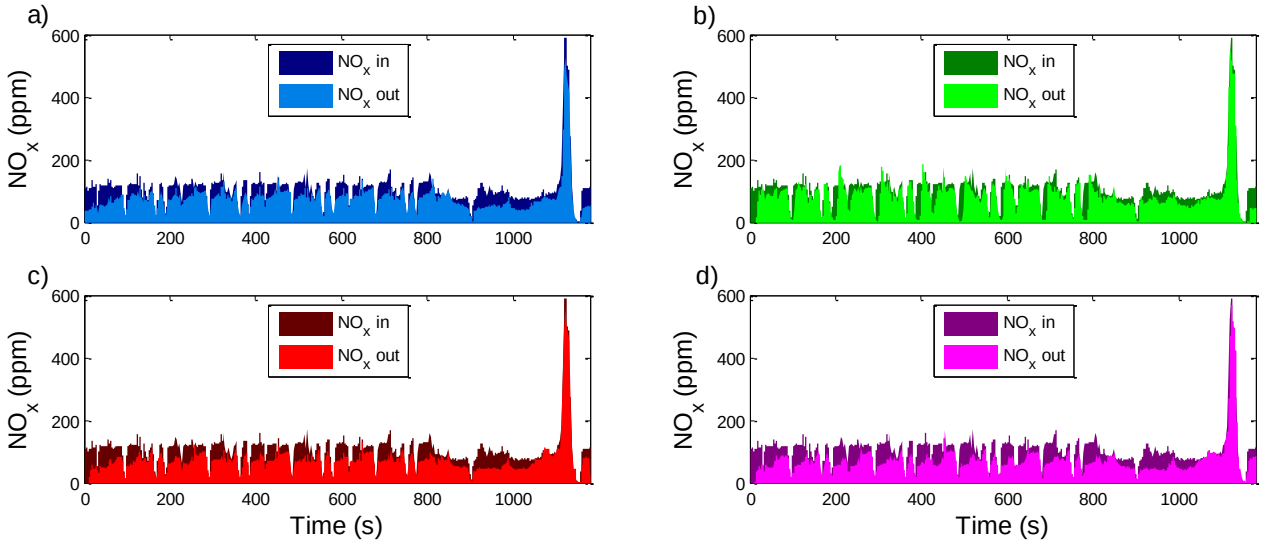

Figure 14 NO_x before (NO_x in) and after (NO_x out) catalysts during NEDC; a) Ag-only, b) Fe-Only, c) dual-Fe/Ag and d) dual-Ag/Fe, NH_3 and H_2 dosing, (only NH_3 for Fe-only).

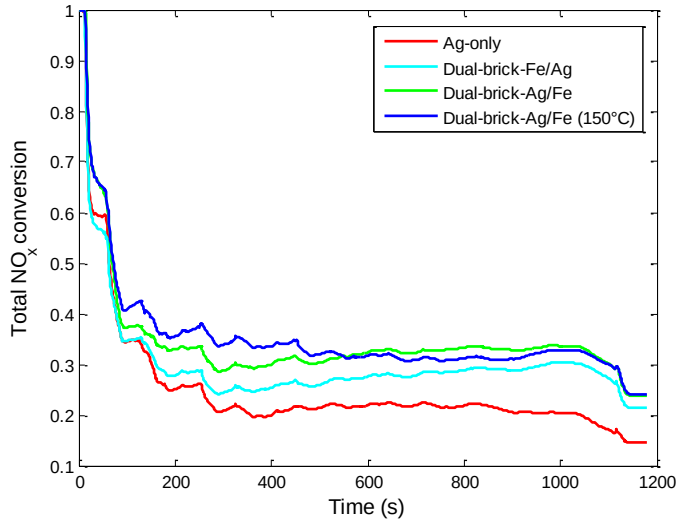

Figure 15 Total NO_x conversions as function of time during NEDC for Ag-only, dual-brick-Fe/Ag, dual-brick-Ag/Fe with NH_3 and H_2 dosing from 120°C. Dual-brick-Ag/Fe with NH_3 and H_2 dosing from 150°C is included for comparison.

Paper IV

Applied Catalysis B: Environmental 117–118 (2012) 49–58

Contents lists available at SciVerse ScienceDirect

Applied Catalysis B: Environmental

journal homepage: www.elsevier.com/locate/apcatb

Sulfur poisoning and regeneration of the Ag/γ-Al_2O_3 catalyst for H_2-assisted SCR of NO_x by ammonia

Dmitry E. Doronkin[a,*], Tuhin Suvra Khan[b], Thomas Bligaard[c], Sebastian Fogel[a,d], Pär Gabrielsson[d], Søren Dahl[a]

[a] Center for Individual Nanoparticle Functionality (CINF), Department of Physics, Technical University of Denmark, Fysikvej 307, 2800 Kgs. Lyngby, Denmark
[b] Center of Atomic-scale Materials Design (CAMD), Department of Physics, Technical University of Denmark, Fysikvej 307, 2800 Kgs. Lyngby, Denmark
[c] SUNCAT Center for Interface Science and Catalysis, SLAC National Accelerator Laboratory, Menlo Park, CA 94025, USA
[d] Haldor Topsøe A/S, Nymøllevej 55, 2800 Kgs. Lyngby, Denmark

ARTICLE INFO

Article history:
Received 1 November 2011
Received in revised form
27 December 2011
Accepted 3 January 2012
Available online 9 January 2012

Keywords:
Ag/Al_2O_3
SO_2
NO_x SCR
Poisoning
Regeneration

ABSTRACT

Sulfur poisoning and regeneration mechanisms for a 2% Ag/γ-Al_2O_3 catalyst for the H_2-assisted selective catalytic reduction of NO_x by NH_3 are investigated. The catalyst has medium sulfur tolerance at low temperatures, however a good capability of regeneration at 670 °C under lean conditions when H_2 is present. These heating conditions can easily be established during soot filter regeneration. Furthermore, two types of active sites could be identified with different regeneration capabilities, namely finely dispersed Ag and larger Ag nanoparticles. The most active sites are associated with the finely dispersed Ag. These sites are irreversibly poisoned and cannot be regenerated under driving conditions. On the other hand the larger Ag nanoparticles are reversibly poisoned by direct SO_x adsorption. The interpretation of the data is supported by DFT calculations.

1. Introduction

Selective catalytic reduction (SCR) is the leading NO_x control technique for diesel vehicles with ammonia used as a reductant. Commonly used catalysts are vanadia-based catalysts and Cu and Fe-containing zeolites. However, none of the systems demonstrate high thermal durability together with a good activity throughout the broad temperature region from 150 to 550 °C which is needed for vehicle applications [1]. Therefore, research of novel non-toxic, inexpensive and durable catalytic systems for NH_3-SCR is still an important focus area.

Recently two research groups suggested to use Ag/Al_2O_3, which is a well-known catalyst for NO_x SCR by hydrocarbons (HC-SCR), for SCR of NO_x by ammonia or urea with co-feeding hydrogen, resulting in nearly 90% NO_x conversion at temperatures as low as 200 °C [2,3]. Still, one of the major obstacles for the application of Ag/Al_2O_3 for NO_x SCR by ammonia is its rather poor sulfur tolerance [4]. A catalyst of 2% Ag/Al_2O_3 demonstrated a decrease in H_2-assisted NO_x conversion by urea from 50% to 30% after 20 h on stream in the presence of 50 ppm SO_2 at 250 °C. This is a rather good result considering the very high GHSV = 380,000 h^{-1} in the tests. However, the large amount of hydrogen (0.5%, 5:1 H_2:NO) used in this study is probably unacceptable for application in diesel vehicles because such a large consumption of hydrogen leads to a high "fuel penalty" [5].

A significant amount of data on sulfur tolerance of Ag/Al_2O_3 catalysts exists for NO_x SCR by hydrocarbons. Meunier and Ross [6] observed strong deactivation of a 1.2% Ag/Al_2O_3 catalyst for propene-SCR by 100 ppm SO_2 in the feed. It is noteworthy that the authors were able to recover most of the catalyst activity by treatment in 10% H_2/Ar at 650 °C or heating in the reaction mixture at 750 °C. Park and Boyer [7] compared the catalytic behavior of 2% and 8% Ag/Al_2O_3 catalysts in the presence of SO_2 and concluded that high Ag loadings may be preferential for making a sulfur tolerant catalyst. The authors demonstrated prominent activation of 8% Ag/Al_2O_3 by SO_2 in the feed and ascribed that to the formation of a very active silver sulfate phase.

When estimating the SO_2 tolerance of Ag/Al_2O_3 catalysts attention should be given also to the process temperature. Satokawa et al. [8] showed a clear dependence of the propane-SCR temperature on the deactivation degree with permanent catalyst deactivation at $T < 500$ °C and furthermore the ability to partially regenerate the catalyst by heating to 600 °C, even without removing low amounts (1 ppm) of SO_2 from the feed. Further studies [8] of sulfation-regeneration mechanisms included obtaining SO_2 TPD profiles and

* Corresponding author. Tel.: +45 4525 3275.
E-mail addresses: dmdo@fysik.dtu.dk, dmitriy.doronkin@gmail.com (D.E. Doronkin).

0926-3373/$ – see front matter © 2012 Elsevier B.V. All rights reserved.
doi:10.1016/j.apcatb.2012.01.002

attribution of peaks to different types of adsorbed SO_2, bound to Ag and alumina. The catalyst regeneration temperature was lower than any of the SO_2 desorption peaks, observed in the study, which did not allow drawing a clear conclusion about the deactivation and regeneration mechanisms.

Breen et al. [9] also demonstrated a drastic dependence of the catalyst degree of poisoning on the temperature of NO_x SCR by octane and toluene. The following was observed; at low temperatures (<235 °C) little deactivation, between 235 and 500 °C – severe deactivation and at $T > 590$ °C – activation due to a suppression of unselective oxidation of hydrocarbons. The low temperature sulfur tolerance was ascribed to low catalyst activity in SO_2 oxidation to SO_3 with the latter considered to be the main poisoning agent for Ag/Al_2O_3. The authors have evaluated a few regeneration options of which heating to 650 °C in hydrogen-containing lean mixture showed promising results rather than regeneration under oxidizing conditions without H_2. The fastest regeneration technique included heating the catalyst in a rich mixture containing CO and hydrogen.

The results of other research groups [10,11] agree with Breen's results in SO_2 oxidation to SO_3 by NO_2 being the major step in the sulfur poisoning of Ag/Al_2O_3 catalysts. Partial regeneration of the catalyst was observed after heating to 600 °C in a hydrocarbon-containing feed.

In this work we have attempted to reveal the Ag/Al_2O_3 sulfation and regeneration mechanisms, which will allow us to develop an efficient regeneration strategy for the ammonia SCR catalyst in question. Special attention was given to the catalyst operation below 300 °C, since for applications in light-duty diesel vehicles low temperatures are of great importance [10]. The suggested mechanism was supported by DFT calculations. A regeneration strategy using the high temperatures developed during Diesel Particulate Filter (DPF) regeneration in diesel cars was evaluated.

2. Experimental

2.1. Catalyst preparation

Parent γ-alumina (Puralox TH 100/150, $S_{BET} = 150\ m^2/g$) was kindly provided by SASOL. 1–3 wt.% Ag/Al_2O_3 were obtained by incipient wetness impregnation of parent γ-alumina by $AgNO_3$ (Sigma–Aldrich) dissolved in deionized water. After impregnation the catalyst was dried at room temperature overnight and calcined at 550 °C for 4 h in static air. The calcined catalyst was tableted, crushed and sieved to obtain a 0.18–0.35 mm fraction (mesh 80–mesh 45) used in the catalytic tests. A new batch of catalyst was sulfated and used to test every new regeneration recipe.

2.2. Determination of the specific surface area

The specific surface areas (S_{BET}) of the catalysts were measured by N_2-adsorption with a Micromeritics Gemini instrument. Untreated catalysts were measured in powder form and for the catalysts after testing a 0.18–0.35 mm fraction of particles (as in catalytic tests) was used for the BET measurement.

2.3. Catalysis

Temperature-programmed activity tests were carried out in a fixed-bed flow reactor (quartz tube with 4 mm inner diameter) in a temperature programmed mode while the temperature was decreased from 400 °C to 150 °C with a rate of 2 °C/min. Prior to the temperature ramp the catalyst was heated to 470 °C for 30 min in the gas mixture used for the tests. The temperature was controlled using an Eurotherm 2408 temperature controller with a K-type thermocouple. 45 mg of catalyst was diluted with 100 mg of SiC (mesh 60) and placed on a quartz wool bed. The bed height was ~11 mm and the GHSV, calculated using the volume of the pure catalyst was ~110,000 h^{-1}. The gas composition normally contained 500 ppm NO, 520 ppm NH_3, 1200 ppm of H_2, 8.3% O_2, and 7% water balanced with Ar. For sulfur poisoning tests 10 ppm SO_2 was admixed to the feed. Water was dosed by an ISCO 100DM syringe pump through a heated capillary. Reaction products were analyzed by a Thermo Fisher Nicolet 6700 FTIR analyzer, equipped with a 2 m gas cell. Gas capillaries were heated to ~130 °C and the FTIR gas cell to 165 °C to avoid condensation of water and formation of ammonium nitrate.

Conversions were calculated using the following equations:

$$X_{NO_x} = 1 - \frac{C_{NO_x}^{outlet}}{C_{NO_x}^{inlet}} \quad (1)$$

and

$$X_{NH_3} = 1 - \frac{C_{NH_3}^{outlet}}{C_{NH_3}^{inlet}} \quad (2)$$

where X_{NO_x} denotes the conversion of NO_x to N_2 and $C_{NO_x}^{inlet}$ and $C_{NO_x}^{outlet}$ are the NO_x concentrations at the inlet and outlet of the reactor respectively, where:

$$C_{NO_x} = C_{NO} + C_{NO_2} + C_{N_2O} \quad (3)$$

and $C_{NH_3}^{inlet}$ and $C_{NH_3}^{outlet}$ are NH_3 concentrations at the reactor inlet and outlet.

2.4. DFT calculations

The plane wave density functional theory (DFT) code DACAPO was used to calculate the adsorption energies and the gas phase energies of the adsorbates [12]. A plane wave cutoff of 340.15 eV and a density cutoff of 680 eV were used in the calculations. The core electrons were described by Vanderbilt ultrasoft pseudopotentials. The RBPE functional was used for describing the exchange correlation energy [13].

The adsorption energies of the SO_2, SO_3, and SO_4 species were studied over the Ag (1 1 1) terrace and (2 1 1) step surfaces, on a γ-Al_2O_3 model step surface, and two single atom Ag sites.

For the Ag (1 1 1) and (2 1 1) surfaces, we used a $4 \times 4 \times 1$ Monkhorst-Pack **k**-point sampling in the irreducible Brillouin zone. We employed a 3×3 surface cell for the Ag (1 1 1) and 3×1 surface cell for the Ag (2 1 1) surfaces. For the (1 1 1) surface we used a four-layer slab where the two top-most layers were allowed to relax, whereas for the (2 1 1) surfaces we used a slab model with nine layers and the topmost three layers are allowed to relax. In all the model calculations, neighboring slabs were separated by more than 10 Å of vacuum.

For the calculation of γ-Al_2O_3 and the adsorption of different species on γ-Al_2O_3 we also used the DACAPO code with a plane wave cutoff of 340.15 eV and a density cutoff of 680 eV. A $4 \times 4 \times 1$ Monkhorst-Pack **k**-point sampling in the irreducible Brillouin zone was used for γ-Al_2O_3. The γ-Al_2O_3 surface was modeled by a step on a non-spinel γ-Al_2O_3 structure which was derived from bulk γ-Al_2O_3 model in [14]. The cell parameters for the γ-Al_2O_3 model step surface are $a = 8.0680$ Å and $b = 10.0092$ Å and $\alpha = \beta = \gamma = 90°$. For the γ-$Al_2O_3$ surface the bottom two layers were fixed whereas the top-most three layers were allowed to relax. In all the model γ-Al_2O_3 surfaces, the neighboring slabs are separated by more than 10 Å of vacuum.

Single atom Ag sites were constructed by replacing one Al atom for Ag in the alumina step surface and by attaching one Ag atom to the γ-Al_2O_3 step (see Supplementary material for the geometries).

SO_x and HSO_x adsorption energies were calculated relative to gas phase energies of SO_2(g), O_2(g) and H_2(g).

For calculation of desorption temperatures for SO_2 and SO_3 we used the following procedure. Starting from the chemical equation:

$$SO_2 + * \leftrightarrow SO_2*, \quad (4)$$

$$SO_2 + 1/2O_2 + * \leftrightarrow SO_3* \quad (5)$$

where * is the free surface site and SO_x* is the adsorbed species. We can write down the ratio of occupied and free adsorption sites:

$$\frac{\theta_{SO_x}}{\theta^*} = K_{ads}P_{SO_x} = \exp\left(-\frac{\Delta G_{ads}}{kT}\right)P_{SO_x} = \exp\left(\frac{-(\Delta G^{\ominus}_{ads} - kT\ln P_{SO_x})}{kT}\right) \quad (6)$$

We assume that at the desorption temperature the numbers of occupied and free adsorption sites will equal ($\theta_{SO_x} = \theta^*$), which gives:

$$\Delta G^{\ominus}_{ads} - kT\ln P_{SO_x} = 0 \quad (7)$$

or

$$\Delta E_{ads} - \Delta ZPE_{ads} - T\Delta S_{ads} - kT\ln P_{SO_x} = 0 \quad (8)$$

We calculate the ZPE (zero point energy) and the entropy of the SO_x in their adsorbed state and so it is possible to calculate the desorption temperature for a given partial pressure of SO_x:

$$T = \frac{\Delta E_{ads}}{k\ln P_{SO_x} - \Delta S_{gas}} \quad (9)$$

The SO_x entropy and ZPE found for the γ-Al_2O_3 model surface were also used for the single Ag atom sites on the γ-Al_2O_3. Standard entropy values for SO_2 and SO_3 from [15] (neglecting entropy change with temperature) and a partial pressure of SO_x 4×10^{-7} bar (0.4 ppm in Ref. [9]) and partial pressure of O_2 is 0.07 bar [9] were used in the calculations.

3. Results and discussion

3.1. Catalyst choice: stability of Ag/Al_2O_3 and options for the regeneration

3.1.1. The catalyst choice

Temperature dependence of NO_x and NH_3 conversions for the fresh 1–3% Ag/Al_2O_3 catalysts is shown in Fig. 1a and b, respectively. 1% Ag/Al_2O_3 exhibits SCR onset at 130 °C reaching 80% NO_x conversion at 200 °C and leveling NO_x conversion at 90% at $T > 300$ °C. This is in agreement with previous studies [2]. 2% and 3% Ag/Al_2O_3 catalysts demonstrate SCR onset shifted by 7 °C to lower temperatures compared 1%, but lower maximum conversion and generally lower SCR activity at higher temperatures, unlike results of Shimizu and Satsuma [3]. The NH_3 conversion follows the NO_x conversion at $T < 270$–300 °C. At higher temperature NH_3 becomes oxidized and the NH_3 conversion is higher than NO_x conversion. Thus, NH_3 oxidation plays some role in the decrease of high temperature NO_x conversion but this is not the main reason. The reason for observing conversion maxima for 2% and 3% Ag/Al_2O_3 catalysts at 200 °C with subsequent drop in NH_3 and NO_x conversions could be direct oxidation of H_2 by oxygen taking over. As it was shown earlier no NO and NH_3 is converted over an Ag/Al_2O_3 catalyst in the absence of H_2 [16]. Another possible reason is the lack of strong acid sites for NH_3 adsorption in the 2–3% Ag/Al_2O_3 catalysts which is demonstrated in [17].

Noteworthy, the tested catalysts demonstrate very high stability at temperature up to 700 °C which has also been shown in the number of papers on HC-SCR [3,9]. To further check the thermal stability of the 1% Ag/Al_2O_3 catalyst it was subjected to hydrothermal deactivation at 750 °C for 16 h. The activity of the obtained catalyst is reported in Fig. 1a and b as gray dotted lines. The low-temperature conversion is only slightly shifted by 3 °C, whereas at $T > 300$ °C one may observe a decrease in NO_x and NH_3 conversions similar to that observed for catalysts with higher Ag loading. This may indicate sintering of Ag particles leading to the increased unselective oxidation of hydrogen. At the same time, the relatively small decrease in the catalyst specific surface area (S_{BET}) does not indicate any significant change in the alumina support (Table 1).

Contrary to the hydrothermal aging, sulfur poisoning of Ag/Al_2O_3 leads to significant catalyst deactivation. Preliminary experiments on the choice of sulfur poisoning temperature showed no catalyst deactivation with SO_2 in the feed at 500 °C and the most severe deactivation in the temperature range 200–300 °C in very good agreement with the earlier reported results for HC-SCR [8,9]. Therefore, preliminary SO_2 deactivation studies of 1–3% Ag/Al_2O_3 were performed at 200–227 °C and all the following deactivation–regeneration studies of 2% Ag/Al_2O_3 were done at 240–250 °C (Fig. 1c). For the comparison of regeneration methods the SO_2 poisoning was obtained by introducing 10 ppm SO_2 to the SCR feed for 4 h.

Catalytic performance of 1–3% Ag/Al_2O_3 in NO_x SCR after such sulfur treatment at 200–227 °C is shown in Fig. 1d. Lowering deactivation temperature from 250 °C to 200 °C leads to a very small shift of the low-temperature activity within 5 °C, therefore, the temperature difference is not the determining factor for the observed activity difference. 1% Ag/Al_2O_3 was poisoned to the highest degree, whereas higher Ag loading led to better sulfur tolerance with 3% Ag/Al_2O_3 showing the highest NO_x conversion at $T < 300$ °C. It should be noted that after exposure to SO_2 (and even after regeneration of 1% and 2% Ag/Al_2O_3 catalysts at 670 °C) the NH_3 conversion profiles coincided with the NO_x conversion profiles for all tested samples. That indicates quenching of NH_3 unselective oxidation over 1–3% Ag/Al_2O_3 by SO_2. Due to the similarity of NO_x and NH_3 conversion curves for the sulfated catalysts only NO_x conversions will be reported throughout the article.

Sulfation of 2 and 3% Ag/Al_2O_3 leads not only to a shift of the maximum NO_x conversion to higher temperatures but also to an increase to significantly higher values than demonstrated over the fresh catalysts. The shift of the maximum activity of 2% Ag/Al_2O_3 along with "activation" of the catalyst at 227 °C (near the conversion maximum of the fresh catalyst) and at 250 °C can be seen in Fig. 1c. Higher SO_2 exposure leads to a shift of the maximum NO_x conversion to higher temperatures along with deterioration of the low-temperature activity. The activity gain induced by sulfation has been observed earlier and attributed to the redistribution of Ag species [4]. However, as we have observed the decrease of unselective NH_3 oxidation after SO_2 exposure, we suppose the SO_x blocking of sites active in NH_3 and H_2 oxidation to play a major role in the increased NO_x conversion over 2 and 3% Ag/Al_2O_3 catalysts. At the same time SO_2 adsorption increases the alumina acidity which can also play the role for the SCR activity as discussed in a separate publication [17].

Several options for the catalyst regeneration under hydrocarbon (HC) SCR have been suggested in the literature. All of them include heating sulfated Ag/Al_2O_3 in different media – oxidizing [9], hydrogen (or hydrocarbon)-containing lean exhaust [6,8–10] or rich exhaust [6,9].

Heating sulfated 2% Ag/Al_2O_3 to 670 °C for 10 min in the NO_x SCR feed without hydrogen leads only to a small 10 °C shift of T50% to lower temperatures (not shown). Therefore, regeneration of Ag/Al_2O_3 for NO_x SCR by NH_3 without co-feeding hydrogen is ineffective. Thus, regeneration at 670 °C in the reaction gas mixture was used to test the regeneration capability of 1–3% Ag/Al_2O_3 catalysts. Activity of the catalysts regenerated during 40 min is reported in Fig. 1e. All catalysts partially regained the low-temperature activity, however, the high-temperature activity of 3% Ag/Al_2O_3 was

Table 1
Specific surface areas of tested catalysts as measured by BET.

Catalyst	Treatment	S_{BET} (m^2/g)
1% Ag/Al_2O_3	–	142
1% Ag/Al_2O_3	Hydrothermal aging (750 °C, 16 h)	126
2% Ag/Al_2O_3	Catalytic test (w/o deactivation)	130
2% Ag/Al_2O_3	Sulfation and 10 min regen. @ 670 °C	129
2% Ag/Al_2O_3	Sulfation and 80 min regen. @ 670 °C	113
2% Ag/Al_2O_3	30 cycles of 1 h sulfation and 10 min regen. @ 670 °C, followed by heating to 950 °C	121
3% Ag/Al_2O_3	–	141

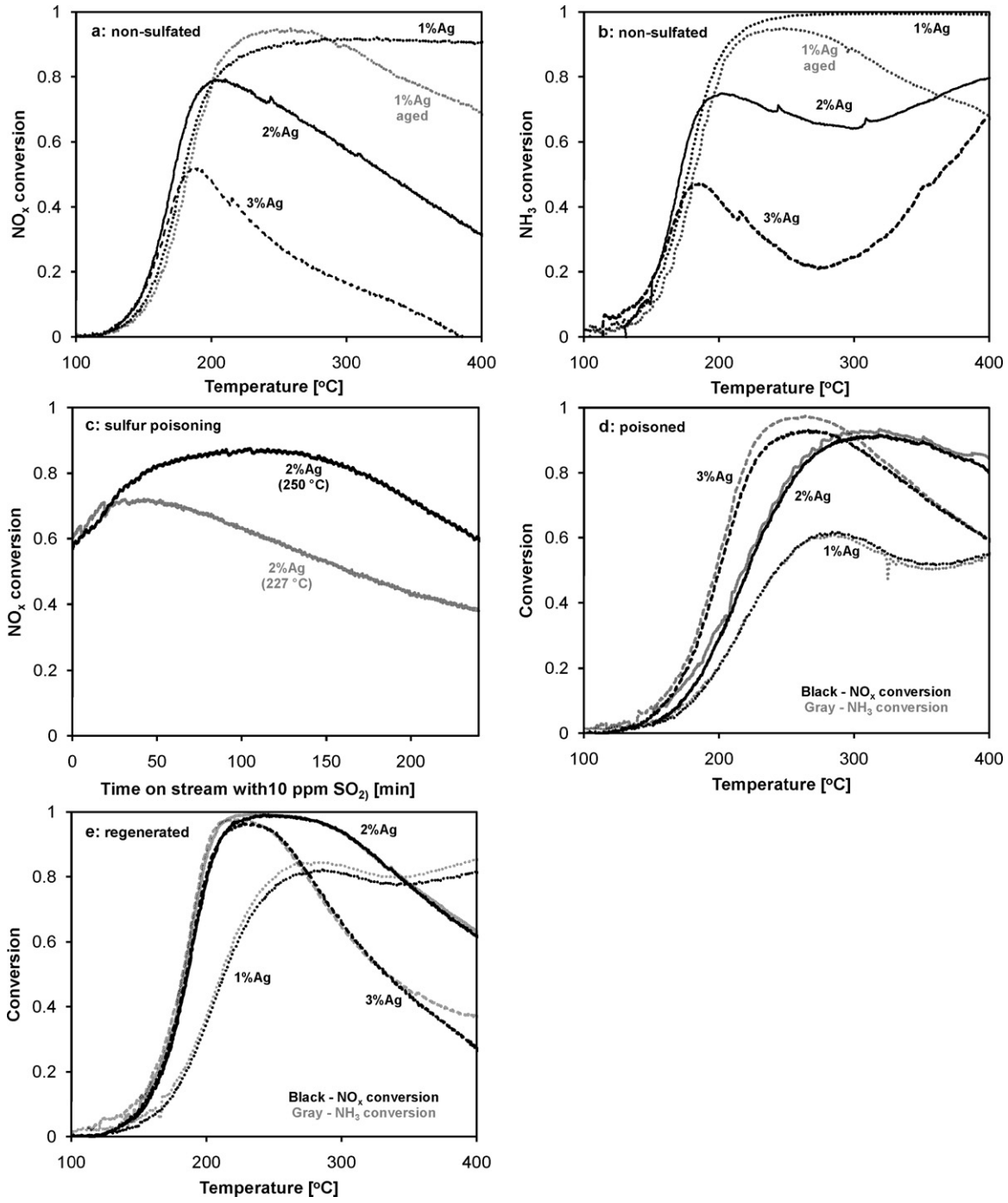

Fig. 1. NO_x (a) and NH_3 (b) conversion profiles obtained over fresh 1–3% Ag/Al_2O_3 (black) and hydrothermally aged 1% Ag/Al_2O_3 (gray dotted) catalysts. (c) Evolution of NO_x conversion at 227 and 250 °C over 2% Ag/Al_2O_3 with 10 ppm SO_2 in the feed. (d) NO_x and NH_3 conversion profiles obtained over sulfur poisoned 1–3% Ag/Al_2O_3 catalysts. (e) NO_x and NH_3 conversion profiles obtained over 1–3% Ag/Al_2O_3 catalysts after 40 min regeneration at 670 °C. Reaction conditions: 500 ppm NO, 520 ppm NH_3, 1200 ppm H_2, 8.3% O_2, 7% H_2O in Ar, GHSV = 110,000 h^{-1}.

decreased compared to the sulfated catalyst. At the same point this catalyst demonstrated a higher conversion of NH_3 compared to NO_x at $T > 350\,^{\circ}C$, indicating NH_3 oxidation. 2% Ag/Al_2O_3 showed the highest NO_x conversion throughout the whole temperature region and will, therefore, be used for the further study. For the simplicity in the text below and the following figures 2% Ag/Al_2O_3 will be referred as Ag/Al_2O_3.

3.1.2. Regeneration options

To simulate regeneration in rich exhaust the catalyst was heated to 670 °C for 1 min with oxygen removed from the feed. The activity following from this rich regeneration is presented in Fig. 2a as a solid line. The profile is significantly shifted to lower temperatures compared to the non-regenerated sample. Another feature is the maximum NO_x conversion (96%), which is now higher than that of both the fresh and the non-regenerated catalysts. Still, regeneration under rich conditions did not allow regaining the low-temperature activity completely.

However, obtaining rich exhaust from diesel engine leads to high fuel consumption and is, therefore, undesirable. Thus, we have preferred relatively fast catalyst regeneration under lean conditions with co-feeding hydrogen. The NO_x conversion profile for Ag/Al_2O_3 regenerated 10 min at 670 °C in the standard NO_x SCR feed (with hydrogen) is shown in Fig. 2a as a dashed line. The catalyst shows the same activity below 200 °C as when regenerated under rich conditions and at higher temperatures even higher conversion (up to 100%). At the same time the surface area of the catalyst regenerated for 10 min is not deteriorated compared to the fresh catalyst (Table 1). This kind of regeneration is very easy to implement in diesel vehicles because it can coincide with regeneration of the DPF, which requires a similar heating strategy.

3.2. Influence of the regeneration time on the catalyst activity

Regeneration time is of high importance for automotive catalysts, as heating the catalyst requires a lot of energy, i.e. fuel to be spent. Influence of the regeneration time (for regeneration under lean conditions with co-feeding hydrogen) on the activity of the regenerated catalyst is shown in Fig. 2b. The value on the *Y*-axis is the shift of temperature for 50% NO_x conversion over the regenerated catalyst relative to the fresh catalyst:

$$T50\%\,\text{shift} = T50\%\,\text{regenerated} - T50\%\,\text{fresh} \quad (10)$$

Zero at the timescale stands for non-regenerated catalyst. Heating to 670 °C for 1 min leads to the shift of *T*50% by 24 °C towards lower temperatures, which is already very good. Heating for 10 min allows us to get 6 °C lower *T*50%, but further treatment at high temperatures does not lead to significant further activation of the catalyst. The best *T*50%, we could get by regenerating Ag/Al_2O_3, is 15 °C higher than *T*50% of the fresh Ag/Al_2O_3. That result is obtained after 40 min of regeneration. Higher regeneration time does not yield better activity but causes loss of the catalyst surface area (Table 1) and is, therefore, undesirable. It is worth noting that we were not able to match the low-temperature activity of the fresh catalyst after regeneration.

3.3. Developing a deactivation–regeneration strategy to mimic automotive catalyst operating conditions

Typical lifecycle of an automotive light-duty Ag/Al_2O_3 NO_x SCR catalyst comprises normal driving, during which the catalyst operates at low temperatures 150–350 °C [10] and is poisoned by sulfur, and regeneration which optimally coincides with regeneration of the DPF. To be more precise, useful vehicle running time according to the modern Euro 5 and Euro 6 standards is 160,000 km [18], and typical intervals between DPF regenerations are 300–900 km (with the modern Volvo D5 light-duty diesel engine as an example) [19], which gives a minimum of 160 catalyst regeneration cycles. Using average fuel consumption of this engine during urban driving (6.7 l/100 km with a manual gearbox), an average diesel fuel density approx. 850 g/l [20], and a maximum allowed sulfur content of 10 ppm in the diesel fuel [21], the total sulfur passed through the catalyst will amount to 91 g or 2.85 mol. Using available data on the volume of monolith catalyst for the mentioned engine (9 l) and the monolith density 2.5 g/in^3 [10], the weight of the washcoat for an automotive catalyst (15% of the total) and the relative weight of the powder catalyst in the washcoat (80%) [22], we get a total of 0.47 g (14.7 mmol) sulfur per gram of powder catalyst during the vehicle lifetime. Therefore, the amount of sulfur per one deactivation cycle will be 83 μmol/g of catalyst, assuming adsorption of all sulfur. In reality, however, not all sulfur will be adsorbed partly due to very high or low temperatures [9].

In our tests we have chosen the scheme involving catalyst poisoning with 10 ppm SO_2 at intermediate temperature of 240 °C for 1 h which gives us a sulfur exposure before regeneration of 65 μmol/g of catalyst, which is close to the theoretical maximum value calculated above. Thus, we will use this protocol as "worst case" scenario.

Fig. 3a and b shows two different ways of testing sulfur tolerance with the same total sulfur exposure (4 h with 10 ppm SO_2, corresponds to 260 μmol/g catalyst) and the same regeneration time, but split by four relatively small regeneration segments in the second case.

The comparison of the catalyst activity after these two tests is given in Fig. 3c. Evidently, the low-temperature activities of the two poisoned catalysts are identical. Different SCR activity at $T > 200\,^{\circ}C$ does not allow us to state that the regenerated catalyst activity observed in Fig. 3c represents "steady state" automotive catalyst activity in both cases. Further testing is needed to reveal "steady state" catalyst activity during sulfation–regeneration cycles.

3.4. Cycling deactivation–regeneration

In order to clarify if the catalyst will be further deactivated after several 1 h. SO_2 poisoning – 10 min regeneration cycles we have carried out 30 deactivation (at 240 °C) – regeneration (at 670 °C) cycles. Evolution of the NO_x and NH_3 conversions during the first 9 cycles of the experiment is shown in Fig. 4.

During the sulfation of the fresh catalyst (first 60 min) NO_x conversion steadily increases. During heating the catalyst to 670 °C the NO_x conversion drops to slightly negative values. According to Eq. (1) in Section 2.3 this is due to a higher NO_x concentration at the reactor outlet than at the inlet. The latter is caused by oxidation of part of ammonia to NO_x at the regeneration temperature which can be seen by the higher conversion of NH_3 compared to NO_x at $T > 500\,^{\circ}C$. To prevent ammonia oxidation in the real life application it is possible to switch off ammonia supply during regeneration without compromising regeneration efficiency.

The NO_x conversion following regeneration is maximal (97%) after the first regeneration and decreases only a little (to 95%) with further regeneration cycles. However, sulfur poisoning of the regenerated sample leads to a decrease in the NO_x conversion at the end of each of the first deactivation cycles. This decrease in NO_x conversion could indicate that during each of these first regenerations the SO_x adsorbed during the preceding deactivation cycle is not completely removed from the catalyst surface. After seven sulfation–regeneration cycles NO_x conversion is stabilized, so each new testing cycle yields the same profile as the previous. Thus, further sulfation and regeneration do not change the catalyst performance.

Integration of the SO_2 signal measured by FTIR during 10th–20th cycles (they are all equal) gives the amount of SO_2 equal to the

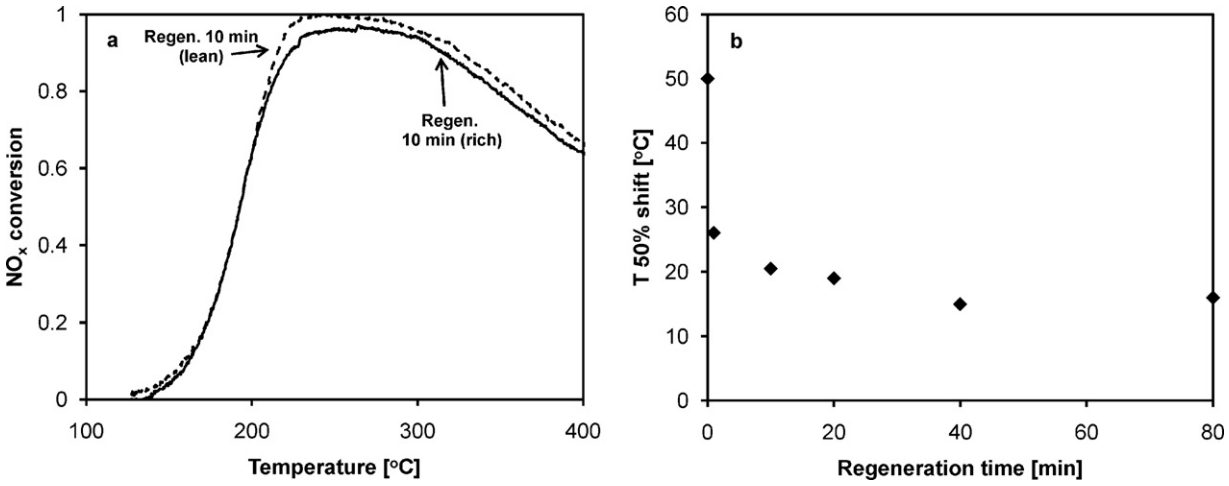

Fig. 2. (a) NO_x conversion profiles obtained over 2% Ag/Al_2O_3 after 10 min regeneration at 670 °C (dashed) and after 1 min regeneration at 670 °C in rich mixture (solid). Reaction conditions: 500 ppm NO, 520 ppm NH_3, 1200 ppm H_2, 8.3% O_2, 7% H_2O in Ar, GHSV = 110,000 h^{-1}. (b) Dependence of shift of temperature of 50% NO_x conversion on the regeneration time. The 0 corresponds to no regeneration.

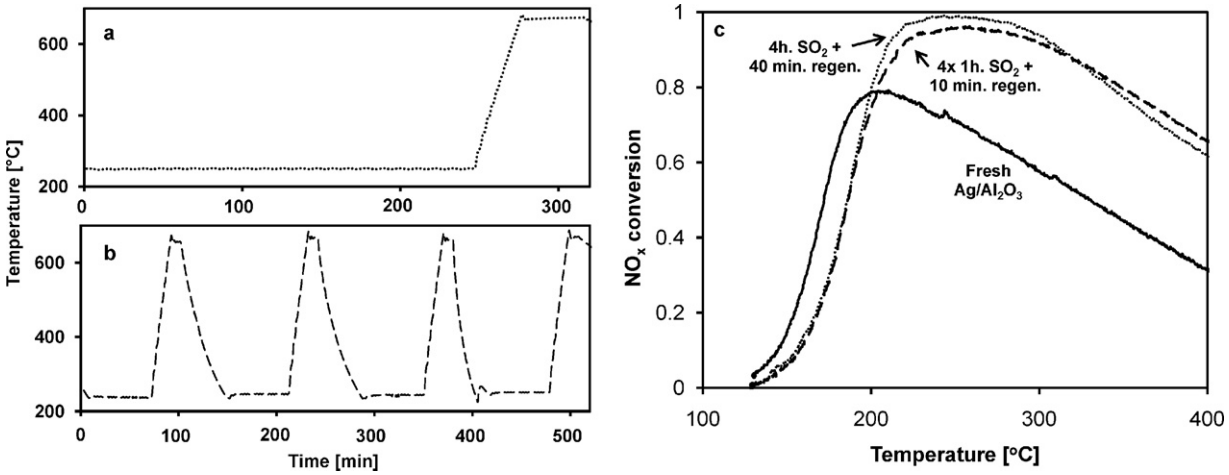

Fig. 3. (a) Temperature profile of 4 h sulfation – 40 min regeneration experiment. (b) Temperature profile of 4 × 1 h sulfation – 10 min regeneration experiment. (c) NO_x conversion profiles obtained over fresh 2% Ag/Al_2O_3 (solid line), 2% Ag/Al_2O_3 after 4 h with 10 ppm SO_2 at 240 °C and 40 min regeneration at 670 °C (dotted line), after 4 cycles 1 h with 10 ppm SO_2 at 240 °C and 10 min regeneration (dashed line).

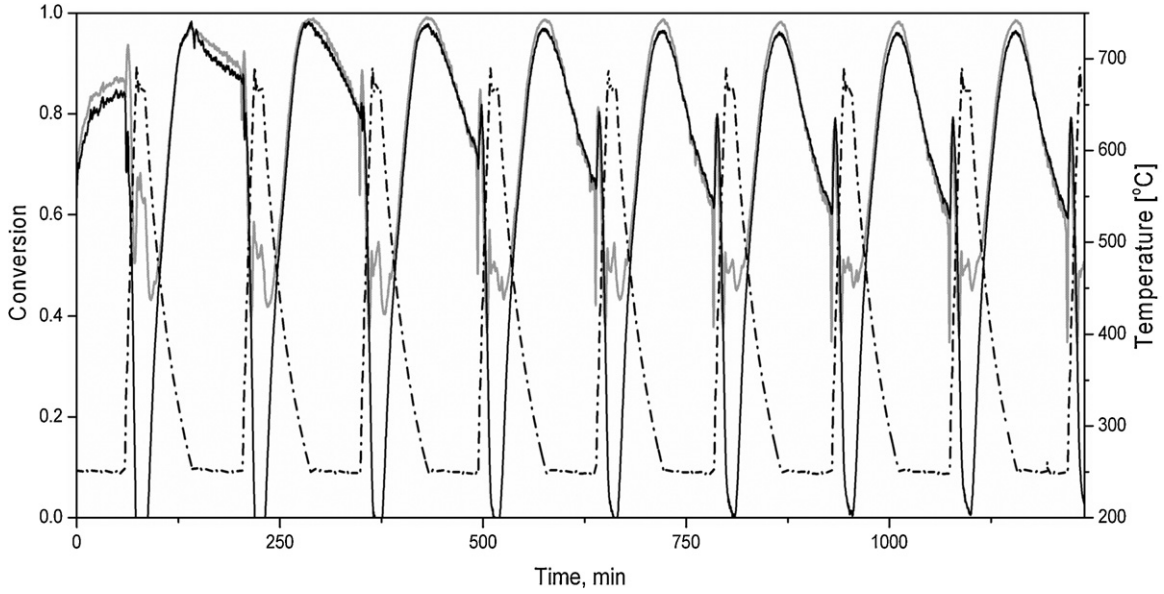

Fig. 4. Evolution of NO_x conversion with time for the first 9 cycles of the long-term stability test of 2% Ag/Al_2O_3. Reaction conditions: 500 ppm NO, 1200 ppm H_2, 8.3% O_2, 7% H_2O in Ar, GHSV = 110,000 h^{-1}. Sulfation with 10 ppm SO_2 for 1 h at 240 °C, regeneration for 10 min at 670 °C.

amount of SO_2 passed through the catalyst during these cycles. Therefore, using FTIR data we can estimate the amount of SO_2, which was accumulated in the catalyst and not desorbed during the first regenerations to be 0.11 mmol/g catalyst.

Our data (not shown) suggests that the SO_2 poisoning effect is cumulative in the range of SO_2 concentrations 0.5–10 ppm, i.e. the catalyst deactivation degree depends only on total SO_2 exposure. Therefore, with the same SO_x exposure between DPF regenerations as in this study real catalyst performance will be high enough even in the end of a sulfation cycle before the next regeneration.

3.5. Mechanism of Ag/Al_2O_3 sulfation and regeneration

The results obtained in the previous Section 3.4 set the ground for a few conclusions regarding the sulfation and regeneration mechanisms for Ag/Al_2O_3 catalysts of hydrogen-assisted NO_x SCR by NH_3.

First of all, some amount of SO_x is not desorbed after regeneration. This amount was estimated in the previous section and is reproducible. At the same time we cannot regenerate the full low-temperature activity of Ag/Al_2O_3, no matter if lean hydrogen-containing or rich mixtures were used for the regeneration. The SCR reaction onset for the sulfated and regenerated catalyst is always shifted to higher temperatures. Therefore, we suppose that a certain type of active sites exists (name it "Type I"), which stand for Ag/Al_2O_3 activity at low temperatures (<200 °C) that are irreversibly poisoned by SO_2 and cannot be regenerated using standard techniques. Taking into account the very low sulfur tolerance of low-loaded Ag/Al_2O_3 [6,7], we can attribute Type I active sites to highly dispersed silver e.g. $Ag^{\delta+}$ atoms or Ag^+ ions [23,24] (see Fig. 5).

SO_x adsorption on the alumina surface (where dispersed silver is localized) blocks these Type I active sites. SO_x can be adsorbed on single-atom Ag sites on the alumina as well as on the neighboring Al atoms. It is impossible to desorb SO_x from the alumina surface by heating the catalyst to 670 °C [25] and, therefore, Type I active sites could not be regenerated.

Another evidence of irreversibly poisoned active sites is the formation of excess of nitrogen dioxide over the fresh catalyst (Fig. 6b, solid line), a catalytic function which is irreversibly poisoned by SO_2 and cannot be regenerated (Fig. 6b, dotted line). Therefore, we also attribute the increased NO oxidation capacity to Type I active sites.

However, the possibility of regeneration of the most of the SCR activity of Ag/Al_2O_3 hints on the existence of "Type II" active sites. As they are more abundant in more SO_2 tolerant high-loaded Ag/Al_2O_3 [7] we attribute them to the surface of Ag nanoparticles. It has been shown that it is possible to desorb SO_2 from the Ag surface at temperatures near 600 °C [25]. Thus, we assume that sulfation and regeneration of these Type II active sites determines the SCR activity of Ag/Al_2O_3 with sulfur-containing fuel in diesel vehicles. According to the SCR mechanism suggested in [16] these Type II species are also capable of oxidizing NO to NO_2 which further reacts with NH_3 over alumina. However, Type II sites are less active which leads to the deficit of NO_2 and prevents observing it in the gas phase when NH_3 is present.

Our assumption about the existence and function of Type I active sites can be verified by the following. As follows from the SO_2 TPD profiles in Refs. [11,25], it is possible to desorb SO_x from alumina surface at ca. 1000 °C. Of course, the alumina will undergo partial restructuring at this temperature [26] accompanied by the formation of the α-Al_2O_3 phase, which will partially ruin the catalyst. However, this may help to test the principle.

The results of heating of sulfated Ag/Al_2O_3 to 950 °C in the SCR gas mixture with further immediate cooling are shown in Fig. 6a and b as dashed lines. By removing SO_x from the alumina surface (observed by FTIR) we were able to regain SCR onset at the same temperature as for the fresh Ag/Al_2O_3 (Fig. 6a). At the same time we were able to regenerate excessive NO_2 production (Fig. 6b) which was impossible to get by any kind of regeneration at lower temperature. Still, the maximum activity of the catalyst was lower than that of the fresh catalyst resembling the activity of 3% Ag/Al_2O_3 (Fig. 1a). The specific surface area of the catalyst regenerated at 950 °C did not change significantly compared to the fresh sample (Table 1), therefore, it is rather sintering of Ag particles which caused a drop in the maximum activity. Thus, we consider possibility of regenerating low temperature activity as an evidence for the existence of several types of active sites in Ag/Al_2O_3 as was previously stated for HC-SCR Ag/Al_2O_3 catalysts [27].

The fact that SO_x irreversibly adsorbed on the alumina surface does not hinder that the SCR reaction can be explained if we assume that Ag species participate in the oxidation of NO to NO_2 and the alumina facilitates further reaction of NO, NO_2 and NH_3 according to the "Fast SCR" mechanism [28]. Since "Fast SCR" occurs over a number of acidic surfaces, sulfated alumina should catalyze SCR as well if SO_x-free Ag surface is left to oxidize NO.

3.6. Evaluation of the proposed sulfation and regeneration mechanism of Ag/Al_2O_3 by DFT

Adsorption energies of SO_2, SO_3, and SO_4 for the most energetically favorable adsorption geometries for different adsorption sites are summarized in Table 2 and the corresponding geometries for the γ-alumina model step surface are shown in Fig. 7. It should be noted that SO_x can be adsorbed on the γ-alumina in different configurations with similar energies and only the lowest energies (strongest adsorption) are shown. The DFT calculation shows that the SO_x adsorbs strongly on the step sites which is expected from the low coordination of these sites and the steric freedom available at the step sites [29–31]. At the same time the surface step is representative of small 1–3 nm nanoparticles containing mostly under-coordinated surface atoms [32].

Two trends can be identified from these values. First global trend is that all types of SO_x bind significantly stronger to the alumina surface than the metal surface. The adsorption sites also include single Ag sites at the alumina surface with Ag atom built in the surface substituting Al is binding SO_x most strongly (see Supplementary material for the exact site geometry). This can be explained by a thermodynamically unfavorable defect structure of this site. Secondly, the oxidation of SO_2 to SO_3 is thermodynamically favorable, with subsequent poisoning of the catalyst surface by the resulting SO_3. This has been suggested in Ref. [9] and probably involves reaction with NO_2 [11]. SO_2 alone cannot be adsorbed on the studied metallic Ag surfaces under reaction conditions and SO_x can, thus, only poison the alumina support or single Ag sites on this surface.

The calculated desorption temperatures (Table 2) are low but the order, at which regeneration of Type II (Ag surface) and Type I (highly dispersed Ag on the alumina) occurs is in agreement with the mechanism of Ag/Al_2O_3 poisoning and regeneration suggested in Section 3.5. The difference between calculated and experimental desorption temperatures [11,25] might indicate the formation of bulk silver sulfate [7,33,34].

At the same time addition of hydrogen significantly enhances catalyst regeneration i.e. removal of SO_x which could be due to the formation of the correspondent HSO_x species with their subsequent desorption. Table 3 shows the energies of the HSO_x species in the gas phase and adsorbed on the most energetically favorable sites. According to the given numbers, the formation of HSO_x is highly favorable on Ag (2 1 1). As the adsorption energies of the HSO_x species with respect to the gas phase species H_2SO_3 (g) and H_2SO_4 (g) are very small they are easily desorbed. The formation of HSO_x is not favorable on the model γ-Al_2O_3 step surface and at the site with Ag built into the γ-Al_2O_3 model step surface. Thus,

Table 2
Adsorption energies and desorption temperatures of SO_x for the most energetically favorable adsorption geometries in case of different adsorption sites.

	Type II (metallic Ag)				Type I (dispersed Ag)					
	Ag (1 1 1)		Ag (2 1 1)		γ-Al_2O_3		Ag built in the γ-Al_2O_3 surface		Ag on the step of γ-Al_2O_3	
	E_{ads} (eV)	T_{des} (K)	E_{ads} (eV)	T_{des} (K)	E_{ads} (eV)	T_{des} (K)	E_{ads} (eV)	T_{des} (K)	E_{ads} (eV)	T_{des} (K)
SO_2	Not adsorbed	–	−0.26	81	−1.43	558	−2.06	791	−1.29	506
SO_3	−1.61	390	−1.82	458	−2.66	630	−3.34	781	−2.64	625
SO_4	−2.65	454	−2.97	597	−1.15	222	−1.77	331	−3.14	572

Table 3
Energies of HSO_x species in the gas phase and adsorbed on the most energetically favorable adsorption sites.

Energy[a] (eV)	HSO_2	HSO_3	H_2SO_3	HSO_4	H_2SO_4
Gas phase	0.21	−0.75	−2.15	−1.48	−3.39
Adsorbed on γ-Al_2O_3	Dissociates	−2.84	−2.18	−3.16	Dissociates
Adsorbed on Ag built in the γ-Al_2O_3	Dissociates	−4.10	−3.38	−3.61	Dissociates
Adsorbed on Ag (2 1 1)	0.02	−2.56	−2.22	−3.94	−3.57

[a] Energy of the HSO_x species is given with respect to SO_2 (g), O_2 (g) and H_2 (g).

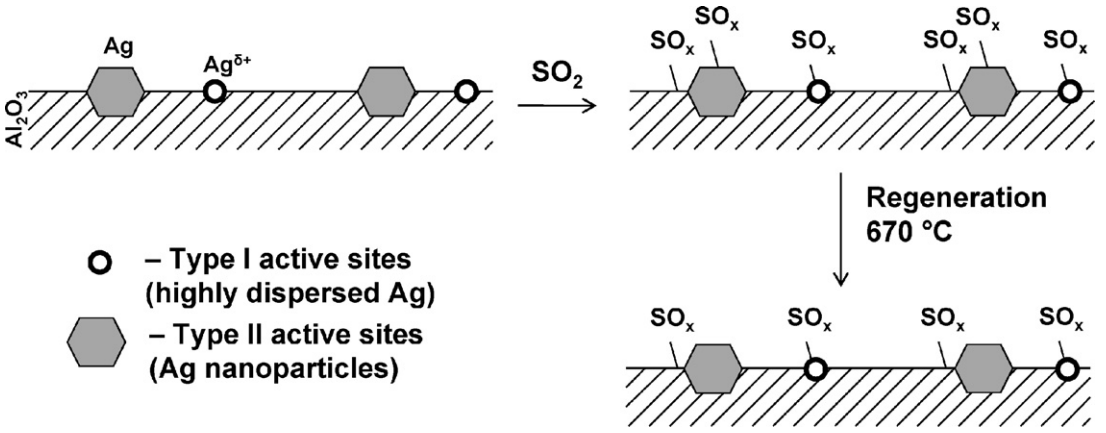

Fig. 5. The scheme of Ag/Al_2O_3 sulfation and regeneration.

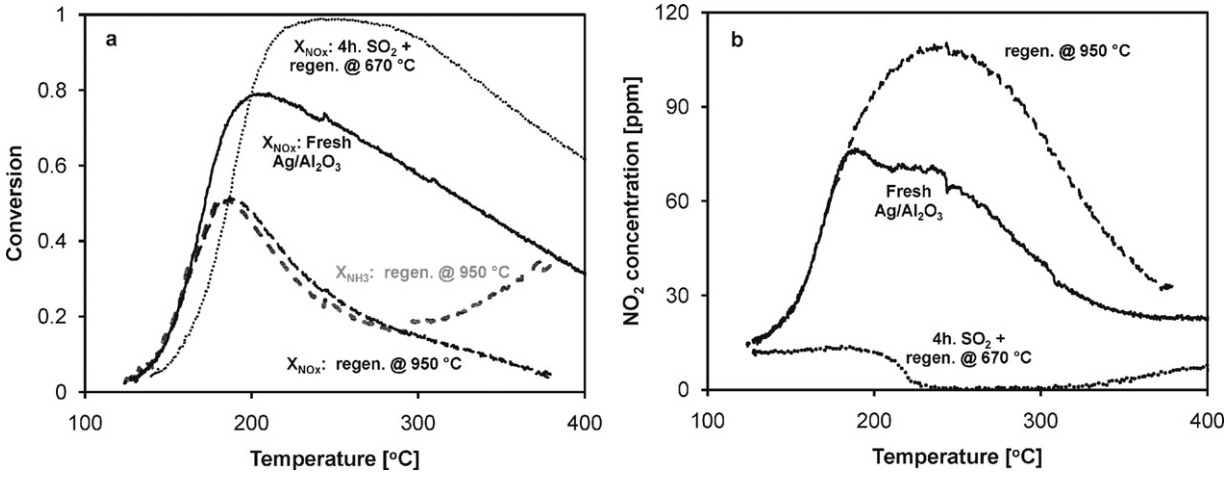

Fig. 6. (a) NO_x conversion profiles obtained over fresh 2% Ag/Al_2O_3 (solid line), 2% Ag/Al_2O_3 after 4 h with 10 ppm SO_2 at 240 °C, followed by 40 min regeneration at 670 °C (dotted line) and after additional regeneration at 950 °C (dashed line). (b) Temperature dependence of NO_2 concentration at the reactor outlet obtained over fresh 2% Ag/Al_2O_3 (solid line), 2% Ag/Al_2O_3 after 4 h with 10 ppm SO_2 at 240 °C, followed by 40 min regeneration at 670 °C (dotted line) and after additional regeneration at 950 °C (dashed line). Reaction conditions: 500 ppm NO, 520 ppm NH_3, 1200 ppm H_2, 8.3% O_2, 7% H_2O in Ar, GHSV = 110,000 h^{-1}.

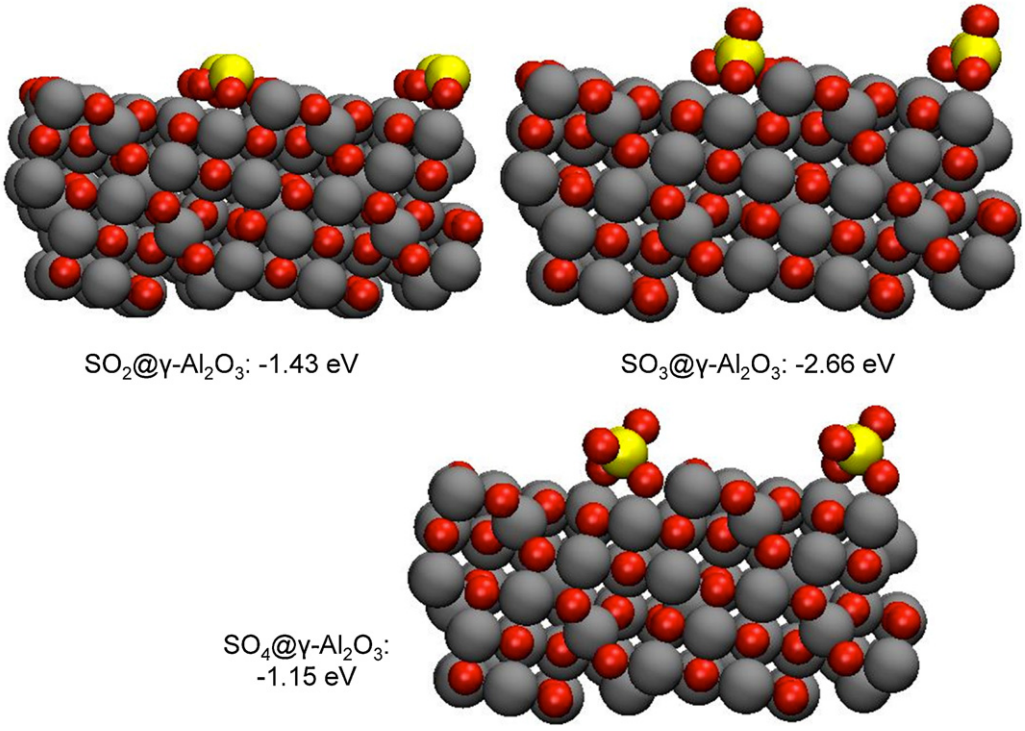

Fig. 7. The most energetically favorable adsorption geometries for adsorption of SO_2, SO_3, and SO_4 on the γ-Al_2O_3 model surface (with corresponding adsorption energies).

presence of H_2 will promote the desorption of SO_x species from the Ag (2 1 1) surface via formation of H_2SO_3 (g) and H_2SO_4 (g) but not for γ-Al_2O_3 surface and the single Ag sites on the γ-Al_2O_3 surface.

4. Conclusions

Sulfur tolerance and regeneration options of 2% Ag/γ-Al_2O_3 catalyst for H_2-assisted NO_x SCR by NH_3 have been tested. The catalyst has medium sulfur tolerance at low temperatures, however a good capability of regeneration. This regeneration should include heating to 650–700 °C for 10–20 min, provided the SCR gas feed is unchanged (ammonia may be removed) and hydrogen is co-fed. Regeneration of Ag/Al_2O_3 without oxygen (rich mixture) leads to essentially the same effect, but requires less time.

Heating to 650–700 °C does not allow full regeneration of low-temperature activity and does not allow recovery of NO_2 formation over Ag/Al_2O_3 in the course of SCR.

During the long-term tests with cycling poisoning–regeneration periods the catalyst activity is regenerated during each regeneration cycle, but at least for the first 6–7 cycles sulfur species are accumulated on the catalyst. Presumably, SO_x is removed from Ag, but not from the alumina surface during standard regeneration, which allows us to make a conclusion on the existence of different active sites in Ag/Al_2O_3, namely finely dispersed Ag ions and Ag nanoparticles.

Acknowledgement

This work was supported by the Danish Council for Strategic Research through grant 09-067233.

Appendix A. Supplementary data

Supplementary data associated with this article can be found, in the online version, at doi:10.1016/j.apcatb.2012.01.002.

References

[1] T.V. Johnson, Int. J. Engine Res. 10 (2009) 275–285.
[2] M. Richter, R. Fricke, R. Eckelt, Catal. Lett. 94 (2004) 115–118.
[3] K.-I. Shimizu, A. Satsuma, Appl. Catal. B 77 (2007) 202–205.
[4] A. Abe, N. Aoyama, S. Sumiya, N. Kakuta, K. Yoshida, Catal. Lett. 51 (1998) 5–9.
[5] H. Kannisto, X. Karatzas, J. Edvardsson, L.J. Pettersson, H.H. Ingelsten, Appl. Catal. B 104 (2011) 74–83.
[6] F.C. Meunier, J.R.H. Ross, Appl. Catal. B 24 (2000) 23–32.
[7] P.W. Park, C.L. Boyer, Appl. Catal. B 59 (2005) 27–34.
[8] S. Satokawa, K.-I. Yamaseki, H. Uchida, Appl. Catal. B 34 (2001) 299–306.
[9] J.P. Breen, R. Burch, C. Hardacre, C.J. Hill, B. Krutzsch, B. Bandl-Konrad, E. Jobson, L. Cider, P.G. Blakeman, L.J. Peace, M.V. Twigg, M. Preis, M. Gottschling, Appl. Catal. B 70 (2007) 36–44.
[10] F. Klingstedt, K. Eränen, L.-E. Lindfors, S. Andersson, L. Cider, C. Landberg, E. Jobson, L. Eriksson, T. Ilkenhans, D. Webster, Top. Catal. 30/31 (2004) 27–30.
[11] Q. Ma, Y. Liu, H. He, J. Phys. Chem. A 112 (2008) 6630–6635.
[12] B. Hammer, L.B. Hansen, J.K. Nørskov, Phys. Rev. B 59 (1999) 7413–7421.
[13] E. Mènendez-Proupin, G. Gutièrrez, Phys. Rev. B 72 (2005) 35116–35119.
[14] M. Digne, P. Sautet, P. Raybaud, P. Euzen, H. Toulhoat, J. Catal. 226 (2004) 54–68.
[15] M.W. Chase Jr., NIST-JANAF Themochemical Tables, fourth edition, J. Phys. Chem. Ref. Data, Monograph 9, 1998, 1–1951.
[16] D.E. Doronkin, S., Fogel, S., Tamm, L., Olsson, T.S., Khan, T., Bligaard, P. Gabrielsson, S. Dahl, Appl. Catal. B, in press, doi:10.1016/j.apcatb.2011.11.042.
[17] S. Fogel, D.E. Doronkin, P. Gabrielsson, S. Dahl, Manuscript in preparation.
[18] Regulation (EC) No. 715/2007 of the European Parliament and of the Council of 20 June 2007, Official Journal of the European Union, (29.6.2007), L 171/1–L 171/16.
[19] VOLVO S80 Instruktionsbok Web Edition http://esd.volvocars.com/site/owners-information/MY11/S80/PDF/S80_owners_manual_MY11_SE_tp11740.pdf (accessed June 2011).
[20] G.M. Wallace, European Diesel Fuel – A Review of Changes in Product Quality 1986–1989, Preprint Archive of the ACS Division of Fuel Chemistry 35 (4) (1990) 1080–1099.
[21] Directive 2009/30/EC of the European Parliament and of the Council of 23 April 2009, Official Journal of the European Union, (5.6.2009), L 140/88–L 140/113.
[22] L. Olsson, H. Sjövall, R.J. Blint, Appl. Catal. B 81 (2008) 203–217.
[23] A. Sultana, M. Haneda, T. Fujitani, H. Hamada, Catal. Lett. 114 (2007) 96–102.
[24] K.-I. Shimizu, J.H.Y. Shibata, A. Satsuma, T. Hattori, Appl. Catal. B 30 (2001) 151–162.
[25] Q. Wu, H. Gao, H. He, J. Phys. Chem. B 110 (2006) 8320–8324.
[26] I. Levin, D. Brandon, J. Am. Ceram. Soc. 81 (1998) 1995–2012.

[27] R. Burch, J.P. Breen, F.C. Meunier, Appl. Catal. B 39 (2002) 283–303.
[28] T.C. Brüggemann, D.G. Vlachos, F.J. Keil, J. Catal. 283 (2011) 178–191.
[29] B. Hammer, J.K. Nørskov, Adv. Catal. 45 (2000) 71–129.
[30] B. Hammer, O.H. Nielsen, J.K. Nørskov, Catal. Lett. 46 (1997) 31–35.
[31] Á. Logadóttir, J.K. Nørskov, J. Catal. 220 (2003) 273–279.
[32] T.V.W. Janssens, B.S. Clausen, B. Hvolbæk, H. Falsig, C.H. Christensen, T. Bligaard, J.K. Nørskov, Top. Catal. 44 (2007) 15–26.
[33] N. Jagtap, S.B. Umbarkar, P. Miquel, P. Granger, M.K. Dongare, Appl. Catal. B 90 (2009) 416–425.
[34] B. Kartheuser, B.K. Hodnett, Alfredo Riva, G. Centi, H. Matralis, M. Ruwet, P. Grange, N. Passarini, Ind. Eng. Chem. Res. 30 (1991) 2105–2113.

Paper V

Applied Catalysis B: Environmental 136–137 (2013) 168–176

Contents lists available at SciVerse ScienceDirect

Applied Catalysis B: Environmental

journal homepage: www.elsevier.com/locate/apcatb

The effect of the gas composition on hydrogen-assisted NH_3-SCR over Ag/Al_2O_3

Stefanie Tamm[a,b], Sebastian Fogel[c,d], Pär Gabrielsson[c], Magnus Skoglundh[a,e], Louise Olsson[a,b,*]

[a] Competence Centre for Catalysis, Chalmers University of Technology, 412 96 Göteborg, Sweden
[b] Chemical Reaction Engineering, Chalmers University of Technology, 412 96 Göteborg, Sweden
[c] Haldor Topsøe A/S, Nymøllevej 55, 2800 Kgs. Lyngby, Denmark
[d] Center for Individual Nanoparticle Functionality (CINF), Department of Physics, Technical University of Denmark, Fysikvej 307, 2800 Kgs. Lyngby, Denmark
[e] Applied Surface Chemistry, Chalmers University of Technology, SE-412 96 Göteborg, Sweden

ARTICLE INFO

Article history:
Received 4 October 2012
Received in revised form 25 January 2013
Accepted 28 January 2013
Available online xxx

Keywords:
Ag/Al_2O_3
H_2-effect
Reaction mechanism
Influence of gas mixture
H_2-assisted NH_3-SCR
Urea

ABSTRACT

In addition to high activity in hydrocarbon-SCR, Ag/Al_2O_3 catalysts show excellent activity for NO_x reduction for H_2-assisted NH_3-SCR already at 200 °C. Here, we study the influence of different gas compositions on the activity of a pre-sulfated 6 wt% Ag/Al_2O_3 catalyst for NO_x reduction, and oxidation of NO and NH_3. The catalyst displays high initial activity for NO_x reduction with a maximum of about 85% at 250 °C. Increasing the concentration of H_2 results in further increased NO_x reduction. Moreover, a global stoichiometry between NO:NH_3:H_2 equal to 1:1:2 is established during selective NO_x reduction conditions. When increasing the concentration of one of the reducing agents only an increase of the H_2 concentration leads to an increase in NO_x reduction, while an increase of the NH_3 concentration only is beneficial to a limit of an equimolar ratio between NO and NH_3. Under transient conditions at constant temperature, the concentration of NO reaches steady state fast, whereas it takes longer time for NH_3 due to accumulated surface species, probably on the alumina. The oxidation of NO to NO_2 is sensitive to the H_2 concentration in similarity to the SCR reaction, while higher amounts of H_2 suppress the oxidation of NH_3. Moreover, the dependency on the O_2 concentration is much higher for the NO and NH_3 oxidation than for the SCR reaction. To explain all these features a reaction mechanism is proposed in which the role of H_2 is to free silver from single oxygen atoms. Ammonia and nitric oxygen can adsorb on these sites and react probably on the border between the silver and alumina or on the alumina surface to N_2.

1. Introduction

Fuel-efficiency in vehicles has become increasingly important owing to increasing oil prices and the concern about climate changes. A more efficient utilization of the energy in the fuel is achieved by combustion in excess oxygen. However, these conditions favor the formation of NO_x as a by-product which needs to be abated due to its negative impact on the environment. Strict emission regulations and low exhaust gas temperatures of fuel efficient engines result in a need for catalysts which can reduce NO_x in oxidizing exhausts already below 200 °C. One concept to reduce NO_x in excess oxygen is selective catalytic reduction (SCR) with either hydrocarbons (HC-SCR) or ammonia/urea (NH_3-SCR) as reducing agent for NO_x.

Silver/alumina is known as a promising catalyst for HC-SCR and shows good catalytic activity at fairly low temperatures when small amounts of hydrogen are added as co-reductant to the feed [1,2]. One major hinder for the practical application of silver/alumina catalysts was the sensitivity to sulphur. However, recently, it was shown, that sulphur poisoned Ag/Al_2O_3 catalysts can be regenerated under conditions which are similar to those during the regeneration of a soot filter [3]. The same authors show, that the activity of an Ag/Al_2O_3 catalyst which has been exposed to sulphur stabilizes after a few exposure and regeneration cycles [3]. Moreover, they showed, that the activity of a silver/alumina catalyst can be higher after sulphur regeneration than freshly prepared [3]. The activity for NO_x reduction varies considerably with the type of hydrocarbon [4]. However, when NH_3 is used as reducing agent 90% conversion can be achieved already at 200 °C [5–7]. In contrast to HC-SCR where H_2 lowers the temperature at which the Ag/Al_2O_3 catalyst is active, Ag/Al_2O_3 is only active for NH_3-SCR in the presence of H_2. The role of this co-reductant as well as the

* Corresponding author at: Chemical Reaction Engineering, Competence Centre for Catalysis, Department of Chemical and Biological Engineering, Chalmers University of Technology, SE-412 96 Göteborg, Sweden. Tel.: +46 31 772 4390; fax: +46 31 772 3035.
E-mail address: Louise.Olsson@chalmers.se (L. Olsson).

0926-3373/$ – see front matter © 2013 Elsevier B.V. All rights reserved.
http://dx.doi.org/10.1016/j.apcatb.2013.01.064

mechanism for HC-SCR have been intensively investigated during the last years [2], since the addition of the reducing agent H_2 unexpectedly leads to an increase of oxidized products as observed both for hydrocarbons [1,8] and nitrogen containing species [4,5]. It has been proposed that the formation of more oxidized products is owing to a change of the state of silver. An increase of the number of small silver clusters has been observed by the addition of H_2 but even by the addition of other reducing agents [9,10]. Moreover, reduction of silver species is discussed but cannot be clearly attributed to the presence of hydrogen [11–13]. Another suggestion is that the reaction mechanism changes by the addition of H_2, which has been exemplified by changing rates of formation and consumption of several carbon-containing intermediates [14,15]. Moreover, NH_3 is proposed to be an intermediate in HC-SCR over Ag/Al_2O_3 [16–18]. This implies, that findings on H_2-assisted NH_3-SCR over Ag/Al_2O_3 also are valid for HC-SCR over the same catalyst. Another area, where similarities might be expected is H_2-SCR over precious metal catalysts [19–22]. However, a substantial difference is that silver/alumina is not active for H_2-SCR; instead, hydrogen acts only as a co-reductant together with either NH_3 or hydrocarbons over silver/alumina catalysts. According to Burch et al. [17] different reaction mechanisms occur over precious metal-based catalysts and oxide based catalysts. One type of reaction mechanism occurs over high loaded silver/alumina catalysts and over precious metals, where substantial amounts of N_2O can be observed. Over low loaded silver/alumina catalysts, the same reaction mechanism has been proposed as over other oxide based catalysts, where the amount of formed N_2O is low.

Although silver/alumina has been studied for a long time, there are no studies available that examine the effect of varying the gas composition on the individual steps in H_2-assisted NH_3-SCR over Ag/Al_2O_3, which is the objective of this work. This is performed in order to achieve fundamental insight into the reactions in this system and propose a mechanism for the H_2 effect. In order to study a highly active catalyst, which is stabilized with sulphur and thus is relevant for real applications, a pre-sulphated catalyst was used in the present study.

2. Materials and methods

Topsøe boehmite alumina was calcined at 500 °C for 2 h. The alumina was then mixed with water and a sufficient amount of $AgNO_3$ was added under intense stirring to give the desired silver loading of 6 wt%. The alumina–Ag slurry was then spray dried and calcined at 400 °C for 2 h. The catalyst was washcoated onto monolith substrate by dipping the monolith in the catalyst slurry. The substrate was a 400 cpsi cordierite monolith with a diameter and a height of 20 mm. After washcoating the monolith was calcined in flowing air at 550 °C for 2 h. The total catalyst load of the monolith was 130 g/L. After calcination the monolith was submerged in an ammonium sulfite solution (sulfite concentration = 2.8 mg/g) for ~10 s. Excess liquid was removed with pressurized air and the monolith was frozen (−30 °C). The water was then removed by sublimation in a vacuum chamber. The amount of sulfur was estimated to 0.7 wt% by weighing the monolith before and after sulfur impregnation.

The specific surface area was 270 m^2/g as measured for the Ag/Al_2O_3 catalyst by N_2-adsorption by single point BET using a Quantachrome Monosorb. The final Ag load was measured to 6.1 wt% by inductively coupled plasma – optical emission spectroscopy (ICP-OES) with a PerkinElmer Optima 3000. Results [3] show that Ag/Al_2O_3 catalysts can be activated by sulfur treatment with SO_2 in the deNO_x feed (O_2, H_2O, NO, NH_3 and H_2). Our results (not published) show that samples also can be activated by impregnation of the catalyst with a sulfur solution (e.g. ammonium sulfite) followed by high-temperature treatment (>600 °C) in deNO_x feed.

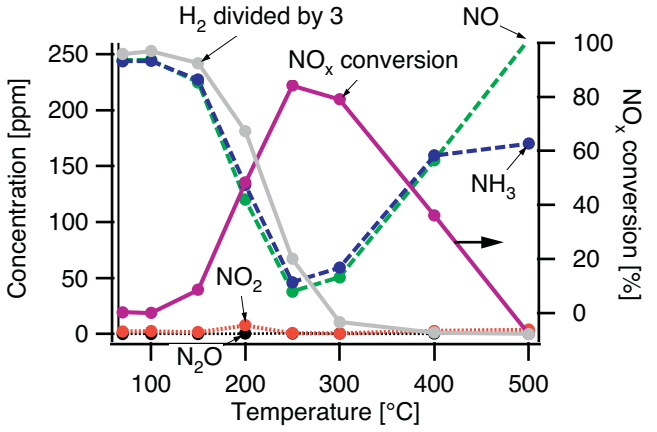

Fig. 1. NO_x conversion and outlet concentrations during H_2-assisted NH_3-SCR over an Ag/Al_2O_3 catalyst as a function of temperature as steady state points. Feed composition: 250 ppm NO, 250 ppm NH_3, 750 ppm H_2, 10% O_2, 5% H_2O in Ar. The concentration of H_2 has been divided by 3.

The samples were freeze dried to ensure that there were no sulfur concentration gradients in the monoliths [23].

Catalytic activity tests were performed in a horizontally mounted quartz tube flow reactor. The quartz tube was 800 mm long with an inner diameter of 20 mm and was externally heated by a heating coil. The monolith was sealed against by-pass flows between the monolith and the wall of the tube with quartz wool and placed in the end of the heated zone. The temperature of the reactor was measured inside a center channel of the monolith sample and controlled 10 mm before the catalyst by a Eurotherm controller. Gases were supplied by separate mass flow controllers and water was added by a controlled evaporation and mixing system (all Bronkhorst Hi-Tech). The outlet gas composition was analyzed using a gas phase FTIR (mks-instruments, MultiGas2030) with the gas cell heated to 191 °C and by a mass spectrometer (Hiden HPR-20 QIC).

All activity tests were carried out using a total flow of 3500 ml/min, resulting in a GHSV of 33 100 h^{-1}. The fresh catalyst was first activated for 5 min at 670 °C in 5% water and then de-greened in 250 ppm NO, 250 ppm NH_3, 10% O_2 and 5% H_2O in Ar at 600 °C for 3 h. In each subsequent experiment the sample was initially pretreated in a flow of 10% O_2 in Ar at 500 °C for 20 min. Afterwards, the catalyst was cooled in 5% water in Ar to 70 °C and exposed to the reaction mixture for 40 min. Then, the temperature was increased in 8 steps with 20 °C/min to 500 °C (100, 150, 200, 250, 300 and 400 °C). Each step lasted at least 20 min to obtain steady state conditions. Moreover, a transient experiment was performed at 200 °C, where NO, NH_3 and H_2 were switched on and off by opening and closing the respective MFC. For the evaluation, the conversion is defined as X conversion [%], which is calculated as $(1 - [X_{out}]/[X_{in}]) \times 100\%$. X consumption [ppm] is calculated as $[X_{in}] - [X_{out}]$, where X is NO_x (NO + NO_2), NH_3 or H_2. Moreover, we calculated the part of NH_3 which is oxidized to NO_x during NH_3 oxidation experiments called NH_3 to NO_x as $[NO_{x,out}]/[NH_{3,in}]) \times 100\%$.

3. Results and discussion

From previous studies it is known, that Ag/Al_2O_3 is active for H_2-assisted NH_3-SCR [5,6]. In contrast to these studies, we here use washcoated monolith catalysts.

3.1. Activity for NO_x reduction

Fig. 1 shows the conversion of NO_x between 70 and 500 °C as a function of temperature during steady state conditions and the

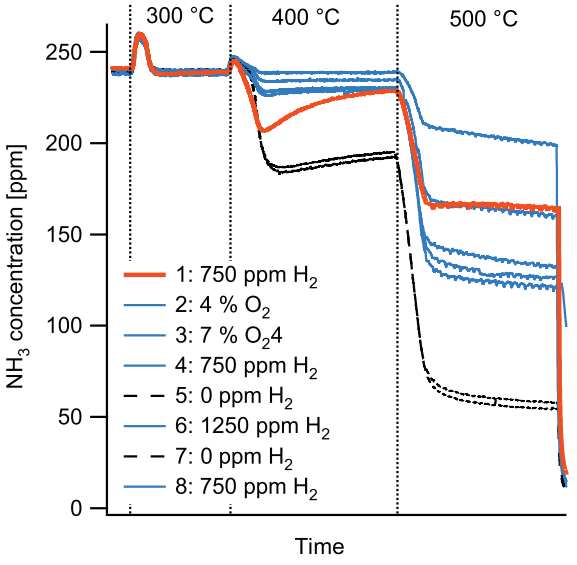

Fig. 2. Outlet concentration of NH_3 during NH_3 oxidation in different gas mixtures as a function of time while increasing the temperature stepwise from 300 to 500 °C with 20 °C/min. Base inlet gas composition: 250 ppm NH_3, 750 ppm H_2, 10% O_2, 5% H_2O in Ar. Modifications are indicated in the figure. The numbers in the figure indicate the order in which the experiments were conducted.

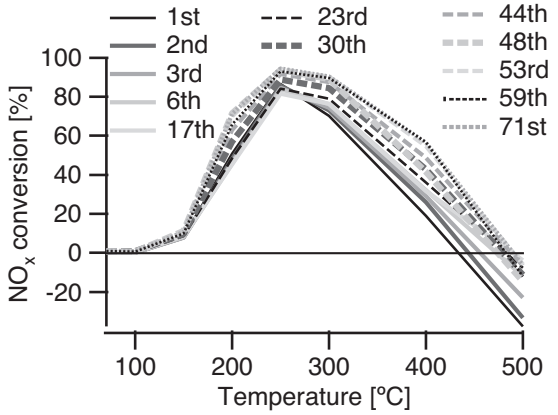

Fig. 3. NO_x conversion after aging of the catalyst with number of experiments. Feed composition: 250 ppm NO, 250 ppm NH_3, 750 ppm H_2, 10% O_2, 5% H_2O in Ar.

outlet concentrations of NO, NO_2, NH_3, N_2O and H_2. The NO_x conversion starts already at 150 °C and reaches a maximum of 85% at 250 °C. In accordance with Ref. [6] the selectivity to N_2 is very high which is indicated by the absence of N_2O throughout the entire temperature range. Moreover, the formation of NO_2 is very low. This is unusual for NH_3-SCR over Ag/Al_2O_3 but can be attributed to the pre-sulfating of the catalyst. Hydrogen, which was shown to be essential for the reaction to occur [5], is completely consumed from 400 °C, limiting the NO_x conversion at these high temperatures. At 500 °C, significant amounts of NH_3 are unselectively oxidized to NO resulting in a negative NO_x conversion in Fig. 1.

The information of Fig. 1 is extracted from a transient experiment, where the catalyst is initially exposed to the reaction gas mixture at 70 °C. Subsequently, the temperature is increased stepwise and the increase of the temperature is accompanied by desorption of NH_3 until 250 °C (see supporting information). In parallel, the NO conversion increases and some NO_2 is initially formed already at 100 °C. From 300 °C, the NH_3 and NO concentrations increase again due to shortage of H_2. Increasing the temperature from 400 to 500 °C causes initially a parallel increase of the NO and NH_3 concentrations until 425 °C, where oxidation of NH_3 starts causing a temporary steep decrease by 90 ppm of the NH_3 concentration accompanied by a further increase of the NO concentration. The NH_3 concentration increases thereafter again and reaches its original level after about 30 min. This transient effect is connected to the presence of NH_3 since it is not observed in NO oxidation experiments. Fig. 2 shows the NH_3 concentration during NH_3 oxidation. When heating the catalyst from 250 to 300 °C, and from 300 to 400 °C small amounts of ammonia desorb from the catalyst. At 300 °C, practically no NH_3 oxidation occurs. This observation is similar for all tested gas compositions. At 400 °C, the ammonia concentration stabilizes after the desorption peak on a stable level in most of the experiments. However, in the first NH_3 oxidation experiment conducted after an SCR experiment, the NH_3 concentration decreases rapidly followed by a slow increase during and after heating from 300 to 400 °C. A similar effect is also observed in the absence of H_2 though not as pronounced. More details of NH_3 oxidation will be discussed later. The transient effect observed between 400 and 500 °C under NH_3-SCR conditions and the effect observed between 300 and 400 °C during NH_3 oxidation are quite similar. One possible explanation for this effect is a slow change in the oxidation state of Ag by a competing reaction between NH_3 and NO_2 or adsorbed NO_x. During NH_3 oxidation small amounts of NO_2 (less than 2 ppm) are formed in the absence of H_2. However, no NO_2 was detected in the presence of more than 750 ppm H_2. In previous studies, Ag/Al_2O_3 catalysts showed good resistance against hydro-thermal treatment below 700 °C [24–26]. Although the Ag/Al_2O_3 catalyst was de-greened at 600 °C in this study, it was not completely stable, and the activity for NO_x reduction improved with time. Fig. 3 shows the activity for NO_x reduction under standard conditions. This activity increased with the number of experiments where one experiment took 8 h. During the first experiments, mainly the activity for NH_3 oxidation decreased as indicated by less negative conversion at 500 °C. This effect can be explained by a loss of loosely bound sulfur, since trace amounts of SO_2 have been detected in the exhaust during the first couple of experiments. However in the following experiments, the activity for NO_x reduction increased in the entire temperature interval between 200 and 500 °C. One explanation for the improved activity could be the loss of further sulfur from the catalyst. However, after the first experiments, no SO_2 was detected in the gas phase after the catalyst. In addition, the largest changes were observed after NH_3 oxidation experiments (between the 30th and 48th experiment) in the absence of NO. After the 59th experiment, the catalyst appears to be stable. Breen et al. [24] report an increase in activity for NO_x reduction in octane-SCR after aging of an Ag/Al_2O_3 catalyst at 600 °C for 16 h and attributed this to coalescing of Ag into small clusters of an average of three atoms. This effect is also reasonable in the present study. Since each experiment started by a pretreatment at 500 °C for 20 min and finished at 500 °C as the highest reaction temperature, the catalyst was in total exposed to 500 °C for more than 30 h during the course of more than 50 experiments. Another possible explanation of the increase in activity is the formation of Ag_2SO_4, which can be expected to occur after the de-greening of the sample. Silver sulfate is reported to decrease low temperature activity [27]. During experiments the less stable Ag_2SO_4 may be converted into more stable $Al_2(SO_4)_3$ like species [28], which could explain the gain in low temperature activity.

3.2. *Influence of the gas composition on the activity for NO_x reduction*

Fig. 4 shows the influence of the concentration of water, oxygen, ammonia and nitric oxide on the NO_x conversion as a function of temperature. Since all the experiments shown in one graph were performed consecutively, changes due to ageing do not need to be

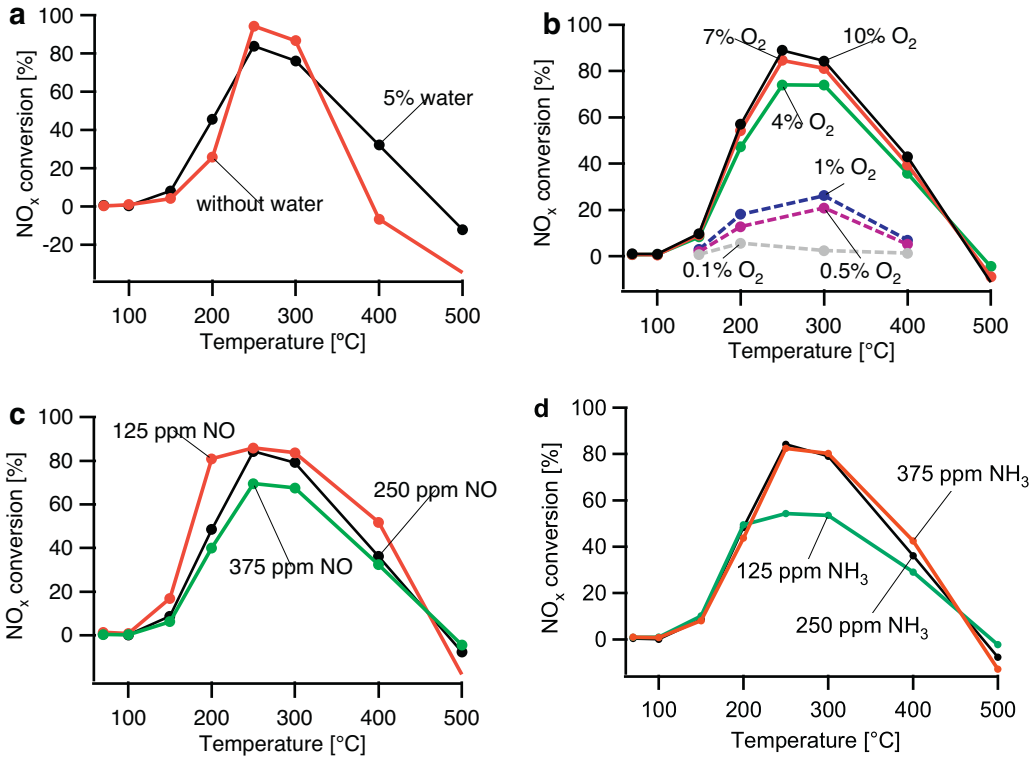

Fig. 4. Influence of the concentration of water (a), oxygen (b), NO (c) and ammonia (d) on the NO_x conversion as a function of temperature. Base inlet gas composition: 250 ppm NO, 250 ppm NH_3, 750 ppm H_2, 10% O_2, 5% H_2O in Ar. Modifications are indicated in the figure.

taken into account for the interpretation. In the presence of water higher activity for NO_x reduction is observed at 200, 250 and 400 °C but the maximum conversion is somewhat lower. Moreover, less NH_3 oxidation occurs at 500 °C. However, no trend can be observed when 4 to 8% of water is present in the feed (not shown). Several roles have been proposed for water. The presence of water can reduce the amount of adsorbed NO_x and reducing agent on the catalyst due to competition of adsorption sites and thus reduce NO_x conversion [29,30]. For long hydrocarbons, this effect is beneficial, since it prevents the formation of coke and thereby increases the NO_x conversion [30]. Ammonia is known to adsorb strongly on the catalyst surface. Therefore, reduction of the amount of NH_3 could be beneficial for NO_x reduction at low temperatures, as it is the case in NH_3-SCR over Fe–zeolites [31]. From 250 °C where the NO_x conversion is high, this effect reduces the overall NO_x reduction. Moreover, it has been proposed, that NO is activated by interaction with hydroxyl groups [32]. In the presence of water, the amount of OH-groups will be higher and could therefore contribute to a higher NO_x conversion.

Fig. 4b shows the effect of different oxygen concentrations on the activity for NO_x reduction. Even when O_2 is provided in large excess, the NO_x conversion increases with increasing of O_2 concentration. This is in accordance with previous results for HC-SCR, where it has been proposed that partial oxidation of the reducing agent (hydrocarbon) is an important part of the reaction mechanism [30,33]. In addition to the partial oxidation of hydrocarbons, partial oxidation of NO and NH_3 have been proposed as initial steps in the reaction mechanism [16,17,34]. These steps also benefit from higher O_2 concentrations. This is further supported by the very low activity with only 0.1% O_2. Although there is still an excess of O_2 present in the feed, the NO_x conversion stays below 5%, demonstrating that O_2 is needed in the SCR reaction. With 0.5 and 1% O_2 in the feed, the maximum conversion occurs at 300 °C, which is higher than for the experiments with higher O_2 concentrations. It is possible that at low O_2 concentrations, less H_2 is unselectively oxidized than at high O_2 concentrations and more hydrogen is thus available for the SCR reaction. Also the effect of changing the NO concentration was studied as shown in Fig. 4c. Decreasing the amount of NO in the feed gas while keeping the concentrations of all other gases constant results in an increased NO_x conversion between 150 and 400 °C. This is in accordance with previous results from HC-SCR and H_2-assisted HC-SCR as reported in Ref. [30] and [35], respectively. At 500 °C, a negative NO_x conversion is observed. The additional NO_x is formed by oxidation of NH_3 to NO. Moreover, the sum of the NH_3 and the NO_x concentrations is about 60 ppm below the inlet values revealing that about 30 ppm N_2 is formed at 500 °C independent on the NO inlet concentration. The N_2 might be formed in the very beginning of the catalyst, where H_2 is available for NH_3-SCR or during the oxidation of NH_3. Since considerable amounts of N_2 are formed during NH_3 oxidation over the present catalyst (see below) the major part of the N_2 formation can be attributed to the NH_3 oxidation. Assuming that N_2 is formed during the NH_3 oxidation and this amount of formed N_2, moreover, is independent of the NO inlet concentration indicates that NH_3 oxidation is independent of the NO concentration in the studied concentration interval.

The change in the NO_x conversion with different NH_3 concentrations is plotted in Fig. 4d. An NH_3 concentration which is significantly lower than the NO_x concentration in the feed leads to a lower NO_x conversion above 200 °C compared to the NO_x conversion with equal amounts of NO_x and NH_3 in the feed. Higher concentrations of NH_3 than NO_x in the feed, however, do not result in higher NO_x conversion. The limit in NO_x reduction seems to contradict the results in Fig. 4c on the variation of the NO_x concentration. However, in Fig. 4c the ratio of both NO to NH_3 and NO to H_2 changes, while in Fig. 4d the ratio between NH_3 to NO and NH_3 to H_2 changes. We can therefore conclude that the limit of NO_x conversion observed in Fig. 4d is caused by the ratio of NO to H_2.

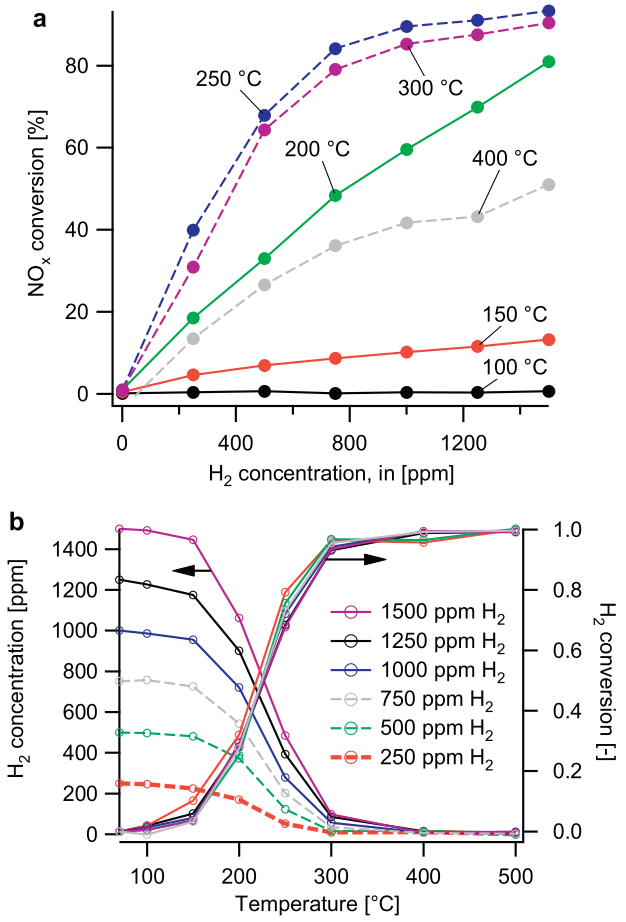

Fig. 5. (a) NO_x conversion as a function of H_2 concentration in the feed at six different temperatures in an inlet feed of 250 ppm NO, 250 ppm NH_3, 0–1500 ppm H_2, 10% O_2 and 5% H_2O in Ar. (b) Hydrogen concentration and hydrogen conversion as a function of temperature for different hydrogen concentrations in a feed gas mixture of 250 ppm NO, 250 ppm NH_3, 0–1500 ppm H_2, 10% O_2 and 5% H_2O in Ar.

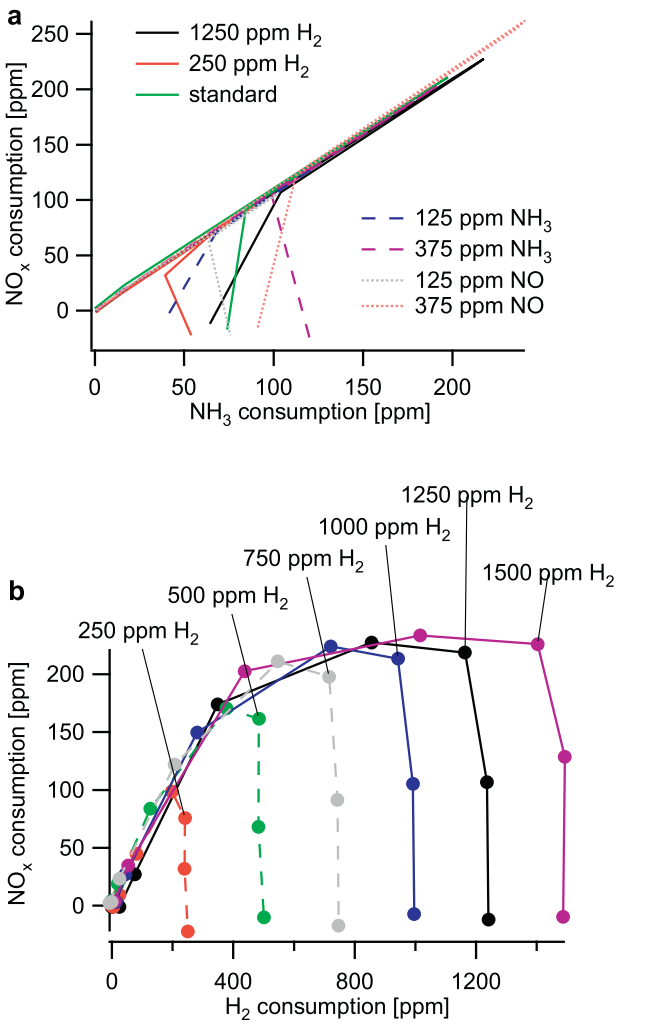

Fig. 6. (a) NO_x consumption as a function of NH_3 consumption for different gas mixtures. Standard inlet gas composition: 250 ppm NO, 250 ppm NH_3, 750 ppm H_2, 10% O_2, 5% H_2O in Ar (light grey solid line). Modifications are indicated in the figure. (b) NO_x consumption as a function of H_2 consumption in different gas mixtures. Inlet gas composition: 250 ppm NO, 250 ppm NH_3, 250–1500 ppm H_2, 10% O_2 and 5% H_2O in Ar.

The dependence of NO_x conversion on the H_2 concentration will be discussed in detail in the following section. The influence of the amount of reducing agent on the NO_x conversion has previously been studied for HC-SCR in the absence of H_2 and gave different results. A constant increase of NO_x reduction with increasing concentration of hydrocarbon was observed [33] while other groups report an increase in NO_x conversion with higher concentrations of hydrocarbons which approaches a limit at high hydrocarbon to NO ratios above certain temperatures [30,36]. This observation is in accordance with our results in Fig. 4d. Moreover, Arve et al. [35] report a higher increase in NO_x conversion with increasing hydrocarbon concentration at high than at low H_2 concentrations.

Fig. 5a shows the NO_x conversion as a function of the inlet H_2 concentration for different temperatures. Without H_2, the catalyst cannot reduce NO_x. However, with increasing H_2 feed concentration the NO_x conversion increases in the entire temperature range, in which the catalyst is active. This increase in NO_x reduction is different at different temperatures. At 250 and 300 °C, the NO_x conversion increases steeply at low H_2 concentrations and approaches slowly 90%. At both lower (150 and 200 °C) and higher (400 °C) temperatures the NO_x conversion increases continuously in the studied concentration interval. Similar trends have previously been reported for NH_3-SCR as well as HC-SCR over Ag/Al_2O_3 catalysts [4,6,35,37].

In addition to the NO_x conversion, the outlet H_2 concentration and H_2 conversion is shown as a function of temperature in Fig. 5b. Hydrogen conversion starts at 150 °C and from 400 °C complete H_2 conversion is seen independently of the H_2 concentration in the feed. In fact, the level of hydrogen conversion (in %) is independent of the hydrogen concentration in the feed revealing that the H_2 conversion is independent of both the NO and the NH_3 concentration. This is valid for a variation of H_2 concentrations at fixed NO and NH_3 concentrations (Fig. 5) and also for variations of the NO, NH_3 and O_2 concentrations (Fig. 4). At 300 °C, about 95% of the H_2 is converted, which might result in a shortage of H_2 in some parts of the catalyst leading to a slightly lower NO_x conversion at 300 °C compared to 250 °C. At even higher temperatures the shortage of H_2 appears to become even more severe, resulting in a clearly lower NO_x reduction. Previously it has been shown that the temperature where complete H_2 conversion is reached is shifted to lower temperatures with increasing silver loading for HC-SCR over Ag/Al_2O_3 [38]. In accordance with the present study, total H_2 conversion was achieved close to 300 °C for the most active sample [38].

In Fig. 6a the NO_x consumption at different NO (Fig. 5c) and NH_3 (Fig. 5d) feed concentrations are combined and the NO_x consumption is plotted as a function of the NH_3 consumption. This type of presentation shows, that there is a fixed molar ratio of 1:1 between NH_3 and NO conversion, which is independent of the NO, NH_3 and H_2 inlet concentrations. Only at 500 °C, where unselective

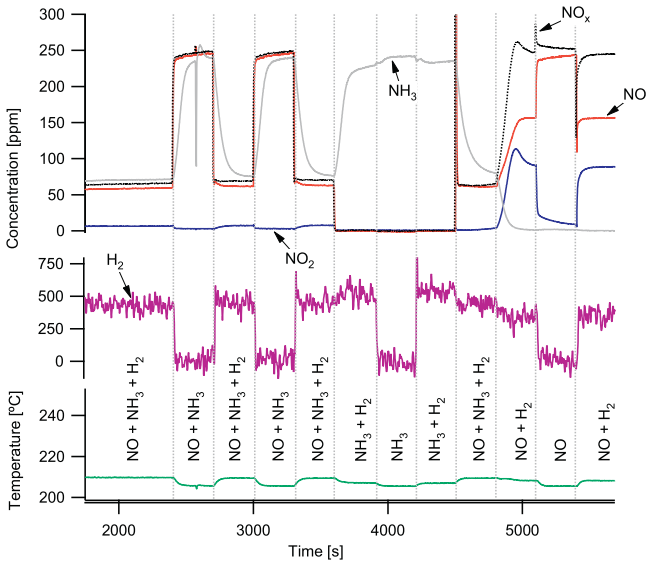

Fig. 7. Transient behavior switching off H_2, NH_3 and NO or combinations of these gases for 5 min at 200 °C under H_2-assisted NH_3-SCR conditions with 250 ppm NO, 250 ppm NH_3, 750 ppm H_2, 10% O_2, 5% H_2O in Ar.

oxidation of NH_3 to NO takes place, this ratio is changed and the points below the main straight line are from these cases. Oxidation of NH_3 to NO results in an NO concentration, which is higher than the inlet NO concentration leading to negative NO_x conversion. Moreover, these results show that below 500 °C all the converted NH_3 is exclusively involved in NO_x reduction. No loss of NH_3 by oxidation to N_2 or N_2O is observed during H_2-assisted NH_3-SCR below 500 °C. In order to establish a ratio between H_2 and NO in the SCR reaction the NO_x consumption is plotted as a function of H_2 consumption. These results are shown in Fig. 6b. From a careful comparison of the values in Fig. 6 with Fig. 5b it is clear that below 250 °C the conversion of H_2 stays below 30% and a linear correlation between NO and H_2 of 1:2 can be established. From 250 °C, unselective oxidation of some H_2 occurs, indicated by a flattening of the curve in Fig. 6b. Here, the unselective oxidation of H_2 is not limiting the NO_x conversion, since the highest NO_x conversion is achieved at 250 °C, where also some unselective oxidation of H_2 occurs. From 300 °C, the unselective oxidation apparently leads to shortage of H_2 in some parts of the catalyst leading to a decrease in the overall NO_x reduction while the H_2 conversion is high. This feature is even more pronounced at higher temperatures. The ratio between NO and H_2 of 1:2 can be explained by assuming that the silver surface is covered by oxygen at low temperatures. This assumption is in accordance to previous results obtained by XPS [13,23]. Hydrogen removes single oxygen atoms from the silver surface freeing single sites which subsequently can be occupied by either NO or NH_3. The adsorbed NO and NH_3 species react and form N_2. This N_2 formation likely occurs on the interface between silver and alumina or on the alumina support, since it has been shown that Al_2O_3 plays an important role in silver/alumina catalysts [5]. Oxygen cannot reoccupy the free single sites on the silver, since it needs two sites to dissociatively adsorb on. This process is limited by the reaction of H_2 with surface oxygen. At somewhat higher temperatures, the reaction of hydrogen with the surface oxygen atoms becomes faster and there is a higher probability that two adjacent oxygen atoms are removed from the silver surface with a short time lag. These sites can be filled with oxygen disturbing the ratio between NO and H_2 of 1:2. At high temperature this process is so fast that the NO_x conversion drops due to a lack of free adsorption sites for the NO and NH_3 on the silver.

Fig. 7 shows the transient behavior of the catalyst upon fast removal of one component from the gas mixture. After reaching steady state conditions for H_2-assisted NH_3-SCR, H_2 is removed from the feed, rapidly halting the NO_x conversion. The NH_3 concentration starts to increase at the same time as the NO concentration. However, it takes almost 5 min for the NH_3 concentration to reach steady state after removal of H_2. A similar behavior is observed, when H_2 is switched on again. The NO_x concentration drops immediately to steady state levels, while this takes longer time for the NH_3 concentration. The different times needed to reach steady state condition for NH_3 and NO indicate different amounts of stored surface species. Previously, we have shown that NH_x species are the predominant species during NH_3-SCR conditions. However, the major parts of the nitrates formed on the surface are stable and will not be removed by NH_3 and H_2 [5]. In accordance with Fig. 1, some NO_2 is formed at 200 °C during H_2-assisted SCR. In the absence of H_2, however, no NO_2 is detected. In the absence of NO, some minor NH_3 conversion occurs in the presence, but not in the absence of H_2, indicating that the presence of H_2 even has a promoting effect on the NH_3 oxidation. This effect will be discussed later in more detail. Removing NH_3 from the feed results in oxidation of about 2/5 of the NO to NO_2 (90 ppm) at steady state. It is interesting to notice, that the NO_2 concentration increases steeply, when NH_3 is switched off and reaches its highest value just after the NH_3 concentration in the outlet has declined to zero. Thereafter, the NO_2 concentration decreases and reaches steady state levels about 5 min after the NH_3 supply has been switched off. No transient effects are observed when H_2 is added to the feed of NO, O_2 and H_2O in Ar. However, the NO_2 production increases significantly. The higher concentration of NO_2 when switching off NH_3 indicates that adsorbed parts of ammonia, like hydrogen, can have a promontory effect on the oxidation of NO to NO_2. However, this effect is only observed when switching out NH_3 from a mixture of NO, NH_3, H_2, O_2 and water. A possible explanation is that the adsorbed NH_3-fragments continue to react with the NO_x and free additional sites, on which NO can be oxidized to NO_2. Finally, some tailing of NO_2 is observed when H_2 is removed from the above mentioned feed while NO reaches steady state more rapidly. All the discussed phenomena of the transient experiment can be explained by the previously proposed mechanism, when assuming that most of the desorbed NH_3 had been adsorbed on the Al_2O_3. Alumina as the main NH_3 storage compound is in accordance with Ref. [39]. Moreover, the tailing of the NO_2 can be assigned to adsorbed NO species on the silver.

In summary, variation of the O_2, NO, NH_3 and H_2 concentration in H_2-assisted NH_3-SCR has similar effects as in H_2-assisted HC-SCR over Ag/Al_2O_3 catalysts. For HC-SCR over Ag/Al_2O_3, a reaction of adsorbed NH_x species with adsorbed NO_x species has previously been proposed as a last step before N_2 formation [16,17,40,41]. This is possibly also the last step in hydrogen-assisted NH_3-SCR over Ag/Al_2O_3. The difference in the reaction mechanisms between NH_3- and HC-SCR is, thus, in the formation of adsorbed NH_x species. Since a similar increase in activity is observed by adding hydrogen to the gas mixture in HC- and NH_3-SCR, it can be assumed that H_2 promotes steps that are either common or at least similar in both reaction mechanisms.

3.3. *Influence of the gas composition on the oxidation of NO and NH_3*

The promotional effect of H_2 on the NO oxidation over Ag/Al_2O_3 catalysts has been shown in several studies [1,5,11,42]. Fig. 8 shows the influence of the H_2, NO and O_2 concentrations on the NO oxidation. Similar to NO_x conversion, the oxidation of NO to NO_2 increases with increasing H_2 concentration (Fig. 8a). The shape of the NO_2 concentration in Fig. 8a resembles in shape that of the NO_x conversion during H_2-assisted NH_3-SCR (see supporting

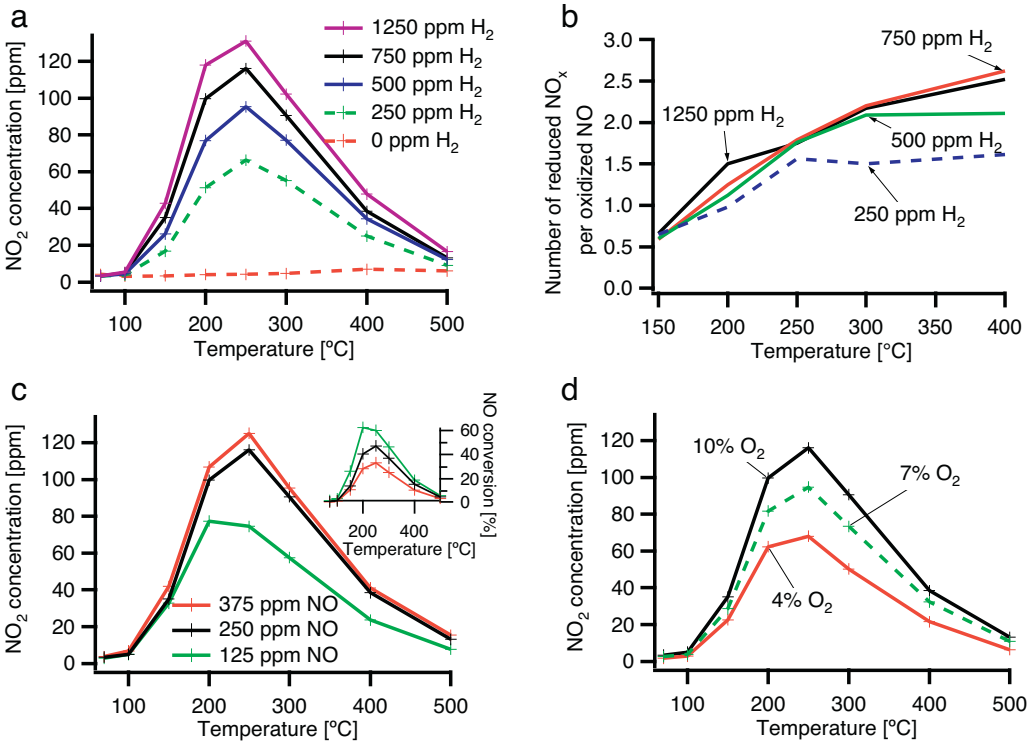

Fig. 8. NO oxidation as a function of the temperature in the presence of different amounts of H_2 (a), Ratio between reduced NO_x in SCR and NO_2 produced in NO oxidation (b), varying NO concentration (c), varying O_2 concentration (d). Base inlet gas composition: 250 ppm NO, 750 ppm H_2, 10% O_2, 5% H_2O in Ar. Modifications are indicated in the figure.

information). Therefore, the molar ratio between reduced NO_x during NH_3-SCR and oxidized NO_2 during NO oxidation was calculated for identical H_2 inlet concentrations and temperatures:

$([NO_{x,in}]\text{-}[NO_{x,out}])_{SCR\ conditions}/([NO_{2,out}])_{NO\ oxidation}$ at fixed NO, O_2, H_2 concentrations and temperatures

In Fig. 8b these results are plotted as a function of temperature for the different H_2 inlet concentrations used. For all H_2 inlet concentrations, one mole of NO_x is reduced during SCR for two moles of NO_2 produced during NO oxidation at 150 °C. This ratio increases reaching a value of about 2.5 moles reduced NO_x per one mole formed NO_2 at 400 °C in the presence of at least 750 ppm H_2. For 250 and 500 ppm H_2, the ratio reaches limits of 1.5 and 2.1, respectively, which are observed already below 400 °C. Since more NO_2 is formed in NO oxidation than NO is reduced during SCR conditions at 150 °C, NO_2 is also expected in the outlet during NH_3-SCR. However, no NO_2 is detected, which can be explained by blocking of the active sites by NH_3 during SCR. Another explanation can be obtained from the mechanistic model proposed above. Assuming that identical concentrations of H_2 free the same amount of sites at a certain temperature NO can occupy twice as many sites during NO oxidation than during SCR, when NH_3 is present. As already stated in the discussion about Fig. 6, more sites are available at higher temperatures leading to a higher ratio of reduced NO_x during SCR to oxidized NO_x during NO oxidation.

In Fig. 8c, the effect of the NO concentration on the NO oxidation is shown. The amount of NO_2 increases as the NO concentration increases but reaches a limit at a H_2:NO ratio of 3:1 in the feed. A higher NO concentration results in the same NO_2 formation. This result is interesting since a similar limit has been observed in Fig. 4d for the influence of NH_3 on the NO_x conversion and can be interpreted as a certain amount of H_2 can only activate a certain amount of NO (probably by oxidation to NO_2) which then can be reduced by an NH_3 derived species. These results do not contradict the ratio between converted H_2:NO of 2:1 established in Fig. 6 since this ratio is only observed for low conversions and is independent of the feed. However, also this result can be explained by H_2 freeing a certain number of sites, on which NO can adsorb. When all these sites are filled higher concentrations do not change the result.

In the insert in Fig. 8c the formation of NO_2 is shown as NO conversion in percent. This insert illustrates that conversion of NO by oxidation increases with decreasing NO concentration mainly as an effect of a higher H_2 to NO ratio. This confirms our results from Fig. 5a, where we showed that the NO_x conversion increases with higher H_2 to NO ratio. Finally, Fig. 8d demonstrates that the NO oxidation is clearly dependent on the O_2 concentration between 150 and 500 °C. This dependency is stronger than the dependency of the NH_3-SCR reaction although the NH_3-SCR reaction appears to be closely related to the oxidation of NO.

To investigate the influence of the NO_2 concentration, activity tests with equimolar amounts of NO and NO_2 as NO_x in the feed were performed (see supporting information). The NO_x reduction is only slightly higher when 50% of the NO_x is NO_2 than when all the NO_x is NO. The largest difference in NO_x conversion is observed at 200 °C were 71% NO_x conversion occurred with only NO in the feed and 85% with a mixture of NO and NO_2, corresponding to 20% higher NO_x conversion at this temperature. This result is in accordance with the study by Doronkin et al., where it was shown that Ag/Al_2O_3 is active for NH_3-SCR without H_2 providing some NO_2 in the feed [5]. Moreover without H_2, the conversion of NO_x is limited to about 30%. This limit is removed by the addition of H_2 showing that H_2 has an important role in NH_3-SCR even in the presence of NO_2 as NO_x. This observation also fits into the framework of the proposed reaction mechanism.

The activity of the catalyst for oxidation of the reducing agent is an important parameter as well. In the literature it has been shown that NH_3 can be oxidized to N_2, N_2O and NO over Ag/Al_2O_3 catalysts [5,43]. The ignition temperature and product distribution vary with the catalyst composition (e.g. Ag loading). Fig. 9 shows the NH_3

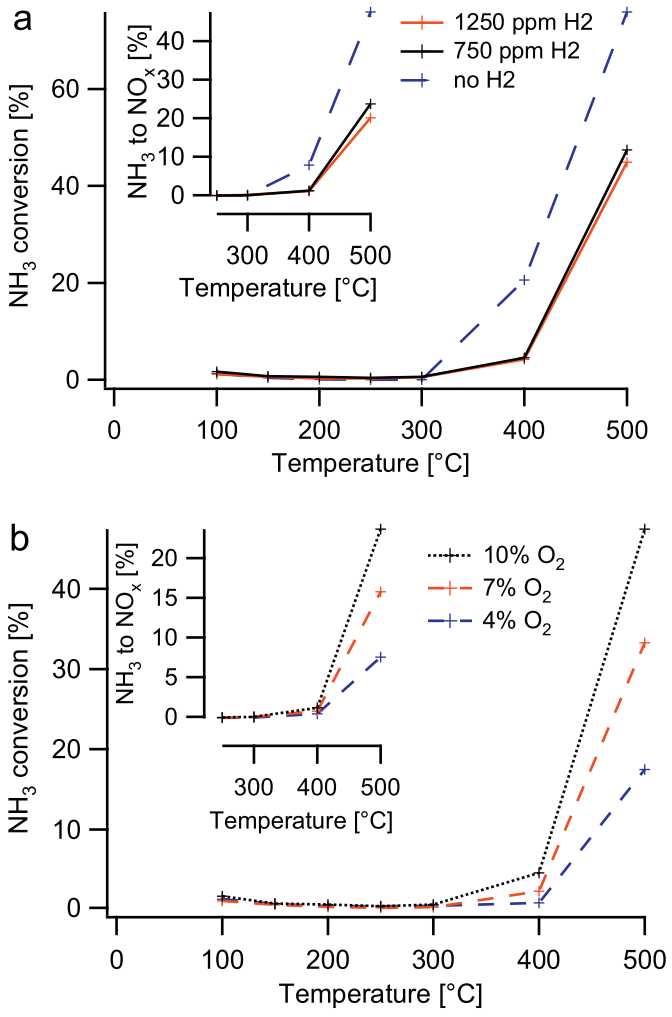

Fig. 9. NH_3 oxidation as a function of temperature in different gas mixtures. Standard gas mixture is 250 ppm NH_3, 750 ppm H_2, 10% O_2 and 5% H_2O in Ar. Modifications are indicated in the figure.

oxidation in different feed compositions as a function of temperature. Without H_2, the oxidation of NH_3 starts at 400 °C and reaches 76% at 500 °C, where 48% of the NH_3 in the feed is oxidized to NO_x over the catalyst, revealing that about two thirds of the oxidized NH_3 forms NO_x and about one third N_2 (Fig. 9a). However in the presence of 750 and 1250 ppm H_2, the oxidation of NH_3 is considerably lower, reaching about 50% at 500 °C. Moreover, only about 25% of the NH_3 in the feed is oxidized to NO_x, i.e. one half of the oxidized NH_3 forms NO_x in comparison to one third in the absence of H_2. These results are reasonable, since NH_3 oxidation is proposed to start by the consecutive braking of N—H bonds over Ag/Al_2O_3 [34]. Assuming equilibrium reaction, the presence of additional hydrogen from H_2 in the feed will shift the equilibrium to the ammonia side. Another explanation for the lower NH_3 oxidation in the presence of H_2 is that hydrogen will decrease the concentration of adsorbed oxygen, which is needed for the oxidation of NH_3. The temperature at which NH_3 oxidation starts in the presence of H_2 is higher in Fig. 9 than expected from the transient experiment in Fig. 7, where some minor NH_3 oxidation is observed at 200 °C in the presence but not in the absence of hydrogen. These contradictory results can be explained by the fact that the catalyst changes during the first NH_3 oxidation experiment as shown in Fig. 2. Moreover, from the reaction mechanism presented above, adsorption of NH_3 also on the silver species can be expected already at 200 °C. However, the reaction mechanism does not predict any reactions on the surface or desorption of species.

Moreover, the oxidation of NH_3 increases at higher O_2 concentrations in the feed (Fig. 9b). Similar to NO oxidation, also NH_3 oxidation is stronger dependent on the O_2 concentration than the SCR reaction. This phenomenon can be rationalized when assuming that higher NO oxidation promotes the SCR reaction while oxidation of NH_3 removes necessary compounds for the reaction. The dependence of these two conflictive effects can explain the minor dependence of the NH_3-SCR reaction on the O_2 concentration.

4. Conclusions

The influence of different gas compositions on the activity for NO_x reduction, and oxidation of NO and NH_3 of a pre-sulfated 6 wt% Ag/Al_2O_3 catalyst has experimentally been studied. It has been shown that:

- The catalyst is initially highly active for NO_x reduction with a maximum of about 85% at 250 °C. The activity increases throughout the course of the experiments due to mild aging of the catalyst at 500 °C.
- An increase in the feed concentration of hydrogen results in increased NO_x reduction. This increase is linear at 150 and 200 °C in the studied H_2 concentration interval but approaches a limit of more than 90% NO_x conversion at 250 and 300 °C.
- An increase of the NH_3 concentration is beneficial to a limit of an equimolar mixture of NO and NH_3. A further increase of the NH_3 concentration above this ratio does not result in further improved NO_x conversion.
- A global stoichiometry between $NO:NH_3:H_2$ equal to 1:1:2 is observed during selective NO_x reduction.
- Under transient conditions at a constant temperature, the concentration of NO reaches steady state fast, whereas the stabilization of the NH_3 concentration takes longer time due to accumulation of surface species. In the presence of NH_x surface species, the concentration of NO_2 takes as long to stabilize as the NH_3 concentration and exhibits a maximum, while in the absence of NH_x surface species the NO_2 concentration stabilizes as fast as the NO concentration.
- The NO oxidation to NO_2 is sensitive to the H_2 concentration in similarity to the SCR reaction. However, the dependence on the O_2 concentration is much higher for the NO oxidation and the NH_3 oxidation than for the SCR reaction. The addition of small amounts of hydrogen during NH_3 oxidation results in decreased NH_3 oxidation and leads to a higher degree of N_2 formation.

All the observations concerning changes in the feed composition can be explained by assuming that the silver surface is covered by oxygen. Oxygen adsorbs dissociatively and competes with NO and NH_3 for the same adsorption sites. Hydrogen can remove single oxygen atoms from that surface freeing adsorption sites for NO or NH_3. These adsorbates can react on the surface forming N_2 probably in the interface between silver and alumina or on the alumina surface. This explains the observed ratio between $NO:NH_3:H_2$ of 1:1:2 and why there is a limit to which NO_x conversion increases for the NH_3 concentration, but not for the H_2 concentration. Moreover, this reaction mechanism explains that twice as much NO_2 is formed during NO oxidation than NO is reduced during SCR at the same temperature and H_2 concentration.

Acknowledgements

This work is financially supported by the Danish Council for Strategic research and was performed at the Competence Center

for Catalysis, Chalmers University of Technology and Haldor Topsøe A/S. The collaboration with Haldor Topsøe, Amminex and DTU is gratefully acknowledged.

Appendix A. Supplementary data

Supplementary data associated with this article can be found, in the online version, at http://dx.doi.org/10.1016/j.apcatb.2013.01.064.

References

[1] R. Burch, J.P. Breen, C.J. Hill, B. Krutzsch, B. Konrad, E. Jobson, L. Cider, K. Eränen, F. Klingstedt, L.E. Lindfors, Topics in Catalysis 30–31 (2004) 19–25.
[2] J.P. Breen, R. Burch, Topics in Catalysis 39 (2006) 53–58.
[3] D.E. Doronkin, T.S. Khan, T. Bligaard, S. Fogel, P. Gabrielsson, S. Dahl, Applied Catalysis B: Environmental 117 (2012) 49–58.
[4] S. Satokawa, J. Shibata, K. Shimizu, S. Atsushi, T. Hattori, Applied Catalysis B: Environmental 42 (2003) 179–186.
[5] D.E. Doronkin, S. Fogel, S. Tamm, L. Olsson, T. Khan, T. Bligaard, P. Gabrielsson, S. Dahl, Applied Catalysis B: Environmental 113–114 (2012) 228–236.
[6] M. Richter, R. Fricke, R. Eckelt, Catalysis Letters 94 (2004) 115–118.
[7] K.I. Shimizu, A. Satsuma, Applied Catalysis B: Environmental 77 (2007) 202–205.
[8] J. Shibata, K. Shimizu, S. Satokawa, A. Satsuma, T. Hattori, Physical Chemistry Chemical Physics 5 (2003) 2154–2160.
[9] J.P. Breen, R. Burch, C. Hardacre, C.J. Hill, Journal of Physical Chemistry B 109 (2005) 4805–4807.
[10] J. Shibata, Y. Takada, A. Shichi, S. Satokawa, A. Satsuma, T. Hattori, Journal of Catalysis 222 (2004) 368–376.
[11] P. Sazama, L. Capek, H. Drobna, Z. Sobalik, J. Dedecek, K. Arve, B. Wichterlová, Journal of Catalysis 232 (2005) 302–317.
[12] R. Brosius, K. Arve, M.H. Groothaert, J.A. Martens, Journal of Catalysis 231 (2005) 344–353.
[13] H. Kannisto, H.H. Ingelsten, M. Skoglundh, Topics in Catalysis 52 (2009) 1817–1820.
[14] S. Chansai, R. Burch, C. Hardacre, J. Breen, F. Meunier, Journal of Catalysis 276 (2010) 49–55.
[15] X.L. Zhang, Y.B. Yu, H. He, Applied Catalysis B: Environmental 76 (2007) 241–247.
[16] S. Tamm, H.H. Ingelsten, A.E.C. Palmqvist, Journal of Catalysis 255 (2008) 304–312.
[17] R. Burch, J.P. Breen, F.C. Meunier, Applied Catalysis B: Environmental 39 (2002) 283–303.
[18] A. Obuchi, C. Wögerbauer, R. Köppel, A. Baiker, Applied Catalysis A-General 19 (1998) 9–22.
[19] C.N. Costa, A.M. Efstathiou, Journal of Physical Chemistry B 108 (2004) 2620–2630.
[20] Z. Liu, J. Li, S.I. Woo, Energy and Environmental Science 5 (2012) 8799–8814.
[21] C.N. Costa, P.G. Savva, C. Andronikou, P.S. Lambrou, K. Polychronopoulou, V.C. Belessi, V.N. Stathopoulos, P.J. Pomonis, A.M. Efstathiou, Journal of Catalysis 209 (2002) 456–471.
[22] P.G. Savva, A.M. Efstathiou, Journal of Catalysis 257 (2008) 324–333.
[23] H. Kannisto, H.H. Ingelsten, M. Skoglundh, Journal of Molecular Catalysis A 302 (2009) 86–96.
[24] J.P. Breen, R. Burch, C. Hardacre, C.J. Hill, B. Krutzsch, B. Bandl-Konrad, E. Jobson, L. Cider, P.G. Blakeman, L.J. Peace, M.V. Twigg, M. Preis, M. Gottschling, Applied Catalysis B: Environmental 70 (2007) 36–44.
[25] V. Houel, D. James, P. Millington, S. Pollington, S. Poulston, R. Rajaram, R. Torbati, Journal of Catalysis 230 (2005) 150–157.
[26] L. Kylhammar, A. Palmqvist, M. Skoglundh, Topics in Catalysis 42–43 (2007) 119–122.
[27] A. Abe, N. Aoyama, S. Sumiya, N. Kakuta, K. Yoshida, Catalysis Letters 51 (1998) 5–9.
[28] S. Satokawa, K.-i. Yamaseki, H. Uchida, Applied Catalysis B: Environmental 34 (2001) 299–306.
[29] Y. Miyahara, M. Takahashi, T. Masuda, S. Imamura, H. Kanai, S. Iwamoto, T. Watanabe, M. Inoue, Applied Catalysis B: Environmental 84 (2008) 289–296.
[30] K. Shimizu, A. Satsuma, T. Hattori, Applied Catalysis B: Environmental 25 (2000) 239–247.
[31] H. Sjövall, R.J. Blint, A. Gopinath, L. Olsson, Industrial & Engineering Chemistry 49 (2010) 39–52.
[32] A. Iglesias-Juez, A.B. Hungria, A. Martinez-Arias, A. Fuerte, M. Fernandez-Garcia, J.A. Anderson, J.C. Conesa, J. Soria, Journal of Catalysis 217 (2003) 310–323.
[33] H.W. Jen, Catalysis Today 42 (1998) 37–44.
[34] E.V. Kondratenko, V.A. Kondratenko, M. Richter, R. Fricke, Journal of Catalysis 239 (2006) 23–33.
[35] K. Arve, H. Backman, F. Klingstedt, K. Eränen, D.Y. Murzin, Applied Catalysis A-General 303 (2006) 96–102.
[36] K. Arve, F. Klingstedt, K. Eränen, J. Wärnå, L.E. Lindfors, D.Y. Murzin, Chemical Engineering Journal 107 (2005) 215–220.
[37] K. Shimizu, A. Satsuma, Journal of Physical Chemistry C 111 (2007) 2259–2264.
[38] M. Richter, U. Bentrup, R. Eckelt, M. Schneider, M.M. Pohl, R. Fricke, Applied Catalysis B: Environmental 51 (2004) 261–274.
[39] Q.Y. Liu, Z.Y. Liu, J.H. Su, Catalysis Today 158 (2010) 370–376.
[40] K. Eränen, F. Klingstedt, K. Arve, L.E. Lindfors, D.Y. Murzin, Journal of Catalysis 227 (2004) 328–343.
[41] R. Matarrese, H.H. Ingelsten, M. Skoglundh, Journal of Catalysis 258 (2008) 386–392.
[42] N.A. Sadokhina, D.E. Doronkin, P.V. Pributkov, V.I. Bukhtiyarov, R.I. Kvon, A.Y. Stakheev, Topics in Catalysis 54 (2011) 1190–1196.
[43] L. Zhang, H. He, Journal of Catalysis 268 (2009) 18–25.

Paper VI

Applied Catalysis B: Environmental 113–114 (2012) 228–236

Contents lists available at SciVerse ScienceDirect

Applied Catalysis B: Environmental

journal homepage: www.elsevier.com/locate/apcatb

Study of the "Fast SCR"-like mechanism of H_2-assisted SCR of NO_x with ammonia over Ag/Al_2O_3

Dmitry E. Doronkin[a,*], Sebastian Fogel[b], Stefanie Tamm[c,d], Louise Olsson[c,d], Tuhin Suvra Khan[e], Thomas Bligaard[f], Pär Gabrielsson[b], Søren Dahl[a]

[a] Center for Individual Nanoparticle Functionality (CINF), Department of Physics, Technical University of Denmark, Fysikvej 307, 2800 Kgs. Lyngby, Denmark
[b] Haldor Topsøe A/S, Nymøllevej 55, 2800 Kgs. Lyngby, Denmark
[c] Competence Center for Catalysis, Chalmers University of Technology, SE-412 96 Göteborg, Sweden
[d] Chemical Reaction Engineering, Chalmers University of Technology, SE-412 96 Göteborg, Sweden
[e] Center for Atomic-scale Materials Design (CAMD), Department of Physics, Technical University of Denmark, Fysikvej 307, 2800 Kgs. Lyngby, Denmark
[f] SUNCAT Center for Interface Science & Catalysis, SLAC National Accelerator Laboratory, Menlo Park, CA 94025, USA

ARTICLE INFO

Article history:
Received 22 September 2011
Received in revised form
15 November 2011
Accepted 24 November 2011
Available online 3 December 2011

Keywords:
Ag/Al_2O_3
Alumina
NO_x SCR
Fast SCR
FTIR

ABSTRACT

It is shown that Ag/Al_2O_3 is a unique catalytic system for H_2-assisted selective catalytic reduction of NO_x by NH_3 (NH_3-SCR) with both Ag and alumina being necessary components of the catalyst. The ability of Ag/Al_2O_3 and pure Al_2O_3 to catalyse SCR of mixtures of NO and NO_2 by ammonia is demonstrated, the surface species occurring discussed, and a "Fast SCR"-like mechanism of the process is proposed. The possibility of catalyst surface blocking by adsorbed NO_x and the influence of hydrogen on desorption of NO_x were evaluated by FTIR and DFT calculations.

1. Introduction

Nitrogen oxides (NO_x) are the most challenging pollutants to address for light-duty diesel vehicles and sophisticated techniques like advanced fuel injection, exhaust gas recirculation (EGR), turbocharging, etc., are used by engine manufactures to reduce emissions. But NO_x removal by exhaust aftertreatment is still required due to stricter emmision regulations and the trade off between fuel consumption and NO_x emmision, i.e., the price for reducing fuel consumption and CO_2 emission by ~15% equals to ~50% increase in NO_x emissions [1].

Selective catalytic reduction (SCR) is the leading NO_x control technique with ammonia as a reductant. Commonly used catalysts are vanadia-based catalysts, Cu and Fe-containing zeolites. However, none of the systems demonstrates high thermal durability together with a good activity throughout a broad temperature region from 150 to 550 °C [1]. This fact explains the reason for the on-going research of novel catalytic systems for NH_3-SCR, which are supposed to be non-toxic, inexpensive and durable.

Alumina supported metals, such as Ag, In, Sn, etc., [2–5] are known to catalyse NO_x SCR by hydrocarbons under the conditions of lean-burn engine exhaust. The major drawback of these catalytic systems is their very poor activity at low temperatures. It has been found that addition of hydrogen to the gas feed can substantially improve the low-temperature activity of Ag/Al_2O_3 [6–8]. Interestingly, several groups have also demonstrated the possibility of Ag/Al_2O_3 to facilitate SCR of NO_x by ammonia or urea with co-feeding hydrogen, resulting in nearly 90% NO_x conversion at temperatures as low as 200 °C [9,10].

Hydrogen for this reaction can be provided on board of the vehicule by two means depending on the used reductant. The required amount of hydrogen can be produced in an on-board fuel reformer without the necessity to change the existing fuel infrastructure. This is convenient for hydrocarbon SCR systems utilizing Ag/Al_2O_3 catalysts and currently leads to fuel penalties from 5 to 10% [11,12] which might be improved by the optimisation of the system. For the NH_3 SCR applications hydrogen can be produced by cracking of part of the ammonia. Pure NH_3 required for this purpose can be stored on board in form of solid metal ammine salts [13]. The suggested system allows accurate and independent dosing of ammonia to the SCR catalyst and to the cracker where it can be decomposed to form the required hydrogen. Using ammonia for hydrogen storage has earlier been suggested for fuel

* Corresponding author. Tel.: +45 4525 3275.
E-mail addresses: dmdo@fysik.dtu.dk, dmitriy.doronkin@gmail.com (D.E. Doronkin).

0926-3373/$ – see front matter © 2011 Elsevier B.V. All rights reserved.
doi:10.1016/j.apcatb.2011.11.042

cell applications but can also be applied for NO_x SCR applications [14,15].

There is no general agreement about the necessary concentration of hydrogen for the effective reduction of NO_x by ammonia over Ag/Al_2O_3. One can find H_2:NO_x ratios varying from 5 to 10 in the literature [9,10,16–18] which is a rather high value. However, Shimizu and Satsuma have demonstrated ever increasing NO_x reduction rate in the interval of H_2:NO_x ratios from 0 to 50 [17] which makes the choice of H_2 concentration a matter of finding the optimum between the amount of ammonia spent on hydrogen production and the SCR efficiency. We are considering a H_2:NO_x ratio 2.4 as an optimum in this work.

Hydrogen has also been considered as the only reductant in H_2-SCR of NO_x, however, currently available catalysts allow effective removal of NO_x only when using H_2:NO_x > 10 and such amount of hydrogen cannot be produced on board at an affordable price [19–21].

In this work we studied several catalysts: Ag supported on different carriers (γ-Al_2O_3, TiO_2 and ZrO_2), Sn and In supported on γ-Al_2O_3 and pure alumina under the conditions of H_2-assisted SCR of NO_x with NH_3. The aim of this study is to investigate the possibility of replacing traditional NO_x SCR catalysts by Ag/Al_2O_3 thus obtaining high catalyst activity even at low temperatures. Another goal of the study is to give insight to the mechanistic aspects of H_2-assisted NO_x SCR by ammonia.

2. Experimental

2.1. Catalyst preparation

Parent γ-alumina (Puralox SCFa-140, 59 ppm Fe_2O_3 content) was kindly provided by SASOL. Prior to its study as a catalyst it was calcined at 550 °C for 4 h in static air.

1%Ag/Al_2O_3, 3%Sn/Al_2O_3 and 3%In/Al_2O_3 were obtained by incipient wetness impregnation of parent γ-alumina by corresponding amounts of $AgNO_3$, $SnCl_4{\cdot}5H_2O$ and $InCl_3{\cdot}4H_2O$ (all from Sigma–Aldrich) solutions in deionised water. 1%Ag/TiO_2 and 1%Ag/ZrO_2 were obtained by incipient wetness impregnation of TiO_2 (anatase containing 10%SiO_2) and ZrO_2 (E10, Magnesium Elektron Ltd.) by the aqueous solution of $AgNO_3$. After impregnation all catalysts were dried at room temperature overnight and calcined at 550 °C for 4 h in static air.

The calcined catalysts were pressed, crushed and sieved to obtain the fraction 0.18–0.35 mm (mesh 80–mesh 45).

2.2. TEM measurements

TEM measurements were carried out in a TECNAI T20 transmission electron microscope equipped with an Oxford Instruments EDX detector. For the measurements the catalyst powder (in a dry form) was dispersed on a copper TEM grid covered with a lacey carbon film. Images were acquired using DigitalMicrograph from Gatan Inc.

2.3. Catalytic studies

The catalytic measurements were carried out in a fixed-bed quartz flow reactor (inner diameter = 4 mm) in a temperature programmed mode while the temperature was decreased from 400 °C to 150 °C with a rate 2 °C/min. The temperature was controlled using an Eurotherm 2416 temperature controller with a K-type thermocouple. 45 mg of catalyst was diluted with 100 mg of SiC (mesh 60) and placed on a quartz wool bed. The bed height was ~11 mm and the GHSV, calculated using the volume of the pure catalyst was ~110,000 h^{-1}. The gas composition normally contained 500 ppm NO, 520 ppm NH_3, 8.3% O_2, and 7% water balanced with Ar. During some tests 1200 ppm of H_2 was added to the gas feed. The gas feed was mixed from 2000 ppm NO in Ar, 2000 ppm NH_3 in Ar, 4000 ppm H_2 in Ar (Air Liquide), oxygen and argon (AGA), dosed by individual mass flow controllers (UNIT Celerity). Water was dosed by an ISCO 100DM syringe pump through a heated capillary. Mixtures of NO and NO_2 were obtained by feeding NO and oxygen through a long capillary, giving NO_x with 26–47% NO_2. Reaction products were analysed by a Thermo Fisher Nicolet 6700 FTIR analyser, equipped with a gas cell (2 m optical pathlength). Gas capillaries were heated to ~130 °C and the FTIR gas cell to 165 °C to avoid condensation of water and formation of ammonium nitrate. To simplify experimental procedure we are not using CO_2 in the study as we have not observed CO_2 effect on the NO_x SCR by NH_3 during the preliminary experiments with Ag/Al_2O_3 catalysts.

Conversions were calculated using the following equations:

$$X_{NO_x} = 1 - \frac{C_{NO_x}^{outlet}}{C_{NO_x}^{inlet}} \quad (1)$$

where X_{NO_x} denotes total conversion of NO_x and $C_{NO_x}^{inlet}$ and $C_{NO_x}^{outlet}$ is the NO_x concentrations on the inlet and outlet of the reactor, where:

$$C_{NO_x} = C_{NO} + C_{NO_2} \quad (2)$$

NH_3 conversion (total), NH_3 conversion to NO_x (when no NO_x is fed) and NO conversion to NO_2 (when no NH_3 was fed) were calculated correspondingly:

$$X_{NH_3} = 1 - \frac{C_{NH_3}^{outlet}}{C_{NH_3}^{inlet}} \quad (3)$$

$$X_{NH_3 \rightarrow NOx} = \frac{C_{NOx}^{outlet}}{C_{NH_3}^{inlet}} \quad (4)$$

$$X_{NO \rightarrow NO_2} = \frac{C_{NO_2}^{outlet}}{C_{NO}^{inlet}} \quad (5)$$

and the ratio of converted NO to converted NO_2 in the experiments with NO and NO_2 mixtures:

$$\frac{C_{NO}^{conv.}}{C_{NO_2}^{conv.}} = \frac{C_{NO}^{inlet} - C_{NO}^{outlet}}{C_{NO_2}^{inlet} - C_{NO_2}^{outlet}} \quad (6)$$

NH_3:NO_x conversion ratio below 400 °C was always 1:0.95–1.05 for all tested catalysts, therefore we are presenting only NO_x conversion values in the discussion.

2.4. DRIFTS studies

In-situ diffuse reflectance infrared Fourier transform spectroscopy (DRIFTS) experiments were performed using a BioRad FTS 6000 FTIR spectrometer equipped with a high-temperature reaction cell (Harrick Scientific, Praying Mantis) with KBr windows. The temperature of the reaction cell was controlled with a K-type thermocouple connected to a Eurotherm 2416 temperature controller. Gases were introduced into the reaction cell via individual mass flow controllers (Bronkhorst Hi-Tech). The gas composition at the outlet of the DRIFTS cell was analysed by a mass spectrometer (Balzers QuadStar 420).

Each experiment was performed using approximately 100 mg of γ-Al_2O_3 powder, using new powder for each experiment. The powder was initially pretreated in a flow of 8% O_2 in Ar at 500 °C for 30 min, subsequently a background spectrum (60 scans, resolution 2 cm^{-1} at 4000 cm^{-1}) was recorded in a flow of Ar. At 500 °C, 185 ppm NO_2, 315 ppm NO, 520 ppm NH_3 and 8.3% O_2 were added to the feed. Then the catalyst was cooled with a ramp rate of 10 °C/min in the reaction mixture to reaction temperature, where

the temperature is held for 10 min for stabilisation. Subsequently, NH_3 is removed from the feed gas mixture for 30 min and added again to it for 10 min. This procedure was repeated once. Thereafter, 1250 ppm H_2 were added for 10 min to the feed gas and, subsequently, NH_3 was removed again. The evolution of absorption bands in the spectra was followed using the kinetic mode (9 scans/spectrum, 6 spectra/min,) at a resolution of 2 cm^{-1} at 4000 cm^{-1}. The data are presented as absorbance, which is defined as the logarithm of the inverse reflectance (log 1/R). All DRIFTS experiments were carried out using a total flow rate of 100 ml/min which corresponds to a space velocity of about 62,000 h^{-1}.

2.5. DFT calculations

Plane wave DFT code DACAPO is used to calculate the adsorption energies and the gas phase energies of the adsorbates. Plane wave cutoff of 340.15 eV and density cutoff of 680 eV are used for the calculations. The core electrons are described by the Vanderbilt ultrasoft pseudopotential [22]. RBPE is used as the exchange correlation energy function [23]. Fermi population of the Kohn-Sham states is $k_bT = 0.1$ eV. The convergence limit is set as maximum change in force constant $f_{max} = 0.03$ eV.

The adsorption energies of O, NO, NO_2 and NO_3 are studied over six different transition metals (Ag, Cu, Pd, Pt, Rh, Ru) on both the (1 1 1) terrace and the (2 1 1) step surfaces. We use a 2×2 surface cell for O and NO for (1 1 1) terrace, 2×1 surface cell for O and NO for (2 1 1) step surface, 3×3 surface cell for NO_2 and NO_3 adsorption study on (1 1 1) terrace and the 3×1 surface cell for NO_2 and NO_3 adsorption study (2 1 1) step surfaces, with $8 \times 8 \times 1$ Monkhorst-Pack **k**-point sampling in the irreducible Brillouin zone for all the 2×2 surface cells, $8 \times 6 \times 1$ Monkhorst-Pack **k**-point sampling in the irreducible Brillouin zone for all the 2×1 surface cells and $4 \times 4 \times 1$ Monkhorst-Pack **k**-point sampling for both 3×3 and 3×1 surface cells. For all the (1 1 1) surfaces we use a four-layer slab where the two topmost layers are allowed to relax whereas for the (2 1 1) surfaces with 2×1 surface cell we use a slab model with twelve layers where the topmost six layers are allowed to relax and for (2 1 1) surfaces with 3×1 surface cell we use a slab model with nine layers where the topmost three layers are allowed to relax.

For the calculation of γ-Al_2O_3 and the adsorption of different species on γ-Al_2O_3 we also used the DACAPO code with a plane wave cutoff of 340.15 eV and a density cutoff of 680 eV. A $4 \times 4 \times 1$ Monkhorst-Pack **k**-point sampling in the irreducible Brillouin zone was used for γ-Al_2O_3. The γ-Al_2O_3 surface was modelled by a step on a nonspinel γ-Al_2O_3 structure which was derived bulk γ-Al_2O_3 model [24]. The cell parameters for the γ-Al_2O_3 step closed packed surface are $a = 8.0680$ Å and $b = 10.0092$ Å and $\alpha = \beta = \gamma = 90^\circ$. For the γ-Al_2O_3 surface the bottom two layers were fixed where as the top three layers were allowed to relax.

In all the model surfaces, the neighboring slabs are separated by more than 10 Å of vacuum.

NO_x and HNO_x adsorption energies were calculated relative to gas phase zero energy points of these species.

The energy minimum adsorption geometries used in the calculations are presented in the supplementary material.

3. Results and discussion

3.1. Unique activity of Ag/Al_2O_3 in H_2-assisted NH_3-deNO_x

NO_x conversions obtained over the prepared catalysts at 380 °C tested under the conditions of SCR of NO_x with NH_3, without and with H_2 in the exhaust, are given in Table 1. In the absence of H_2 all the catalysts are inert with respect to NO_x reduction or ammonia oxidation at temperatures below 400 °C. The hydrogen effect was observed only for Ag/Al_2O_3, Ag/TiO_2 and In/Al_2O_3 (Fig. 1). The former catalyst demonstrates extremely high performance with NO_x conversion exceeding 80% at 200 °C at GHSV = 110,000 h^{-1}. No more than 5 ppm N_2O was observed in the products. Ag/TiO_2 is much less active with maximum NO_x conversion of 25% at 380 °C. The activity of In/Al_2O_3 below 400 °C is only marginal. Therefore only Ag/Al_2O_3 may be considered for practical applications among the tested catalysts. Futhermore, it is evident that both silver and alumina are nesessary components of the catalyst to obtain a high performance in deNO_x. Removal or change of each of these components lead to almost inactive catalysts. Therefore, it is likely that both silver and alumina take part in the catalytic cycle or the active site is positioned on the interface between Ag and Al_2O_3.

Table 1
Studied catalysts and NO_x conversions obtained at 380 °C without and with H_2 in the feed gas. Reaction conditions: 500 ppm NO, 520 ppm NH_3, 8.3% O_2, 7% H_2O in Ar, GHSV = 110,000 h^{-1}.

Catalyst	Metal loading, wt%	Support BET surface area, m^2/g	NO_x conversion	
			0 ppm H_2	1200 ppm H_2
Al_2O_3	–	140	0	0
Ag/Al_2O_3	1	140	0	94
Ag/TiO_2	1	110	1.5	25
Ag/ZrO_2	1	14	0	0
Sn/Al_2O_3	3	140	0	0
In/Al_2O_3	3	140	0	10.5

3.1.1. TEM data on Ag/Al_2O_3 and Ag/TiO_2

In order to clarify if it is the catalyst morphology that determines the drastic difference in the SCR performance of Ag/Al_2O_3 and Ag/TiO_2, TEM images of the samples were obtained. These micrographs are compared in Fig. 2. The choice of the catalysts in question is dictated by their common properties (Ag loading, BET surface area of the support, preparation technique), which is in contrast to their very different catalytic activity.

EDX shows the presence of ~1% Ag in the both depicted catalyst grains. However, we were unable to locate any metal particles with diameters larger than 2–3 nm in both catalyst samples. This confirms a high dispersion of Ag in both Ag/Al_2O_3 and Ag/TiO_2

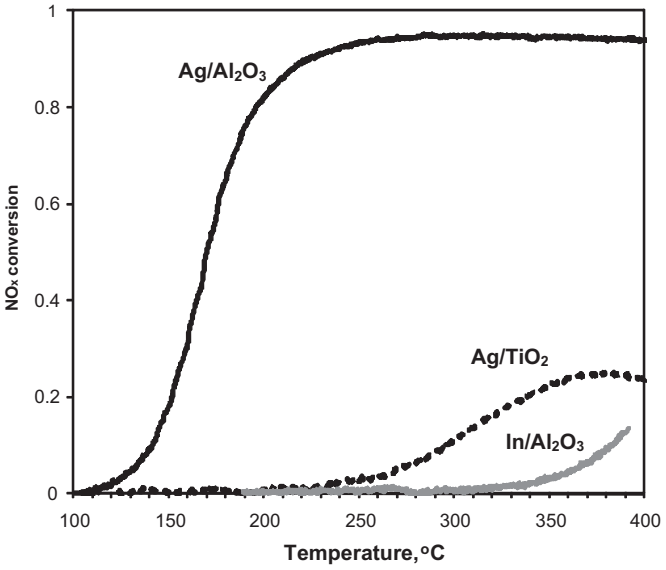

Fig. 1. NO_x conversion profiles obtained over Ag/Al_2O_3, Ag/TiO_2, and In/Al_2O_3. Reaction conditions: 500 ppm NO, 520 ppm NH_3, 1200 ppm H_2, 8.3% O_2, 7% H_2O in Ar, GHSV = 110,000 h^{-1}.

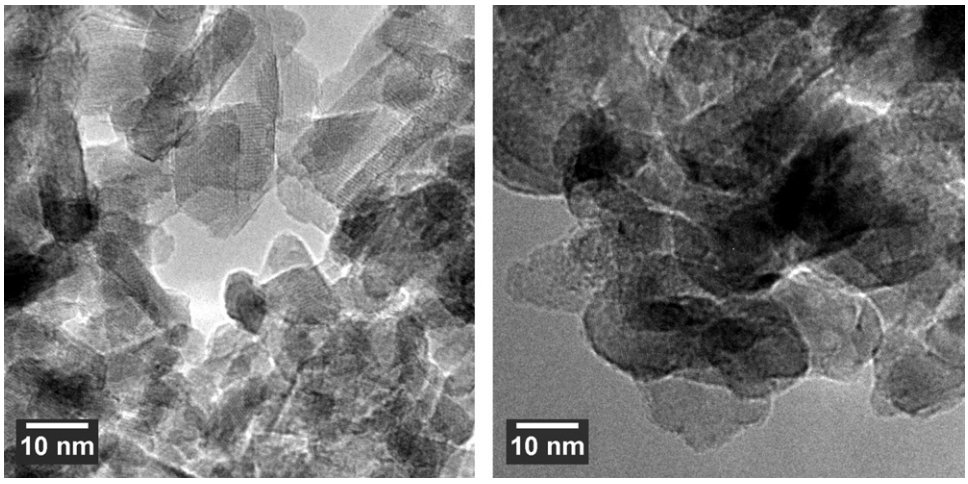

Fig. 2. TEM images of Ag/Al_2O_3 (left) and Ag/TiO_2 (right) calcined at 550 °C in air.

catalysts, which might be in the form of clusters of 4–8 Ag atoms as suggested by Kondratenko et al. [16]. Therefore the large difference in SCR activity of Ag/Al_2O_3 and Ag/TiO_2 is not due to a large difference in Ag dispersion.

3.2. Study of the mechanism of H_2-assisted NH_3-deNO_x

3.2.1. Experiments with Ag/Al_2O_3 where components of the feed are omitted

Studies of the mechanism of hydrogen-assisted NO_x SCR by NH_3 on Ag/Al_2O_3 were already performed before [16,17], where the attention was drawn to the state of silver. Our catalytic experiments show a uniqueness of the Ag/Al_2O_3 catalytic system, in which both components play a vital role.

To have a notion of the individual reactions occuring during NO_x SCR by NH_3 we consequtively run catalytic tests with one of the components absent in the feed.

According to the results obtained so far it is already clear that the removal of hydrogen leads to a completely inactive catalyst with regards to NH_3-deNO_x (Table 1) or ammonia oxidation. The concentration of all monitored gases remained constant during temperature ramping from 400 to 100 °C when no H_2 was in the feed. The same is true for the removal of oxygen from the feed – no NO reduction or NH_3 oxidation was observed without O_2.

When NH_3 was removed from the gas feed, a pronounced oxidation of NO to NO_2 starting from 100 °C was observed (Fig. 3, solid line). Together with that a very low NO_x to N_2 conversion (dotted line, max. 4%) was observed indicating that hydrogen normally acts not as the main reductant but as a co-reductant. When both ammonia and hydrogen were removed from the feed, no oxidation of NO to NO_2 was observed.

The latter observation agrees with the data obtained in [6,16]. As suggested in [6], hydrogen addition promotes oxidation of NO. However, we observed no oxidation of NO to NO_2 during the experiments with Ag/TiO_2 and Ag/ZrO_2 catalysts. This shows once again that not only Ag, but also the support plays an important role in the catalytic activity of Ag/Al_2O_3 which also agrees with the data on C_3H_8-SCR reported in [6].

The mechanism of O_2 activation by hydrogen has been suggested earlier [25,26] as follows. On the first step hydrogen dissociates on active Ag_n+ sites on alumina to form an acidic proton and hydride Ag_n–H. This hydride later reacts with oxygen to form a reactive oxidant, such as hydroperoxy radicals (HO_2), peroxide (O_2^{2-}), or superoxide ions (O_2^-) all of which later oxidise NO to NO_2.

When removing NO from the NO, NH_3, H_2, O_2 and H_2O containing feed, NH_3 oxidation to N_2 (Fig. 4, solid line) and to NO_x (Fig. 4, dotted line) occurs at temperatures higher than 200 °C. Comparison of the data in Fig. 3 and Fig. 4 suggests that NO oxidative acivation starts at significantly lower temperature (corresponding to the NH_3-deNO_x light-off temperature) than NH_3 oxidative activation. Therefore it is more likely that oxidative activation of NO is an important step in the overall catalytic mechanism of NO_x SCR over Ag/Al_2O_3.

The data does not support a hypothesis of oxidative dehydrogenation of NH_3 (or NH_3-assisted NO decomposition) being the main catalysed step of H_2-assisted NH_3-deNO_x over Ag/Al_2O_3 [18]. Ag/Al_2O_3 rather participates in NO activation and possibly in the reaction of NH_3 with NO_x intermediates [16].

The hydrogen promoted oxidative activation of NO has been already reported by Satokawa et al. for NO_x SCR by C_3H_8 [6]. However in that study oxidative activation of NO was not enough to initiate SCR and activation of C_3H_8 by H_2 has been reported to be necessary which makes it different from SCR by NH_3.

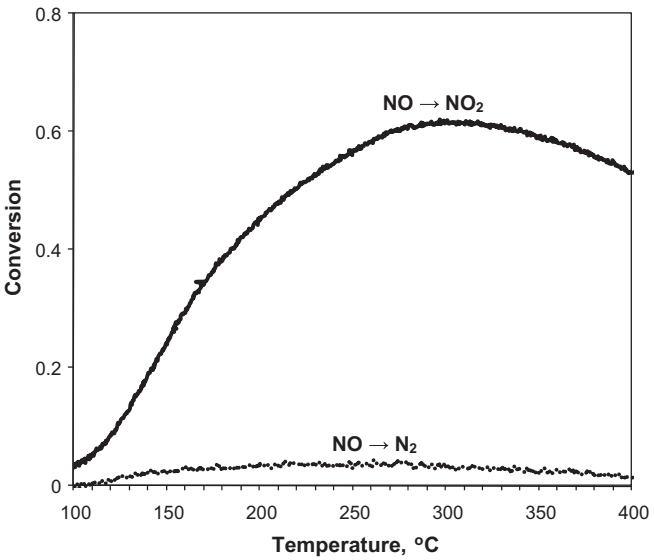

Fig. 3. NO conversion to NO_2 (solid line) and NO_x conversion to N_2 (dotted line) over Ag/Al_2O_3 without ammonia in the feed. Reaction conditions: 500 ppm NO, 1200 ppm H_2, 8.3% O_2, 7% H_2O in Ar, GHSV = 110,000 h^{-1}.

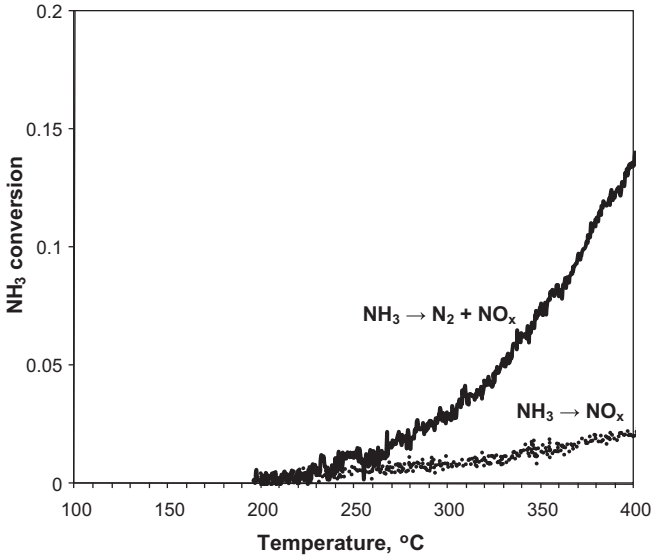

Fig. 4. Total NH_3 conversion (solid line) and NH_3 conversion to NO_x (dotted line) over Ag/Al_2O_3 with no NO in the feed. Reaction conditions: 520 ppm NH_3, 1200 ppm H_2, 8.3% O_2, 7% H_2O in Ar, GHSV = 110,000 h^{-1}.

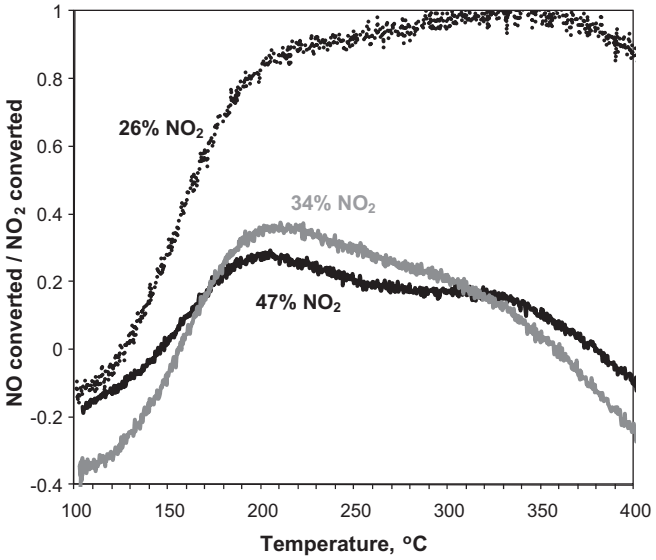

Fig. 6. Ratio of consumed NO to consumed NO_2 for simultaneous NO + NO_2 reduction by NH_3 over Ag/Al_2O_3. Reaction conditions: 500 ppm NO_x (NO_2 fraction is stated near the corresponding curves), 520 ppm NH_3, 8.3% O_2, 7% H_2O in Ar, GHSV = 110,000 h^{-1}.

3.2.2. Experiments with feeding NO and NO_2 mixtures over Ag/Al_2O_3 and Ag/ZrO_2

After realizing that the hydrogen promoted oxidation of NO to NO_2 may be the first step in the H_2-assisted NH_3-deNO_x we decided to do catalytic tests with a feed containing a mixture of NO and NO_2 as NO_x. Since H_2 facilitates reversible NO-NO_2 tranformation, undesirable for these experimens, no H_2 was co-fed.

Fig. 5 shows NO_x conversions to N_2 obtained over Ag/Al_2O_3 when a NO and NO_2 mixture is fed as NO_x (containing 26, 34 and 47% NO_2) and over Ag/ZrO_2 with 34% NO_2 in NO as NO_x. Surprisingly for all three cases we observe nearly equal, maximum 30%, NO_x conversion which changes only slightly with temperature. NH_3 conversion profiles follow the NO_x conversion profiles and they are therefore not shown. This observation allows us to conclude that oxidation of NO to NO_2 over Ag/Al_2O_3, at least, partially accounts for the activity of this catalyst in the NO_x SCR. This agrees with previous works, evidencing oxidation of NO to NO_2 involving H_2 [25] and supposing it to be crucial for low-temperature NO_x SCR by hydrocarbons [27].

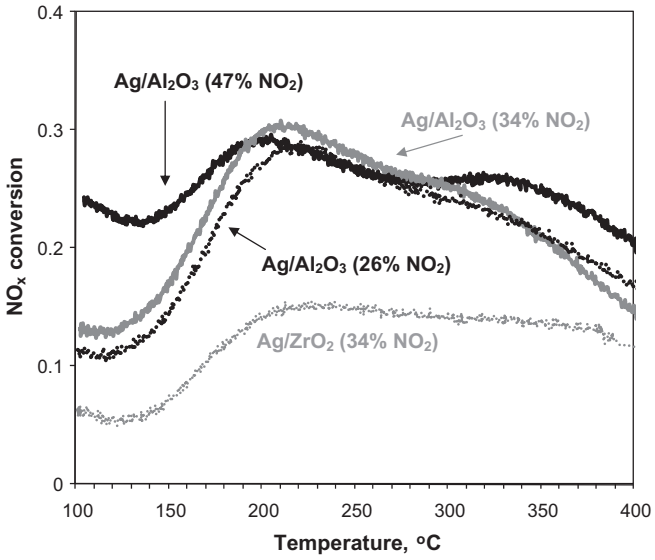

Fig. 5. NO_x conversion over Ag/Al_2O_3 and Ag/ZrO_2 without H_2 in the feed, when NO and NO_2 mixture is fed as NO_x (NO_2 content is specified, NO is the rest of 500 ppm NO_x). Conditions: 500 ppm NO_x, 520 ppm NH_3, 8.3% O_2, 7% H_2O in Ar, GHSV = 110,000 h^{-1}.

Moreover, SCR of the NO and NO_2 mixture by NH_3 is not a unique feature of Ag/Al_2O_3 but was also observed for other supports though to a less extent, e.g. with 15% maximum NO_x conversion in the case of Ag/ZrO_2 (see Fig. 5, gray dotted line). Thus, metal oxides other than alumina can catalyse NO + NO_2 SCR by NH_3 but Ag/Al_2O_3 with H_2 co-feeding is required to oxidise NO at low temperatures. Therefore, we are focusing our study on Ag/Al_2O_3 catalysts and the corresponding alumina support.

The effect of increasing the NO_x SCR rate by feeding NO and NO_2 mixture has already been noticed for other catalytic systems including vanadia-based catalysts [28] and zeolites [29]. The effect is called "Fast-SCR" and characterised by a well-defined stoichiometry of NO:NO_2 being 1:1.

To check if the NO:NO_2 conversion without H_2 in the feed can be ascribed to "Fast SCR" [29], we calculated the ratio of consumed NO to consumed NO_2 (Fig. 6). In our case the ratio of consumed NO to consumed NO_2 changed with temperature from negative values (only NO_2 is consumed and a small amount of NO is produced from it) to positive values up to 1 in case of feeding 26% NO_2 (Fig. 6). Interestingly, the temperature at which NO starts to be consumed (~150 °C) coincides with the onset temperature of H_2-assisted SCR (Fig. 1). Therefore, we can suppose that parts of the mechanisms of both H_2-assisted NO SCR by NH_3 and NO + NO_2 SCR by NH_3 are similar. But in case of NO + NO_2 SCR we observed a conversion limit at ~30%, when almost 100% conversion is obtained in H_2-assisted NO_x-SCR. This could be explained by blocking of the catalyst surface by adsorbed nitrate species [25]. The poisoning effect of surface nitrates for propane-SCR was observed in [26], where the authors also demonstrated the ability of hydrogen to effectively remove adsorbed nitrate species. Thus, introduction of hydrogen may facilitate not only NO to NO_2 conversion, but also regeneration of the catalyst surface, which removes the 30% conversion limit.

In general, the ratio of converted NO to converted NO_2 depends on the total amount of NO_2 in the feed and decreases with increase in NO_2 content. The higher the NO_2 content – the larger is the part of NO_2 in the NO_x that is converted to N_2. Independent on this,

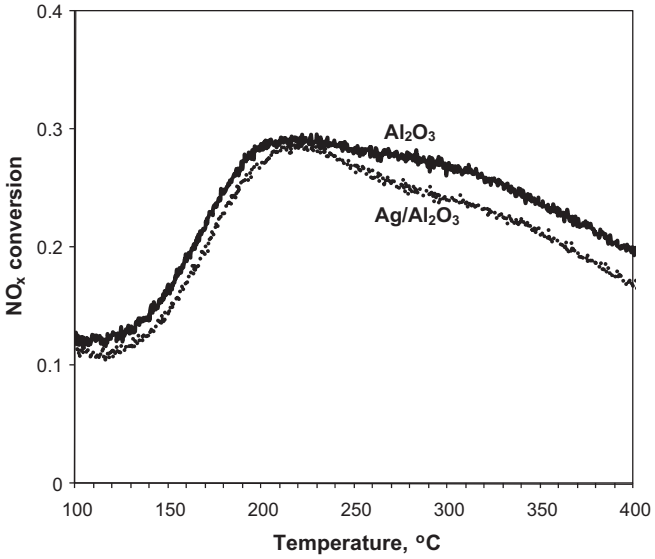

Fig. 7. NO_x conversion over Al_2O_3 (solid line) and Ag/Al_2O_3 (dotted line, for a comparison) without H_2 in the feed, when NO and NO_2 mixture is fed as NO_x. Reaction conditions: 500 ppm NO_x (37% NO_2), 520 ppm NH_3, 8.3% O_2, 7% H_2O in Ar, GHSV = 110,000 h^{-1}.

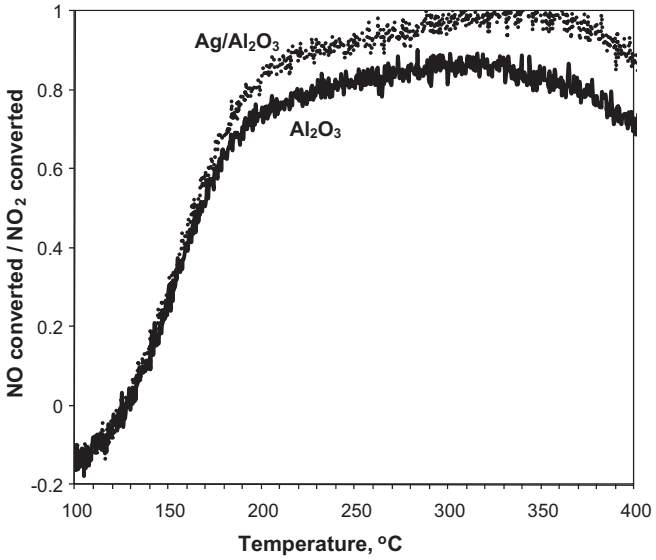

Fig. 8. Ratio of consumed NO to consumed NO_2 for NO + NO_2 simultaneous reduction by NH_3 over Al_2O_3 (solid line) and Ag/Al_2O_3 (dotted line, for a comparison). Reaction conditions: 500 ppm NO_x (26% NO_2), 520 ppm NH_3, 8.3% O_2, 7% H_2O in Ar, GHSV = 110,000 h^{-1}.

the ratio of converted NO_x to converted NH_3 was always 1:1 and maximum conversion remained constant at ~30%.

3.2.3. *Experiments with feeding NO and NO_2 mixtures over pure γ-Al_2O_3*

In some of the papers on H_2-assisted NO SCR by NH_3, published earlier [16,17], alumina was considered only as a support for the active Ag nanoparticles. In this case, the properties of alumina could influence the catalyst activity indirectly by tuning the Ag particle size and distribution. In the following we test this assumption.

With or without hydrogen γ-alumina stays inactive under the experimental conditions of NO_x SCR by ammonia when NO is the only component of NO_x in the feed. This changes when NO_2 is introduced. Fig. 7 shows a comparison of NO_x (26% NO_2 of total NO_x at the reactor inlet) conversion by NH_3 obtained over pure Al_2O_3 (solid line) and Ag/Al_2O_3 (dotted line) with no H_2 in the feed. The profiles are almost identical indicating that presence of Ag in the catalyst is important only for the H_2-assisted reaction. Taking into account the overall quantity of NO_2, which can be produced from NO in presence of H_2 over Ag/Al_2O_3 (Fig. 3), it is evident that alumina can significantly contribute to the overall H_2-assisted NO SCR mechanism. Thus, it cannot be neglected that alumina is an active part of the catalyst. Moreover the stoichiometry of NO + NO_2 SCR conversion over alumina follows the same trend as for the Ag/Al_2O_3 (Fig. 8), which may demonstrate the same mechanism is working in both cases. Running NO + NO_2 SCR with H_2 in the feed over pure Al_2O_3 yield almost the same NO_x conversion as as for the test without H_2 (Fig. 7, solid line).

Thus, the presence of Ag and H_2 is mostly important for oxidative activation of NO and possibly removal of adsorbed species blocking the catalyst surface. The reaction of NO and NH_3 with the obtained NO_2 can proceed further over pure Al_2O_3 yielding N_2. This result agrees with the results of Lee et al. [30], who demonstrated the ability of pure alumina to catalyse the reduction of NO, activated over Ag/Al_2O_3, by partially oxidised hydrocarbons. At the same time, Meunier and Ross [31] observed the ability of pure alumina to run the propene SCR of NO_2 (but not of NO).

From the analysis of the stoichiometry of the NO + NO_2 SCR reaction (Figs. 6 and 8) it can be concluded that at temperatures lower than 150 °C only NO_2 reacts with NH_3. The production of NO from NO_2 can also be observed, which is thermodynamically not possible and is likely due to an uncomplete SCR reaction between NO_2 and NH_3. Above 350 °C NO_2 decomposition to NO is thermodinamically favorable, and this may be a reason of decreasing apparent amount of consumed NO [32]. Only between 150 and 350 °C NO consumption is significant and almost equal to NO_2 consumption in the case of 26% NO_2 in NO_x feed. Based on the knowledge of the "Fast SCR" [29] the following reactions can be proposed:

$$2NH_3 + H_2O \leftrightarrow 2NH_4^+ + O^{2-} \quad (7)$$

$$2NO_2 \leftrightarrow N_2O_4 \quad (8)$$

$$N_2O_4 + O^{2-} \leftrightarrow NO_2^- + NO_3^- \quad (9)$$

$$NO_2^- + NH_4^+ \leftrightarrow [NH_4NO_2] \rightarrow N_2 + 2H_2O \quad (10)$$

$$NO_3^- + NH_4^+ \leftrightarrow NH_4NO_3 \quad (11)$$

$$NH_4NO_3 \leftrightarrow N_2O + 2H_2O \quad (12)$$

$$NO + NO_3^- \leftrightarrow NO_2 + NO_2^- \quad (13)$$

According to the scheme, at temperatures higher than 150 °C reactions (7)–(11) take place yielding nitrogen and surface nitrate species. Disproportionation of adsorbed NO_2 (8), (9) was also suggested by DFT calculations earlier [33]. A small part of the surface nitrates is decomposed to N_2O (12), trace amount of which (<5 ppm) is observed in the reaction products at high temperatures. NO production from NO_2 (negative $NO_{converted}/NO_{2converted}$ ratio at $T < 150$ °C on Fig. 6) and the observation that the higher the NO_2 content – the larger is the part of NO_2 in the NO_x that is converted to N_2 in the NO/NO_2 experiments can be explained by reverse (13). NO reacts with surface nitrates according to (13) to form NO_2 and nitrite, which is readily decomposed to nitrogen (10). With that nitrates are partly removed from the catalyst surface and higher NO_x conversion is obtained.

With decreasing reaction temperature from 400 to 200 °C an increase in the NO_x conversion is observed. The effect is particularly evident for the 47% NO_2 + NO mixture (Fig. 5, solid curve) and may be due to the formation of surface NH_4NO_3. NH_4NO_3 formation is also consistent with decreased $NO_{converted}/NO_{2converted}$ ratio below 180 °C (Fig. 8) due to reaction stoichiometry:

$$2NH_3 + 2NO_2 \rightarrow NH_4NO_3 + N_2 + H_2O, \quad (14)$$

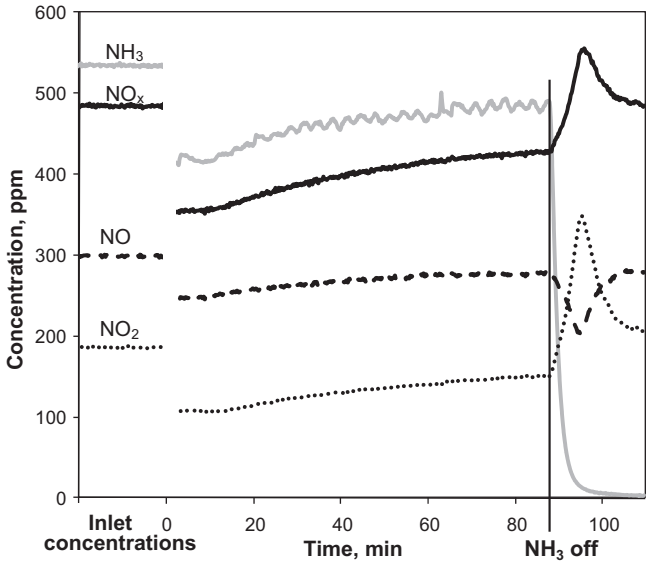

Fig. 9. Change of NO, NO_2 and NO_x concentrations after removing NH_3 from the feed. Catalyst: Al_2O_3. Reaction conditions: 500 ppm NO_x (37% NO_2), 520 ppm NH_3, 8.3% O_2, 7% H_2O in Ar, GHSV = 110,000 h^{-1}, temperature 210 °C.

which is, in fact, a combination of (7)+(8)+(9)+(10)+(11), but without (12) and (13), which are too slow at this temperature. It is also rather indicative of NH_4NO_3 formation that below 200 °C we do not observe N_2O evolution, while above this temperature its decomposition (12) yields N_2O. Therefore, below 200 °C nitrate formation and subsequent blocking the alumina surface limits NO_x conversion.

To check the reaction scheme during an Al_2O_3 activity test, temperature ramping was stopped at 500, 210 and 100 °C. After the concentrations of the outlet gas components were stabilised, NH_3 was switched off from the feed. Following the removal of NH_3 from the inlet gas at 500 and 100 °C the concentrations of NO and NO_2 equalled these concentrations at the reactor inlet (no reaction with adsorbed nitrates (13) was observed). However, the removal of NH_3 from the feed at 210 °C (Fig. 9) resulted in consumption of NO and release of NO_2. This is in agreement with NO consumption in the NO_x SCR over alumina, which takes place between 150 and 350 °C (Fig. 8). The ratio of evolved NO_2 to consumed NO was approximately 1.7. This ratio can be achieved by combination of the competing reactions (10), which gives no NO_2, reverse (9) and (8), which give 2 NO_2 molecules, and, of course (13), which initiates the NO consumption and yields 1 NO_2 molecule. Thus the mechanism of NO_x SCR by NH_3 over Al_2O_3 and Ag/Al_2O_3 could share most of the reaction steps with "Fast SCR".

3.2.4. *Surface species during NH_3-SCR over Al_2O_3*

Diffuse reflectance infrared spectroscopy is a powerful tool to complement observations from catalytic experiments with observations of surface species. Fig. 10 shows the evolution of species on the Al_2O_3 surface, when switching off NH_3 from a feed containing NO, NO_2, NH_3 and O_2 at 150 °C and at 500 °C. Similar spectra were observed at 300 and 400 °C but not shown. The first spectra are taken in a feed containing NH_3 and the following spectra 5, 10, 15 and 25 min after the NH_3 was switched off. When all gases are present in the first spectra, bands at 1690, 1623, 1533, 1474, 1398, 1314 and 1236 cm^{-1} can be distinguished at 150 °C. According to literature, the bands at 1623, 1533 and 1236 cm^{-1} which are accompanied by bands at 3355, 3271 and 3173 cm^{-1} (not shown) can be assigned to deformation vibrations and stretching vibrations of ammonia, respectively [34–37]. Bands at 1690 and 1474 cm^{-1} have previously been assigned to deformation vibrations of NH_4^+

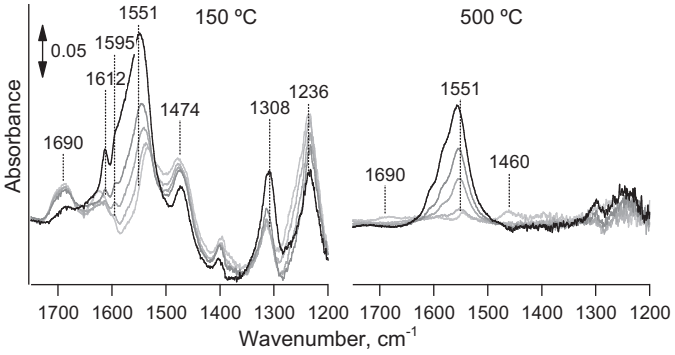

Fig. 10. Change in surface species after removing NH_3 for the first time from the feed over a fresh Al_2O_3 catalyst. Reaction conditions: 500 ppm NO_x (37% NO_2), 520 ppm NH_3, 8.3% O_2 in Ar. Spectra were taken from gray to black: with NH_3 in the feed, and 5, 10, 15 and 25 min after switching off NH_3.

or NH_3 [34,35,37]. At 500 °C all the bands are much smaller. But even there, mainly bands due to NH_3 or NH_4^+ can be observed. Thus under NH_3-SCR conditions, mainly ammonia is adsorbed on Al_3O_2 and very little nitrates and nitrites are adsorbed. When turning off ammonia in the feed first the bands of adsorbed NH_3 at 1236, 1623, 3355, 3271 and 3173 cm^{-1} decrease at 150 °C. Somewhat later, the NH_4^+ bands at 1690 and 1474 cm^{-1} start to decrease and two new bands at 1612 and 1585 cm^{-1} grow. At the same time, the bands around 1551 and 1308 cm^{-1} shift in wavenumber and increase. The shifts in wavenumber as well as the new bands are all caused by the stretching of the N=O bond of differently bound nitrate species [35–45] which start accumulating in the absence of NH_3. That the bands of adsorbed NH_3 diminish before the bands of adsorbed NH_4^+ species start to decrease is in accordance with reaction (14). Switching back to SCR reaction conditions, the NH_3 and NH_4^+ species start growing again at 150 °C while the nitrate species decrease but do not completely disappear, even in the presence of H_2 as shown by the first spectra in Fig. 11.

At 500 °C, the bands of adsorbed NH_4^+ at 1690 and 1464 cm^{-1} disappear previous to the bands of adsorbed NH_3 between 3355 and 3173 cm^{-1} (not shown), while the nitrate band at about 1551 cm^{-1} increases. The remaining nitrates may be regarded as inactive. However, whether the accumulation of these species reduce the

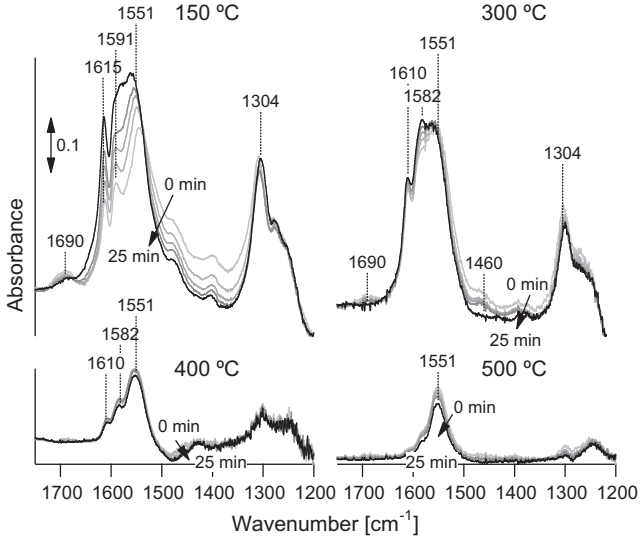

Fig. 11. Change in surface species after removing NH_3 from the hydrogen-containing feed over Al_2O_3. Reaction conditions: 500 ppm NO_x (37% NO_2), 520 ppm NH_3, 1250 ppm H_2, 8.3% O_2 in Ar. Spectra were taken from gray to black: with NH_3 in the feed, and 5, 10, 15 and 25 min after switching off NH_3.

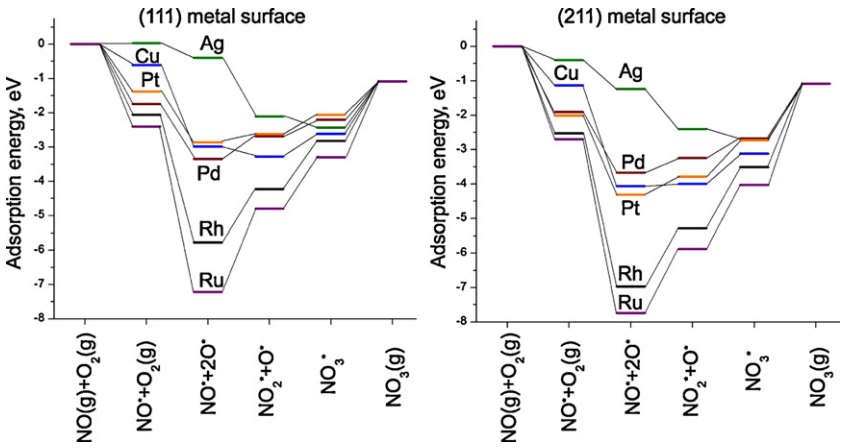

Fig. 12. Potential energy surface diagram for the formation of NO_x via the oxidation of NO over (1 1 1) and (2 1 1) surfaces of the selected transition metals.

activity for NO_x reduction and, thus, poison the surface or only act as spectator species, cannot be answered by the available data.

Fig. 11 shows, moreover, the evolution of bands when switching off NH_3 from a H_2 containing feed at different temperatures. At all temperatures, the spectra are dominated by nitrates with bands at 1551, around 1585, 1612 and around 1304 cm^{-1}. The amount of adsorbed species decreases with increasing temperature as indicated by fewer and smaller peaks at higher temperatures. When the ammonia is switched off from the feed containing H_2 at 150 °C the bands assigned to NH_3 and NH_4^+ species on the surface decrease while the nitrate bands around 1615, 1585, 1551 and 1301 cm^{-1} increase. This evolution of the bands is similar to the case without H_2 in the feed. At 300 °C, only the nitrate band at 1585 cm^{-1} increases, while the other nitrate bands are stable or decrease. At even higher temperatures, all NH_x bands are very tiny or hardly visible while all nitrate bands clearly decrease showing that the addition of H_2 to the feed has an influence on γ-Al_2O_3 without silver. For this observed effect of hydrogen at high temperatures (400 and 500 °C) there are two reasonable explanations: hydrogen may either itself reduce the nitrates as observed by [26,31,46] on Ag/Al_2O_3 or it partially reduces some of the NO_2 to NO which in turn can reduce nitrates to nitrites (reaction (13)). Moreover, less new nitrates will be formed on the catalyst surface when the NO_2 concentration is decreased by partial reduction to NO.

3.3. DFT calculations

3.3.1. Oxidation of NO to NO_2 and NO_3 on the surface of transition metals

Fig. 12 shows the potential energy surface diagram for the absorption of NO and O_2 leading to NO_x, i.e., NO_2 and NO_3 calculated for 6 different transition metal catalysts Ag, Cu, Pd, Pt, Rh and Ru. For all six different transition metal catalysts both the (1 1 1) terrace surface model and (2 1 1) step surface model were investigated and the results are similar for both surfaces. The diagram shows that among the transition metals studied the formation of NO_2 on (1 1 1) terraces is favorable for both Ag and Cu, whereas the formation of NO_3 is favorable only on Ag. On (2 1 1) step surface the formation of NO_2 and NO_3 via oxidation of NO is significantly favorable only on Ag. For other metals NO adsorption without oxidation to NO_x is preferred. That supports the idea of Ag being necessary catalyst component for the oxidation of NO to NO_x species as potentially first step of NO SCR.

3.3.2. Adsorption of NO_x and HNO_x on the step γ-Al_2O_3 surface

The model of the step on the γ-Al_2O_3 (representing uncoordinated Al sites) was used for calculations of NO_x adsorption energy as the most abundant surface of γ-Al_2O_3 crystals is the step surface [24]. It has been demonstrated by Mei et al. [33] that NO_3 adsorbs rather strongly on the γ-Al_2O_3 (1 0 0) and γ-Al_2O_3 (1 1 0) surfaces than compared to NO and NO_2.

A clear decrease of concentration of surface nitrates has been observed by FTIR after addition of hydrogen at high temperatures (experiments at 400 and 500 °C in the Section 3.2.4). Such removal of strongly bound nitrates which block the alumina surface can partly explain the positive effect of H_2 on the activity of Ag/Al_2O_3 catalysts in NO_x SCR.

Though authors of [33] have done extensive calculation for the adsorption of NO_x on γ-Al_2O_3 (1 0 0) and γ-Al_2O_3 (1 1 0) surfaces, however, no effect of H_2 on the stability of surface nitrates on γ-Al_2O_3 has been considered.

We have calculated the adsorption energy of NO_3 and HNO_3 on our model γ-Al_2O_3 step surface representing uncoordinated Al surface sites. Five different uncoordinated Al sites are present

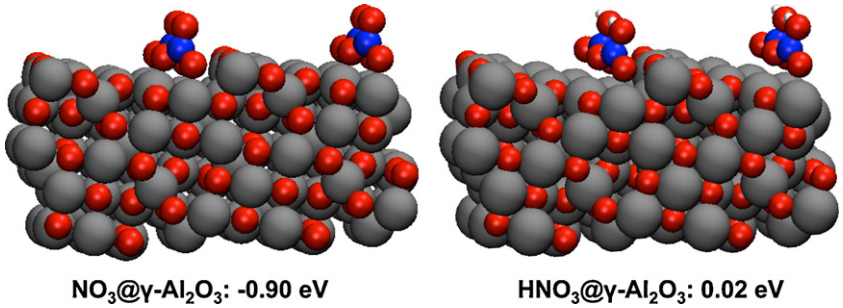

Fig. 13. NO_3 and HNO_3 adsorption geometries and adsorption energies on the model step closed packed gamma alumina surface. All the adsorption energies are given with the reference to the gas phase zero energy points of the respective species.

in our model alumina surface as derived from the bulk γ-Al_2O_3 geometry in [24]. These have all been used for the calculations, however, only the most energetically favorable (energy minimum among studied) adsorption geometries with two oxygen atoms of NO_3 and HNO_3 bridging with two Al sites of γ-Al_2O_3 are reported here. See supplementary information for more details on the used geometries.

The calculated adsorption energy of HNO_3 (Fig. 13) on the model surface of γ-alumina is considerably smaller than that of NO_3 (which agrees with [33]), which increases the probability of HNO_3 removal from the alumina surface compared to NO_3 in the absence of hydrogen. This supports the suggestion of H_2 facilitating removal of strongly bound NO_3 from the alumina.

The mechanism of reduction of adsorbed NO_x species by hydrogen with the formation of N_2 has been previously suggested for $Pt/MgO–CeO_2$ catalysts for H_2-SCR of NO_x [20,21]. This mechanism includes dissociative adsorption of hydrogen on the metal nanoparticle, spillover of the formed atomic hydrogen on the support to the two neighboring NO_x species and their reduction with subsequent release of surface sites. However, this is not a major pathway of the SCR in our case because SCR in the absence of NH_3 is insignificant (Fig. 3, dotted line). Here we suggest that atomic hydrogen reacts rather with a single nitrate or nitrite group with subsequent release of HNO_x and adsorption sites on alumina. The evolved HNO_x can recombine with the formation of water and nitrogen oxides.

4. Conclusions

Ag supported on γ-Al_2O_3 is a very promising catalytic system which can be used for the removal of nitrogen oxides from the exhaust of diesel engines in the presence of H_2. It is vital that both Ag and alumina are present in the catalyst formulation. The primary role of Ag is the H_2-assisted oxidative activation of NO and the reaction of oxidised NO and NH_3 can proceed further on alumina. Hydrogen also facilitates removal of nitrates from the alumina surface, as supported by DRIFTS experiments and DFT calculation.

The studied catalysts facilitate $NO + NO_2$ mixture reduction without H_2 in the feed with the Al_2O_3 support defining the catalytic activity. Therefore, tuning the alumina support, not only the metal, is vital for obtaining active Ag/Al_2O_3 catalyst.

Acknowledgements

This work was supported by grant 09-067233 from The Danish Council for Strategic Research. TEM images were acquired with the support of Center for Electron Nanoscopy (DTU CEN) and personally by Thomas W. Hansen. We acknowledge the supply of the commercial alumina for the study by the SASOL Germany.

The authors also wish to thank Dr. Alexander Yu. Stakheev and Dr. Jakob Weiland Høj for fruitful discussions.

Appendix A. Supplementary data

Supplementary data associated with this article can be found, in the online version, at doi:10.1016/j.apcatb.2011.11.042.

References

[1] T.V. Johnson, Int. J. Engine Res. 10 (2009) 275–285.
[2] S. Subramanian, R.J. Kudla, W. Chun, M. Chatth, Ind. Eng. Chem. Res. 32 (1993) 1805–1810.
[3] T. Miyadera, Appl. Catal. B 2 (1993) 199–205.
[4] G.E. Marnellos, E.A. Efthimiadis, I.A. Vasalos, Appl. Catal. B 48 (2004) 1–15.
[5] Z.M. Liu, K.S. Oh, S.I. Woo, Catal. Lett. 106 (2006) 35–40.
[6] S. Satokawa, J. Shibata, K. Shimizu, S. Atsushi, T. Hattori, Appl. Catal. B 42 (2003) 179–186.
[7] R. Burch, J.P. Breen, C.J. Hill, B. Krutzsch, B. Konrad, E. Jobson, L. Cider, K. Eranen, F. Klingstedt, L.E. Lindfors, Top. Catal. 30–31 (2004) 19–25.
[8] M. Richter, U. Bentrup, R. Eckelt, M. Schneider, M.M. Pohl, R. Fricke, Appl. Catal. B 51 (2004) 261–274.
[9] M. Richter, R. Fricke, R. Eckelt, Catal. Lett. 94 (2004) 115–118.
[10] K.-i. Shimizu, A. Satsuma, Appl. Catal. B 77 (2007) 202–205.
[11] H. Kannisto, X. Karatzas, J. Edvardsson, L.J. Pettersson, H.H. Ingelsten, Appl. Catal. B 104 (2011) 74–83.
[12] S. Bensaid, E.M. Borla, N. Russo, D. Fino, V. Specchia, Ind. Eng. Chem. Res. 49 (2010) 10323–10333.
[13] T. Johannessen, H. Schmidt, US patent 2010/0021780 A1.
[14] C.H. Christensen, R.Z. Sørensen, T. Johannessen, U.J. Quaade, K. Honkala, T.D. Elmøe, R. Køhler, J.K. Nørskov, J. Mater. Chem. 15 (2005) 4106–4108.
[15] A. Klerke, C.H. Christensen, J.K. Nørskov, T. Vegge, J. Mater. Chem. 18 (2008) 2304–2310.
[16] V.A. Kondratenko, U. Bentrup, M. Richter, T.W. Hansen, E.V. Kondratenko, Appl. Catal. B 84 (2008) 497–504.
[17] K.-i. Shimizu, A. Satsuma, J. Phys. Chem. C 111 (2007) 2259–2264.
[18] E. Kondratenko, V. Kondratenko, M. Richter, R. Fricke, J. Catal. 239 (2006) 23–33.
[19] P.G. Savva, C.N. Costa, Catal. Rev. – Sci. Eng. 53 (2011) 91–151.
[20] C.N. Costa, A.M. Efstathiou, J. Phys. Chem. C111 (2007) 3010–3020.
[21] P.G. Savva, A.M. Efstathiou, J. Catal. 257 (2008) 324–333.
[22] E. Mènendez-Proupin, G. Gutièrrez, Phys. Rev. B 72 (2005) 35116–35119.
[23] B. Hammer, L.B. Hansen, J.K. Nørskov, Phys. Rev. B 59 (1999) 7413–7421.
[24] M. Digne, P. Sautet, P. Raybaud, P. Euzen, H. Toulhoat, J. Catal. 226 (2004) 54–68.
[25] P. Sazama, L. Čapek, H. Drobná, Z. Sobalík, J. Dědeček, K. Arve, B. Wichterlová, J. Catal. 232 (2005) 302–317.
[26] K.-i. Shimizu, J. Shibata, A. Satsuma, J. Catal. 239 (2006) 402–409.
[27] V. Houel, P. Millington, R. Rajaram, A. Tsolakis, Appl. Catal. B 77 (2007) 29–34.
[28] G. Madia, M. Koebel, M. Elsener, A. Wokaun, Ind. Eng. Chem. Res. 41 (2002) 3512–3517.
[29] A. Grossale, I. Nova, E. Tronconi, D. Chatterjee, M. Weibel, J. Catal. 256 (2008) 312–322.
[30] J.H. Lee, S.J. Schmieg, S.H. Oh, Appl. Catal. A 342 (2008) 78–86.
[31] F.C. Meunier, J. Ross, Appl. Catal. B 24 (2000) 23–32.
[32] J.G.M. Brandin, L.H. Andersson, C.U.I. Odenbrand, Acta Chem. Scand. 44 (1990) 784–788.
[33] D. Mei, Q. Ge, J. Szanyi, C.H.F. Peden, J. Phys. Chem. C 113 (2009) 7779–7789.
[34] A.A. Tsyganenko, D.V. Pozdnyakov, V.N. Filimonov, J. Mol. Struct. 29 (1975) 299–318.
[35] J.B. Peri, J. Phys. Chem. 69 (1965) 231–239.
[36] A.A. Davydov, Infrared Spectroscopy of Adsorbed Species on the Surface of Transition Metal Oxides, John Wiley & Sons, Chichester, New York, Brisbane, Toronto, Singapore, 1984.
[37] G. Busca, H. Saussey, O. Saur, J.C. Lavalley, V. Lorenzelli, Appl. Catal. 14 (1985) 245–260.
[38] A. Iglesias-Juez, A.B. Hungria, A. Martinez-Arias, A. Fuerte, M. Fernandez-Garcia, J.A. Anderson, J.C. Conesa, J. Soria, J. Catal. 217 (2003) 310–323.
[39] S. Tamm, H.H. Ingelsten, M. Skoglundh, A.E.C. Palmqvist, J. Catal. 276 (2010) 402–411.
[40] S. Tamm, H.H. Ingelsten, A.E.C. Palmqvist, J. Catal. 255 (2008) 304–312.
[41] S. Kameoka, Y. Ukisu, T. Miyadera, Phys. Chem. Chem. Phys. 2 (2000) 367–372.
[42] F.C. Meunier, J.P. Breen, V. Zuzaniuk, M. Olsson, J.R.H. Ross, J. Catal. 187 (1999) 493–505.
[43] K.I. Hadjiivanov, Catal. Rev. Sci. Eng. 42 (2000) 71–144.
[44] G.G. Ramis, G. Busca, V. Lorenzelli, P. Forzatti, Appl. Catal. 64 (1990) 243–257.
[45] M. Schraml-Marth, A. Wokaun, A. Baiker, J. Catal. 138 (1992) 306–321.
[46] H. Kannisto, H.H. Ingelsten, M. Skoglundh, Top. Catal. 52 (2009) 1817–1820.